Laser Interstitial Thermal Therapy in Neurosurgery

Veronica L. Chiang
Shabbar F. Danish
Robert E. Gross
Editors

Springer

Laser Interstitial Thermal Therapy in Neurosurgery

Veronica L. Chiang • Shabbar F. Danish
Robert E. Gross
Editors

Laser Interstitial Thermal Therapy in Neurosurgery

Springer

Editors
Veronica L. Chiang
Department of Neurosurgery
Yale University School of Medicine
New Haven, CT
USA

Shabbar F. Danish
Department of Neurosurgery
Rutgers-RWJ Medical School
New Brunswick, NJ
USA

Robert E. Gross
Department of Neurosurgery
Emory University School of Medicine
Atlanta, GA
USA

ISBN 978-3-030-48046-2 ISBN 978-3-030-48047-9 (eBook)
https://doi.org/10.1007/978-3-030-48047-9

This Springer imprint is published by the registered company Springer Nature Switzerland AG
The registered company address is: Gewerbestrasse 11, 6330 Cham, Switzerland

Foreword

Laser Interstitial Thermal Therapy (LITT), also known as Laser Induced Thermal Therapy, Stereotactic Laser Ablation, or, simply, Laser Ablation, for CNS disorders is not new. Pioneers in Germany and Boston, Massachusetts, set forth to try to treat brain tumors using various versions of laser-generated heat in the 1990s. Although there were some promising early results, it was clear that this was an idea that was ahead of its time due to the limitations of contemporary technologies.

A decade later saw a new generation of LITT, with sophisticated, self-cooling laser probes that use near-infrared wavelength energy to heat and coagulate brain tissues, monitored in real time by magnetic resonance thermography. Whether or not used in conjunction with robotic probe-driving control and the choice of side-firing versus the more traditional diffuse radiant pattern, LITT systems today promise a new, minimally invasive approach to neurosurgery. LITT ablation of CNS tissue is currently used for the treatment of a number of brain disorders, including primary and secondary tumors, adverse radiation effects, epilepsy, some movement disorders, and even some spinal tumors.

This book describes the pioneering efforts of the authors contained herein and is an excellent resource that provides state-of-the-art information on the latest indications and results for LITT in CNS applications as well as prerequisite historical perspective and technical fundamentals. An added bonus is Steve Tatter's practical guide to starting up a LITT practice in the current medical socioeconomic environment. The result is a comprehensive guide to "all things LITT" at the end of the second decade of the second millennium. While it is anticipated that the field will continue to advance rapidly, we certainly have come a long way since the pioneering efforts of Schwarzmaier [1] and Jolesz [2] in the 1990s.

Cleveland, OH, USA — Gene H. Barnett, MD

References

1. Kahn T, Bettag M, Ulrich F, Schwarzmaier HJ, Schober R, Fürst G, et al. MRI-guided laser-induced interstitial thermotherapy of cerebral neoplasms. J Comput Assist Tomogr. 1994;18(4):519–32.
2. Jolesz FA. MR-guided thermal ablation of brain tumors. AJNR Am J Neuroradiol. 1995;16(1):49–52.

Preface

Following in the footsteps of antisepsis, cautery, stereotaxis, and microsurgery, MRI-guided laser interstitial thermal therapy (LITT) is the latest great addition to the field of neurosurgery. As with all disruptive innovations, adoption of its use has been slow, and even two decades after its inception, it is still considered by many to be experimental despite FDA clearance to ablate soft tissue in the brain.

The purpose of this book is to serve as a foundation for MRI-guided LITT across neurosurgical diseases. Within this book, the authors have reviewed the historical development of LITT, the technical and technological components required to perform LITT, its indications and contraindications, areas that still require investigation, LITT complications, and challenges to starting up LITT within one's practice. Given that all the authors were early adopters of the technology, there is much sage advice included within the text that reflects the initial learning curves of many of the users. It is therefore the hope of the authors that this text will allow all neurosurgeons interested in LITT to successfully adopt the technology and incorporate its use seamlessly, safely, and appropriately into their individual practices.

Many thanks go to all the authors for their time and for generously sharing their knowledge. Thanks also to Megan Ruzomberka and Connie Walsh, our developmental editors, who worked tirelessly to make this text possible.

Most of all we give thanks to our patients and their families who have allowed us to participate in their neurosurgical care and were the bravest of pioneers as we sought to understand the impact of this technology.

New Haven, CT, USA — Veronica L. Chiang
New Brunswick, NJ, USA — Shabbar F. Danish
Atlanta, GA, USA — Robert E. Gross

Contents

1 **Magnetic Resonance-Guided Laser Interstitial Thermal Therapy: Historical Perspectives and Overview of the Principles of LITT** 1
Richard Tyc, Mark G. Torchia, Kevin Beccaria, Michael Canney, and Alexandre Carpentier

2 **Technical Considerations for LITT: Getting Through the Procedure** 19
Nitesh V. Patel, Simon Hanft, Veronica L. Chiang, David D. Gonda, Joseph S. Neimat, and Shabbar F. Danish

3 **Special Technical Considerations: LITT in the Awake Patient and the Pacemaker Patient** 37
Brian D. Toyota, Jamie Joseph Van Gompel, and Sanjeet S. Grewal

4 **Complications of LITT** 45
Michael Schulder and Nick Kleiner

5 **LITT for Metastatic In-Field Recurrence** 51
Nanthiya Sujijantarat, Shabbar F. Danish, and Veronica L. Chiang

6 **LITT Treatment of High-Grade Gliomas** 65
Daria Krivosheya, Gene H. Barnett, and Alireza M. Mohammadi

7 **LITT for Pediatric Brain Tumors** 75
George W. Koutsouras, Monserrat Almaguer Ascencio, and Zulma Tovar-Spinoza

8 **LITT in the Treatment of Adult Epilepsy** 85
Bartosz T. Grobelny, Jon T. Willie, and Robert E. Gross

9 **LITT in Adult Functional Neurosurgery: Movement Disorders** 105
Meghan Harris and Jessica Anne Wilden

10 **LITT for Intractable Psychiatric Disease** 119
Wael F. Asaad and Nicole C. R. McLaughlin

11 LITT in Pediatric Epilepsy 127
Sara Hartnett and Daniel J. Curry

12 LITT for Spine Tumors 151
Rafael A. Vega, Dhiego C. A. Bastos, and Claudio E. Tatsui

13 Building a LITT Practice 167
Stephen B. Tatter, Adrian W. Laxton, and Daniel E. Couture

Index 177

Contributors

Wael F. Asaad, MD, PhD Departments of Neurosurgery and Neuroscience, Brown University and Rhode Island Hospital; The Carney Institute for Brain Science, Brown University, Providence, RI, USA

Monserrat Almaguer Ascencio Department of Neurosurgery, Hospital Civil de Guadalajara "Dr. Juan. I. Menchaca", Guadalajara, Jalisco, Mexico

Gene H. Barnett, MD, MBA Rose Ella Burkhardt Brain Tumor and Neuro-Oncology Center, Department of Neurosurgery, Cleveland Clinic, Cleveland, OH, USA

Dhiego C. A. Bastos, MD, MSc Department of Neurosurgery, The University of Texas MD Anderson Cancer Center, Houston, TX, USA

Kevin Beccaria, MD Neurosurgery Department, Sorbonne University School of Medicine, Paris, France

Michael Canney, PhD CarThera, Institut du Cerveau et de la Moelle épiniére (ICM), Paris, France

Alexandre Carpentier, MD, PhD Neurosurgery Department, Sorbonne University School of Medicine, Paris, France

Veronica L. Chiang, MD Department of Neurosurgery, Yale University School of Medicine, New Haven, CT, USA

Daniel E. Couture, MD Department of Neurosurgery, Wake Forest School of Medicine, Winston-Salem, NC, USA

Daniel J. Curry, MD Department of Neurosurgery, Section of Pediatric Neurosurgery, Texas Children's Hospital/Baylor College of Medicine, Houston, TX, USA

Shabbar F. Danish, MD Department of Neurosurgery, Rutgers University, New Brunswick, NJ, USA

Jamie Joseph Van Gompel, MD Department of Neurological Surgery, Mayo Clinic Hospital – St. Mary's Campus, Rochester, MN, USA

David D. Gonda, MD Department of Neurological Surgery, University of California San Diego, San Diego, CA, USA

Sanjeet S. Grewal, MD Department of Neurological Surgery, Mayo Clinic Florida, Jacksonville, FL, USA

Bartosz T. Grobelny, MD Neurological and Spine Surgery, Saint Luke's Hospital of Kansas City, Kansas City, MO, USA

Robert E. Gross, MD, PhD Department of Neurosurgery, Emory University School of Medicine, Atlanta, GA, USA

Simon Hanft, MD Department of Neurological Surgery, Rutgers-Robert Wood Johnson Medical School, New Brunswick, NJ, USA

Meghan Harris, MD Department of Neurology, Highland Clinic, Shreveport, LA, USA

Sara Hartnett, MD Neurosurgery and Brain Repair, University of South Florida, Tampa, FL, USA

Nick Kleiner, BS Department of Neurosurgery, Northwell Health, Lake Success, NY, USA

George W. Koutsouras, DO, MPH, MS Department of Neurosurgery, Upstate University Hospital, Syracuse, NY, USA

Daria Krivosheya, MD Department of Neurosurgery, Cleveland Clinic, Cleveland, OH, USA

Adrian W. Laxton, MD Department of Neurosurgery, Wake Forest School of Medicine, Winston-Salem, NC, USA

Nicole C. R. McLaughlin, PhD Department of Psychiatry and Human Behavior, Butler Hospital/Alpert Medical School of Brown University, Providence, RI, USA

Alireza M. Mohammadi, MD Department of Neurosurgery, Cleveland Clinic, Cleveland, OH, USA

Joseph S. Neimat, MD Department of Neurological Surgery, University of Louisville, Louisville, KY, USA

Nitesh V. Patel, MD Department of Neurosurgery, Robert Wood Johnson-Barnabas University Hospital, New Brunswick, NJ, USA

Michael Schulder, MD, FAANS Department of Neurosurgery, Zucker School of Medicine at Hofstra/Northwell, Lake Success, NY, USA

Nanthiya Sujijantarat, MD Department of Neurosurgery, Yale-New Haven Hospital, New Haven, CT, USA

Claudio E. Tatsui, MD Department of Neurosurgery, The University of Texas MD Anderson Cancer Center, Houston, TX, USA

Stephen B. Tatter, MD, PhD Department of Neurosurgery, Wake Forest School of Medicine, Winston-Salem, NC, USA

Mark G. Torchia, MS, PhD Department of Surgery, Max Rady College of Medicine, University of Manitoba, Winnipeg, MB, Canada

Zulma Tovar-Spinoza, MD Department of Neurosurgery, SUNY Upstate Medical University, Syracuse, NY, USA

Brian D. Toyota, MD, CM, FRCSC, FAANS Department of Neurosurgery/Surgery, Kingston General Hospital, Kingston, ON, Canada

Richard Tyc, MSc, PEng Monteris Medical Inc., Winnipeg, MB, Canada

Rafael A. Vega, MD, PhD Division of Neurosurgery, Beth Israel Deaconess Medical Center, Harvard Medical School, Boston, MA, USA

Jessica Anne Wilden, MD Surgical Movement Disorder Clinic, Tristate Neurosurgery, Willis-Knighton Hospital System, Shreveport, LA, USA

Jon T. Willie, MD, PhD Department of Neurosurgery, Emory University School of Medicine, Atlanta, GA, USA

1 Magnetic Resonance-Guided Laser Interstitial Thermal Therapy: Historical Perspectives and Overview of the Principles of LITT

Richard Tyc, Mark G. Torchia, Kevin Beccaria, Michael Canney, and Alexandre Carpentier

Introduction

Laser use in neurosurgery was described almost immediately after their invention in the late 1950s. Lasers were used as free beam devices during open surgical procedures (e.g., 10.6 μm CO_2 laser) or as components of a surgical instrument ("laser scalpel"). Both brain and spinal surgery benefitted from this use. However, the need for the surgeon to directly visualize the effect of the laser on tissue has limited their use until more recently, when other sophisticated radiological imaging techniques became available.

The combination of the introduction of interstitial hyperthermia by Sutton [1], and the utility of laser as a heat source [2] provided the background to laser interstitial thermal therapy (LITT). Sugiyama et al. [3] in 1990 treated 5 patients (gliomas, $n = 3$, and metastatic lung carcinoma, $n = 2$) with LITT using in situ thermocouples to control temperatures. This work was expanded by Roux et al. with the treatment of a thalamic melanoma metastasis; however, the tumor recurred and the patient died 4 months later [4]. The first reports of MRI to monitor tissue changes post LITT were by Kahn et al. [5, 6] and Schwabe et al. [7] treating brain metastasis. MR imaging was expanded to include MRI thermometry by Schulze et al. [8]. Carpentier et al. [9] reported LITT results of 15 radiosurgery-resistant focal metastatic intracranial tumors in six patients. No perioperative mortality occurred and morbidity was limited (one probe misplacement, one transient increase in cerebellar syndrome, one transient aphasia resolving after 2 weeks). No recurrence occurred by 12 months in patients with complete ablation coverage. In patients receiving partial ablation coverage, peripheral recurrence was visible at 3 months. Overall the estimated median survival was 17.4 ± 3.5 months with two patients alive at 30 and 19 months [10]. Sloan et al. [11] reported LITT results of recurrent glioblastoma (GBM) in ten patients in a dose-escalating first-in-man safety trial of the NeuroBlate System (Monteris Medical). LITT was monitored using real-time MRI thermometry and software that provided predictive thermal damage feedback for surgeons.

R. Tyc (✉)
Monteris Medical Inc., Winnipeg, MB, Canada
e-mail: rtyc@monteris.com

M. G. Torchia
Department of Surgery, Max Rady College of Medicine, University of Manitoba, Winnipeg, MB, Canada

K. Beccaria · A. Carpentier
Neurosurgery Department, Sorbonne University School of Medicine, Paris, France

M. Canney
CarThera, Institut du Cerveau et de la Moelle épiniére (ICM), Paris, France

V. L. Chiang et al. (eds.), *Laser Interstitial Thermal Therapy in Neurosurgery*,
https://doi.org/10.1007/978-3-030-48047-9_1

Remote control was used by the surgeon for probe rotation and depth, in an effort to tailor the zone of treatment. Treatment-related necrosis was evident on MRI studies at 24 and 48 hours. The median survival was 316 days (range: 62–767 days). Three patients improved neurologically, six remained stable, and one worsened. Steroid-responsive treatment-related edema occurred in all patients except one.

Since 2008, two commercial systems Visualase (Medtronic) and NeuroBlate (Monteris Medical) have received FDA and other regulatory clearances. See Table 1.1 for a comparison of the two systems. Many centers across the USA, Canada, and the EU are now using these LITT devices in patients with primary and metastatic brain tumors, epilepsy, and post-SRS radionecrosis [12–21]. More than 270 peer-reviewed papers have been published since 2016 on the application and results of LITT in brain.

Lasers

Optical Radiation on the Electromagnetic Spectrum

Light amplification by stimulated emission of radiation (LASER) devices emit spatially and temporally coherent light that maintains a continuous narrow beam (continuous wave) over long distances tuned to a specific wavelength. In some lasers, a wider wavelength spectrum is created but the light is delivered at extremely short durations (<1 ns). Commercially available lasers represent a broad range of possible output wavelength from <160 nm (ultraviolet) to 570,000 nm (far infrared). Lasers used in medical applications typically have wavelengths in the range of 325–10,600 nm.

When laser light impacts a material, the light is, to some extent, reflected, transmitted, absorbed,

Table 1.1 Comparison of two systems (NeuroBlate and Visualase) commonly used for LITT neurosurgical applications

	NeuroBlate (Monteris Medical)	Visualase (Medtronic)
Laser	Diode, 1064 nm wavelength, continuous wave, pulse mode	Diode, 980 nm wavelength, 15 W continuous wave, adjustable power
Laser delivery device	SideFire® and FullFire® probes, 2.2 and 3.3 mm diameter	Laser applicator, 1.65 mm diameter catheter - (internal laser diffusing fiber with 3 or 10 mm length energy output)
Insertion method	Rigid laser delivery probe via Mini-Bolt to target, integrated to probe driver	Stiffening stylet for delivery via bone anchor, stylet replaced with diffusing fiber optic for treatment
Probe tip cooling	Internalized gas cooling with temperature control, 1–14 °C range	Circulating sterile saline to probe tip at room temp
Stereotactic placement of laser device in OR	Both compatible with many common neurosurgical techniques including frame-based and frameless systems, surgical robots, frameless microtargeting platforms (STarFix [FHC]; ClearPoint, etc.)	
Cranial access	MiniBolt affixed via 4.5 mm twist drill hole	Skull anchor affixed via 3.2 mm twist drill hole
Patient fixation and transport	Integrated head fixation and patient transfer board for MR use as option	None; uses site supplied equipment as needed
MRI	Both integrated with 1.5 T and 3 T MRI systems from Siemens, GE, IMRIS, and Philips	
Temperature monitoring	PRF method, multi-slice 2D GRE, TruTemp (Monteris Medical) optimization	PRF method, variable slice 2D GRE (user-defined)
Prediction of ablation	Thermal dose estimation, CEM43 method	Thermal damage estimation, Arrhenius method
Probe protection safety measures	Probe temperature control via fiber optic sensor	User-defined temperature target points on image for auto shutoff
User interface and display features	Trajectory planning and treatment functions, probe's eye and Ax/Cor/Sag views, pre-, intra-, and post-op MR image integration, user-defined regions, and image registration	Real-time thermal map and damage estimate, trajectory views, damage estimate overlays, and split window

and scattered, depending on the optical and thermal properties of the material and the wavelength, waveform, and power of the laser. In tissue, the relative contribution of the various processes is primarily determined by the amount of absorption which is, in turn, related to the concentration of the various chromophore tissue components, including water, hemoglobin, and melanin. Heating of tissue requires absorption of the laser energy and for almost all medical applications, water is the primary chromophore involved. Given the absorption spectrum of water, lasers with the wavelength range below 1200 nm provide deeper penetration of light [22]. Hemoglobin is a chromophore of blood also found in most tissues. Its absorption is significant in the water absorption range, but increases at lower wavelengths. Comparing the spectra for both water and hemoglobin (Fig. 1.1), a wavelength range between 800 and 1100 nm is considered the therapeutic window for deeper penetration of light and optimal for LITT [22].

Lasers Used in LITT

Many hundred types of lasers exist; however, only a few are used for neurosurgical procedures. Nd:YAG (1064 nm) lasers were used in the earliest clinical applications of LITT [23]. More recently, diode lasers, which produce laser energy using a completely solid state semiconductor system, have been utilized. Compared to the flash-lamped based Nd:YAG lasers, the diode laser systems are compact, less expensive, and can be manufactured to produce a variety of wavelengths. The two most common diode laser wavelengths in use for LITT today in neurosurgery are 980 nm (Visualase) and 1064 nm (NeuroBlate) [11, 24].

Mechanisms of Laser Interactions with Tissue

For any application of lasers to tissue, there are four possible mechanisms of *immediate* laser interactions [25], which are characterized by the following four mechanisms:

1. *Photothermal Effect*: light is converted into heat in the tissue. It is this effect that is the basis for LITT.
2. *Photochemical Effect*: there is a reaction between the laser light and tissue containing a photosensitizing agent. The latter is activated by light, leading to phototoxic reaction in the tissue (photodynamic therapy).
3. *Photomechanical Effect*: high intensity, short laser pulses can create local shock waves and mechanical stress (e.g., laser lithiasis).
4. *Photoablative Effect*: cell molecular bonds are broken, which disintegrates the tissues (e.g., photorefractive keratectomy).

Secondary Mechanisms of Laser Interactions with Tissues

Alterations to cells and tissues that result from heating depend on the tissue being treated and on the intensity and the duration of heating. In LITT, both *hyperthermia* (tissue temperatures of 40–45 °C) and *coagulation* (tissue temperatures of 50–95 °C) occur. Depending on the thermal dose (see Thermal Dosimetry section below), the cells may be killed instantaneously or may die over a more prolonged period of time (24–72 hours). However, there are also additional consequences of heating beyond direct cell death that can then have consequent impacts locally or systemically. These can include long- or short-term opening of the blood-brain barrier [26] and immune modulation [27].

Measurement of Tissue Temperature

Thermal Dosimetry

The neurosurgical use of LITT requires control of the heat distribution in tissue and monitoring the extent of cell death during the procedure.

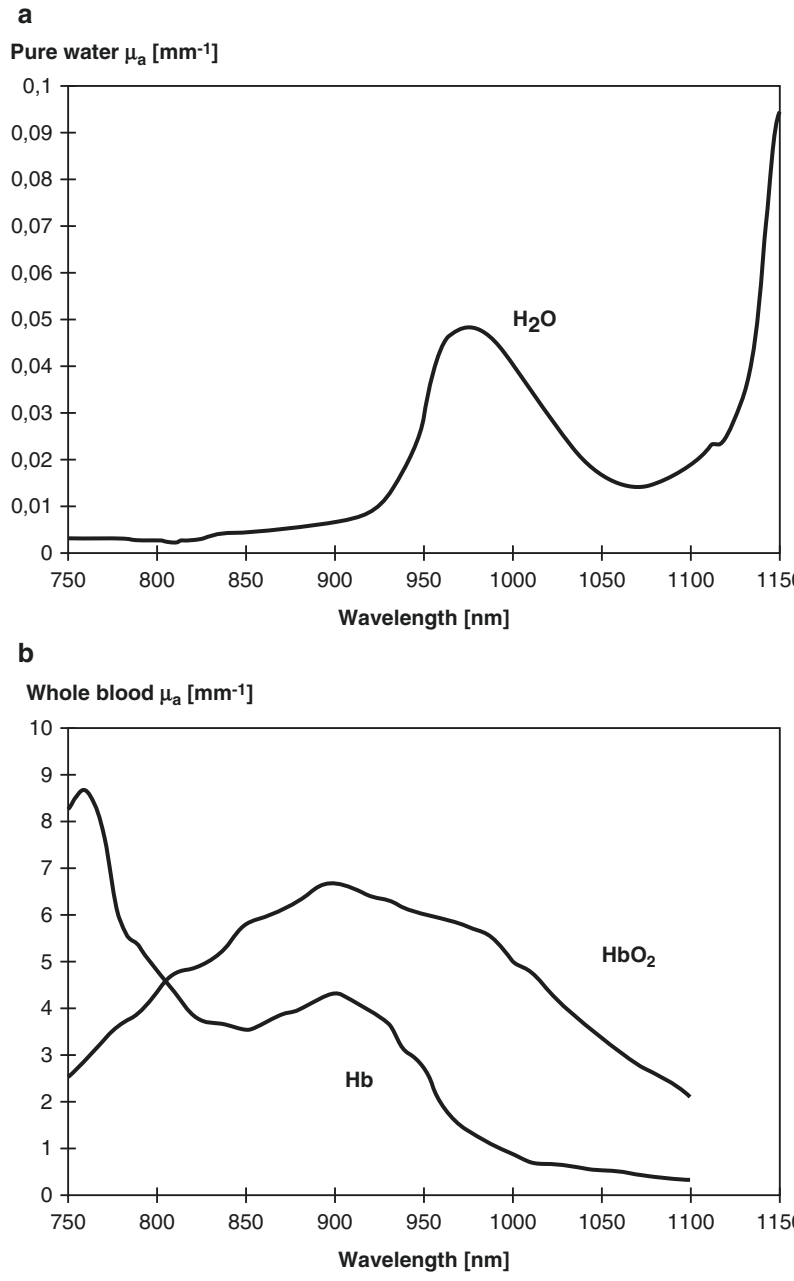

Fig. 1.1 Absorption spectra of pure water (**a**) and oxy- and deoxy-hemoglobin (**b**) in the therapeutic window for deep penetration of light. (Reprinted with permission from Muller and Roggan [48])

Heat-sensitive MRI sequences allow for the creation of a tissue spatiotemporal temperature history. Three thermal models have been described [28] to predict the result of tissue heating. First, the Arrhenius rate analysis models damage as a change in the state of the tissue with the recognition that coagulation occurs between 54 and 60 °C, with denaturation of proteins and cellular components [29] and cell death. Second, the CEM43 model is based on the Arrhenius model and empirical data from hyperthermia observations. In the CEM43 model, cell damage is quantified by relating the temporal temperature history to a reference constant temperature of 43 °C. CEM43 is the Cumulative Equivalent Minutes equivalent to the time at the reference

temperature of 43 °C [30]. Third, the threshold temperature model assumes that tissue is irreparably damaged instantaneously once it reaches 60 °C. This third model does not take into account the temperature history and is really only adapted to rapid tissue ablation [31] rather than LITT procedures. This third model can significantly underestimate the tissue damage if the thermal gradient is in LITT.

MRI Thermal Imaging Sequences

MRI use in LITT was first described in 1988 by Jolesz et al. [32] who interpreted irreversible and complete signal loss as a combination of tissue water loss and altered tissue water mobility, and the surrounding reversible signal loss as an effect of a local temperature rise. Tracz et al. [33] also observed similar MRI changes around the fiber tip during LITT. However, such MRI signal changes are insufficient to monitor LITT as it is not possible to distinguish coagulation from temperature elevation. In LITT, necrosis of the tissue evolves up to about 72 hours post treatment so an acute morphological image will not correspond to the final lesion.

To overcome these limitations, Bleier et al. [34] proposed and demonstrated the dynamics of temperature-related signal intensity changes in the regions irradiated by laser. Although a number of other imaging methods have been tested to measure temperature and the results of LITT (ultrasound, CT, and MRI [35]), only MRI has emerged to become the standard for image-guided LITT ablation procedures in the brain [36]. Unlike MRI, quantifying temperature changes using CT or ultrasound is difficult due to both the impact of heat-induced changes and tissue type on the temperature-dependent property being exploited.

Several parameters of MRI are temperature-dependent including T1 and T2 relaxation time, proton density, diffusion coefficient, magnetization transfer, and the proton resonant frequency (PRF) [37]. PRF has proven to be most effective for monitoring thermal therapies due to its tissue independence (except for adipose tissue) and its linear correlation with temperature over a wide range (20–100 °C) [38]. The shift in the proton resonance is due to temperature-induced changes in intermolecular hydrogen bonding [36, 38].

The frequency shift of the proton resonance signal can be encoded in sequential MR phase images acquired by a variety of MR pulse sequences, including both 2D and volumetric 3D types. The successive phase data acquired by such MR acquisitions is then converted into relative temperature changes. Absolute tissue temperature can also be determined when the baseline temperature at the beginning of the acquisition is known.

Several groups have evaluated the temperature dependence of the water PRF shift in both human and animal tissues [37], and most have found agreement with the pure water value of -0.01 ppm $°C^{-1}$ found by Hindman [38]. MR thermometry using the PRF method has now been used for decades to monitor LITT procedures and is the technique used by commercial LITT systems today for MR-guided ablation in the brain.

Despite its origins in the data generated through MR acquisitions, MR thermometry is not currently provided by the MRI vendors as a fully integrated feature. Rather, tissue temperature quantification using MRI is a method developed external to the MRI system, most often implemented within third-party software. This software integrates with the MRI to retrieve and process temperature-sensitive MR data and provide useful temperature information to the surgeon to guide LITT. The most important elements of the MRI system necessary to provide the raw data stream are: (1) the pulse sequence and imaging hardware (e.g., radiofrequency [RF] coils) available to encode the PRF shift into image data of sufficient quality and (2) the capability to provide such data in "pseudo" real-time after each MR measurement for processing into temperature data to monitor the treatment.

Today, many thermal-sensitive pulse sequences are available to provide temperature-sensitive data using the PRF technique. The most commonly used MR pulse sequence for PRF-based MR thermometry is the 2D gradient

recalled echo (GRE) widely available on modern clinical MRI systems. This acquisition can be single or multi slice and acquired orthogonal or perpendicular to the laser probe or catheter in the region of tissue heating.

When considering other sequences, it is important to note that custom pulse sequences, beyond those directly available at the MR console, may only be used for research purposes. A recent summary of such "stock" MR pulse sequences [39] confirms the variety of available sequences on Siemens, GE, and Philips MR systems.

Current LITT system software provides rapid processing of MR data to produce pseudo real-time quantitative temperature maps, estimates of thermal ablation zones, and computer-controlled feedback during treatments [9, 11].

Tissue Changes and LITT

Histology of LITT-Induced Ablations in Brain Tissue

Histological changes in human brain tissue treated by LITT were reported from a single clinical case by Elder [40], where *en bloc* resection of the treated GBM and adjacent tissue was required 2 weeks post LITT due to progressive edema. Three distinct zones with specific staining patterns were identified:

- Zone 1: Central necrotic area with no cells, poor staining, and resorption at the boundary.
- Zone 2: Rim of granulation tissue in which vascular proliferation was occurring and various immune cells could be identified (lymphocytes and CD68- and CD45-positive microglia); this margin demonstrated mesenchymal and glial reactions.
- Zone 3: Region beyond the granulation tissue, which included GFAP-positive astrocytes.

Additional immunological study demonstrated similar features described in numerous studies in animal models [24, 31, 32, 41–44]. In Elder's study, Zone 2 also demonstrated multinucleated giant cells, while axonal spheroids and neuronal and cell body injury were seen in Zones 1 and 2. Zone 1 demonstrated thrombotic occlusion of blood vessels especially adjacent to the ablative area. In animal studies, the LITT lesion has shown blood-brain-barrier opening which is stronger in this last zone of edema [42, 45]. Blood brain barrier opening followng LITT has also been demonstrated in humans [46].

Following LITT, the size of the ablation lesion changes over time [24, 42] with an initial expansion, thought to be due to vascular damage at the lesion margins [24], delayed hyperthermic cell death at the periphery, or intrafocal edema [31]. Edema spreads to the adjacent normal brain tissue and typically peaks 3–6 days post LITT [24, 42]. Some cases have demonstrated liquefaction of the central necrosis area and the formation of an encapsulated cyst structure after a few months.

Evolution of Cerebral Thermal Ablations on MRI

Many studies have described the MRI appearance of thermally induced ablations in both humans and animal models [5, 7, 24]. The typical MRI lesion architecture immediately following treatment is five concentric zones: the fiber/probe artifact, the central zone, the peripheral zone, a thin rim at the outer border of the peripheral zone, and perifocal edema [7]. In T1-weighted images, probe artifact and peripheral zones are hypointense while the central zone is hyperintense. The perifocal edema is slightly hypointense. The thin rim at the border of the peripheral zone is hypointense with enhancement after gadolinium injection. On MRI, the peripheral zone typically can expand up to 45% in diameter during the first 10 days after LITT [5, 7]. Later, the lesion begins to shrink to reach approximately 50% of the initial size within a mean of 90 days.

Perifocal edema can begin to appear 1–3 days post LITT and can continue to increase up to 3–4 weeks post treatment, with resolution, in some cases, requiring an additional 2–3 weeks [7, 24]. The severity of edema generally does not appear to coincide with the tumor grade or the applied laser energy [5].

With increasing time from ablation, the enhancing rim shows a continuous reduction in diameter and enhancement but often remains visible long after treatment [5, 7]. The internal part of the lesion evolves into an area with a more homogeneous appearance due to the loss of the demarcation of zones. In animals, this MRI zonal architecture corresponds to the zones described in histological studies [42], with MRI central zone possibly corresponding to increasing concentrations of methemoglobin and the collection of proteinaceous fluid.

Elder et al. [40] indicated that ablative changes in tissue (detected histologically) are well represented by MR images within the first 14 days following LITT treatment.

LITT Systems

In general, MR-guided LITT procedures follow a common workflow from the OR to the MR with some differences depending on surgeon preference, MRI equipment, and site layout. In most cases, workflow begins in the operating room for cranial fixation and stereotactic placement of the laser delivery device. (The site- and surgeon-specific method of stereotactic placement drives the most variability to LITT workflow.) Newer devices, such as the ClearPoint system (MRI Interventions), allow for MR-guided stereotactic planning, twist drill hole, and probe insertion to take place in the MRI suite. Figure 1.2 shows a typical workflow. Variations include location of device insertion (OR vs MRI suite), target registration method, coordination with LITT planning software, MRI thermal imaging, and manipulation of device position intraoperatively (within MRI suite or remotely).

This multi-step LITT process demands integration of LITT system hardware and software components to achieve the desired outcomes. The integration of image guidance as a core feature in commercial LITT systems requires MR imaging to provide both planning and treatment functions. As such, subcomponents integrate with the MRI and allow stereotactic targeting and ablation of the defined region of interest. Some of the hardware must reside in the MRI suite (intraoperative or diagnostic) during treatment while others may

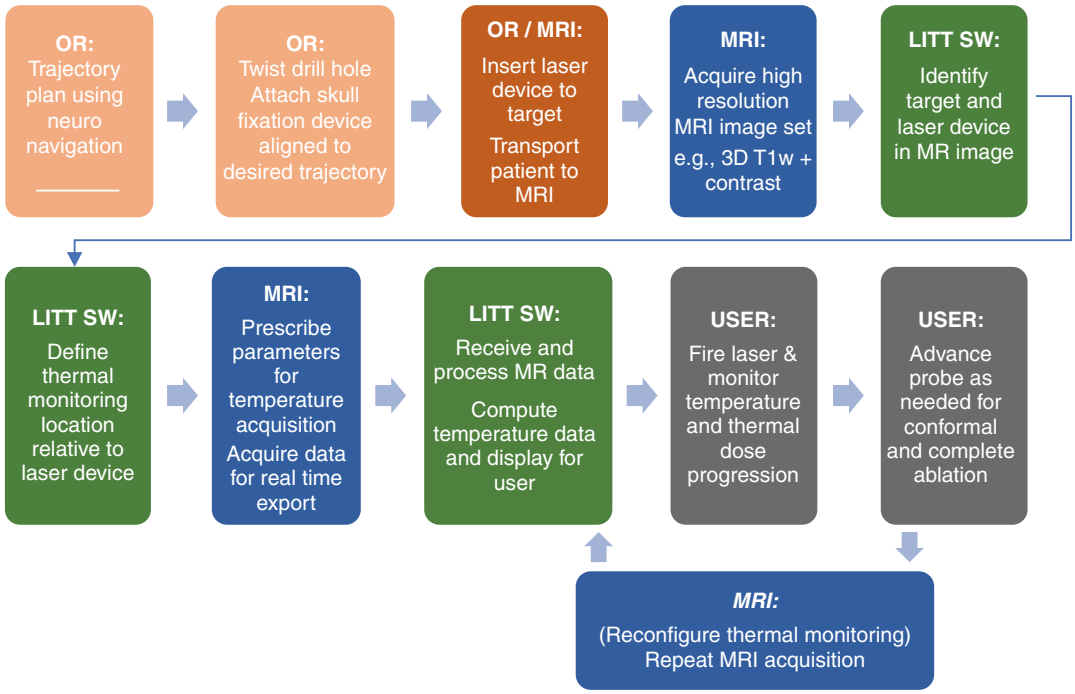

Fig. 1.2 Common workflow steps for MR-guided LITT procedures

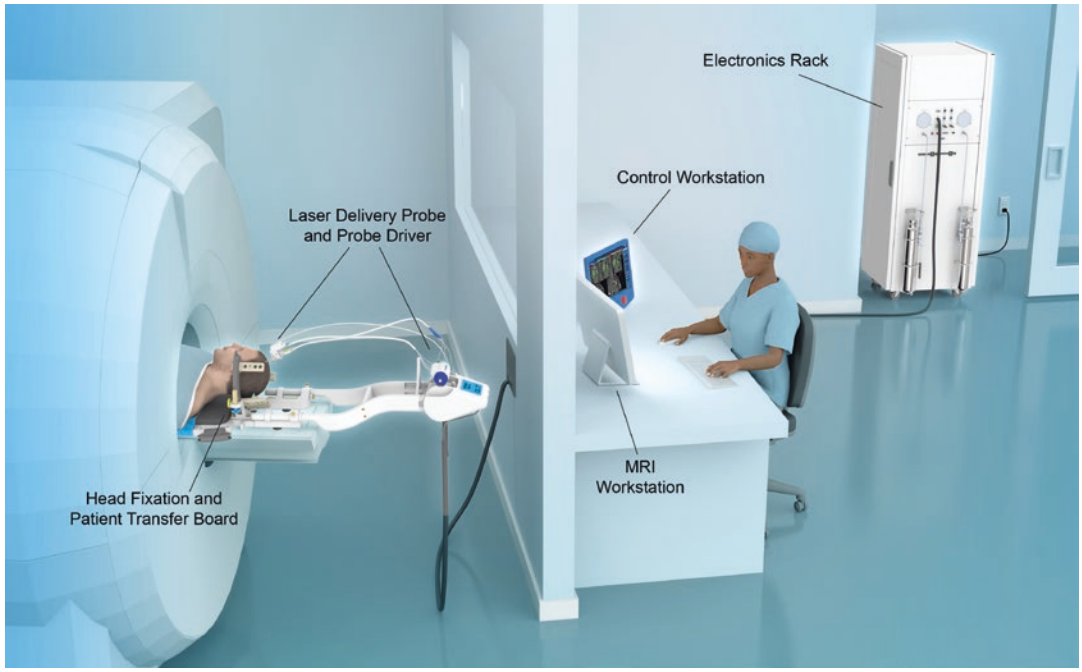

Fig. 1.3 LITT system integrated into the MR suite. (Used with permission. © 2019 Monteris Medical)

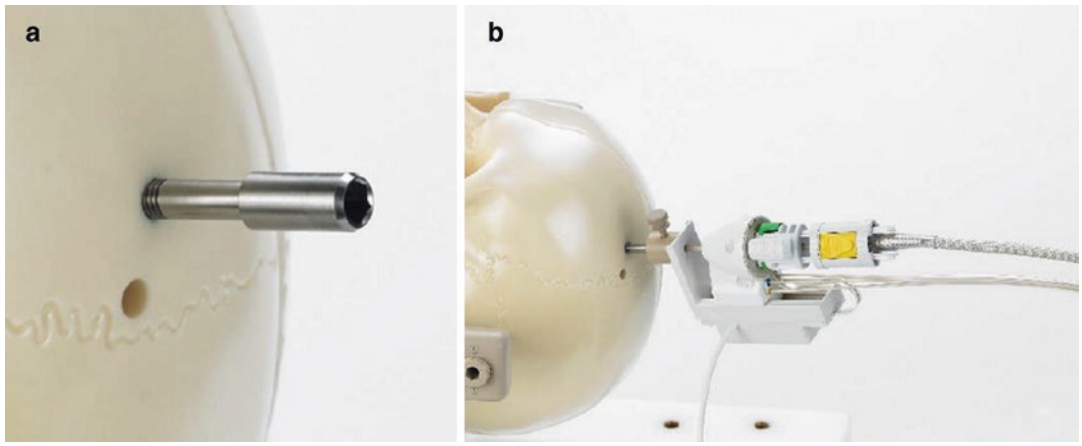

Fig. 1.4 The NeuroBlate Mini-Bolt (**a**) with a robotic probe driver attached (**b**). (Used with permission. © 2019 Monteris Medical)

only be used in the operating room for stereotactic positioning of the laser delivery devices (Fig. 1.3).

Skull-Mounted Trajectory Device

A means of stereotactic placement and retention of trajectory alignment prior to MR imaging is required to provide accurate placement of the laser energy delivery device to the target tissue. Typically, a skull-mounted trajectory device is affixed through a twist drill hole in the skull using a threaded "bolt." The twist drill hole is aligned along the desired target trajectory using one of several methods of stereotactic placement (frame or frameless). Such bolts must be compatible for use in the MRI. Figure 1.4 illustrates the non-magnetic titanium Mini-Bolt (Monteris

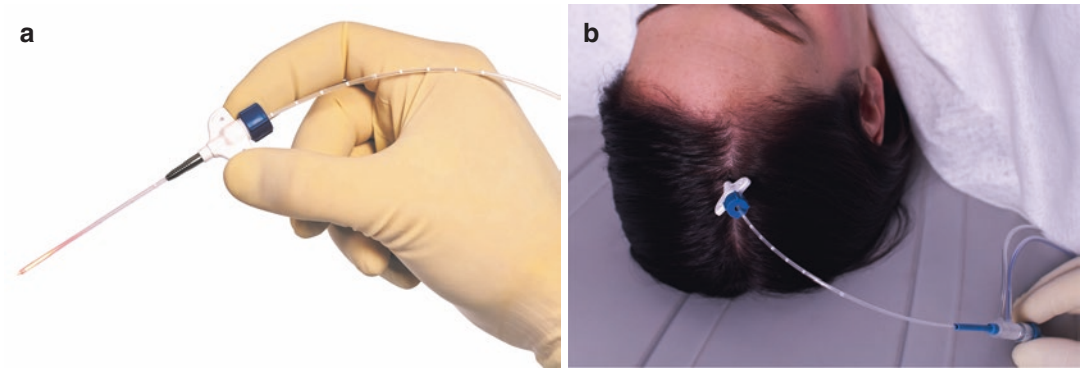

Fig. 1.5 Visualase bone anchor with laser applicator inserted (a). (Used with permission. ©2019 Medtronic)

Medical) with threading to engage a 4.5 mm twist drill hole. Once affixed to the skull, the Mini-Bolt defines the trajectory to the target for the laser delivery probe and provides a mounting platform for a robotic probe driver. Multiple trajectories can be accomplished using two or more bolts as needed. Figure 1.5 illustrates the polymer-based bone anchor from Visualase.

Fiber Probes and Cooling

The transmission of laser energy to the tissue is provided by a fiber optic consisting of a silica-based core (400–600 μm) surrounded by a thin cladding of silica or a hardened polymer. The difference in refractive index between the core and the cladding of the fiber optic results in total internal reflection along the fiber. In this way, large amounts of energy can be transmitted over a long distance with good efficiency. Specific optical alterations or additions to the tip of the fiber can result in directional or diffuse laser output profiles.

In the early clinical reports, bare fibers without cooling were applied directly to the tissue. To prevent fiber damage and tissue charring, the laser output was restricted to lower power and short application times. Cooled laser fibers/probes allow for the treatment of larger volumes with additional thermal control. Modern commercial LITT systems use more sophisticated probes or catheters with integrated cooling at the probe tip. Figure 1.6 shows the NeuroBlate Optic Laser Probe (Monteris Medical). This rigid device has a polymer shaft and sapphire lens at the tip and is capable of direct insertion to target. It is available in 2.2 or 3.3 mm diameter having either a diffuse emission pattern or a side fire energy emission pattern at the tip. Pressurized CO_2 gas internal to the probe is used during energy delivery to regulate probe tip cooling to 1–14 °C depending on the application. The Visualase system provides a double-lumen applicator for the fiber (Fig. 1.7) that allows circulation of room-temperature sterile saline for cooling [9].

Position Control Methods of Laser Delivery Probe

Complete thermal ablation of the targeted region is the goal for any LITT system. Often the ablation zone coverage from laser application at a single position within or adjacent to the target is insufficient to meet this goal. In addition, by moving the probe or fiber, complex and irregular volume lesions can also be generated [29, 42]. The method of adjusting probe position control may be as simple as manual manipulation of the probe by the surgeon when the patient is within the MRI (Visualase) or remote and automated robotic control of the laser delivery device allowing remote manipulation (NeuroBlate).

NeuroBlate uses a robotic probe driver (Fig. 1.8) to manipulate the laser delivery probe both along the line of trajectory and in rotation, which is useful for a probe with directional out-

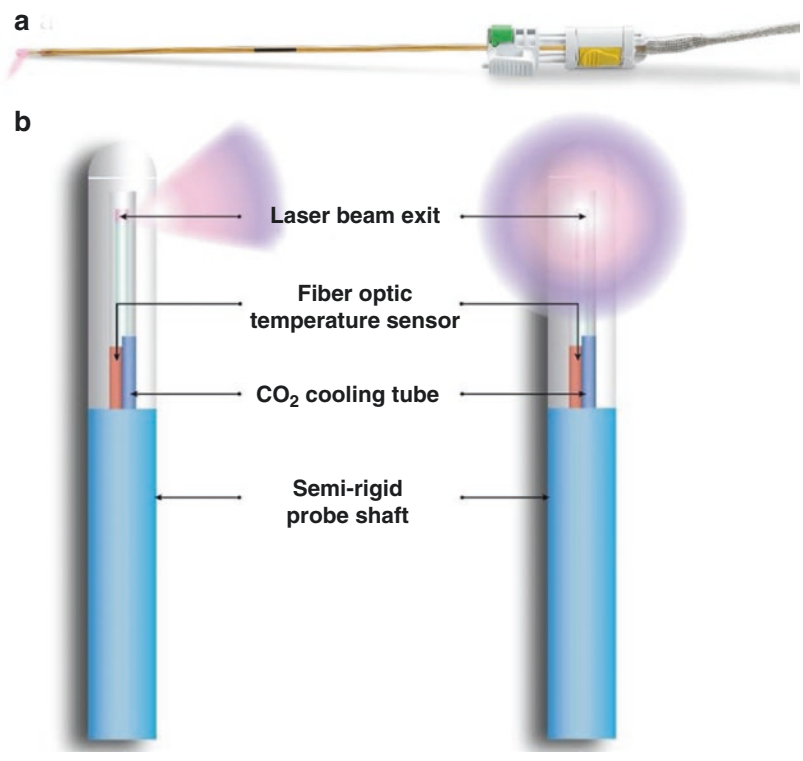

Fig. 1.6 The Optic Laser delivery probe (**a**) and its two types of energy patterns available (**b**): SideFire (left) and FullFire (right). (Used with permission. © 2019 Monteris Medical)

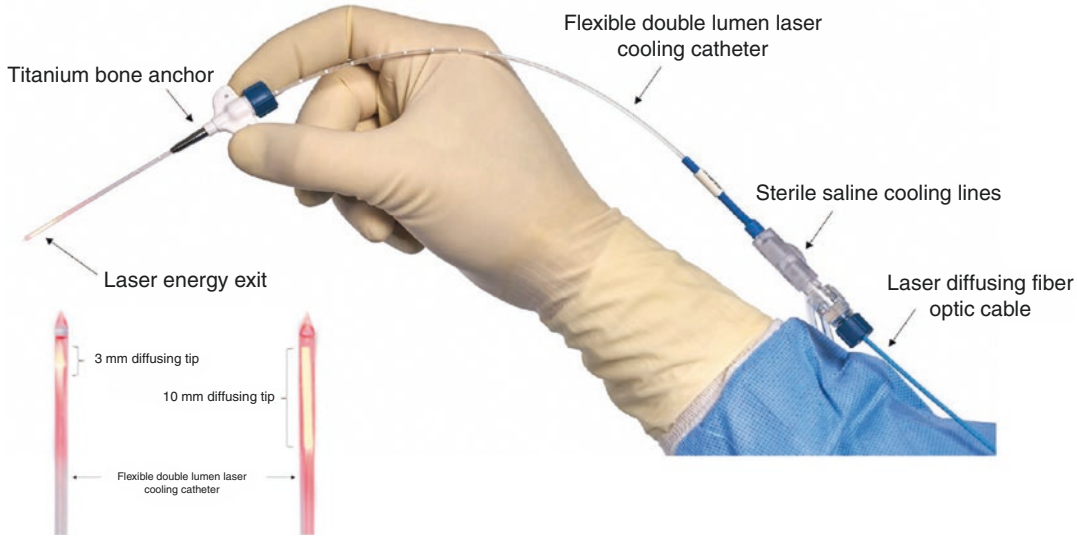

Fig. 1.7 The Visualase Cooling Catheter System and its two types of energy patterns available (*inset*). (Used with permission. ©2019 Medtronic)

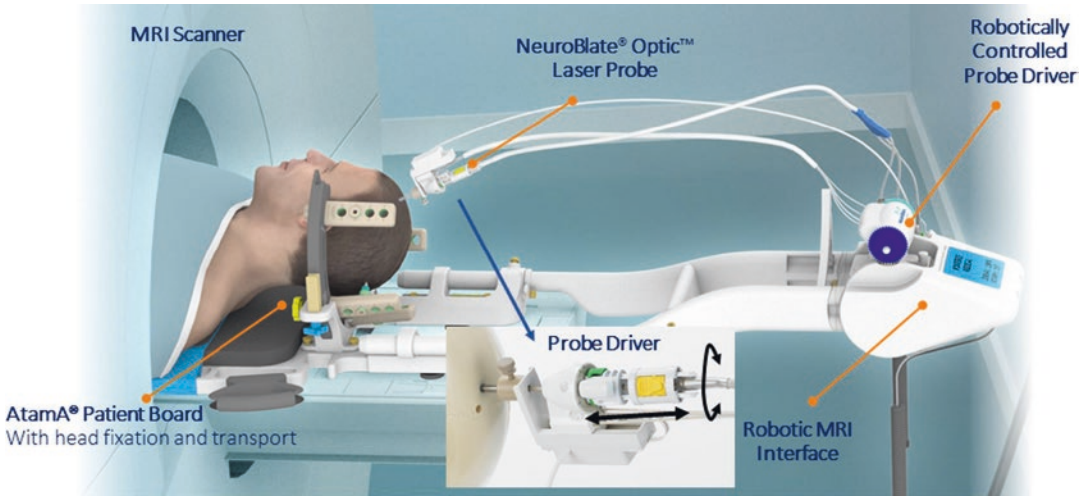

Fig. 1.8 The NeuroBlate system shown within the MRI with the robotic probe driver affixed to the Mini-Bolt and the laser delivery probe inserted via probe driver. (Used with permission. © 2019 Monteris Medical)

put (SideFire; Monteris Medical). Once the probe is inserted and connected to the probe driver, the probe position is remotely controlled by the surgeon from the MR control room where the NeuroBlate system user interface is located.

In the Visualase system, the laser applicator is inserted to its deepest target position by the surgeon in the operating room and then locked into the bone anchor. Then linear position control can be affected manually within the MRI suite as needed by unlocking the laser fiber and retracting the device along its axis inside of the external cannula to a desired position (Fig. 1.9).

Fig. 1.9 The Visualase system shown within the MRI with the bone anchor, laser cooling catheter, and fiber. The laser fiber adjustment occurs at gloved hand position. (Used with permission. ©2019 Medtronic)

Control Computer, Electronics, and User Interface

LITT systems require computer-controlled laser energy delivery, a user interface for the planning and treatment phase of the procedure, and network connectivity to the MRI for data streaming. Additional various electro-mechanical subsystems are also required, depending on the LITT system; however, all demand a set of core system features:

1. Control computer(s): One or many computers control all aspects of providing and controlling such features as: safety monitors, laser energy settings, probe cooling, MR connectivity and DICOM image transfer, graphical user interface (GUI), and display/interaction devices.
2. Electronic subsystems: Including power supplies, safety E-Stops, cooling system pumps or pressure regulation, cables and fiberoptic delivery to MRI suite, filter panel connectivity into MR room, and motion control for robotic devices.

3. User interface: The surgeon interacts with a dedicated GUI that assists in planning and monitoring treatment in addition to providing system diagnostic information. Such interfaces vary among LITT systems but generally provide several key features to guide the user during the ablation process. This includes real-time update of the MR thermometry data for the acquired slice locations defined during the planning process. Temperature data can be displayed as a color-coded temperature image overlaid against a reference diagnostic image providing anatomical information (e.g., 3D T1-weighted high-resolution MRI scan).

The NeuroBlate system GUI is shown in Fig. 1.10a during the laser energy delivery phase of a procedure when one of many MR measurements of the MR thermal acquisition has been processed for display. In this system, three slice planes (red lines in lower views) are acquired perpendicular to the laser delivery probe aligned to the energy exit location. These are shown in the top three views as a color-coded temperature overlay against a 3D T1-weighted diagnostic MRI scan which includes fiber tracts embedded within the image (solid white regions). Diagnostic reference images can include such fiber tractography from DTI data providing a local region of interest for surgical assessment during heating. The lower views show an alternate view of the data parallel to the laser delivery probe while the right side of the GUI contains diagnostic information about the laser, an MR measurement counter, and other user controls.

The Visualase system GUI is shown in Fig. 1.10b during the laser energy delivery phase of a procedure. In this system, 1–3 slice planes are selected to ensure visualization of nearby critical anatomical structures. Typically, slice planes are selected to visualize the length of the laser catheter thereby capturing all potential laser heating locations for a given procedure. In the primary viewing panes, users can select the desired images including a damage estimate overlay on a high-resolution image, a color-coded temperature overlay on a real-time structural image, or a split/combination of the two. Additionally, the upper view contains a temperature over time chart of all set temperature targets, and the lower view contains all user controls for temperature target and visualizations.

MR Imaging and LITT Systems

Medical imaging is essential during LITT to define target(s), select trajectory, track the probe/fiber, monitor thermal dose, predict of final lesion size, and subsequent follow-up of induced lesions. MRI has high soft tissue contrast, multiplanar imaging capabilities, high spatial resolution, temperature sensitivity, and has become the de facto imaging modality for neurological application of LITT.

MRI systems currently integrated with LITT include both diagnostic and intraoperative MRI suites at 1.5 T and 3 T field strengths. Intraoperative MRI suites have dedicated patient handling technology to quickly move the patient in and out of the MRI. Only the IMRIS intraoperative MRI suite allows for a static patient position table while the MRI magnet is moved into place when necessary for LITT treatment.

To provide optimal MR imaging of the brain for LITT, specific RF coils are used to increase the signal-to-noise ratio. These coils often require flexibility in both their overall positioning and how the coil remains adjacent to the head. Various commercial coil types and styles that can be used for LITT are available. In some cases, standard head coils can be used if the trajectory and laser applicator do not impinge on the coil. In other situations, "flex coils" can be used as their design allows for alternate positions adjacent to the head to allow for interaction with the LITT device (Figs. 1.11 and 1.12).

As for all MRI procedures, patient position stabilization is critical because motion will interfere with imaging. This is particularly important during PRF-based MR thermometry as the process assumes tissue spatial location is fixed in successive MR acquisitions. In most LITT cases, the patients are under general anesthesia, although LITT has been used with awake procedures [47]. Patient stabilization can be as

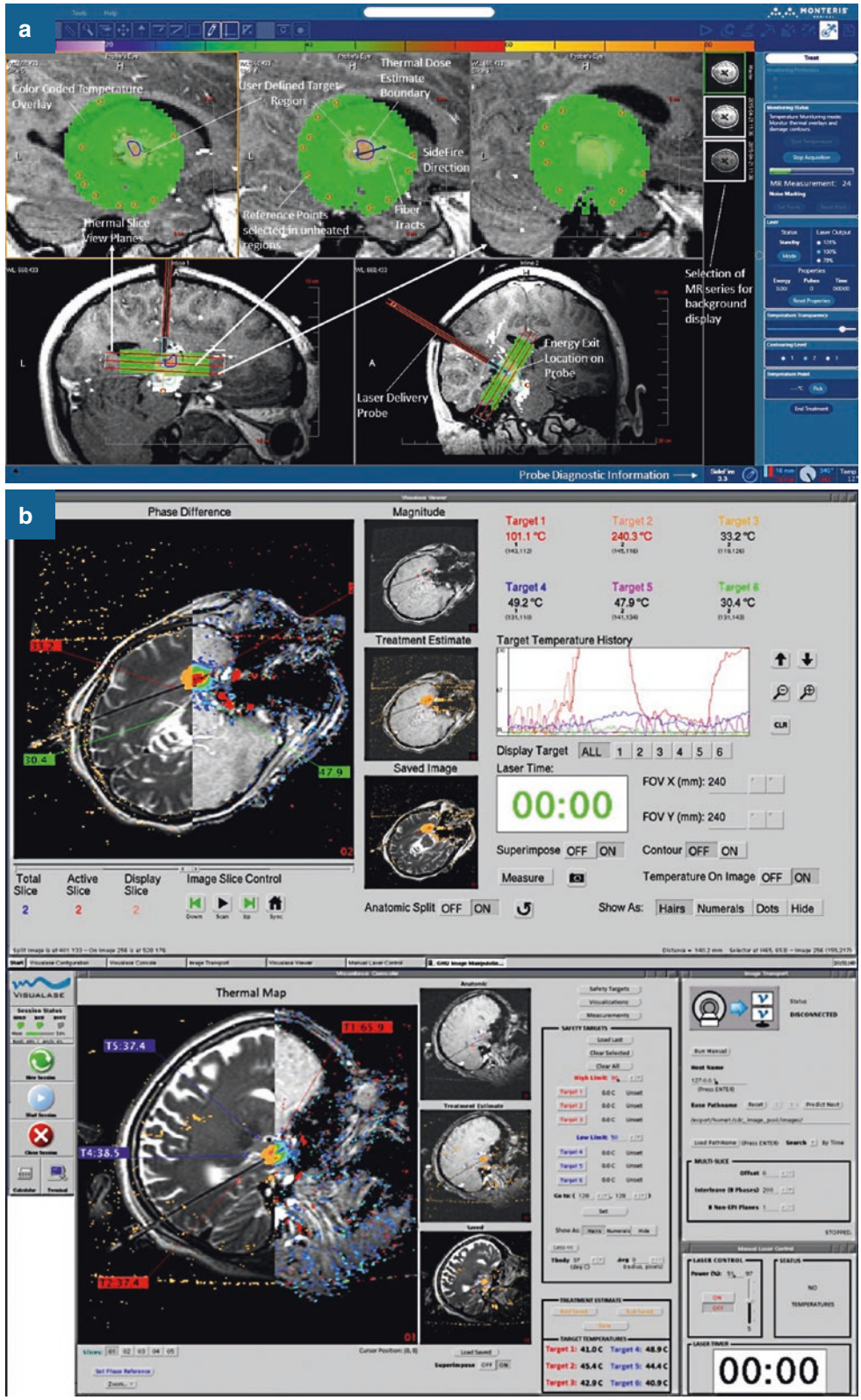

Fig. 1.10 (**a**) NeuroBlate GUI during MR-guided laser thermal therapy (Used with permission. © 2019 Monteris Medical); (**b**) Visualase GUI during MR-guided laser thermal therapy. (Used with permission. ©2019 Medtronic)

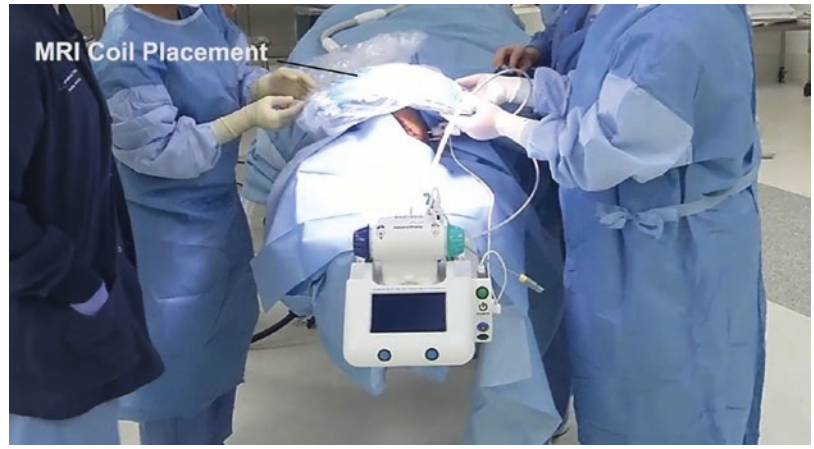

Fig. 1.11 RF coil setup for a LITT procedure using IMRIS setup. Anterior flex coil shown; posterior flex coil is beneath Mayfield skull clamp (Integra LifeSciences) hidden from view

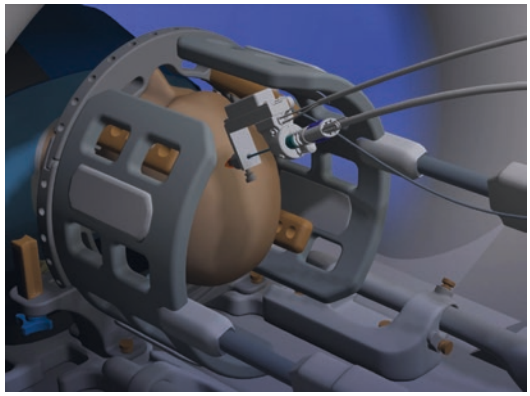

Fig. 1.12 LITT procedure setup using two RF flex coils. (Used with permission. © 2019 Monteris Medical)

simple as restraining the head with straps, pads, or other passive supports, or more rigid fixation provided by MR compatible head fixation devices. Such fixation may be integrated into the patient table (common to intraoperative MRI suites) or integrated into portable patient tables capable of easy transport of the patient from OR to MRI.

MR imaging used for monitoring thermal ablation introduces other sources of error which must be considered. The static magnetic field can drift or vary over time, which can impact the accuracy of MR thermometry. For example, a 0.02 ppm/hr. magnetic field drift can generate a temperature error of ±2 °C [48]. Techniques can be used to compensate for field drift such as external references at known temperatures or, more commonly, internal references such as unheated tissue regions.

During initial MRI thermometry measurements, and with the laser temporarily locked, the NeuroBlate system establishes an optimized reference data set from the temperature-sensitive phase data (∅) of the MR thermometry scan. This referencing improves the accuracy of tissue temperature and therefore computation of thermal dose. The NeuroBlate system computes a baseline phase reference ($\varnothing_{baseline}$) from the average of a minimum of eight MR thermometry measurements to avoid single measurement noise error. This baseline phase reference is the mathematical surrogate for the actual time = 0 patient baseline temperature entered into the system ($T_{patient\ baseline}$). This optimized baseline phase data set is subtracted from subsequent MR measurements during heating to provide accurate relative temperatures (ΔT_n) for when laser energy delivery is enabled. To compensate for phase drift within the MR data, the user selects multiple reference points surrounding the target region in unheated tissue (see Fig. 1.10a) during the initial reference data set collection period. These reference point locations allow the system to create an optimal correction map to monitor and correct for non-thermal phase drift across the monitored anatomical location ($\varnothing_{drift\ correction}$). This phase drift can then be removed from each acquired MR phase measurement ($\varnothing_n$) to ensure that the calculation of relative tissue temperature

represents only true tissue temperature changes as follows:

$$T_{tissue,n} = T_{patient\ baselne} + \Delta T_n$$

$$\text{where } \Delta T_n \sim \Delta\varnothing_n = \varnothing_n - \varnothing_{baseline} - \varnothing_{drift\ correction,n}$$

The Visualase system can monitor temperature drift in unheated regions to determine the amount of drift that is present. A new phase reference can be set after each laser-on event after the tissue has cooled to baseline. The duration between resetting the phase reference is important as inaccuracy can accumulate with drift over time. With Visualase, typical laser-on times range from 1 to 3 minutes with times rarely exceeding 5 minutes when using lower laser powers. When drift is acceptable after monitoring, resetting the phase reference periodically will ensure minimal impact on MR thermometry and Thermal Damage Estimate accuracy during the ablation procedure.

RF noise within the MRI suite can also be a source of error although this is typically controlled during installation and qualification of the MRI site. MR-guided LITT procedures often introduce equipment into the MRI suite, such as anesthesia, and care must be taken to ensure new sources of RF noise are not introduced corrupting both diagnostic imaging and MR thermometry. Magnetic susceptibility artifacts within the MR image due to device presence or air-tissue interfaces in the target region (e.g., entrapped air from biopsies) can also lead to localized uncertainty in temperature calculations. Such device-related image artifacts are typically constrained to close proximity of the device and are generally worse at 3 T than 1.5 T. These artifacts are often mitigated through both device design and material property selection of the laser applicator and pulse sequence parameter selection. Temperature-dependent susceptibility error in water-based tissue is small [48] and thus not significant in brain applications. Intra-scan motion due to cardiac or respiratory influences can also create temperature uncertainty [49] although this is generally not relevant in brain imaging.

Conclusions

It is important to have a sense of the historical concepts as well as of the basic principles that ultimately guide laser therapy for intracranial pathologies. The technologies will likely continue to evolve as our understanding of lasers and laser-tissue interactions increases.

The increasing sophistication of LITT systems, MRI imaging and thermometry, and surgical navigation has resulted in the adoption of LITT as a minimally invasive option for a diverse group of neurological lesions.

References

1. Sutton CH. Tumor hyperthermia in the treatment of malignant gliomas of the brain. Trans Am Neurol Assoc. 1971;96:195–9.
2. Bown SG. Phototherapy in tumors. World J Surg. 1983;7(6):700–9.
3. Sugiyama K, Sakai T, Fujishima I, Ryu H, Uemura K, Yokoyama T. Stereotactic interstitial laser-hyperthermia using Nd-YAG laser. Stereotact Funct Neurosurg. 1990;54–55:501–5.
4. Roux FX, Merienne L, Fallet-Bianco C, Beuvon F, Devaux B, Leriche B, et al. Stereotaxic laser interstitial thermotherapy. A new alternative in the therapeutic management of some brain tumors. Neurochirurgie. 1992;38(4):238–44.
5. Kahn T, Bettag M, Ulrich F, Schwarzmaier HJ, Schober R, Fürst G, et al. MRI-guided laser-induced interstitial thermotherapy of cerebral neoplasms. J Comput Assist Tomogr. 1994;18(4):519–32.
6. Menovsky T, Beek JF, van Gemert MJ, Roux FX, Bown SG. Interstitial laser thermotherapy in neurosurgery: a review. Acta Neurochir. 1996;138(9):1019–26.
7. Schwabe B, Kahn T, Harth T, Ulrich F, Schwarzmaier HJ. Laser-induced thermal lesions in the human brain: short- and long-term appearance on MRI. J Comput Assist Tomogr. 1997;21(5):818–25.
8. Schulze PC, Vitzthum HE, Goldammer A, Schneider JP, Schober R. Laser-induced thermotherapy of neoplastic lesions in the brain--underlying tissue alterations, MRI-monitoring and clinical applicability. Acta Neurochir. 2004;146(8):803–12.
9. Carpentier A, McNichols RJ, Stafford RJ, Itzcovitz J, Guichard JP, Reizine D, et al. Real-time magnetic resonance-guided laser thermal therapy for focal metastatic brain tumors. Neurosurgery. 2008;63(Suppl 1):ONS21–8. https://doi.org/10.1227/01.neu.0000335007.07381.df.

10. Carpentier A, McNichols RJ, Stafford RJ, Guichard JP, Reizine D, Delaloge S, et al. Laser thermal therapy: real-time MRI-guided and computer-controlled procedures for metastatic brain tumors. Lasers Surg Med. 2011;43(10):943–50.
11. Sloan AE, Ahluwalia MS, Valerio-Pascua J, Manjila S, et al. Results of the NeuroBlate system first-in-humans phase I clinical trial for recurrent glioblastoma. J Neurosurg. 2013;118(6):1202–19. https://doi.org/10.3171/2013.1.JNS1291.
12. Kamath AA, Friedman DD, Hacker CD, Smyth MD, Limbrick DD, Kim AH, et al. MRI-guided interstitial laser ablation for intracranial lesions: a large single institution experience of 133 cases. Stereotact Funct Neurosurg. 2017;95(6):417–28. https://doi.org/10.1159/000485387.
13. Chaunzwa TL, Deng D, Leuthardt EC, Tatter SB, Mohammadi AM, Barnett GH, et al. Laser thermal ablation for metastases failing radiosurgery: a multicentered retrospective study. Neurosurgery. 2018;82(1):56–63. https://doi.org/10.1093/neuros/nyx142.
14. Ali MA, Carroll KT, Rennert RC, Hamelin T, Chang L, Lemkuil BP, et al. Stereotactic laser ablation as treatment for brain metastases that recur after stereotactic radiosurgery: a multiinstitutional experience. Neurosurg Focus. 2016;41(4):E11.
15. Dadey DY, Kamath AA, Leuthardt EC, Smyth MD. Laser interstitial thermal therapy for subependymal giant cell astrocytoma: technical case report. Neurosurg Focus. 2016;41(4):E9.
16. Tovar-Spinoza Z, Ziechmann R, Zyck S. Single and staged laser interstitial thermal therapy ablation for cortical tubers causing refractory epilepsy in pediatric patients. Neurosurg Focus. 2018;45(3):E9. https://doi.org/10.3171/2018.6.FOCUS18228.
17. Ahluwalia M, Barnett GH, Deng D, Tatter SB, Laxton AW, Mohammadi AM, et al. Laser ablation after stereotactic radiosurgery: a multicenter prospective study in patients with metastatic brain tumors and radiation necrosis. J Neurosurg. 2018;130(3):804–11. https://doi.org/10.3171/2017.11.JNS171273.
18. Beaumont TL, Mohammadi AM, Kim AH, Barnett GH, Leuthardt EC. Magnetic resonance imaging-guided laser interstitial thermal therapy for glioblastoma of the corpus callosum. Neurosurgery. 2018;83(3):556–65. https://doi.org/10.1093/neuros/nyx518.
19. Petito GT, Wharen RE, Feyissa AM, Grewal SS, Lucas JA, Tatum WO. The impact of stereotactic laser ablation at a typical epilepsy center. Epilepsy Behav. 2018;78:37–44. https://doi.org/10.1016/j.yebeh.2017.10.041.
20. Wright JM, Staudt MD, Alonso A, Miller JP, Sloan AE. A novel use of the NeuroBlate SideFire probe for minimally invasive disconnection of a hypothalamic hamartoma in a child with gelastic seizures. J Neurosurg Pediatr. 2018;21(3):302–7. https://doi.org/10.3171/2017.9.PEDS1747.
21. Mohammadi AM, Hawasli AH, Rodriguez A, Schroeder JL, Laxton AW, Elson P, et al. The role of laser interstitial thermal therapy in enhancing progression-free survival of difficult-to-access high-grade gliomas: a multicenter study. Cancer Med. 2014;3(4):971–9. https://doi.org/10.1002/cam4.266.
22. Laurent D, Oliveria SF, Shang M, Bova F, Freedman R, Rahman M. Techniques to ensure accurate targeting for delivery of awake laser interstitial thermotherapy. Oper Neurosurg (Hagerstown). 2018;15(4):454–60. https://doi.org/10.1093/ons/opx290.
23. Roux FX, Merienne L, Devaux B, Leriche B, Cioloca C. YAG laser in neurosurgery. Neurochirurgie. 1992;38(4):229–34.
24. Kangasniemi M, McNichols RJ, Bankson JA, Gowda A, Price RE, Hazle JD. Thermal therapy of canine cerebral tumors using a 980 nm diode laser with MR temperature-sensitive imaging feedback. Lasers Surg Med. 2004;35(1):41–50.
25. Tew JM Jr, Tobler WD. The laser: history, biophysics, and neurosurgical applications. Clin Neurosurg. 1983;31:506–49.
26. Leuthardt EC, Duan C, Kim MJ, Campian JL, Kim AH, Miller-Thomas MM, et al. Hyperthermic laser ablation of recurrent glioblastoma leads to temporary disruption of the peritumoral blood brain barrier. PLoS One. 2016;11(2):e0148613. https://doi.org/10.1371/journal.pone.0148613.
27. Keisari Y. Tumor abolition and antitumor immunostimulation by physico-chemical tumor ablation. Front Biosci (Landmark Ed). 2017;22:310–47.
28. Yung JP, Shetty A, Elliott A, Weinberg JS, McNichols RJ, Gowda A, et al. Quantitative comparison of thermal dose models in normal canine brain. Med Phys. 2010;37(10):5313–21.
29. Stafford RJ, Fuentes D, Elliott AA, Weinberg JS, Ahrar K. Laser-induced thermal therapy for tumor ablation. Crit Rev Biomed Eng. 2010;38(1):79–100.
30. Sapareto SA, Dewey WC. Thermal dose determination in cancer therapy. Int J Radiat Oncol Biol Phys. 1984;10(6):787–800.
31. Schulze PC, Kahn T, Harth T, Schwurzmaier HJ, Schober R. Correlation of neuropathologic findings and phase-based MRI temperature maps in experimental laser-induced interstitial thermotherapy. J Magn Reson Imaging. 1998;8(1):115–20.
32. Jolesz FA, Bleier AR, Jakab P, Ruenzel PW, Huttl K, Jako GJ. MR imaging of laser-tissue interactions. Radiology. 1988;168(1):249–53.
33. Tracz RA, Wyman DR, Little PB, Towner RA, Stewart WA, Schatz SW, et al. Magnetic resonance imaging of interstitial laser photocoagulation in brain. Lasers Surg Med. 1992;12(2):165–73.
34. Bleier AR, Jolesz FA, Cohen MS, Weisskoff RM, Dalcanton JJ, Higuchi N, et al. Real-time magnetic resonance imaging of laser heat deposition in tissue. Magn Reson Med. 1991;21(1):132–7.
35. McDannold N. Quantitative MRI-based temperature mapping based on the proton resonant frequency

shift: review of validation studies. Int J Hyperth. 2005;21(6):533–46.
36. De Poorter J, De Wagter C, De Deene Y, Thomsen C, Ståhlberg F, Achten E. Noninvasive MRI thermometry with the proton resonance frequency (PRF) method: in vivo results in human muscle. Magn Reson Med. 1995;33(1):74–81.
37. Rieke V, Butts PK. MR thermometry. J Magn Reson Imaging. 2008;27(2):376–90.
38. Hindman JC. Proton resonance shift of water in the gas and liquid states. J Chem Phys. 1966;44:4582–92.
39. Odéen H, Parker DL. Improved MR thermometry for laser interstitial thermotherapy. Lasers Surg Med. 2019;51(3):286–300. https://doi.org/10.1002/lsm.23049.
40. Elder JB, Huntoon K, Otero J, Kaya B, Hatel J, Eltobgy M, et al. Histological findings associated with laser interstitial thermotherapy for glioblasoma multiforme. Diagn Pathol. 2019;14(1):19. https://doi.org/10.1186/s13000-019-0794-4.
41. Canney M, Carpentier A, Beccaria K, Souchon R, Chavrier F, Lafon C, et al. MR-guided interstitial thermal therapy for the treatment of brain tumors with a multi-element ultrasound probe. AIP Conference Proceedings. 2012;1481:32.
42. Schober R, Bettag M, Sabel M, Ulrich F, Hessel S. Fine structure of zonal changes in experimental Nd:YAG laser-induced interstitial hyperthermia. Lasers Surg Med. 1993;13(2):234–41.
43. Vogl TJ, Mack MG, Roggan A, Straub R, Eichler KC, Müller PK, et al. Internally cooled power laser for MR-guided interstitial laser-induced thermotherapy of liver lesions: initial clinical results. Radiology. 1998;209(2):381–5.
44. Higuchi N, Bleier AR, Jolesz FA, Colucci VM, Morris JH. Magnetic resonance imaging of the acute effects of interstitial neodymium:YAG laser irradiation on tissues. Investig Radiol. 1992;27(10):814–21.
45. Salehi A, Paturu MR, Patel B, Cain MD, Mahlokozera T, Yang AB, Lin T-H, Leuthardt EC, Yano H, Song S-K, Klein RS, Schmidt R, Kim AH, Therapeutic enhancement of blood-brain and blood-tumor barrier permeability by laser interstitial thermal therapy. Neuro-Oncology Advances. vdaa071.
46. Leuthardt EC, Duan C, Kim MJ, Campian JL, Kim AH, Miller-Thomas MM, Shimony JS, Tran DD, Abdollahi A. Hyperthermic laser ablation of recurrent glioblastoma leads to temporary disruption of the peritumoral blood brain barrier. PLOS ONE. 2016;11(2):e0148613.
47. Schatz SW, Bown SG, Wyman DR, Groves JT, Wilson BC. Low power interstitial Nd:Yag laser photocoagulation in normal rabbit brain. Laser Med Sci. 1992;7:433–9.
48. Muller G, Roggan A, editors. Laser-induced interstitial thermotherapy. Bellingham: SPIE Optical Engineering Press; 1995.
49. Winter L, Oberacker E, Paul K, Ji Y, Oezerdem C, Ghadjar P, et al. Magnetic resonance thermometry: methodology, pitfalls and practical solutions. Int J Hyperth. 2016;32(1):63–75. https://doi.org/10.3109/02656736.2015.1108462.

2 Technical Considerations for LITT: Getting Through the Procedure

Nitesh V. Patel, Simon Hanft, Veronica L. Chiang, David D. Gonda, Joseph S. Neimat, and Shabbar F. Danish

Introduction

Laser-induced thermal therapy (LITT) has become a widely used minimally invasive technique for the treatment of intracranial pathology [1–5]. Lesions previously thought to be inaccessible or untreatable may now be managed using LITT. As its popularity grows and efficacy becomes increasingly well-established, LITT is now considered a first-line approach for a variety of intracranial pathologies [2, 4].

N. V. Patel (✉)
Department of Neurosurgery, Robert Wood Johnson-Barnabas University Hospital, New Brunswick, NJ, USA
e-mail: patel236@njms.rutgers.edu

S. Hanft
Department of Neurological Surgery, Rutgers-Robert Wood Johnson Medical School, New Brunswick, NJ, USA

V. L. Chiang
Department of Neurosurgery, Yale University School of Medicine, New Haven, CT, USA

D. D. Gonda
Department of Neurological Surgery, University of California San Diego, San Diego, CA, USA

J. S. Neimat
Department of Neurological Surgery, University of Louisville, Louisville, KY, USA

S. F. Danish
Department of Neurosurgery, Rutgers University, New Brunswick, NJ, USA

The two commonly used wavelengths for LITT are 980 nm (Medtronic Visualase™; Medtronic, Inc., Minneapolis, MN) and 1064 nm (Monteris NeuroBlate™; Monteris Medical, Inc., Plymouth, MN) [5]. Early experiments in canines and porcine models led to the identification of the wavelengths facilitating optimal ablation [5]. The 1064 nm wavelength is absorbed slightly less in water and blood when compared to 1064 nm resulting in theoretically better lesion to surrounding edema definition at the higher wavelength [5].

Laser therapy delivery is accomplished via long optical fibers, and fiber tip shape can affect how therapy is delivered. Diffusing tips (full-fire) allow for three-dimensional radial delivery while directional firing tips (side-fire) can conform to complex geometry. Each of the two commercially available systems uses a different tip style. The Medtronic Visualase™ system utilizes a radial diffusing tip while the Monteris NeuroBlate™ system has both diffuse and directional firing tip options (Fig. 2.1). Additionally, the Monteris system has multiple size options for laser catheter diameter, which can affect the power of ablation (as measured in watts, W).

Laser systems tend to max out at the 15 W range [3]. Choosing the appropriate power is highly dependent on lesional metrics and operator experience/preference. In order to protect the laser tip from thermal damage, a CO_2 gas or flowing saline system is employed [5, 6]. Laser cath-

V. L. Chiang et al. (eds.), *Laser Interstitial Thermal Therapy in Neurosurgery*,
https://doi.org/10.1007/978-3-030-48047-9_2

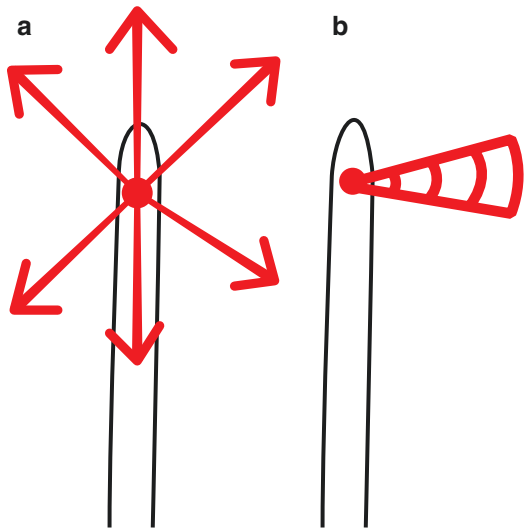

Fig. 2.1 Laser catheter types – (**a**) Demonstrates a radial diffusing laser tip while (**b**) demonstrates a side-fire or directional tip. The Visualase system features only the radial diffusing tip option while the Monteris system offers both

eters are sheathed in a co-axial cooling system allowing the flow of CO_2 or water bi-directionally [5, 6].

This chapter focuses on the existing LITT systems and technical considerations for operators. Although there is some variability in LITT hardware, the procedure can be broken down into three major parts:

1. Choosing Laser Trajectory, Laser Type, and Number of Lasers
2. Laser Fiber Insertion
3. Laser Ablation

Planning

Determining Trajectory and Number of Laser Fibers

Typically, the determination of the trajectory is pre-planned. At the present time, regardless of laser type, there is a diameter limit to which heat can be delivered, and this is dependent on several target tissue variables. Delivery is perpendicular to the laser tip and depth of placement is only limited by regional anatomy. Typically, the target's long axis is the easiest along which to deliver ablation, since the ablation can be delivered at several segments along a single axis. This can result in some novel trajectories that are not usually thought of when considering traditional approaches; innovation in trajectory planning needs only take into account traditional planning rules such as avoiding highly vascular and eloquent areas. An MRI with gadolinium (or CT with contrast) with fiducials prior to trajectory planning can allow avoidance of cortical vasculature when planning trajectories. If this is not possible then trajectory entry over a gyrus (rather than a sulcus) should minimize the risk of intracerebral hemorrhage. Measures in addition to these general principles include:

1. *Target Diameter:* If target diameter in any direction exceeds the heating diameter of the laser fiber then more than one trajectory may need to be chosen. The exact limits of ablation are dependent on several variables, but in general 8–9 cc volumes can usually be ablated with a single trajectory. Targets exceeding these thresholds may require multiple trajectories and pre-planning on navigational workstations. Alternatively, as seen in elliptical targets such as the hippocampus, the laser can be sequentially pulled back to create a column of ablation.
2. *Eloquent Structures:* If there is a critical structure adjacent to the area of ablation, operators should carefully plan and review trajectories, especially if multiple lasers are to be used. There is usually a minimal anterior spread of thermal energy from the laser. It is therefore sometimes advisable to place the laser such that its deepest point abuts the critical structure. Lateral heating from the laser is less controllable and placing critical structures in this position could either result in inadequate treatment of intended targets, since heating may need to be prematurely stopped to avoid heating of critical structures, or excessive heating of critical structures can occur in order to complete target treatment.

3. *Obtaining Tissue Diagnosis:* A biopsy may be required to obtain tissue prior to the LITT procedure. Biopsy can be completed prior to the placement of the LITT anchor bolt using the same trajectory as planned for the LITT procedure. Because of the offset required for the laser bolts, care must be taken in understanding the trajectory length to the biopsy target, and ensuring that the biopsy needle is long enough to reach. Additionally, the user must be aware that multiple core biopsies will introduce air and blood into the track, and this may negatively affect the ability to see thermal information during the LITT procedure.
4. *Heat Sink:* Fluid spaces, including larger blood vessels, can act as heat sinks, where heat from the laser tip diffuses less predictably (Fig. 2.2). Placement of the fiber trajectory down the center of the target typically allows for even heating around the laser fiber. If there are specific structures that could divert heat, such as ventricles or large vascular structures, then the trajectory may be better placed closer to these structures to ensure adequate heating of the tissues between the laser and the heat sink.

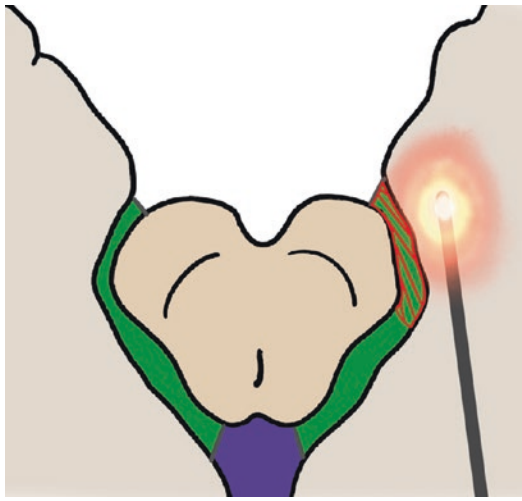

Fig. 2.2 Heat sink effect for laser ablation – Shown is a laser catheter targeting the medial temporal lobe. The ambient cistern (green) and quadrigeminal cistern (purple) are shown. The ambient cistern can function as a heat sink and therefore shield the midbrain from the laser's heat

Deciding on the Type of Laser Fiber to Use

Each of the available laser fibers can only be used with their respective LITT system. The Visualase system utilizes a single catheter size measuring 1.65 mm diameter. The catheters' size provides a robust but smaller pathway like a biopsy needle trajectory. The catheter houses the surgeon's choice of two laser diffusing fiber (LDF) lengths; 3 mm or 10 mm. Choosing which LDF is typically based on the desired ablation volume and geometry as well as surgeon experience.

1. *3 mm LDF:* Neurosurgeons will often utilize the 3 mm when a small ablation is required, the geometry of the target tissue is spherical, and lower wattage can be of benefit when monitoring the laser emission. The 3 mm LDF is therefore typically used for brainstem tumors, hypothalamic hamartomas, pallidotomies, and thalamotomies.
2. *10 mm LDF:* With a longer diffusing tip, the Visualase 10 mm LDF can deliver up to a 15-watt laser energy output. Therefore, the fiber can provide larger ablations resulting in 4–8 cc volumes needed for the ablation of various larger targets.

The NeuroBlate system has two types of laser fibers – the full-fire and side-fire – and two different available diameters −2.2 mm (full-fire only) or 3.3 mm (full and side-fire available). Choosing which laser fiber to use is dependent on surgeon choice and is again based on experience. A few guiding principles exist:

1. *Smaller Diameter:* Neurosurgeons typically feel more comfortable passing a thinner probe further into the brain. Therefore, the treatment of temporal lobe targets from an occipital approach, callosotomy trajectories, and the same deeper targets as for the 3 mm LDF catheter above is typically performed using the 2.2 mm fiber.
2. *Larger Diameter:* The NeuroBlate 3.3 mm full-fire laser allows for the delivery of more power and therefore can achieve a larger abla-

tion size. The 3.3 mm full-fire fiber has the potential to achieve the largest ablation diameter, sometimes exceeding 4 cm in diameter (30 cc in volume). Therefore, for targets that are 3–4 cm diameter, with few restrictions for heating, the 3.3 mm full-fire catheter allows for the most effective heat delivery.

3. *Laser Emission Type:* The side fire laser, while not necessarily resulting in unidirectional heating at smaller diameters, can result in more asymmetric heating at larger diameters. In irregular lesions, typically tumors, or in the case of a heat sink, such as a ventricle or a large cerebral artery, the side fire laser can encourage heat to move in a specific direction to overcome the heat sink.

Laser Insertion

Techniques

Placement of LITT catheters is performed stereotactically using a variety of commercially available platforms (Table 2.1). Frame-based, trajectory-guided platforms, and frameless approaches and/or a combination of these have all been successfully used for laser placement [6]. The key point here is to recognize that the choice of system requires two core components: (1) a fiducial system and (2) a targeting device. Stereotactic frames have both of these components while trajectory-guided platforms and frameless approaches separate these components. System choice is usually dependent upon institution availability and surgeon preference. The majority of LITT procedures today are performed using a trajectory-guided platform or frameless approach given the familiarity and availability of these systems [6–8]. Most centers use head fixation for laser insertion to ensure accurate laser trajectory. Head fixation for trajectory-guided platforms could include any standard head fixation system, including the Mayfield head holder, if the patient is being transported to a diagnostic magnet for laser ablation. However, if an intraoperative MRI is being used then MR-compatible head fixation systems can be used throughout the laser insertion and ablation steps. Some centers use the Atama™ (Monteris Medical, Inc., Plymouth, MN) board. This is a transfer board with an attached split-ring head fixation allowing the patient to remain in the same position as they are transported to the MRI unit from the operating room.

Table 2.1 Laser insertion techniques

Frame-based	Frameless[a]
Traditional stereotactic frames 1. Leksell frame 2. Cosman-Roberts-Wells (CRW) frame *Trajectory-guided mini-frames* 1. ClearPoint® System 2. STarFix™ Platform	1. BrainLab Varioguide™ 2. Medtronic StealthStation® with bone fiducials 3. Robot-guided stereotaxy

[a]Note that multiple iterations are possible with all of these systems and other options are available – these are the most commonly used and discussed in this chapter

Frame-Based LITT

Stereotactic Frames

Use of stereotactic frames for LITT usually involves one of the commercially available stereotactic frames (Fig. 2.3) such as the Leksell (Elekta Inc., Norcross, Georgia) or Cosman-Roberts-Wells (CRW Frame; Integra, Inc., Plainsboro, New Jersey) [9, 10]. Both have been employed successfully for laser catheter placement [10, 11]. Historically frames have been associated with a high degree of accuracy when reaching deep targets. The surgical steps are essentially the same as those for a stereotactic biopsy or the anchoring of a stereoelectroencephalography electrode bolt. For the LITT procedure specifically, a series of guiding cannulas will be necessary. Placement of the frame typically occurs in the operating room and is followed by a volumetric MRI or CT (subsequently merged with a preoperative MRI). The target is identified, and coordinates are defined. The coordinates can then be dialed into the stereotactic frame and the entry point can be identified on the patient's scalp. Of note, however, unlike

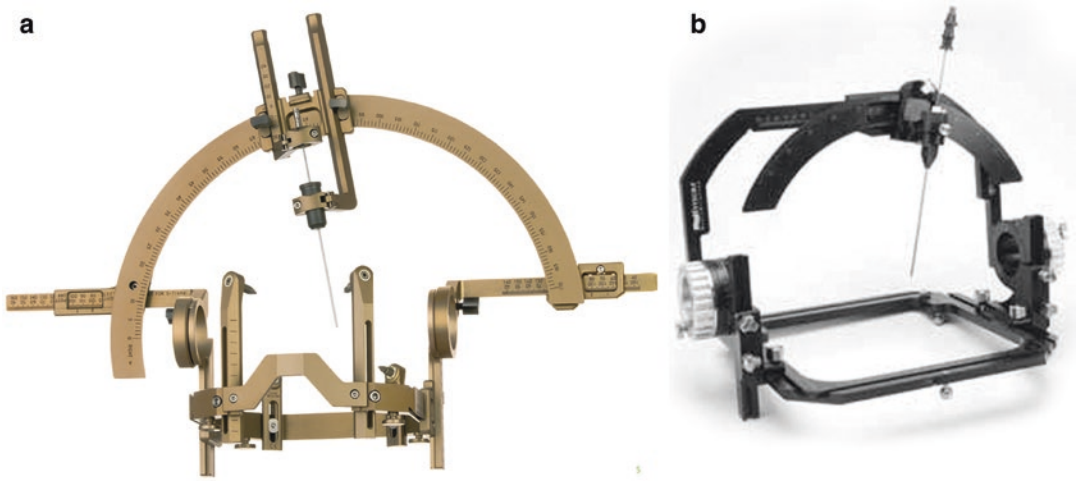

Fig. 2.3 Stereotactic frames – (**a**) Demonstrates the Leksell Stereotactic frame while (**b**) demonstrates the Cosman-Roberts-Wells (CRW) frame. Both achieve similar goals for laser ablation and are routinely used in functional neurosurgery for targeting

a stereotactic biopsy or deep brain stimulation procedure, for LITT trajectories, the scalp entry point is also predetermined and planning for this requires extending the trajectory beyond the scalp to ensure there is space for the laser bolt. Use of the CRW frame will require calculation of an offset to accommodate the bone anchor in longer trajectories. One solution to ensure adequate space for the anchor using CRW is to move the target back along the target trajectory during stereotactic planning, effectively moving the frame back. Planning two trajectories is the most commonly used method; the first trajectory is the intended planned trajectory to the target while the second trajectory is the same as the first but with the target shifted proximally along the trajectory creating an offset to create space above the scalp. The plan versus offset trajectories are checked for accuracy using the CRW Phantom Base. Of note, a second offset trajectory is used to accommodate the anchor and it is important to add the distance back into the final catheter measurement. Leksell planning does not require an offset.

Each frame utilizes reducing tubes and bushings (CRW) or stops and guides (Leksell) to drill the skull, open the dura, affix a bolt to the skull, and guide the laser along trajectory to the target. Size of tubes and guides are based on the hole required for the bone anchor and the alignment device needed to align such bone anchor as well as the laser's intended pathway to the target.

CRW Frame

Using the CRW frame for Visualase catheter placement requires a 190 mm 3.2 mm sharp drill bit, a 3.2 mm guide tube, as well as a 2.7 mm guide tube with a 1.9 mm reducing tube inserted. Once the bolt is secured, a measurement is taken by inserting the ruler provided in CRW tray through the carrier until it meets the top of the bone anchor. The measurement from the top of the carrier to the anchor is then subtracted from 160 mm, which is the distance to the target in the CRW system. This calculation becomes the length to the target for the laser catheter. As noted above, if an offset was included during planning the measurement should be added as well. Trajectory planning with a CRW frame requires creating a 50 mm offset from the scalp to ensure space for the laser bolt with the Visualase system.

When using the NeuroBlate system, this offset is not required. The user will need a 4.5 mm drill bit to create the burr hole. The T-handle fits end to end with the NeuroBlate bolt through the reducing tube such that an offset is not required.

The CRW Arc is removed before the catheter is placed to the target.

Leksell Frame

Use of the Leksell frame also requires stops, guides, and reducing tubes. Visualase insertion requires the 4.0 mm guide and stop, 3.2 mm reducing tube, and 190 mm 3.2 mm drill bit. Once the 3.2 mm opening is drilled in the skull, a 2.1 mm guide and stop will align the bone anchor and guide the catheter into place. The guide and stop's clamshell design allow for catheter insertion through the frame which will break away around the catheter at the procedure's end. As a result, there is no need to calculate an offset into the trajectory length.

The Leksell Arc's scale will provide the measurement needed to mark the catheter's length to the target. If the Arc's carrier was adjusted to zero, it will measure 190 mm. If the carrier was advanced or backed away from zero, the difference should be included in the measurement.

Trajectory-Guided Mini-Frames

Separation of the fiducial system from the targeting device facilitates the smaller footprint for trajectory-guided mini-frames (Fig. 2.4). These devices come in various versions and are often skull-mounted MRI compatible systems that may be used to perform LITT entirely in the MRI suite [6, 8]. The STarFix™ microTargeting Platform (FHS, Bowdoin, Maine) is used in deep brain stimulation procedures and was the basis for the MRI-compatible version used for LITT [*J. Neimat – Unpublished Communication*]. Small modifications were made to adapt the platform for the appropriate drill guides bolt reducers. The NexFrame™ (Medtronic, Louisville, Colorado) uses real-time tracking feedback for adjustments and was the basis for the most commonly used trajectory-guided platform: the ClearPoint system (MRI Interventions, Inc., Irvine, California) [6, 12].

The ClearPoint software allows for preoperative planning; however, other commercial stereotactic systems including both BrainLab and StealthStation systems may be used. Plans can then be transferred into the ClearPoint workstation. The ClearPoint system allows for the entire procedure to be performed within the MRI unit. After the patient is anesthetized and intubated, the patient can be fixed in pins in the MRI unit. The patient is then prepped and draped, and the fiducial grid is fixed to the scalp in the region of the intended entry. The patient may be positioned prone, semi-lateral, or supine, although the goal is to place the target as close as possible to the MRI center – this minimizes distortion. The initial target is then selected on the ClearPoint workstation and using the fiducial

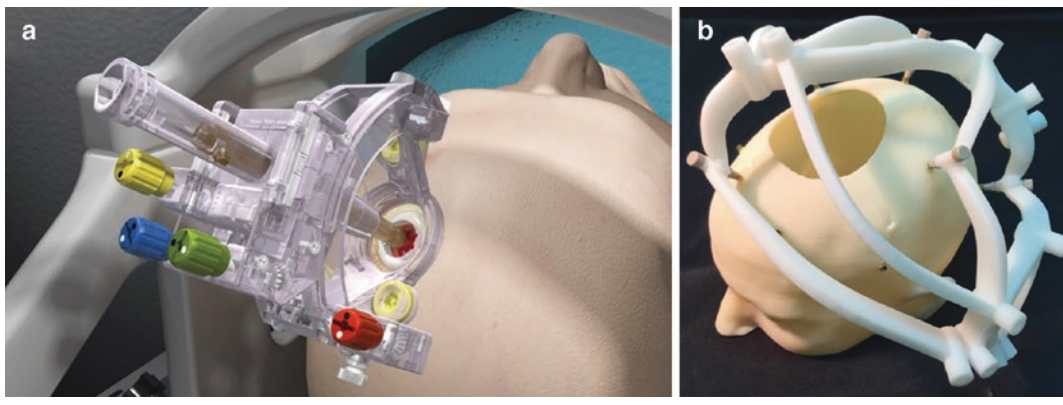

Fig. 2.4 Trajectory-guided mini-frames – (**a**) The ClearPoint® tower is shown as it appears when anchored to the patient's head. (**b**) An example of a custom, multi-trajectory STarFix™ frame is shown. These frames are custom designed based on the patient's anatomy and intended target(s)

grid, a safe trajectory is planned. The fiducial grid allows entry point marking directly onto the patient's scalp. The ClearPoint ScalpMount™ (MRI Interventions, Inc.) frame base is then percutaneously mounted with 3–6 lag screws and 4 circumferential offset skull pins. This configuration allows for a stable position of the base.

The adjustable TwistPoint XG™ frame tower (MRI Interventions, Inc.) is then locked into the ScalpMount and localizer MRI scans are obtained. The ClearPoint software can then be used to make calculated fine adjustments to the tower and mount to refine the trajectory. Adjustments are usually made until the level of accuracy reaches <0.5 mm radial error. Once error is minimized, the mount and tower are locked with thumbscrews and local anesthetic is applied to the entry site on the scalp. A small stab incision is followed by the system's MRI-compatible 3.2 or 4.5 mm bitted hand drill to create a burr hole craniectomy. Durotomy is most easily performed using the drill and a ceramic rod can be inserted to verify target accuracy along the trajectory. The rod is then replaced with the laser fiber assembly and confirmatory images are once again obtained prior to laser ablation.

For operators who utilize the STarFix system the procedure is divided into a preoperative fiducial placement (which can be done in the OR or Clinic under regional or general anesthesia) and the LITT procedure itself. The fiducial placement involves the insertion of 4 or more bone screws into the skull and closure of small incisions. The placement is typically stereotyped although there is a broad flexibility of these techniques to allow for all possible trajectories. Fiducial insertion is typically performed 5–7 days before the ablation procedure. After fiducial placement, a volumetric CT is obtained on which the fiducials and their orientation can be identified. This is referenced to a preoperative MRI on which the intended treatment trajectory can be planned. Based on this plan, a 3-D printed custom platform is created and sent to the facility before the day of the intended surgery. On the day of the LITT procedure, the platform is simply attached to the bone fiducials sterilely to achieve the planned stereotactic trajectory. Drilling the pilot hole and driving the bolt are performed easily through the frame with STarFix guides, and, because all stereotactic registration and planning have been previously performed the procedure on the day of surgery is typically expeditious and relatively hassle-free. A high degree of Stereotactic accuracy with the STarFix system has been well demonstrated making this a useful choice for hippocampal trajectories that demand high precisions [13].

Frameless LITT

A complete separation of the fiducial and targeting device is characteristic of frameless systems [6]. Theoretically, frameless systems allow for greater flexibility, reduced physical bulk, and eliminate the risk of frame displacement. At the same time, the operator is dependent on the integrity of reference fiducials in relation to the patient's head. A variety of reference fiducial techniques exist: pattern tracing, anatomic landmarks, contrast-enhanced stick-on fiducials, and implantable skull fiducials (skull pins). There is also a range of common stereotactic software systems that have been employed with all of these fiducial techniques. Both Medtronic StealthStation (Medtronic, Inc.) and Brainlab (Brainlab AG, Feldkirchen, Germany) have been commonly used for LITT. Both options can be used with either of the currently available LITT systems. Targeting robots have also become a rapidly expanding part of the neurosurgical armamentarium. As they have been used to stereotactically place depth electrodes, they have also been applied to LITT.

Regardless of which frameless approach is used, all patients undergo preoperative contrast-enhanced MRI including a high-resolution stereotactic scan. A high-resolution T2 or fluid-attenuated inversion recovery (FLAIR) sequence may also be obtained in cases where lesions have non-enhancing components. Obtaining these

studies under general anesthesia is an option as it reduces movement error and provides more optimal imaging; however, it is not mandatory. Patients are intubated for the surgical procedure and fixed in 3-point fixation – such as a Mayfield head holder.

BrainLab

The Brainlab approach is used in conjunction with the VarioGuide™ system and VectorVision Cranial™ (Brainlab AG) software package (Fig. 2.5). A high-resolution computed tomog-

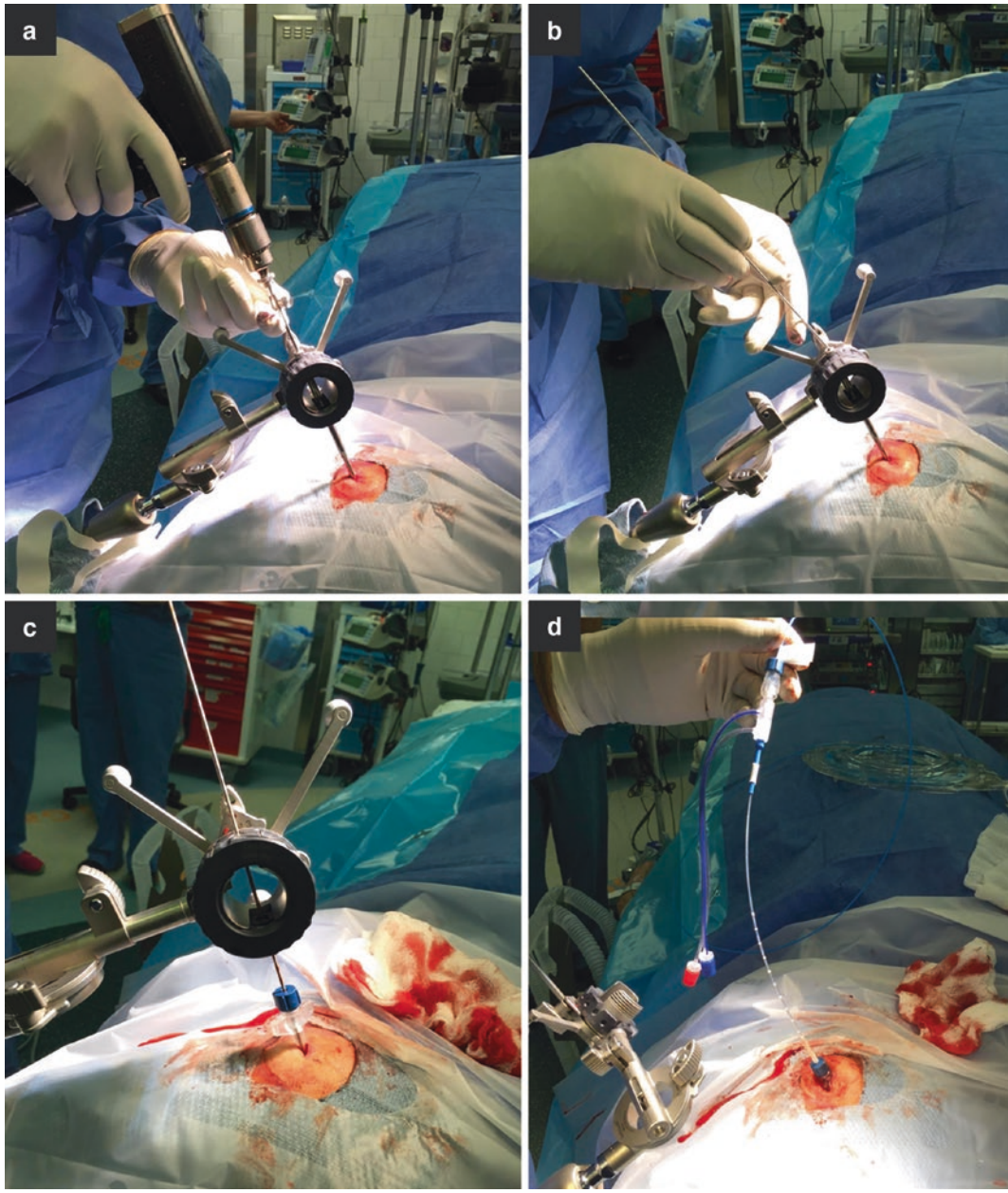

Fig. 2.5 BrainLab™ VarioGuide system – (**a**) With the VarioGuide arm locked in placed (after stereotactic guidance), a small incision is made at the entry site and the automated drill is inserted through the guiding cannula. (**b**) A rigid stylet is then passed to check the completeness of the burr hole and (**c**) the bone anchor is screwed into the created hole. After the dura is perforated, the guiding arm is used to insert the laser catheter through the cannula and the laser is secured into the anchor (**d**). (From Patel et al. [6]. Reprinted with permission from Oxford University Press)

raphy (CT) scan of the head is optimal for the Z-touch and Softouch-based registration. This CT can be merged with a high-resolution MRI. The iPlan software allows for the creation of multiple candidate trajectories which can then be reviewed using a "probe's eye" feature. Patient registration is performed using a non-sterile reference array and arm. Antibiotics and steroids (usually 10 mg IV dexamethasone) are administered. The non-sterile reference array is removed; the patient is prepped and draped in the usual fashion. A sterile reference array is attached to the arm used previously, and accuracy is confirmed relative to the patient's anatomy. It is important to note that, much like in frame-based approaches for LITT, an offset of 40–50 mm is important to accommodate the laser bolt. The VarioGuide arm is connected to the operating table. BrainLab's wizard-guided trajectory software leads the positioning of the three arm joints to align with the intended trajectory. After target alignment is achieved, the black ring assembly acts as a reducing sleeve accommodating 1.8–8.0 mm diameters. Reducing tubes can be placed in the black ring fitting the drill bit required for the procedure. The drill bit diameter must equal that of the LITT bone anchor. Because frameless navigation does not provide the rigidity of a traditional stereotactic frame, it is critical the entire length of the drill maintains the anticipated trajectory. Once the hole is drilled, durotomy is performed. The black ring is then used to align and affix the bone anchor to the skull. Using Brainlab navigation, the distance is taken from the black ring to the target. The calculated distance to the target determines the distance the laser catheter is inserted. Laser insertion can then be performed, and if desired post-insertion confirmation obtained with intra-operative imaging or transfer to an imaging unit.

Medtronic

The Medtronic StealthStation system also allows for frameless LITT catheter insertion (Fig. 2.6). There are two approaches for StealthStation frameless registration. The first uses the StealthStation Tracer® or O-arm™ imaging system to register anatomy. This registration method is similar to a biopsy workflow. Tracer or O-Arm registrations are convenient methods when a target is easily accessible. The more common frameless approach for LITT is to use bone fiducials or screws with a point merge registration method. Utilizing bone fiducials has shown to provide an increased level of accuracy when using a frameless system. This can benefit when submillimetric accuracy is required to deliver a laser catheter along several targeted points of the desired ablation volume as well as small or deep lesions. With this method, the patient's anatomy is marked by circumferentially placing small screws around the calvarium [14]. Patients are brought into the operating room and conscious sedation is given. This is followed by injection of local anesthetic (lidocaine 1–2% with epinephrine) at six sites around the skull – usually two frontal, two parietal, and two occipital. Sequentially, small stab incisions are made at this sites, and screws are implanted. They are often referred to as skull pins or bone fiducials measuring 1.5 mm and 7–20 mm (Medtronic, Inc., Minneapolis, MN & Depuy-Synthes Inc., West Chester, Pennsylvania). However, operators may use any type of screw whose head can be imaged. Once screws are implanted, a high-resolution CT is obtained. If intraoperative CT is available, the head clamp may need to be appropriately incorporated into the operating room bed adapter. The CT is merged with the preoperative MRI. The patient is then placed under general anesthesia and placed in 3-pin head fixation. Registration is then carried out using the implanted screws as the fiducials and attachment of the Stealthstation star to a Vertek™ Arm (Medtronic, Inc.) secured to the Mayfield head holder via a triple star adapter. Once registration is complete, the navigation probe is used to approximate the entry point on the scalp. Registration error should be kept to approximately 0.5 mm. A second Vertek Arm is then sterilely placed onto the dual star adapter and the Precision Aiming Device (PAD) is attached to the Vertek Arm. Medtronic cranial reducing tubes (CRT) are inserted into the PAD when needed in the procedure to accommodate the instrument being used. The first CRT will

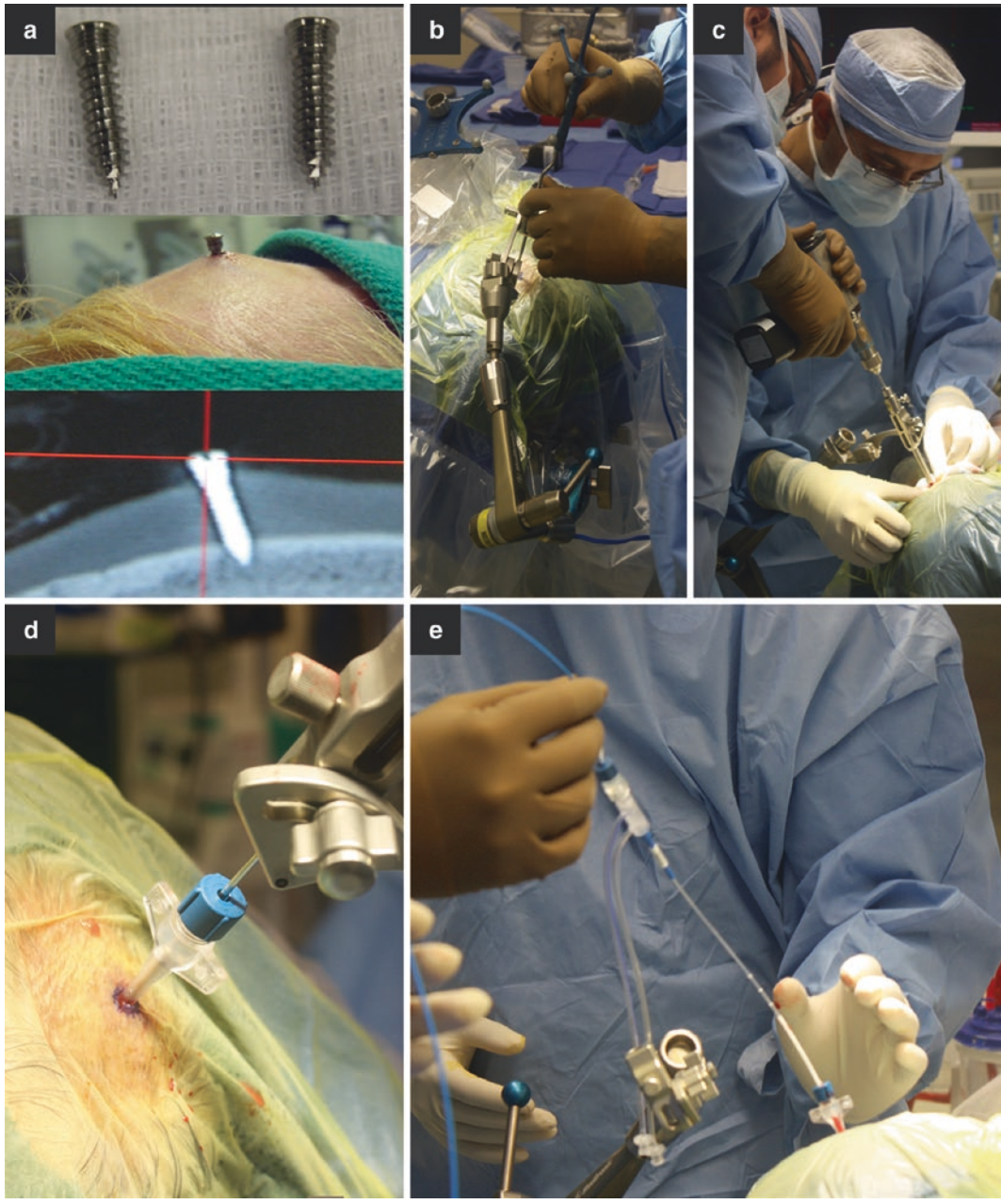

Fig. 2.6 Medtronic StealthStation® with bone fiducials – General Steps for Laser Catheter Placement: (**a**) The pins (screws) shown are placed circumferentially in the skull, typically totaling to about 6 pins. The pin heads are used as registration points. (**b**) The Precision Aiming Device (PAD) is aligned with the planned trajectory using the stereotactic handheld probe and the PAD is then locked. (**c**) An automated drill is used to drill a burr hole and a reducing cannula followed by a rigid stylet is passed to ensure completeness of the burr hole. Next the bone anchor is placed and the dura is perforated (**d**). The laser catheter is then passed to the planned depth (**e**). (From Patel et al. [6]. Reprinted with permission from Oxford University Press)

accommodate the passive planar blunt probe. A sterile passive planar probe is then placed into the PAD and Vertek Arm's articulating points are adjusted to line with the planned trajectory. Care should be taken to ensure that the target alignment error remains under 0.5 mm. Once the Vertek is aligned with the plan trajectory, securing the arm will be crucial in guiding the anchor and catheter's trajectory. The passive planner probe is removed. Local anesthetic is applied at the entry site and a stab incision is made. Insert the 3.2 mm CRT for the Visualase system, or the 4.5 mm CRT for NeuroBlate. Navigation can be used to approximate the skulls thickness and set a drill stop. Once drilling is completed, remove the drill bit and guide from the PAD. The Visualase bone anchor will be placed using the 1.7 mm CRT. The 1.7 mm is inserted into the PAD. The alignment rod is placed through the CRT and used to align the bone anchor. The bone anchor is placed under the PAD near the skull. The alignment rod will be guided through it into the bone anchor stopping just inside the skull. The bone anchor is turned until it is securely purchased to the skull. As the alignment rod is removed, it is critical the bone anchor not shift from the planned trajectory. The NeuroBlate system utilizes a T-handle that is guided through the PAD. The NeuroBlate anchor is secured by turning the instrument. Once bone anchor is secure, the navigation system is used to calculate the measurement to the target. The calculated distance to the target determines the distance the laser catheter is inserted. Laser insertion can then be performed, and if desired post-insertion confirmation obtained with intraoperative imaging or transfer to an imaging unit. Table 2.2 summarizes these steps along with the steps for the BrainLab system.

Table 2.2 Summary of steps for BrainLab and Medtronic techniques

BrainLab	Medtronic[a]
1. Perform frameless navigation using the BrainLab software system using the Z-touch or other BrainLab registration tools 2. Calibrate and "zero" the VarioGuide arm 3. Use this arm to then align the system to the intended trajectory 4. Minimize predicted errors on the workstation 5. sMark the intended entry point	1. Perform frameless stereotactic registration using bone-implanted fiducials and ensure registration error is sub-millimeter, ideally <0.5 mm. 2. Attach the articulating secondary Vertek® arm and precision-aiming device (PAD). 3. Change the view on the workstation to "Guidance View." 4. Maneuver the PAD to line it with the goal trajectory line, achieving a target alignment error (TAE) <1.0, ideally <0.5. 5. Based on this trajectory, mark the scalp at the planned entry point.

[a]This is specific to the Medtronic StealthStation® approach using bone-implant fiducials

Robotic Placement

LITT trajectories are preoperatively planned using the ROSA software system and high-resolution MRI (Fig. 2.7). Planning can be done on the ROSA mobile workstation and imported into the robotic device or it can be performed on the robotic device itself. The ROSA system is designed to optimize the placement of multiple trajectories efficiently. Both the "probe's eye" view and "view along trajectory" are reviewed to confirm no intersection with vascular structures along the trajectory.

The patient's head is then fixed into any of the commercially available headframes. The headframe is then connected to the robotic apparatus. There are several options for registering the patient's head position for the stereotaxy once in a fixed position. One option is to perform laser scanning of the patient's facial surface anatomy. Facial anatomical landmarks are defined on a 3D modeled reconstruction of the patient's face on the planning software. The distance sensor is then attached to the robotic arm and manipulated passively by the operator to point at each of the previously identified landmarks. The robotic arm then captures additional landmarks with the distance sensor through a course of automated scans over the patient's facial anatomy.

For lesions that are smaller in size or require longer trajectories necessitating a higher degree of accuracy, it is preferred to register using in-

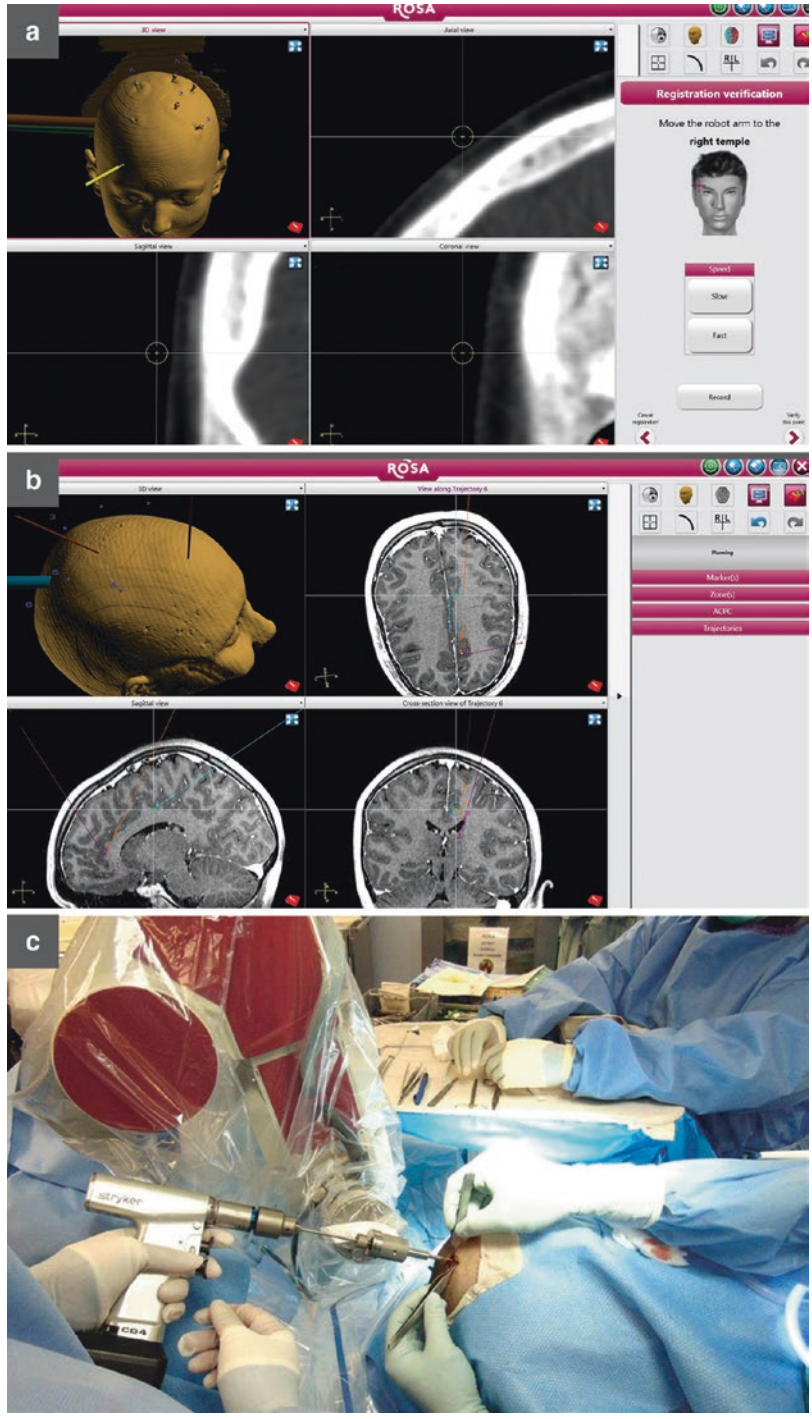

Fig. 2.7 ROSA robotic system for LITT – (**a**, **b**) Demonstrate the registration and planning portions of the ROSA system while (**c**) shows the creation of the entry burr hole with the ROSA robotic arm as a guide

bone fiducials inserted into the skull. These bone fiducials are typically placed after the patient has gone under anesthesia. For each fiducial insertion, a small stab incision is made through the scalp and a bone screw is passed into the outer cortex of the calvarium using a small powered driver. A total of 5 or 6 fiducials are inserted and then a high-resolution CT scan of the head

is obtained. The CT scan is then uploaded and merged with the preoperative imaging plan. Each of the fiducial screws is marked and defined on the 3D modeled reconstruction of the patient's anatomy using the ROSA software. A touch probe is applied to the robotic arm. The robotic arm is passively manipulated by the operator to make contact with each of the fiducial markers for registration. Following the insertion of the fiber-optic laser catheters, the fiducials are removed from the skull with each site being closed with a simple 4-0 monocryl stich prior to the patient being transferred to the MRI.

The third option for positional registration with accuracy comparable to using in-bone fiducials is to use a Leksell headframe for cranial stabilization. The headframe is applied before or after the patient is placed under anesthesia and a CT scan of the head is obtained for fusion to the preoperative plan. The headframe is then attached to the robotic apparatus and the touch probe is used to identify the labeled markers of the Leksell headframe.

Once registration is complete, the patient is prepped and draped in the usual sterile fashion. The operator selects their desired trajectory on the ROSA user interface screen and the robotic arm will then drive itself into the correct position. The operator must exercise caution during the automated arm movements to ensure that the arm does not collide with the headframe in route to the trajectory. Once in position, an appropriately sized steel bushing is placed within the instrument holder attached to the robotic arm. The steel bushing serves as a drill guide for creating the burr hole of entry. The robotic arm is then switched into a passive axial movement mode that allows the operator to position the instrument holder nearer or further from the head while maintaining the desired trajectory. The entry site of the scalp is injected with a local anesthetic. A stab incision using a No. 15 blade is made into the scalp. The drill bit is then passed through the steel bushing guided by the ROSA arm along the desired trajectory and a burr hole is made through the skull. The steel bushing is then swapped out with a 1.8 mm diameter PEEK bushing to guide the insertion of the alignment rod. A k-wire is first inserted through the bushing to make a perforation through the dura. The ROSA software calculates the distance to the target based on the position of the robotic arm. An alignment rod is then inserted through the 1.8 mm PEEK bushing to the depth of the target and the LITT bolt-anchor is twisted into the skull around the alignment rod until secure. The alignment rod is then removed, and the robotic arm is repositioned away from the patient's head so that the fiberoptic catheter can be inserted into the bolt-anchor to the target distance.

For multiple trajectories, the process can easily be repeated for any additional LITT fiberoptic catheters being inserted. The next trajectory is chosen on the ROSA user interface and the robotic arm drives into the desired position for placement.

Laser Catheter Placement

The Visualase laser catheter is marked (typically using a steri-strip) for trajectory length, with an accommodation for the length of the bolt-anchor. The laser catheter is then passed through the bolt-anchor until the depth marked by the steri-strip is reached. Once the catheter is placed to the target, the laser diffusing fiber (LDF) is inserted into the catheter. The lure lock of the LDF is tightened on the catheter and the bolt compression cap tightened to secure the catheter that now houses the LDF. A designated team member is then set to monitor the laser catheter and the remainder of the team works to remove drapes and arrange for transfer to the MRI suite (if intra-operative MRI is unavailable). The catheter is somewhat flexible, and at some distance is usually taped to the chest to act as a strain-relief.

For NeuroBlate laser insertion, the laser can be held at the skull using a titanium bolt or it can be held in place with the Clearpoint tower or the STarFix system. The major difference here for a workflow that does not use Clearpoint is that the bolt is placed in the operating room, but the actual laser is placed in the MRI suite. The bolt allows the attachment of the robotic driver that then allows the surgeon to remotely drive

the laser deeper or shallower very precisely in single millimeter changes. This is different from the Visualase system, where the user must enter the MRI and manually change the position of the laser in-between ablations. Placement of the bolt along the laser trajectory is therefore key. For trajectories that enter the skull perpendicularly, the drill bit appropriate for the laser diameter required can be used directly to drill through the skull. However, for trajectories that enter the skull tangentially it is key to ensure that the drill bit does not slide along the skull prior to entry into the bone. For this reason, if the 3.3 mm diameter laser is needed, then a 2.2 mm non-skiving drill bit is used to create a pilot hole first before using the 4.5 mm drill bit. The bolt is then solidly screwed into place. Laser fiber length to be introduced is pre-measured and then the laser is introduced through the robotic driver and bolt to its target. Once the laser fiber is secured in place then the patient can be brought into the MRI unit.

Laser Ablation

Patient Positioning

In the setting of intraoperative MRI where the placement of laser fiber and ablation will all occur in the same position, it is important to ensure that the patient and all the laser equipment will fit comfortably into the bore of the magnet. The laser target should be as close as possible to the isocenter so the imaging is optimal at that point. When possible, the trajectory of the laser needs to emerge from the head parallel to the length of the bore. Since this is not always possible, to maximize space for the laser, patients may be pinned in a head holder that does not drop down too low relative to the bed and the long axis of the head holder should ideally be in line with the bed itself. This means that to pin the patient, the head itself should be positioned relative to the head holder rather than the other way around. The most difficult targets to access in the magnet therefore are those that are suboccipital. For these targets, the patient may need to be in a lateral position or prone on gel rolls – which take up space in the magnet – and the head may need to be flexed to try to aim the laser fiber out the bore. A ring of the size of the magnet bore can be used to test to see if a patient, when fully padded and wrapped for surgery, can fit in the magnet.

Quality of Thermometry Imaging

Many factors that are outside the depth of this chapter can affect the quality of thermometry imaging. These can include factors such as:

1. Technical magnet-related factors such as the location of the target relative to the isocenter of the magnet and having the magnet "shimmed" appropriately for thermometry
2. Image acquisition factors such as phase encoding directions of imaging acquisition
3. The presence of radiofrequency artifact within the MR room (for example, having calf pneumatic boots running while imaging)
4. Having blood products, calcium, melanin, or air within the target lesion
5. Anatomical concerns such as difficulty imaging adjacent to the bone – both calvarial and base of the skull

An example of thermometry imaging is shown in Fig. 2.8. If the signal is suboptimal with the extensive artifact, then it is important to work with the physicist or MR technologist to improve signal prior to ablation.

Ablation

Once the patient is arranged in the MRI, the ablation probe and cooling lines are connected to the workstation (either Medtronic Visualase or Monteris NeuroBlate) and initial images are obtained. The MRI technician begins to scan with a localization or survey image. A 3D volume of the patient's head is imaged. At this point the surgeon needs to determine that the laser is in the intended position and that an insertional hemorrhage has not occurred. Using the 3D volume, monitoring planes are obtained based on the

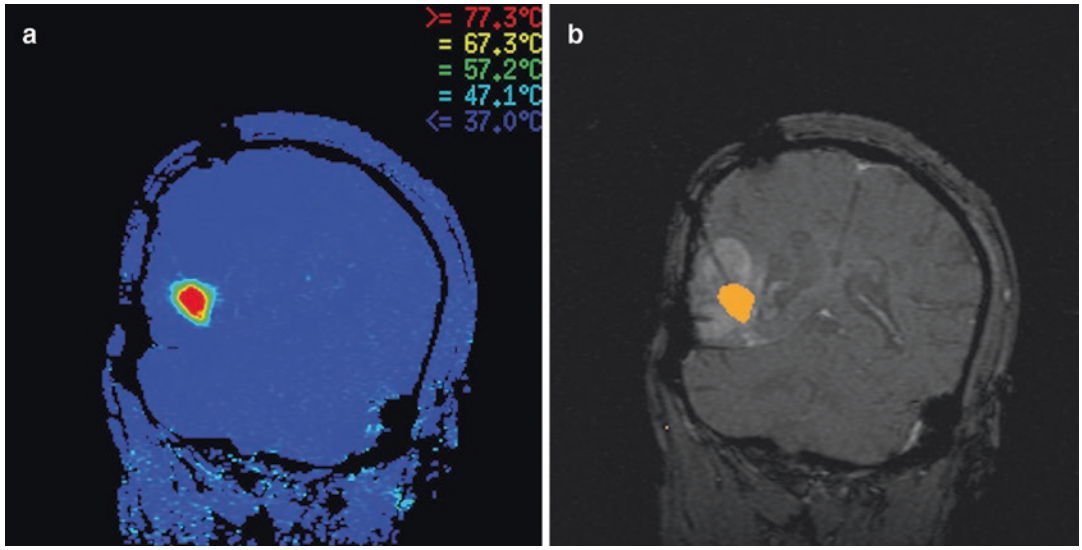

Fig. 2.8 Thermal monitoring features of Visualase – (**a**) Shows the temperature map that is seen during ablation for the Visualase system. (**b**) Shows the thermal damage estimate (TDE) that is calculated based on the Arrhenius model incorporating pixel-based magnetic resonance change during ablation. The Monteris system also has similar capabilities as previously described in Chapter 1

target and critical surrounding structures. A high-quality T1 and/or T2 image is then obtained and transferred to the LITT workstation to serve as the reference images. Monitoring planes are then determined for the gradient echo scan (GRE) needed for thermal imaging.

For the Visualase system, the high-quality images chosen earlier are interpreted on the system. The catheter can be imaged in-line, as probes eye, and/or as an anatomical view. It is important to note that the image refresh rate will slow a few seconds with every additional image and therefore unidimensional thermal monitoring allows for more frequent imaging during laser on time at the expense of multidimensional detail. The high-quality T1-weighted image is overlaid onto the near-real-time thermal and tissue death calculations. Reference thermal images are acquired at baseline brain temperature and temperature targets are then set on these images (Fig. 2.9). High-temperature targets are usually set in the vicinity of the catheter tip (90 °C) while low-temperature limits are set near the boundaries of the lesion (43–50 °C). The ablation procedure can then proceed dependent on the operator's preferences. Monitoring is performed via the LITT workstation and sequential MRI images. Thermal heating change is interpreted on the workstation as color change of red, yellow, green, light blue, and dark blue as heat spreads through the tis-

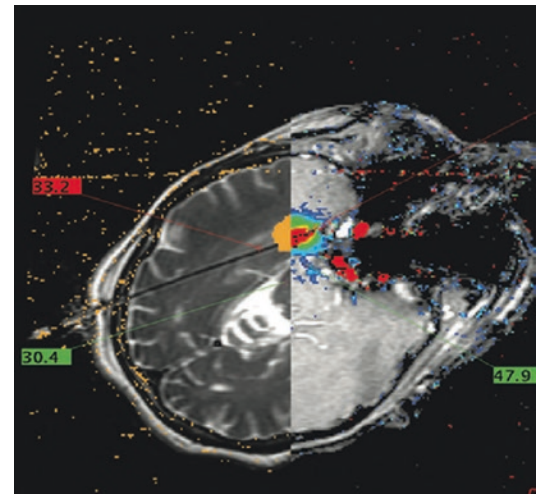

Fig. 2.9 Temperature safety points – Shown in green and red are safety checkpoints that can be customized and placed by the operator at key points in the target's vicinity. These checkpoints can give temperature information and also function as automatic shut-off points that can stop ablation once a certain temperature threshold is crossed.

sue. Real-time thermal damage is calculated by the system based on the MRI pixel shift of the target tissue in response to thermal damage. As tissue denaturation/damage is achieved, each image voxel is colored orange. The orange damage calculation will increase in size as the volume of cell death is achieved. The high-quality image and temperature limits as well as real-time thermal and damage imaging are all viewed on a transition window. Laser power level can be controlled up to 15 Watts. Ablation imaging begins, and a phase reference is set to define baseline temperature before the laser power is increased. To start, the surgeon delivers an initial test dose at 20–30% of maximum power followed by therapeutic doses at 60–100% maximum power. Choosing the appropriate power is highly dependent on lesional metrics and operator experience/preference [15]. In neurologically critical areas, the wattage can be deceased to enable control whereas in larger lesions, wattage should be increased to maximize treatment efficiency.

For the NeuroBlate system, if target outlining is required, the baseline T1 and T2 images may need to be acquired in the plane of contouring even though the images can be reconstructed in three planes for visualization. In addition, any structure to be avoided can then be imported at this point from the stereotactic planning workstation and overlaid over the MR images as part of ablation planning.

Prior to the initiation of heating, the cooling system and laser are separately tested to ensure adequate functioning. Prior to the initiation of laser use, MR thermometry images are acquired, and baseline intracerebral temperature is obtained. System cooling is then initiated and MR thermometry is able to detect the region of temperature change in tissue to ensure that laser placement is accurate. Once temperature is again stabilized around the laser then heating can begin. Tissue heating can be seen as graded color change around the laser and point temperatures can also be obtained. With the passage of time, color change will appear on the thermal damage map. For the NeuroBlate system, calculated protein denaturation (yellow) and cell kill (blue and white) lines will then appear superimposed upon the heat map showing damage estimation in real-time. The NeuroBlate system allows visualization of 3 slabs of imaging perpendicular to the laser trajectory as well as 2 planes of reconstruction along the laser fiber. Sometimes not all areas of heating will be visible since visualization of heating is limited to a 15 mm slab but using the 3.3 mm fullfire laser a diameter of 3–4 cm can be reached. Judgment is therefore sometimes required at this stage as to which slices the surgeon wishes to observe when treating larger lesions. When heating at the deep end of the lesion, especially if a critical structure is present here, then it is possible to watch for heating beyond the lesion and therefore to stop heating if heat appears in the structure at risk. It is important to note however that when doing this, heating proximally along the laser may extend beyond the visible slices if heating is of protracted duration. On the NeuroBlate system, this can be seen as a plateauing of the yellow and blue lines in the most proximal slice of imaging Fig. 2.10.

Post-ablation

Once ablation is complete, a post-ablation gadolinium-enhanced MRI can be obtained. Some centers may consider giving a half-dose of gadolinium for this scan as it reduces the amount of total gadolinium given for perioperative time period. This image typically shows a thin eggshell rim of enhancement surrounding the lesion or intended area of ablation. If the region of ablation is satisfactory then the laser catheter and bolt-anchor can be removed while in the MRI suite or in the OR and a single absorbable suture or staple is used to close the scalp entry site. The patient is then moved to a recovery unit for monitoring. In some institutions, patients may be moved to a step down or general floor bed on the same day with discharge within 24 hrs post-procedure if medically ready. Steroid and anticonvulsant use varies across centers and by disease process but typically reflect post-craniotomy practices. Differing post-procedure imaging is obtained varying from 24 h to 2 weeks after LITT dependent on the pathology treated and surgeon's pro-

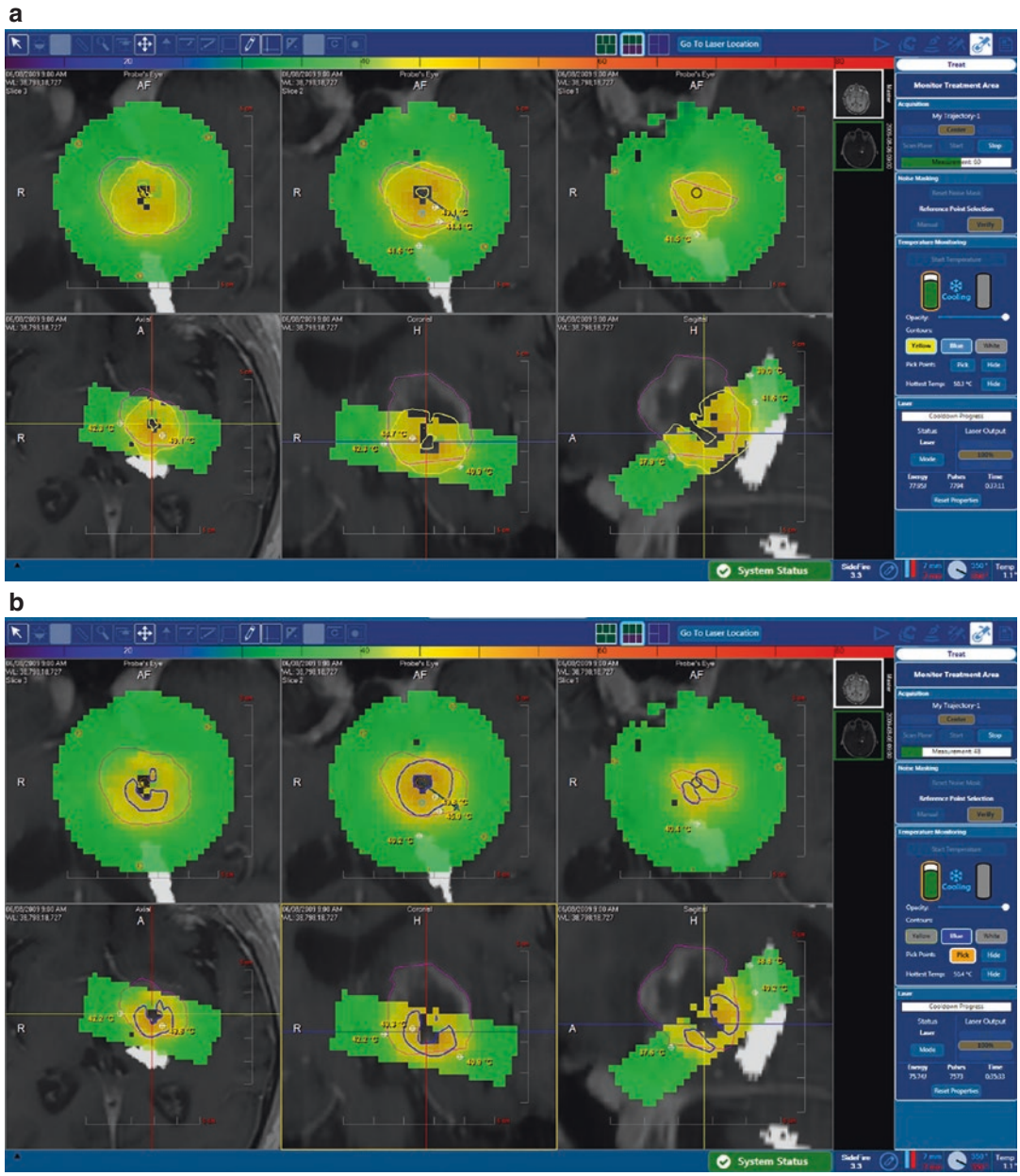

Fig. 2.10 Thermal monitoring features of Monteris system - Shows the temperature map and superimposed thermal damage estimate (Tdt line) calculated during ablation – (**a**) Shows the yellow Tdt line which correlates histologically to zone of protein denaturation (**b**) Shows the blue Tdt line which correlates histologically with zone of cell death. Pink lines are outline of the lesion. Solid white structure in both (**a**) and (**b**) are the corticospinal tracts mapped from the navigation system into the thermal map to enable safe avoidance of critical structures

tocols. Discharge medications may include a steroid taper and the next follow-up MRI may be performed within 30–90 days.

Disclosures Dr. Danish has received honoraria from Medtronic. Dr. Chiang has received honoraria from Monteris Medical Inc.

References

1. Ashraf O, Patel NV, Hanft S, Danish SF. Laser-induced thermal therapy in neuro-oncology: a review. World Neurosurg. 2018;112:166–77.
2. Hale AT, Sen S, Haider AS, et al. Open resection vs laser interstitial thermal therapy for the treatment of pediatric insular epilepsy. Neurosurgery. 2019;85(4):E730–6.
3. Jethwa PR, Barrese JC, Gowda A, Shetty A, Danish SF. Magnetic resonance thermometry-guided laser-induced thermal therapy for intracranial neoplasms: initial experience. Neurosurgery. 2012;71(1 Suppl Operative):133–44; 144–135.
4. Mohammadi AM, Sharma M, Beaumont TL, et al. Upfront magnetic resonance imaging-guided stereotactic laser-ablation in newly diagnosed glioblastoma: a multicenter review of survival outcomes compared to a matched cohort of biopsy-only patients. Neurosurgery. 2019;85(6):762–72.
5. Stafford RJ, Fuentes D, Elliott AA, Weinberg JS, Ahrar K. Laser-induced thermal therapy for tumor ablation. Crit Rev Biomed Eng. 2010;38(1):79–100.
6. Patel NV, Mian M, Stafford RJ, et al. Laser interstitial thermal therapy technology, physics of magnetic resonance imaging thermometry, and technical considerations for proper catheter placement during magnetic resonance imaging-guided laser interstitial thermal therapy. Neurosurgery. 2016;79(Suppl 1):S8–s16.
7. Brandmeir NJ, McInerney J, Zacharia BE. The use of custom 3D printed stereotactic frames for laser interstitial thermal ablation: technical note. Neurosurg Focus. 2016;41(4):E3.
8. Ho AL, Sussman ES, Pendharkar AV, et al. Improved operative efficiency using a real-time MRI-guided stereotactic platform for laser amygdalohippocampotomy. J Neurosurg. 2018;128(4):1165–72.
9. Awad AJ, Nguyen HS, Arocho-Quinones E, Doan N, Mueller W, Lew SM. Stereotactic laser ablation of amygdala and hippocampus using a Leksell stereotactic frame. Neurosurg Focus. 2018;44(VideoSuppl2):V1.
10. Fayed I, Sacino MF, Gaillard WD, Keating RF, Oluigbo CO. MR-guided laser interstitial thermal therapy for medically refractory lesional epilepsy in pediatric patients: experience and outcomes. Pediatr Neurosurg. 2018;53(5):322–9.
11. Laurent D, Oliveria SF, Shang M, Bova F, Freedman R, Rahman M. Techniques to ensure accurate targeting for delivery of awake laser interstitial thermotherapy. Oper Neurosurg (Hagerstown, MD). 2018;15(4):454–60.
12. Franck JI, Haer FC, Franklin RJ, et al. Instrument guidance for stereotactic surgery. Google Patents; 2001.
13. D'Haese PF, Pallavaram S, Konrad PE, Neimat J, Fitzpatrick JM, Dawant BM. Clinical accuracy of a customized stereotactic platform for deep brain stimulation after accounting for brain shift. Stereotact Funct Neurosurg. 2010;88(2):81–7.
14. Attaar SJ, Patel NV, Hargreaves E, Keller IA, Danish SF. Accuracy of laser placement with frameless stereotaxy in magnetic resonance-guided laser-induced thermal therapy. Oper Neurosurg (Hagerstown, MD). 2015;11(4):554–63.
15. Munier SM, Hargreaves EL, Patel NV, Danish SF. Ablation dynamics of subsequent thermal doses delivered to previously heat-damaged tissue during magnetic resonance–guided laser-induced thermal therapy. J Neurosurg. 2018;131:1958–65. https://doi.org/10.3171/2018.7.JNS18886.

3 Special Technical Considerations: LITT in the Awake Patient and the Pacemaker Patient

Brian D. Toyota, Jamie Joseph Van Gompel, and Sanjeet S. Grewal

LITT in the Awake Patient

The benefits of laser interstitial thermotherapy (LITT) have been well described [1–3]. In our experience, the advantages have included risk avoidance (i.e., minimally invasive), patient-friendliness, cost-effectiveness, and real-time imaging quantification of tumor eradication/eloquent tissue preservation. The vast majority of centers performing focused laser ablation utilize general anesthetic-endotracheal intubation [4–6]. The University of Florida has reported on their experience with local anesthesia on ten patients [7].

In our institution, all laser cases (28) have been done using local anesthetic for the ablative stage of the procedure. We have employed this strategy for several reasons, including patient safety, stacking procedures, and deployment of resources.

B. D. Toyota
Department of Neurosurgery/Surgery, Kingston General Hospital, Kingston, ON, Canada

J. J. Van Gompel (✉)
Department of Neurological Surgery, Mayo Clinic Hospital – St. Mary's Campus, Rochester, MN, USA
e-mail: VanGompel.Jamie@mayo.edu

S. S. Grewal
Department of Neurological Surgery, Mayo Clinic Florida, Jacksonville, FL, USA

Patient Safety

Although modern general anesthetic strategies carry an extremely low risk of morbidity and mortality, the attendant physiologic alterations and pharmacologic interactions still pose a potential threat to any surgical patient. For those institutions that use a diagnostic MRI for the laser ablation, transport of a patient under general anesthetic involves a caravan of healthcare personnel. There is an inherent risk of mishap in the transfer of an intubated patient under general anesthetic from the operating room to the MR suite. Equipment dislodgment, anesthetic complications, drug accessibility, timing delays, discordant scheduling, and personnel availability can compound to increase the risk to the patient [8].

Our experience with the use of local anesthesia has proven that general anesthesia, even if it is low risk, is not necessary for the safe performance of laser ablation.

In addition, laser ablation with an awake patient, analogous to awake craniotomies, allows for real-time clinical monitoring of neurologic function. Continual communication and intraprocedural testing during the laser ablation allow one to assess neurologic function in real-time as the laser is deployed near eloquent tissue. Our experience has shown that neurologic deficits that manifest during the early stages of ablation are typically reversible if the lasing is aborted. Presumably, the deficits were a manifestation of

V. L. Chiang et al. (eds.), *Laser Interstitial Thermal Therapy in Neurosurgery*,
https://doi.org/10.1007/978-3-030-48047-9_3

low levels of heating that proved to be reversible once the heat dissipated prior to reaching tumor-kill intensity [9].

Stacking Procedures and Reduced Patient Turnaround Time

Local anesthesia makes it easier for both staged procedures in the same patient and performing ablations on more than one patient on a given day. For large tumors (>4 cm), we have chosen to stage the ablation to minimize the risk of morbid cerebral edema. After the first ablation, the patient returns to the ward with the laser bolt under sterile protection. Approximately 48 hours later, upon satisfactory assurance of edema control, the patient can easily be returned to the MR suite for further ablation. We have also been able to perform three laser procedures over fewer than 4 hours, largely due to the modest turn-around time afforded by using the local anesthetic technique. Patients can sit comfortably as they await their turn for tumor ablation, and the time devoted to general anesthetic induction, reversal, and recovery is precluded.

Deployment of Resources

There is also a strategic advantage to using local anesthesia from a financial and managerial perspective. From the perspective of cost, significant savings were validated at our institution by minimal use of operating room resources, including anesthesiology, avoidance of the critical care units (post-anesthetic recovery and neuro-intensive care), rapid procedural times, expedited patient recovery, modest pharmacologic costs, and negligible personnel/equipment costs related to transport.

Implementation strategies are also greatly favored by using local anesthesia rather than general endotracheal anesthetic. LITT is unique as a surgical procedure as it spans geographically from the operating room to the radiology department. Gaining acceptance of magnetic resonance-guided laser ablation (MRgLA) requires various silos to communicate and cooperate across separate budgets and agendas. These silos include the operating room, anesthesia, nursing, respiratory technicians, radiology department, radiologists, and radiology technologists. Performing LITT under local anesthesia makes the coordination much easier. The most prominent advantages from this perspective are the avoidance of the "anesthesia train" transferring the patient to diagnostic MR and the organization of ventilatory support in the MR suite. Having the patient conscious and cooperative makes the trans-hospital journey smooth and simple to orchestrate.

The greatest fear in using local anesthesia is intra-procedural patient movement at critical moments. The MR-laser software interface requires geometric accuracy to depict the MR thermographic image on which the clinician depends. If there is patient movement, this accuracy deteriorates and the software has a default setting to abort the procedure. A general anesthetic with pharmacologic paralysis ensures rigid fixation and patient immobility. Our local anesthetic technique has not shown patient movement to be a major problem, with only two of 30 cases having to be reset due to patient movement. This chapter describes this technique and pearls of utilization.

Considerations for Choosing Appropriate Patients

Although we have never refused a patient for treatment under local anesthetic, there are situations which need to be scrutinized. Understandably, patients who are likely to be physically uncomfortable inside the bore for prolonged periods of time need greater preparatory work and vigilance for movement. This category of patients includes the near-claustrophobic, large body mass index, position-based respiratory compromise, and degenerative spinal pain. The procedure requires exquisite patient cooperation, and hence the patient who is even modestly confused is not likely to succeed an awake procedure. Equally the elderly patient who is vulnerable to medication-induced cognitive impairment needs

to be considered cautiously. The oncology patient with an escalating seizure history is likely to be vulnerable to hyperthermia-induced convulsions, and hence having that patient under local anesthesia would be problematic. Finally, like all surgical procedures, ensuring that the appropriate resources are available prior to commencement is crucial. Time efficiency is paramount while a patient is awake, and it is incumbent that preparations include the presence of well-trained clinical support and radiology personnel as well as all the necessary disposables, laser probes, and hardware. Any indication of shortcomings in these areas should postpone the ablation procedure.

Technique of MR-Guided Laser Ablation Under Local Anesthetic

Laser ablation can be split into two technical stages: (1) trajectory planning with skull perforation and (2) laser probe placement and activation.

In the early days of our experience, both stages had been performed under local anesthesia. This has since evolved into incorporating general anesthesia on select cases for the first stage of trajectory planning, skull perforation, and placement of the laser-support device (i.e., bolt). The rationale for this is that the outcome of MRgLA is greatly dependent on the initial trajectory plan, which in turn is only accurately realized if the skull perforation and laser-support device are done with precise technique. Simply put, if the trajectory and skull perforation is not precise, the entire enterprise will be sub-optimal. This precision is better accomplished with a deep neuroleptic or general anesthetic. Like most institutions, we perform this first stage in the operating room where anesthetic support/personnel are readily available. Hence adding a deeper level of anesthetic does not add significantly to patient flow or resource allocation while at the same time ensuring the most accurate trajectory execution possible.

Stage 2 for all our cases is done using local anesthesia. Since the trajectory for the laser probe is already embedded when the patient reaches the MR suite, there is scant ability to accurately re-orient the probe at this stage. For the laser ablation stage, the only patient requirement is to remain immobile during the actual lasing process. To accomplish this under local anesthetic, the following issues are crucial:

- Preparation:
  - Preoperative discussion with the patient
  - Pharmacology
  - Technical
  - Positioning of the patient
  - Catheterization and I.V. access
- Support personnel
  - Drug availability
  - Patient rapport
- Patient reassurance
  - Verbal/physical/pharmacologic

Preoperative patient preparation is crucial for all surgical cases under local anesthetic. In the case of LITT, the key issue is to ensure that the patient understands the need to maintain immobility while the laser is activated. Since all such patients have had lengthy experiences inside an MRI gantry, the preoperative discussion regarding this aspect of the procedure with the patient is generally straight-forward. However, in addition, it is necessary to reassure the patient that (1) the intracranial hyperthermia is not palpable, (2) movement during the laser will not "ruin" the process nor cause danger, and (3) continuous communication will take place during the procedure.

Pharmacologic preparation involves patients being routinely started on a high dose of dexamethasone (4 mg QID) for at least 24 hours prior to the procedure, with an extra 10 mg bolus prior to ablation. (This continues over the subsequent days titrated against patient status and imaging.) As the patient enters the MR suite, a bolus of 4 mg of intravenous (IV) midazolam is administered. We prefer midazolam [10] for its sedative, anti-anxiety, and amnestic features, as well as its suppression of seizures. We specifically aim to avoid pharmacologic complications such as respiratory suppression, cardiovascular lability, confusion, or excessive drowsiness. All anti-epileptics are kept on schedule, and a bolus

dosage is provided also on the way into the MR suite. It is important to have IV medications ready to be administered quickly inside the MR suite. This requires preparation of syringes and IV access made easily accessible and not buried in clothes/blankets. Midazolam, analgesics, and anti-epileptics are all kept on standby. One person is designated for this task upon demand, typically a nurse or resident staff.

Technical preparation is also paramount. Patients can remain immobile for long periods of time, but excessive downtime will inevitably lead to restlessness. Hence, it is crucial that both the running of the MR and the laser set-up is smooth and efficient. The MR technician needs to be familiar with the sequences and to dialogue with the laser clinical-support personnel. Similarly, the clinical-support personnel must be very familiar with the specific MR in use, with the radiology technician and have the laser ready for deployment as soon as possible once the patient is positioned inside the gantry.

Patient positioning is crucial when doing laser ablation under local. The ability to remain motionless during the ablation is significantly easier while comfortable. Hence, all patients are maintained in a neutral supine position or straight lateral position. This consideration in turn requires careful trajectory planning. Some approaches, while convenient for planning purposes, require awkward positioning inside the MR magnet. While this is not an issue under general anesthetic, the conscious patient will not tolerate awkward spine, especially neck, orientations. It is worthwhile spending time ensuring patient comfort prior to entering the MR suite as prolonged patient comfort diminishes the risk of movement and will allow for prolonged lasing if needed.

Positioning also requires anticipating the use of a head coil. Consideration needs to be given to how potential collision with the laser probe can be avoided and how the coil can be fixed over the patient's head without causing irritation or exaggerated claustrophobia. Wireless head coils are particularly useful in MRgLA, and in the unconscious patient, they can simply be placed directly on the head. This, however, is not feasible in the conscious patient. As there are no commercial products to adequately position the coil over the patient, we have improvised various foam and plastic parts to create a shield that allows proximity of the coil to the head but avoids contact with the patient's face.

All patients have bladder catheters, placed during Stage 1 in the operating room. A well-functioning, comfortable, and easily accessible IV line is established. No central lines are needed. Basic remote MR-compatible heart rate and blood pressure monitors are employed. Nasal prongs for oxygen supplementation is available but has been rarely used, and if not needed, is one less irritation to the patient's comfort.

Once the patient is inside the magnet, the laser is set up and placed through the skull into the lesion. Preparatory MR runs are performed and laser probe position is validated. Complete immobility at this stage is not pivotal. However, once all these steps are completed, the next stage, which is quality assurance thermography and the actual lasing, is crucial for patient immobility. It is necessary to return to the patient's side to communicate this and to ensure that the patient is comfortable, e.g., if a stretch by the patient or body realignment is required, if there is pain or restlessness. Any shifting or itching should be attended to immediately prior to laser deployment.

Finally, the speaker-microphone apparatus is tested and revealed to the patient. Ongoing communication is comforting, allowing patients to communicate concerns and likewise for the team to announce timing, progress, and expectations. For a patient who indicates a level of heightened anxiety, we administer an additional bolus of midazolam. If possible, it is ideal to delegate someone to liaise with the patient throughout the process to build trust and rapport. This person is responsible for the continual communication with the patient regarding comfort, concerns, reassurance, and medications. While the responsible surgeon can play this role, it is less ideal as technical and imaging issues may distract from the immediate needs of the patient.

Once the patient has been informed to remain motionless, it is especially important to keep the

team working crisply. Conscientious preparation should allow for efficient quality assurance protocols, thermographic imaging, and laser deployment; needless delays and idle chatter only add time and thus increase the likelihood of patient movement.

There are natural interruptions in the process which can be used to re-enter the magnet, speak with the patient, allow them to shift their body to a limited degree, and administer additional medications if required.

While seemingly ideal, we prefer not to have the patient fall asleep. While a conscious patient makes a dedicated effort not to move, someone who arouses from sleep will inevitably be disoriented, if not confused, and head movements can be expected.

After the ablation has been completed, the laser probe is quickly removed and the patient is brought out of the magnet. In the MR-receiving area, we remove the laser anchor/bolt. Upon arrival in the ward, the patient has the small incision cleansed and sutured in layers.

Patients are brought to a step-down unit, not a formal intensive care unit. Our laser ablations take place in the evening (after diagnostic MR time) and hence they are observed overnight and discharged the following day. As mentioned, we maintain patients on a high dose of dexamethasone for several days after the procedure. We have not typically performed repeat imaging within 24 hours unless there is a concern for problematic cerebral edema.

Procedural Pearls

We have never had to abort or curtail an ablation due to issues of local anesthesia. However, experience has revealed several important nuances of the process.

Current iterations of LITT are heavily reliant on clinical support personnel. It follows that such personnel need to be incorporated as critical members of the procedural team, both in the operating room as well as the MR suite. The ability of clinical support to work seamlessly and collaboratively with both teams is a particularly valuable skill set. Based on daily exposure to ablation cases, they offer a broad experience from which the responsible surgeon can draw. The technical set-up and smooth running of the laser apparatus and software are fundamental to a smooth, trouble-free ablation session. This is especially critical in an awake case, where patient endurance is precious, and time cannot be wasted.

By extension, the MR technicians who run the MR controls must also be engaged members of the ablation team. Their familiarity with the required algorithms and sequences will ensure that delays are avoided. While "learning on the fly" is a luxury with a patient under general anesthetic, such educational time expenditure is not ideal for a patient who is awake for the procedure.

Clinical Pearls

Each patient will respond differently to the ablation experience, and hence each can present unique challenges. As discussed in the previous section, physical and psychological comfort is paramount for a successful awake ablation case.

Physical comfort requires attentiveness to a variety of aspects. Head and body positioning must be carefully scrutinized since the patient must remain relatively immobile for up to a few hours. If there is an extensive delay between scalp incision and MR ablation, the incision itself can become uncomfortable. We routinely infiltrate the incision with Marcaine before leaving the OR to provide as durable cutaneous anesthesia as possible. In the MR suite, we keep Marcaine available should there be breakthrough incisional pain. For lesions proximate to a dural surface, especially pain-sensitive areas such as the tentorium, caution, and awareness are needed as the patient will likely feel the burn of the hyperthermia. On one occasion, this resulted in the need for IV analgesia as well as a modification of our ablation plan.

Psychological comfort is equally critical. It is imperative to discuss what the patient can expect to experience, to reassure that he or she will get forewarning of each step, that any pain or discomfort will be addressed quickly, that two-

way communication will be constant, and that the process can be safely aborted at any time. Tolerance to the claustrophobic atmosphere is variable despite all patients having familiarity with the MR procedure. On occasion, a member of the team will sit inside the MR suite, providing constant physical and verbal reassurance as the actual lasing takes place. One elderly patient became confused toward the end of the procedure—this was not an unexpected sequela from a long day, the age of the patient, a steroid boost and some analgesics, and the biologic impact of the tumor. A similar strategy of bedside presence and modifying the pharmaceuticals allowed for the successful ablation of a large occipital glioblastoma in the patient.

Anecdotal Pearls

Three specific cases highlight issues related to the use of treating the awake patient.

Case 1

There was a singular experience with an awake patient for epilepsy ablation. The left medial temporal lobe structures had been targeted and within seconds of the ablation, the patient, perhaps not unexpectedly, suffered a generalized seizure. Seizures have not been an issue for the neoplastic population, and we ensure adequate blood levels of anti-epileptics are present, a top-up bolus is given prior to ablation and IV anti-epileptics (e.g., benzodiazepine) are readily at hand during the procedure. From this experience, it seems reasonable to conclude that the awake patient is not ideal when attempting to ablate epileptic tissue.

Case 2

Early in our experience, a patient awoke from falling asleep during ablation resulting in significant movement. This led to the software shutting down the procedure, and more significantly, movement of the head position by 1 cm. As we were in the later stages of ablation, instead of recalibrating, we completed the final lasing by extrapolating the hyperthermic effect based on the new positioning. We were benefited by the location of the tumor in the non-eloquent region and opted for additional ablation within a comfortable buffer of tissue of a large malignancy. Significant head movement will undermine useful geometric targeting; however, one can extrapolate with reasonable confidence if not dealing with the eloquent brain.

Case 3

In one case, a malignancy was situated on the right medial homunculus, presenting with mild left leg weakness. During the ablative process, the patient noted left leg sensations and leg flexor weakness, even while lying still in the gantry. He indicated this via the intercom, and we aborted the process. Much of the new leg weakness recovered over minutes. We readjusted the probe to a more superficial location and continued the ablation with constant monitoring of his leg. We succeeded in an aggressive ablation of a recurrent malignant glioma that had failed previous therapies. However, the patient was left with a mildly worsened proximal leg weakness. The weakness resolved over the subsequent weeks with the addition of prolonged steroids and rehabilitation. We felt that despite incurring worsened weakness, the deficit would likely have been more profound and irreversible if it had been done under general anesthetic.

LITT in the Pacemaker Patient

More than 1.8 million people in the United States have a cardiac implantable electronic device (CIED), such as a pacemaker or implantable cardioverter-defibrillator (ICD), which have until recently been considered to be contraindications to MRI. In the setting of epilepsy, MR-guided LITT is increasingly being employed as a treatment of mesial temporal lobe epilepsy. This procedure necessitates the use of MRI, and we have increasingly encountered patients with epilepsy who have an ICD or pacemaker. This section discusses a protocol for safely performing MR-guided LITT in patients with ICDs [11].

When considering MR-guided LITT in patients with ICDs or pacemakers, a team-based approach

is essential. Prior to proceeding with the procedure, an evaluation by cardiology or a pacemaker nurse is important to determine whether the pacemaker is MRI compatible and whether the patient is pacemaker-dependent. Additionally, the procedure should be completed in a 1.5 T MRI. The team needed for the day of the procedure should include: surgeon, neuroradiologist, medical physicist, and pacemaker nurse.

When performing MR imaging on patients with pacemakers, most published studies recommend careful patient monitoring, reprogramming pacemakers prior to an MRI, and some sites limit specific absorption rate (SAR) to less than 1.5–2 W/kg during the scanning. However, there are studies in which patients were scanned safely without specific limits on SAR, but these still recommend appropriate device programming, constant physiologic monitoring, and adjusting of imaging parameters to maintain clinically adequate imaging [12–14]. SAR is the power absorbed per unit of mass tissue, and this is the key determinant of heating secondary to radiofrequency pulses in an MRI. By limiting SAR, and monitoring it throughout the procedure, we can potentially minimize the risk of damage to myocardial tissue at the tips of the leads due to excessive heating and minimize the risk of CIED dysfunction. In vitro evidence shows that by limiting SAR and using a 1.5 T MRI, typical temperature changes at pacemaker leads of ≤0.5 °C were noted [15].

Prior to obtaining an MRI, the patient's pacemaker is interrogated and reprogrammed from DDDR mode to DDD. A cardiology nurse and medical physicist are present for the entire time the patient requires interaction with the MRI suite. A cardiology nurse, along with the anesthesiology service while the patient is under general anesthesia, continually monitor the patient's cardiac function through ECG and pulse oximetry. The physicist assists the MRI technologist in monitoring and adjusting pulse sequence parameters to limit the possibility of excessive heating of pacemaker leads or of the MRI interfering with the function of the pacemaker. The MRI procedure is performed on a 70 cm bore 1.5 T Espree scanner (Siemens; Erlangen, Germany) in the normal operating mode for both SAR and gradient switch rates. In addition, the exposed-body SAR is monitored to verify that its value remains below 1.5 W/kg, which is a consensus value for safe scanning of patients with non-MRI-conditional pacemakers at our institution [16, 17]. Following a scout series, a post-gadolinium volumetric magnetization-prepared gradient echo (MP-RAGE) sequence is executed (SAR = 0.1 W/kg) for treatment planning. The imaging sequence and SAR values have been reported in our prior manuscript (Table 3.1) [11]. It is important to evaluate a CIED pre- and post-MRI to ensure that the CIED is functioning and that there have not been any pacing threshold changes, which would be likely attributed to heating at the lead-tissue interface.

Table 3.1 Imaging sequence and SAR values

Sequence	Purpose	Whole Body SAR (W/kg)
MP-RAGE (3D T1 GRE)	Fiber localization/ post-procedure evaluation	0.01
T1 FLASH (3 planes of single-slice acquisition)	Anatomical reference images of the treatment zone	0.03
3-Plane GRE (single slice in each plane)	Thermal mapping of the treatment zone	0.01
SPACE (3D T1 FLAIR)	Post-procedure evaluation	0.03
T1 GRE	Post-procedure evaluation	0.004
T2 FLAIR	Post-procedure evaluation	0.2
DWI	Post-procedure evaluation	0.07

SAR specific absorption rate, *MP-RAGE* magnetization-prepared gradient echo, table, *GRE* gradient echo, *FLASH* fast low angle shot, *SPACE* sampling perfection with application-optimized contrasts using different flip angle evolution, *FLAIR* fluid-attenuated inversion recovery, *DWI* diffusion-weighted MRI

From Grewal et al. [11]. (Reprinted with permission from Oxford University Press)

Conclusions

Our experience has shown that awake MRgLA of tumors is not only a feasible option, but also carries many advantages. In our institution, it has proven to be cost-effective and resource-efficient.

We have managed to avoid risks associated with general endotracheal intubation and to create a platform on which multiple cases can be done in a compact amount of time.

The pivotal maneuver in our success is the preparation of the patient and of deployment of the technology. We have been satisfied with our results to date and plan to continue with our paradigm of local anesthesia for laser ablation. We are committed to further refining the patient flow and the laser technology and supportive apparatus. In our view, the entire process of LITT has a significant place in the treatment of brain neoplasia, and advances in the technology will ensure broader adoption and application.

LITT is also possible in the pacemaker patient in institutions using a 1.5 T MRI. As with the awake LITT procedure, a dedicated team that is knowledgeable about the pacemaker and the procedure is essential for the success of these cases.

References

1. Ashraf O, Patel NV, Hanft S, Danish SF. Laser-induced thermal therapy in neuro-oncology: a review. World Neurosurg. 2018;112:166–77. https://doi.org/10.1016/j.wneu.2018.01.123.
2. Keen JR, Vigneswaran K, McCracken DJ, Olson JJ. Advancements in the use of stereotactic laser ablation for high-grade gliomas. Contemp Neurosurg. 2017;39(9):6. https://doi.org/10.1097/01.CNE.0000520801.40184.79.
3. Mohammadi AM, Sharma M, Beaumont TL, Juarez KO, Kemeny H, Dechant C, et al. Upfront magnetic resonance imaging-guided stereotactic laser-ablation in newly diagnosed glioblastoma: a multicenter review of survival outcomes compared to a matched cohort of biopsy-only patients. Neurosurgery. 2018;85(6):762–72. https://doi.org/10.1093/neuros/nyy449.
4. Jimenez-Ruiz F, Arnold B, Tatsui CE, Cata J. Perioperative and anesthetic considerations for neurosurgical laser interstitial thermal therapy ablations. J Neurosurg Anesthesiol. 2018;30(1):10–7. https://doi.org/10.1097/ANA.0000000000000376.
5. Eseonu CI, ReFaey K, Garcia O, John A, Quiñones-Hinojosa A, Tripathi P. Awake craniotomy anesthesia: a comparison of the monitored anesthesia care and asleep-awake-asleep techniques. World Neurosurg. 2017;104:679–86. https://doi.org/10.1016/j.wneu.2017.05.053.
6. Prabhakar H, Mahajan C, Kapoor I. Anesthesia for minimally invasive neurosurgery. Curr Opin Anaesthesiol. 2017;30(5):546–50. https://doi.org/10.1097/ACO.0000000000000499.
7. Laurent D, Oliveria SF, Shang M, Bova F, Freedman R, Rahman M. Techniques to ensure accurate targeting for delivery of awake laser interstitial thermotherapy. Oper Neurosurg (Hagerstown). 2018;15(4):454–60. https://doi.org/10.1093/ons/opx290.
8. Knight P, Maheshwari N, Hussai J, Scholl M, Hughes M, Papadimos TJ, et al. Complications during intrahospital transport of critically ill patients: focus on risk identification and prevention. Int J Crit Illn Inj Sci. 2015;5(4):256–64. https://doi.org/10.4103/2229-5151.170840.
9. Munier SM, Hargreaves EL, Patel NV. Danish SF0. Effects of variable power on tissue ablation dynamics during magnetic resonance-guided laser-induced thermal therapy with the Visualase system. Int J Hyperth. 2018;34(6):764–72. https://doi.org/10.1080/02656736.2017.1376355.
10. Conway A, Rolley J, Sutherland JR. Midazolam for sedation before procedures. Cochrane Database Syst Rev. 2016;20(5):CD009491. https://doi.org/10.1002/14651858.CD009491.pub2.
11. Grewal SS, Gorny KR, Favazza CP, Watson RE, Kaufmann TJ, Van Gompel JJ. Safety of laser interstitial thermal therapy in patients with pacemakers. Oper Neurosurg (Hagerstown). 2018;15(5):E69–72. https://doi.org/10.1093/ons/opx292.
12. Roguin A, Schwitter J, Vahlhaus C, Lombardi M, Brugada J, Vardas P, et al. Magnetic resonance imaging in individuals with cardiovascular implantable electronic devices. Europace. 2008;10(3):336–46. https://doi.org/10.1093/europace/eun021.
13. Russo RJ, Costa HS, Silva PD, Anderson JL, Arshad A, Biederman RW, et al. Assessing the risks associated with MRI in patients with a pacemaker or defibrillator. N Engl J Med. 2017;376(8):755–64. https://doi.org/10.1056/NEJMoa1603265.
14. Sommer T, Naehle CP, Yang A, Zeijlemaker V, Hackenbroch M, Schmiedel A, et al. Strategy for safe performance of extrathoracic magnetic resonance imaging at 1.5 tesla in the presence of cardiac pacemakers in non-pacemaker-dependent patients: a prospective study with 115 examinations. Circulation. 2006;114(12):1285–92. https://doi.org/10.1161/CIRCULATIONAHA.105.597013.
15. Shellock FG, Fischer L, Fieno DS. Cardiac pacemakers and implantable cardioverter defibrillators: in vitro magnetic resonance imaging evaluation at 1.5-tesla. J Cardiovasc Magn Reson. 2007;9(1):21–31. https://doi.org/10.1080/10976640600897237.
16. Boilson BA, Wokhlu A, Acker NG, Felmlee JP, Watson RE Jr, Julsrud PR, et al. Safety of magnetic resonance imaging in patients with permanent pacemakers: a collaborative clinical approach. J Interv Card Electrophysiol. 2012;33(1):59–67. https://doi.org/10.1007/s10840-011-9615-8.
17. Korutz AW, Obajuluwa A, Lester MS, McComb EN, Hijaz TA, Collins JD, et al. Pacemakers in MRI for the Neuroradiologist. AJNR Am J Neuroradiol. 2017;38(12):2222–30. https://doi.org/10.3174/ajnr.A5314.

Complications of LITT

4

Michael Schulder and Nick Kleiner

Introduction

The modern era of laser interstitial thermal therapy (LITT) began in 2008, with the publication of Carpentier demonstrating the use of this technology in treating patients with metastatic brain tumors [1]. One of the presumed benefits of LITT is its minimal invasiveness and decreased associated surgical risks. However, the incidence of such risks cannot (of course) be zero, considering that LITT is in fact a surgical procedure that includes the deposition of energy as a means of tissue ablation. In fact, studies have shown that potential complications of LITT are not rare and must be taken into account in patient discussions and management decisions [2]. This chapter will discuss the types of complications to be expected when performing LITT, and their frequency and severity.

M. Schulder (✉)
Department of Neurosurgery, Zucker School of Medicine at Hofstra/Northwell, Lake Success, NY, USA
e-mail: mschulder@northwell.edu

N. Kleiner
Department of Neurosurgery, Northwell Health, Lake Success, NY, USA

Laser Misplacement

Inaccurate laser fiber placement can prevent adequate hyperthermic treatment of the planned target, or worse, intracranial hemorrhage. We found that using a stereotactic frame for twist-drill guidance and the subsequent placement of a skull bolt for laser fixation greatly reduced the risk of laser misplacement [2]. In addition, the transition to titanium skull anchors, from the "first-generation" plastic bolts, has also decreased the rate of laser misplacement. It may seem obvious, but is worth noting, that this problem in general can be avoided in centers where LITT is performed from start to finish in a high-field MRI. This can be accomplished by dedicated intraoperative imagers that support stereotactic targeting, imaging of the fibers, and repositioning as needed, or by the temporary "conversion" of a diagnostic magnet into an interventional device (MRI Interventions, Irvine, CA). For small deep targets, special attention needs to be paid to creating a trajectory that is as perpendicular to the skull surface as possible. If this is not possible then when drilling the skull it is important to ensure that the drill bit does not slip along the curvature of the skull. Lastly, in lesions that may be evolving quickly with time, the ability to fuse new images to planning scans is essential to ensure that trajectory is still correct.

V. L. Chiang et al. (eds.), *Laser Interstitial Thermal Therapy in Neurosurgery*,
https://doi.org/10.1007/978-3-030-48047-9_4

Case Illustration: Misplacement of Laser Fiber

A 56-year-old woman had undergone prior craniotomy and multiple treatments with stereotactic radiosurgery for metastatic non-small-cell lung carcinoma. She now had tumor recurrence in the region of the medial right parietal falx, in an area treated before with SRS. Laser placement was done using the Precision Aiming Device (PAD; Medtronic Surgical Technologies, Louisville, CO). MRI showed the laser fiber to have missed the target (Fig. 4.1). The procedure was aborted, and the patient agreed to return for an ultimately successful LITT tumor ablation two weeks later, using a stereotactic frame.

Intracranial Hematoma

Intracranial hematomas from LITT can result from hemorrhage located epidurally (from inadequate dural puncture at the time of twist-drill drilling), or subdurally and intracerebrally from laser fiber insertion. This is a risk common to all stereotactic cannula-based procedures, including biopsy and deep brain stimulation. Avoiding this purely surgical risk can be done by paying close attention to the technical details of any standard stereotactic surgery. Pre-operative normalization of coagulation factors, platelet count and cessation of non-steroidals and anticoagulation therapy also remains essential.

Case Illustration: Hematoma from Laser Insertion

This 24-year-old woman had medically refractory gelastic seizures and a hypothalamic hamartoma. A left coronal insertion was planned for the placement of a single laser fiber. MRI revealed an epidural hematoma, no doubt because of inadequate dural puncture and secondary stripping of the dura (Fig. 4.2). LITT was successfully completed, after which the patient was returned to the OR for craniotomy and hematoma evacuation. No neurological deficit occurred, and she was seizure-free at the time of the last follow-up.

Given the need for the drill to penetrate the dura at the time of bony opening, the underlying cortex could also be entered. Surgical navigation systems have become the standard method of

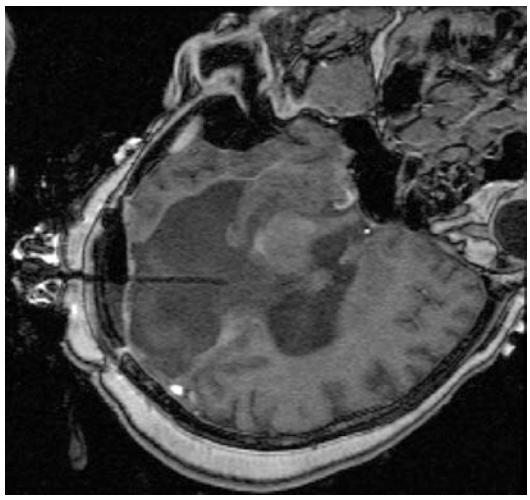

Fig. 4.1 Misplacement of laser fiber using the PAD. (From Pruitt et al. [2]. Reprinted with permission from the Journal of Neurosurgery)

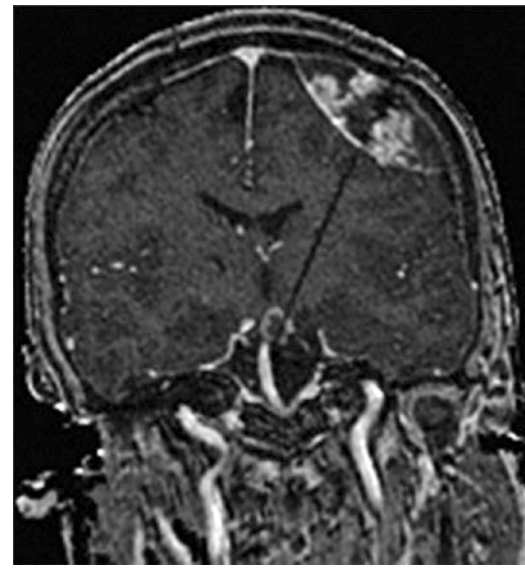

Fig. 4.2 Epidural hematoma due to inadequate dural puncture at the time of twist drill for laser fiber insertion. Laser tip is in the hypothalamic hamartoma, and LITT has been successfully completed. (From Pruitt et al. [2]. Reprinted with permission from the Journal of Neurosurgery)

planning such procedures, even when a stereotactic frame is used. It is mandatory, when the surgical plan is being created, to ensure that the cannula or laser fiber will not be traversing a sulcus or visibly crossing paths with an artery or vein. A contrast-enhanced stereotactic MRI, or a CT angiogram, can be used for direct targeting, or can be registered for the purpose of surgical planning. After defining the entry and target points, the planned pathway of the laser fiber can be visualized and the trajectory adjusted as needed to minimize the risk of hemorrhage. A similar consideration is the avoidance of passage through a cerebral ventricle. Although this matter is debated, going through a ventricle probably increases the risk of a bleed as passage through two subependymal surfaces will result.

Lastly, laser overheating can also cause bleeding if the laser is not properly cooled, which will cause nearly instant overheating and charring of the tip. Removing of the laser can then cause bleeding from the charred tissue when the laser is removed [2]. Concern for hemorrhage should be considered if any sudden changes of MR gradient echo sequence signal occur during laser ablation, especially if heating in the area is occurring quickly. The best sequences for detecting hyperacute hemorrhage are susceptibility-weighted and T2-weighted images [3]. While there are theoretical concerns about causing hemorrhage in highly vascular lesions such as melanoma brain metastases, this risk has not been borne out by anecdotal experience.

Hyperthermic Complications

Heat causes ablation by energy transmission, just as ionizing radiation does in the form of radiation therapy or stereotactic radiosurgery. However, as far as is known, hyperthermia does not leave the biological "footprint" created by radiation. Presumably hyperthermia can be repeated as needed, and does not carry the same risk of secondary neoplasia (of course, a moot issue in patients with malignant tumors, but not in those with epilepsy). It is tempting, therefore, to consider LITT as somehow "immune" from causing direct neurological injury caused by the treatment itself. But this is not the case. In our series of 49 LITT treatments in 46 patients there were 3 patients in whom a new neurological deficit resulted from hyperthermia itself [2]. This does not preclude the repeat administration of LITT to a given intracerebral target, but means that in any given patient the volume, duration of treatment, and neurological "eloquence" of the target must be carefully considered. In addition, in a study by Sharma et al., diffusion tensor imaging was performed in 80 patients prior to LITT and then the overlap of hyperthermia region with clinically significant tracts was measured and correlated with temporary and permanent post-op neurological deficits. What this study showed was that even an overlap as small as 0.1 cm^3 could result in a permanent motor deficit [4].

Ensuring that structures at risk are defined prior to start of ablation and setting constraints to turn off the laser when temperatures exceed a designated level can limit the risk of hyperthermic injury. However, in doing so, these limits should not be so restrictive as to render the treatment ineffective. LITT must be not only safe but effective, as well.

Case Illustration: Hyperthermic Injury

This 29-year old man had been treated at other centers for a supratentorial high-grade astrocytoma (initially deemed grade 3, and more recently as grade 4) with two prior craniotomies, along with radiation therapy and chemotherapy. He now developed new tumor growth in his cerebellum, adjacent to the fourth ventricle, causing mild gait ataxia (Fig. 4.3a). He was referred for LITT as a means of treating this new tumor focus with a (presumed) lesser chance of causing edema and obstructive hydrocephalus compared to stereotactic radiosurgery.

Under general anesthesia, a single laser fiber was inserted through the tumor (Fig. 4.3b) and the whole enhancing volume was treated to a temperature of 43 °C (Fig. 4.3c). The patient awoke with new bilateral palsies of cranial nerves 6 and 7, and worsened ataxia. These deficits

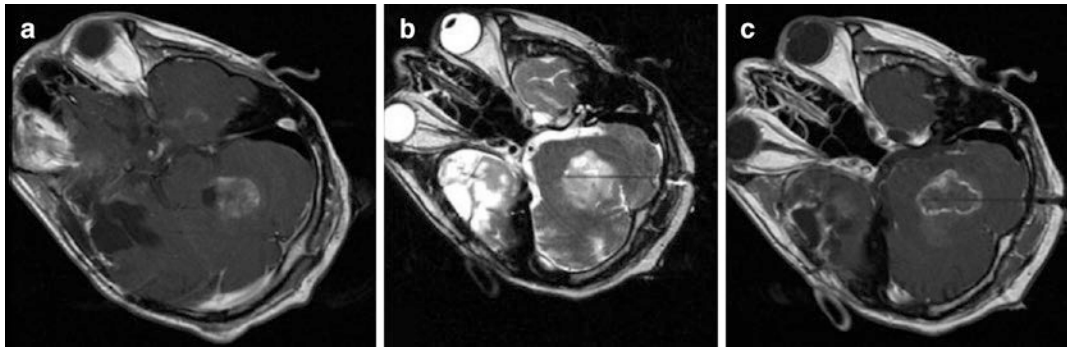

Fig. 4.3 (**a**) T1W MRI with contrast showing the new tumor growth. (**b**) T2W MRI with laser fiber inserted. (**c**) T1W MRI with contrast acquired immediately upon completion of LITT, showing the expected central loss of enhancement with a thin rim of residual contrast. The entire lesion was treated. (From Pruitt et al. [2]. Reprinted with permission from the Journal of Neurosurgery)

improved slightly if at all, and the patient died of progressive glioblastoma six months later.

Unpredictable Technological Complications

One of the biggest challenges in the performance of LITT is the procedure's heavy dependence upon novel technology. As was seen in Chap. 2, the minimum technology required to successfully perform LITT is a highly accurate navigation system that needs to be compatible with a fully functional laser system inside an MRI. That MRI must provide high-quality non-distorted multimodality imaging, and be able to support continuous communication with the laser system. The success of this multi-step procedure is dependent upon the completion of each step along the way.

In the traditional neurosurgical procedure, the neurosurgeon is usually well trained in the technical aspects of running all the equipment required. For LITT, however, this is not at all the case. In fact, it would be the rare neurosurgeon who would be well versed in deciding which MR coils to use or how to run an MRI. The laser systems and some of the newer navigation systems are also similarly complex, which is why clinical representatives from the relevant companies are often available to assist in the use of the devices. It must be remembered that while the awareness of LITT is growing rapidly in the neurosurgical community, the number of centers at which these procedures are being done remains limited. Breakdown of any key piece of equipment from navigation to MRI and the laser itself will have devastating effects on the ability to complete a LITT procedure. Similarly, having either institutional staff or industry representatives that are unfamiliar with the set-up of the LITT procedure and equipment can result in errors and complications. Lastly, while neurosurgeons are typically well trained at the interpretation of basic MR images, acute changes that might occur intraoperatively are not routinely learned in residency or as part of regular practice. Neuroradiological consultations may be available, but even neuroradiologists may not fully appreciate the significance of imaging changes obtained during LITT. In addition, interpretation of real-time changes on MR thermometry can be subjective due to the vagaries of MR data that may be of marginal quality, being part of a surgical procedure. Lack of experience on the part of the neurosurgeon and/or the clinical representative can result in errors of interpretation and therefore complications or errors in management also.

Realistically, then, the list of potential complications that can arise due to the overall complexity of the technology needed for LITT and its multiple "moving parts" can be highly unpredictable. While not necessarily putting the patient directly at risk, problem solving outside the neurosurgeon's capability can delay comple-

tion of the surgery, even up to leaving catheters in the brain overnight while critical equipment is flown in, or to aborting the procedure. It therefore remains critical that neurosurgeons continue to recognize that LITT remains novel technology at this time.

Discussion

LITT was first described in the 1980s, but its practical introduction was just over a decade ago, with the practical and routine availability of MRI thermometry. In comparison to radiofrequency lesioning, this allowed for confirmation of probe location and also of real-time knowledge of how much temperature was going where. Likewise, this contrasted LITT to SRS, in which the effects of ionizing radiation are delayed, and reliance on the spatial accuracy of treatment delivery is the only means of ensuring proper outcome. As time has passed and LITT has become a mature treatment, reporting of complications has confirmed the obvious fact that while experience and attention can minimize complications, they cannot completely eliminate them. Our group reported 11 adverse events in 49 procedures, including 4 patients with misplaced catheters, 1 whose procedure was aborted after overheating occurred after the saline coolant was depleted, 3 patients with intracranial hemorrhage, and 3 new deficits from laser hyperthermia [2].

In recent years, the preponderance of patients treated using LITT have been those with medically refractory epilepsy (Medtronic Visualase, Houston, TX, unpublished data). A recent review found that in these patients, LITT-induced deficits tended to be transient. While observation has suggested that some of the memory-related side effects of resective mesial temporal surgery are mitigated using LITT (at the price of somewhat decreased seizure control), this has not been clearly proven [5]. In addition, new hyperthermia-related complications can occur that are unique to LITT. For example, the occipital approach for mesial temporal epilepsy can result in a visual field cut associated with hyperthermic injury to the lateral geniculate nucleus which lies medial to the tail of the hippocampus. In a series of 17 children, the majority of whom had focal cortical dysplasia, one patient sustained intraventricular hemorrhage and secondary aseptic meningitis. No hyperthermia-related deficits were noted [6]. A case report described delayed intraparenchymal and intraventricular hemorrhage in an 18-year-old man. This manifested itself on the 9th postoperative day, and required a craniotomy to evacuate the hematoma. The authors speculate that the cause of hemorrhage was pseudoaneurysm creation from mechanical injury or from the hyperthermia, though they furnished no evidence of that [7].

Other authors have added to the evidence that LITT by and large is a safe procedure. In one series of 133 patients, there were 3 complications, and in another group of 54 patients with glioblastoma, there were 9 such events [8, 9]. In each of these series hyperthermia-induced deficits were the minority.

Conclusion

When performed with the necessary attention to technical and clinical detail, LITT is a form of minimally invasive neurosurgery that is safe. Given that is proposed as such, it is especially incumbent on the neurosurgeon to avoid complications from the procedure, which can be worse than the natural history of the condition being treated and perhaps be more severe than those of open surgery. It is particularly important to recognize that technology-driven factors outside those typically dictated by the surgery itself can influence the risk of complications for this procedure.

References

1. Carpentier A, McNichols RJ, Stafford RJ, Itzcovitz J, et al. Real-time magnetic resonance-guided laser thermal therapy for focal metastatic brain tumors. Neurosurgery. 2008;63(Suppl 1):ONS21–8; discussion ONS28-9.
2. Pruitt R, Gamble A, Black K, Schulder M, Mehta AD. Complication avoidance in laser interstitial

thermal therapy: lessons learned. J Neurosurg. 2017;126(4):1238–45.
3. Linfante I, Llinas RH, Caplan LR, Warach S. MRI features of intracerebral hemorrhage within 2 hours from symptom onset. Stroke. 1999;30:2263–7.
4. Sharma M, Habboub G, Behbahani M, Silva D, Barnett GH, Mohammadi AM. Thermal injury to corticospinal tracts and postoperative motor deficits after laser interstitial thermal therapy. Neurosurg Focus. 2016;41(4):E6.
5. Alattar AA, Bartek J Jr, Chiang VL, Mohammadi AM, Barnett GH, Sloan A, Chen CC, et al. Stereotactic laser ablation as treatment for brain metastases recurring after stereotactic radiosurgery: a systematic literature review. World Neurosurg. 2019;128:134–42.
6. Lewis EC, Weil AG, Duchowny M, Bhatia S, Ragheb J, Miller I. MR-guided laser interstitial thermal therapy for pediatric drug-resistant lesional epilepsy. Epilepsia. 2015;56(10):1590–8.
7. Barber SM, Tomycz L, George T, Clarke DF, Lee M. Delayed intraparenchymal and intraventricular hemorrhage requiring surgical evacuation after MRI-guided laser interstitial thermal therapy for lesional epilepsy. Stereotact Funct Neurosurg. 2017;95(2):73–8.
8. Kamath AA, Friedman DD, Hacker CD, Smyth MD, et al. MRI-guided interstitial laser ablation for intracranial lesions: a large single-institution experience of 133 cases. Stereotact Funct Neurosurg. 2017;95(6):417–28.
9. Kamath AA, Friedman DD, Akbari SHA, Kim AH, Tao Y, Luo J, Leuthardt EC. Glioblastoma treated with magnetic resonance imaging-guided laser interstitial thermal therapy: safety, efficacy, and outcomes. Neurosurgery. 2018;84(4):836–43.

LITT for Metastatic In-Field Recurrence

5

Nanthiya Sujijantarat, Shabbar F. Danish, and Veronica L. Chiang

Abbreviations

BBB	blood-brain barrier
BSE	brain-specific enolase
HVLT-R	Hopkins Verbal Learning Test-Revised
ICH	intracerebral hemorrhage
KPS	Karnofsky Performance Score
LAASR	Laser Ablation After Stereotactic Radiosurgery study [5]
LITT	laser interstitial thermal therapy
MMSE	Mini-Mental State Examination
MRI	magnetic resonance imaging
N/A	not available
PFS	progression-free survival
POD	progression of disease
QOL	quality of life
RN	radiation necrosis
SF-36	Short-Form Health Survey
SRS	stereotactic radiosurgery
TR	tumor regrowth
WBRT	whole brain radiation therapy

N. Sujijantarat
Department of Neurosurgery, Yale-New Haven Hospital, New Haven, CT, USA

S. F. Danish
Department of Neurosurgery, Rutgers University, New Brunswick, NJ, USA

V. L. Chiang (✉)
Department of Neurosurgery, Yale University School of Medicine, New Haven, CT, USA
e-mail: veronica.chiang@yale.edu

Introduction

The management of patients with brain metastases has become increasingly complex with advancements in systemic therapies resulting in increased duration of survival in cancer patients. Typically a late-term complication, brain metastases represent the most common brain tumors diagnosed and their presence can significantly impact patients' overall survival and quality of life (QOL). The treatment of brain metastases has undergone multiple shifts in recent decades. Most significantly, stereotactic radiosurgery (SRS) has evolved to become first-line treatment for many patients.

The cumulative incidence of recurrent tumor or radiation necrosis after SRS is reported to be up to 9.2–14% in patients surviving beyond one year [1]. While these entities have distinct pathophysiologies, when symptomatic, patients present with similar symptoms related to mass effect and edema as seen as progressive enhancement on magnetic resonance imaging (MRI) sometimes causing focal neurological deficits and seizures, among other symptoms.

Radiation necrosis is typically a result of a late irreversible injury to the brain surrounding the tumor after SRS. Risk factors for its development include large lesional volume, higher radiation dose, and adjuvant chemotherapy around the time of SRS [1, 2]. Multiple hypotheses exist in the pathophysiology of radiation

V. L. Chiang et al. (eds.), *Laser Interstitial Thermal Therapy in Neurosurgery*,
https://doi.org/10.1007/978-3-030-48047-9_5

necrosis, including endothelial cell damage causing capillary dysfunction and injury to glial cells leading to demyelination and necrosis [2, 3]. Radiation necrosis can occur months to years after SRS treatment and its incidence has been rising with the increased use of immunotherapies. Given that not all radiation necrosis becomes symptomatic, the initial treatment of radiation necrosis is typically conservative. Corticosteroids are used if patients develop neurological symptoms. If lesional regrowth or symptoms are progressive, especially despite corticosteroid therapy, surgical resection is an option to relieve the mass effect caused by radiation necrosis.

In contrast, the recurrent tumor has a more straightforward pathophysiology and often results from incomplete resection or radiation, regrowth of treatment-resistant tumor cells, or invasion of metastatic cells to the previously treated site. The incidence of tumor regrowth is related to the type of primary tumor, the size of the initial target, and the radiation dose. Recurrent metastases can be treated with a surgical resection or additional radiation in the form of SRS, whole brain radiation therapy (WBRT), or a combination of the two.

In practice, it is often difficult to distinguish between radiation necrosis and tumor regrowth by means of imaging or presentation alone [4]. When progressive and symptomatic, the management of both entities often converges. For these reasons, some authors have proposed the use of the term "metastatic in-field recurrence" to include and sometimes obviate the need to distinguish between radiation necrosis and tumor regrowth. Craniotomy for resection of metastatic in-field recurrence offers excellent local control but may result in prolonged recovery time, worsening neurological deficits, infection, and significant psychiatric implication including depression [5]. Laser interstitial thermal therapy (LITT) has emerged as a minimally invasive treatment option for metastatic in-field recurrence especially in tumors that are difficult to access surgically. This chapter will discuss the current evidence for LITT as a treatment of metastatic in-field recurrence, including patient selection, outcome, imaging changes, and its role in disrupting the blood-brain barrier (BBB).

Patient Selection

The use of stereotactic laser therapy for the treatment of brain tumors was described as early as 1966 [6]. As discussed in the previous chapters, the availability of MRI for the guidance of stereotaxis and heat delivery has expanded the current interest in and use of LITT. In the early studies, the indications for using LITT for metastatic in-field recurrence were less clear. The cases that were described largely used thermal therapy to treat tumors that had previously exhausted other treatments, were about 2–3 cm in diameter or less, and were deemed accessible by LITT in patients who had good expected survival [7, 8]. Subsequently, the selection criteria have evolved to highlight some of the strengths of LITT, which will be discussed in the following sections. In the most recent LAASR (laser ablation after stereotactic radiosurgery) multicentered study, patients who qualified for LITT were those with metastases from a known primary cancer who previously underwent SRS treatment for the LITT-intended lesion, with KPS score $\geq$60 and age $\geq$18 years, and who were deemed to be suitable surgical candidates [5]. In another study by Rao et al., stricter KPS scores of >70 were used as a cutoff [9]. LITT was reported to be used for lesions with volumes ranging from 0.4 to 38.9 cm^3 [5, 9–12].

Aside from the patient's age and functional status, other indications for LITT can include patients with radiographically regrowing treated brain metastases who need biopsy for diagnosis, or those in whom symptoms related to the regrowth are not controllable with steroids [1]. Patel et al. proposed that LITT should be considered in a progressive lesion that meets any of the following criteria: (1) patient requiring long-term low-dose steroid or (2) the lesion has grown at least 1 cm, grown by 50% in two out of three linear dimensions, and has grown on two consecutive scans [13]. The authors concluded that patients who required higher preoperative steroid dosages were unlikely to benefit from LITT, and

a craniotomy should be considered in these cases, if possible, to immediately address the mass effect. The idea here is that the LITT procedure can increase edema and mass effect in the acute phase and the natural course of edema after LITT can sometimes take weeks, if not months, to resolve [14].

In general, therapeutic decision making for radiographic regrowth after SRS follows the principle that tumor regrowth typically requires immediate treatment whereas radiation necrosis can be followed and treated only if progressively symptomatic. However, this last indication is changing with the increasing use of immunotherapy and the need to wean off steroids quickly to enable restarting of cancer treatment. This is also challenging when in the midst of attempting to resolve the underlying pathophysiology, the growth can become exponential, and one can miss the window to treat irrespective of the underlying physiology [4, 15]. When LITT is proposed as a treatment modality, however, authors have failed to achieve consensus on whether or not to perform a biopsy for diagnosis prior to LITT. On one hand, complete ablation of the lesion using LITT has been shown to be effective for both diagnoses and eliminates the need to distinguish between these two pathologies. The concern about the biopsy arises because bleeding in the area can make intraoperative LITT imaging, specifically that related to the Visualase System (Medtronic), more difficult to interpret, thus compromising the treatment [13]. Furthermore, within SRS-treated targets, there can be areas where both radiation necrosis and tumor coexist and sampling errors can occur making the value of biopsy debatable. However, from a cancer management standpoint, it can be critically important to understand if cancer control is being achieved in the brain using SRS. Many patients have multiple brain metastases treated using SRS and the presence or absence of tumor within the biopsy sample likely reflects the pathology of the next regrowing lesion. In the experience of some authors, the presence of any tumor, regardless of the presence of radiation necrosis, should be treated as tumor recurrence [16]. In the age of targeted therapies and immunotherapies, biopsy is an opportunity not only to make a diagnosis but also to determine whether the genetic profile of the tumor is the same in the brain as it is peripherally in the cases of regrowing tumors, thus helping to determine if the systemic therapy being prescribed might be effective in the brain.

The LAASR study revealed that both survival and local control outcomes after LITT alone are significantly better for patients with radiation necrosis than those with tumor regrowth [5]. Additional analysis of the results was performed based on the completeness of LITT ablation for 21 patients. For patients with radiation necrosis, resolution of the LITT lesion was seen in 100% of the treated lesions with both total and subtotal ablation. This was compared with tumor patients where 75% resolved with total ablation, 25% of lesions partially resolved with total ablation, and 63% of lesions progressed if subtotally ablated. Not only does this translate in the radiation necrosis patients to an overall better prognosis and therefore continued aggressive cancer care, but for the progressive tumor patient, a possibly different discussion regarding goals of care and whether adjuvant radiation after LITT may be needed. In addition, from a technical standpoint, complete ablation was necessary for controlling a regrowing tumor whereas the subtotal ablation of radiation necrosis could still result in local control, thus affecting the goals of the LITT procedure. These authors therefore recommended that a biopsy be performed where possible at the time of LITT as it can guide follow-up care decisions. The decision to perform a biopsy in the setting of lesional regrowth after SRS needs to take the care of the patient holistically into the context relative to the capability of the LITT technology.

Technical Aspects

Like gliomas, the locations of metastatic in-field recurrence can vary significantly as can the prior management of the patients. Because of this, some preoperative planning is required to ensure successful access to the target and then complete coverage with the ablation. Given the lack of pre-

procedural planning ability within the current software packages, goals to be achieved by the surgery and approach limitations need to be considered prior to surgery. In general, one of the most important factors to be determined is trajectory. Preoperative MRI brain with and without contrast should be reviewed preoperatively. General anesthesia is preferred given the sometimes complex trajectories and target locations. Patients undergo preoperative MRI with fiducials which is then transferred to the stereotactic navigation system. Given that the diameter of the deliverable heat region is typically 2–3 cm in maximum dimension, planning to place the laser fiber along the long axis of the target typically allows for best LITT coverage. Many of the trajectory planning systems allow for a diameter circle to be created around the planned trajectory and this often enables the surgeon to visualize which parts of the target can be ablated with the planned trajectory and what normal brain may be at risk as the cylinder of heating is created. Figure 5.1 demonstrates a typical trajectory used for an occipital regrowing tumor in a patient with metastatic breast cancer (NeuroBlate System; Monteris Medical).

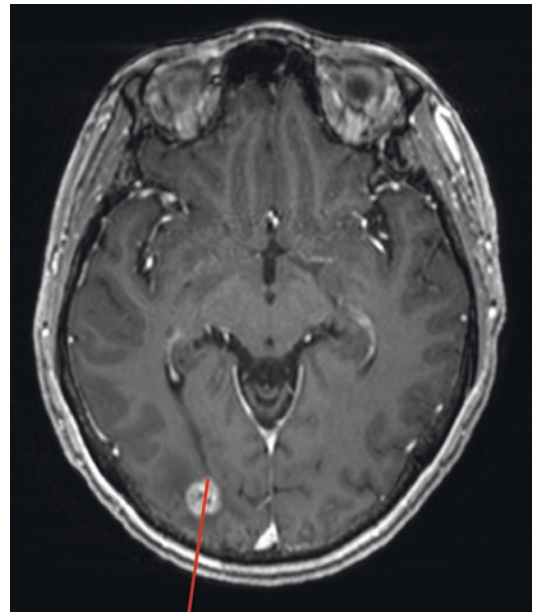

Fig. 5.1 A typical trajectory used for an occipital regrowing tumor

Figure 5.2, however, shows how planning may vary depending upon the goals of the surgery. This example shows a patient with metastatic melanoma who was treated with radiosurgery to a right basal ganglia lesion with SRS followed by the initiation of ipilimumab and nivolumab. Unfortunately, the metastatic focus (medial portion of the enhancing region) did not decrease in size in response to SRS but rather enlarged laterally within the next 3 months. Systemic response to immunotherapy in contrast was excellent.

Due to its deeper location, LITT was felt to be a reasonable option but biopsy was also needed to understand the discrepancy in response to immunotherapy between the intracranial disease and the systemic disease. The NeuroBlate System was also used in this example. Given the difference in radiographic appearance between the medial nodule and the more lateral changes, it was decided to plan trajectory to allow for separate biopsies of the two areas (Fig. 5.2a) rather than along the classical long axis of the lesion (Fig. 5.2b). This was possible in this scenario because the longest length of the target in the AP direction was still less than 3 cm. In addition, given that this target almost abutted the internal capsule, having the structure at risk at the end of the laser (Fig. 5.2a) rather than on the side of the laser (Fig. 5.2b) also allowed for the safest heat delivery. Heat emanates from the sides of the tip of the NeuroBlate laser and forward heat delivery is limited and therefore unlikely to spread out of control. Three specimens were sent for pathology, and a diagnosis of radiation necrosis was made from the lateral specimen compared with residual tumor from the medial portion. The follow-up MRI approximately one month after LITT demonstrated improved perilesional edema and mass effect.

The other major consideration in trajectory planning is the presence of a prior craniotomy. Usually there is scarred dura and/or dural substitute which can increase the insertional hemorrhage rate or cause catheter deviations. Therefore, choosing a trajectory outside of the original surgery can be advantageous. Figure 5.3 demonstrates a trajectory that may be used for a patient who previously underwent a craniotomy.

Lastly, odd target configurations and locations, as well as the need to treat multiple lesions,

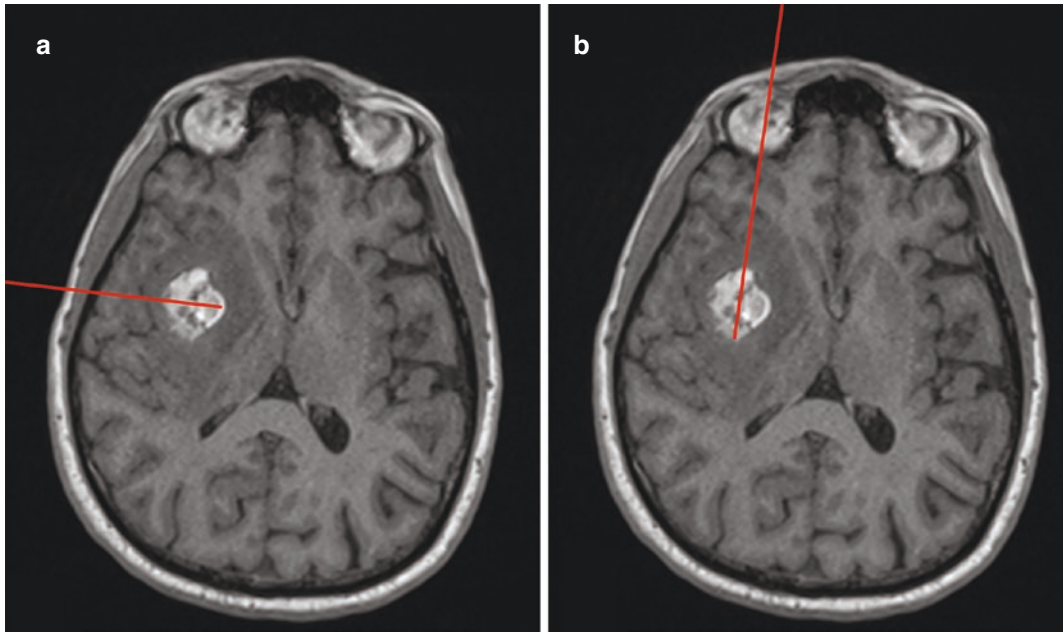

Fig. 5.2 Trajectory planning in a patient with metastatic melanoma with a right regrowing basal ganglia lesion. The trajectory was planned to allow for separate biopsies of the medial nodule and the more lateral changes (**a**), rather than along the classical long axis of the lesion (**b**)

can pose a challenge largely unique to metastatic cancer patients. Figure 5.4 demonstrates some examples of how LITT can be planned and used for bilateral occipital regrowing tumors (Fig. 5.4a) or unique trajectories across midline (Fig. 5.4b).

Most patients receive 10 mg of dexamethasone and 1 g of levaciteram intraoperatively. A stab incision followed by a twist drill burr hole is made through this system, and the laser introduction bolt is secured to the skull. A biopsy is performed at this point if needed. Following the biopsy, a laser fiber is introduced and a repeat MRI obtained to confirm its position prior to initiation of LITT.

From a technical standpoint, an early report from the Case Comprehensive Cancer Center in patients with gliomas using the NeuroBlate System suggested a possible risk of proximal seeding of tumor along the laser tract, and recommendations were made for heat delivery to start at the shallowest point and advance to the deepest point [17]. Since this initial report, however, no further cases have been reported and this practice has not been instituted in our practice.

Immediately postoperatively, LITT patients are monitored in the neuro-intensive care unit. CT head without contrast is obtained postoperatively to rule out immediate periprocedural complications. Most patients are continued on a steroid taper postoperatively varying from 5 days to 2 weeks depending on steroid dependence preoperatively. Patients are followed up at 2 weeks postoperatively with an MRI and for wound check. They then typically undergo surveillance MRIs at 1.5, 3, and 6 months.

Complications and Postoperative Management

Adverse outcomes following LITT for metastatic in-field recurrence have varied depending on the definitions used in the studies. In the LAASR study, adverse outcomes were defined as any undesirable medical occurrence regardless of its association with the use of the device itself [5]. The most common side effects were headache, nausea/vomiting, cardiopulmonary events including pneumonia, urinary tract infection, and complications from

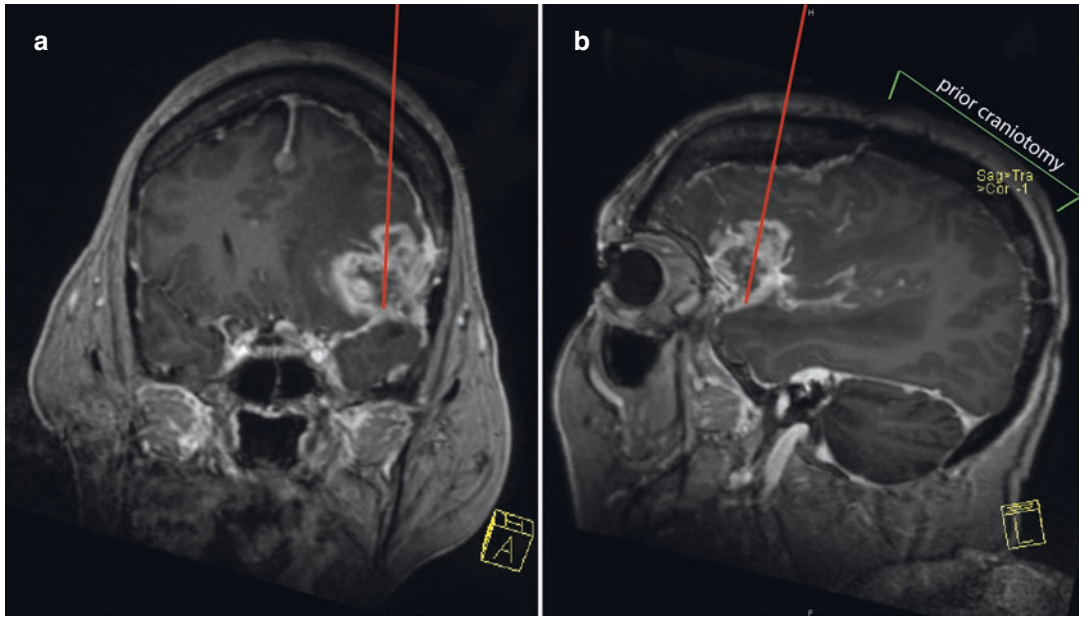

Fig. 5.3 (**a**) Example of a trajectory that may be used for a patient with a regrowing left frontal tumor who previously underwent a craniotomy (**b**)

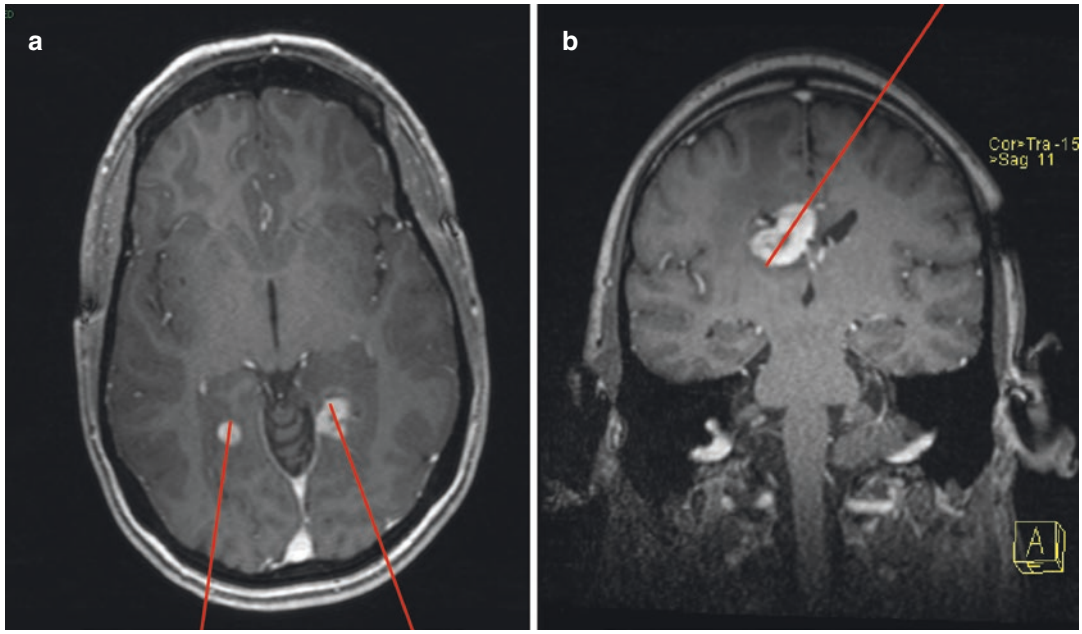

Fig. 5.4 Examples of trajectories used for bilateral occipital regrowing tumors (**a**) or a unique trajectory across midline (**b**)

the progression of systemic cancer. When considering only LITT-related neurological complications, 12% of the patients had adverse outcomes including weakness, paralysis, and neglect. In 80% of these patients, LITT was performed adjacent to the motor, sensory, or speech areas. Asymptomatic intracerebral hemorrhage (ICH) occurred in 2% of the patients and seizures in 17%. The rates of com-

plications overall did not differ between the tumor regrowth group and the radiation necrosis group in this study.

Overall, ICH was reported in 2–13% of cases in the published studies [5, 9, 11]. The Chaunzwa et al. series of 30 patients reported a 13% incidence of ICH, occurring during the LITT portion rather than the biopsy portion of the case, but very few resulted in worsening of preoperative symptoms. Rao et al. reported an asymptomatic ICH in one patient (7%) in their series of 15 patients. One out of 23 patients who had left thalamic metastasis in the Ali et al. series developed hydrocephalus requiring a temporary ventricular drainage after LITT, and one patient developed malignant cerebral edema requiring an emergency hemicraniectomy [10]. See Table 5.1 for a listing of the complications.

It can be concluded that while the scalp and bony access to the target is less invasive compared to a craniotomy, the risks associated with LITT are similarly dependent on several variables including lesion location, pre-ablation edema, and size of the pre-ablation targets. Postoperatively, LITT patients therefore require observation in a setting equivalent to a neuro-intensive care unit. Time to recovery after an uncomplicated procedure and anesthesia, however, is still relatively short compared to a standard craniotomy, with the median length of hospital stay after LITT being 1–2 days [4, 5, 9, 11]. See section later in this chapter, Outcomes of LITT for Metastatic In-field Recurrence, for discussion of postoperative steroids management.

Imaging Changes after LITT

Radiographic changes after LITT can be variable but generally follow a trend of an initial increase in the size of the contrast-enhanced volume followed by a steady decrease. In the initial series published by Carpentier et al., the thermal ablation zone showed postoperative expansion of the necrotic area followed by a decrease in size [7]. Interestingly, the authors noted that the FLAIR volume did not increase postoperatively. These results are comparable in the subsequent larger series. Rao et al. reported that in the majority of targets treated (12 out of 14), the immediate postoperative volume had an average increase to 2.78 times the preoperative volume [9]. Thereafter, some treated areas continued to increase in size up to 2–4 weeks, followed by a gradual decrease in size. The majority of these treated areas returned to their preoperative sizes by 16 weeks. Chaunzwa et al. found that at 6 weeks, the contrast-enhanced volume showed a median increase in the volume of up to 34%, but this was associated with a median reduction in FLAIR volume of 36% [11]. At 3 months, the contrast-enhanced volume largely returned to their preoperative baseline, but the FLAIR volume continued to decrease to 74% of the baseline volume. At 6 months, the contrast-enhanced volume showed a decline in size compared to the preoperative volume, with an overall median reduction of 34%. The median FLAIR reduction was 77% at

Table 5.1 Published rates of complications associated with LITT for metastatic in-field recurrence

Series	Number of patients	ICH	Headache	Weakness and paresis	Hydrocephalus requiring intervention	Malignant edema requiring craniotomy
Rao, 2014 [9]	15	6.7%	N/A	6.7%	0%	0%
Ali, 2016 [10]	23 (26 lesions)	0%	N/A	13%	4%	4%
Smith, 2016 [12]	7	0%	N/A	14%	0%	0%
Patel, 2016 [17]	37	3%	N/A	19%	0%	0%
Hernandez, 2018 [4]	59	0%	N/A	15%	0%	0%
Chaunzwa, 2018 [11]	30	13%	N/A	8% (2/25)	0%	0%
Ahluwalia, 2018 [5]	42	2.4%	2.4%	9.6%	0%	0%

ICH intracerebral hemorrhage, *N/A* not available

this time point. Beechar et al. reported similar response, with the median post-contrasted volume increase at 3 months, followed by a decrease at 6–9 months post-LITT [18]. Similarly, the FLAIR volumes at 6 months demonstrated significant reduction compared to pretreatment volumes. Figure 5.5 showcases an example of imaging changes after LITT.

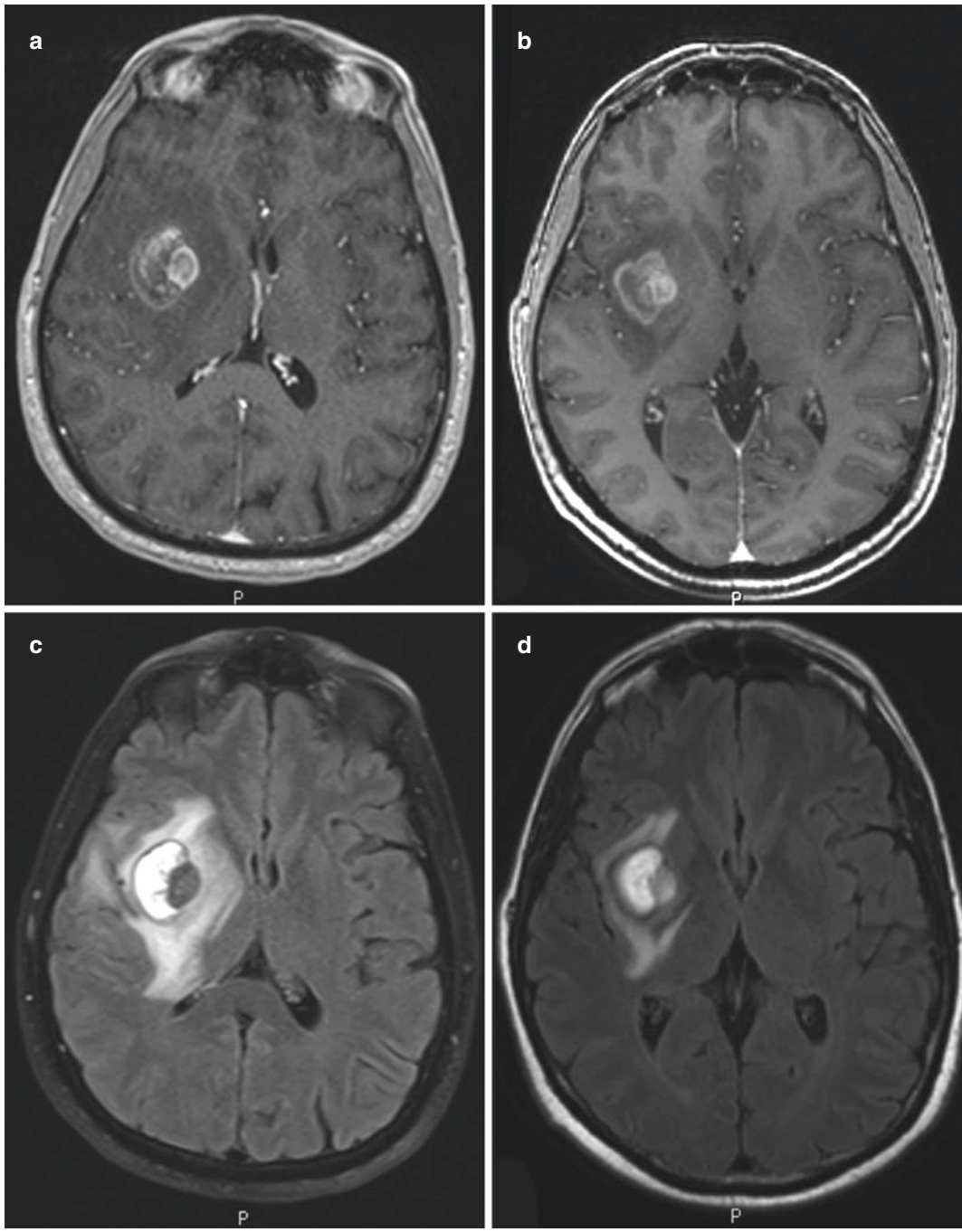

Fig. 5.5 Contrast-enhanced T1W imaging in a patient with metastatic melanoma showed no significant change in the contrast-enhancing lesion size on preoperative imaging (**a**) and postoperative imaging at two weeks (**b**), but a significant reduction in associated FLAIR volumes between preoperative imaging (**c**) and postoperative imaging (**d**)

Compared to these series, Smith et al. reported a similar increase in volume followed by a decrease, but the trend observed in this study appeared to be on a longer time course [12]. Most notably, an increase in the lesional volume was observed in the majority of patients all the way up to their 6-month follow-up, and the volume reduction only began to be observed in the majority of the patients at 12 months. One explanation here may be that this study included patients with both primary and secondary brain tumors failing radiosurgery as opposed to metastatic in-field recurrence alone. The degree and timing of FLAIR signal resolution has also not been well studied or well stratified by pre-LITT lesional sizes. Whereas no significant associations were found with these factors in the LAASR study [5], Beechar et al. found that the smaller preoperative volumes respond better radiographically than those with larger volumes [18]. The authors postulated that this may be because of residual tumor cells that may be left unablated in patients with larger tumor volumes.

Overall, these results cautioned against interpreting LITT failure as an increase in the lesional volume alone. As these studies would suggest, capturing imaging changes at an early time point could lead to an inaccurate interpretation that the treatment has failed. Treatment response may be more accurately represented by a trend in the lesional volumes and the FLAIR volumes over time.

Outcomes of LITT for Metastatic In-Field Recurrence

Local Control and Overall Survival

In 2008, Carpentier et al. described their group's initial experience with real-time MRI-guided LITT for metastatic in-field recurrence [7]. Their series included four subjects who were previously treated with chemotherapy or radiotherapy (SRS or WBRT) who were not candidates for craniotomy. Following LITT treatment using a prototype Visualase System, the authors reported no tumor recurrence within the thermal ablation zone. In patients whose treatment was partial, peripheral recurrence was observed, making the rate of local control approximately 50% overall at 90 days after LITT. In 2013, Torres-Reveron et al. described the use of LITT in six patients who had metastatic in-field recurrence after gamma knife SRS [8]. This was the first series for which all patients with metastatic in-field recurrence underwent a biopsy at the time of the procedure, and pathology was consistent with radiation necrosis in all cases. One patient died of systemic progression, and local control was seen in 80% of the remainder of the patients at 3 months. Rao et al. series reported a similar local control rate of 75.8% at a median follow-up time of 6 months [9]. However, pathology was not available in this series.

In 2016, Ali et al. reported their results in 26 brain metastases and observed local control in 65% of their patients over a median follow-up duration of 4.7 months (range 2.1–26.5 months) [10]. Interestingly, <80% ablation was achieved in patients who were later noted to have a progression of the disease. In patients who underwent postoperative adjuvant SRS for consolidation of <80% ablation with LITT, 100% control rate was obtained, leading to a suggestion that hypofractionated SRS may enhance the efficacy of LITT. Pathology was also not available in this series. During the same year, Smith et al. described single-institution long-term outcomes for 25 patients with biopsy-proven radiation necrosis [12]. The primary targets were metastasis in seven cases. In these patients, mean survival from LITT was 19.2 months, and progression-free survival was 11.4 months.

In the following years, larger multicentered series were added to the body of experiences of LITT as a treatment of metastatic in-field recurrence. Chaunzwa et al. reported an overall survival rate of 52.3% at 6 months [11]. Pathology reports were available in 80% of the cases and radiation necrosis made up 79% of the cases versus tumor regrowth in 21%. Most recently published was the multicentered LAASR study [5]. Here, all patients underwent a biopsy at the time of the surgery, with an approximately equal distribution between radiation necrosis and recurrent tumor (45.2% and 47.6%, respectively).

Progression-free survival was 74% and overall survival was 72% at 6.5 months. Progression-free survival was significantly different at 3 months between the radiation necrosis group and the recurrent tumor group (100% vs 54%, respectively), and trended toward significance at 6 months (90.9% vs 62%, respectively). Of note, patients who had progression of disease after LITT had a lower preoperative baseline KPS score than those without progression (70 vs 90). Table 5.2 summarizes the outcomes of these series.

Heterogeneity may exist in the rate of local control and survival between these series for multiple reasons. In the early series, partial treatment was elected in some cases for safety reasons [19], as was seen in the Carpentier et al. series. Smith et al.'s reported local control rate of 14.3% was a stark difference compared to other series, whose local control rates ranged from 65% to 92.9% [5, 8–11]. It is worth mentioning that Smith's series median follow-up time is longer than most other series (12.1 months vs 3–6 months), and that their progression-free survival was impressive at 11.4 months. As was discussed in the prior section, lesions treated by LITT tend to initially undergo an increase in the volume before a decrease. As a result, one may argue that capturing these volumes at earlier time points could overestimate the rate of LITT failure, and that the local control rate may be better defined as a trend in volume reduction over multiple time points. Unfortunately, the failure of LITT was not uniformly defined. For example, while one study defined local control as the absence of regrowth on MRI associated with increase in FLAIR and no recurrence of symptoms [11], another study defined local control as a decrease in size of the ablated targets, or <25% enlargement in volume compared to volume 24 hours after the procedures, and absence of new enhancement progressing over two MRIs [9]. In many studies, however, definitions were not provided [8, 12].

While their reported local control rate may be different, Smith et al.'s progression-free survival of 11.4 months was not inconsistent with the LAASR data in the patient group with radiation necrosis. This raises the question of whether survival outcomes may be affected by the pathology at hand. Unfortunately, pathology reports were not uniformly available in all series, and a biopsy may not always be feasible due to the differences in the LITT procedure set-up available at each institution. As discussed previously, the LAASR data showed significant difference in progression-free survival between the tumor regrowth and the radiation necrosis cohorts at 3 months and rates of progres-

Table 5.2 Published local control and survival rates in LITT patients with metastatic in-field recurrence

Series	Number of patients	Median follow-up (months)	Local control	PFS	Overall survival	Pathology
Carpentier, 2008 [7]	4	3	50%	33.3%	100%	N/A
Torres-Reveron, 2013 [8]	6	3	80%	66.7%	83%	100% RN
Rao, 2014 [9]	15	6	75.8%	42.9%	57%	N/A
Ali, 2016 [10]	23 (26 lesions)	4.7	65%	65%	100%	N/A
Smith, 2016 [12]	7	12.1	14.3%	14.3%	57.1%	100% RN
Chaunzwa, 2018 [11]	30	6	92.9%	N/A	52.3%	16.7% TR 63.6% RN 20% unknown
Hernandez, 2018 [4]	59	11.2	83.1%	N/A	N/A	N/A
Ahluwalia, 2018 [5]	42	6.5	74%	74%	72%	47.6% TR 45.2% RN 7.1% unknown

N/A not available, *PFS* progression-free survival, *RN* radiation necrosis, *TR* tumor regrowth

sion-free survival remained higher for the radiation necrosis group at 6 months compared to the tumor regrowth group. Thus, from a cancer-control perspective, biopsy at the time of LITT is recommended as long as it does not compromise the ability to perform LITT therapy, since the lower local control rate achieved by LITT in the tumor regrowth group may be curbed by considering postoperative radiation or systemic therapy [5].

Quality of Life (QOL) and Neurological Outcome

Both radiation necrosis and tumor regrowth can present similarly with neurologic deficits from mass effect. In patients with metastatic in-field recurrence, LITT was reported to improve neurological symptoms in approximately 27.3–71.4% of cases [5, 8, 9, 11]. These symptoms included motor deficits, speech difficulties, and ambulatory status, among others. The median time to symptom resolution was reported to be 2 weeks in the series by Chaunzwa et al. [11].

Overall, the functional outcomes following a LITT surgery for metastatic in-field recurrence have focused on stabilization of the KPS score. Untreated, both radiation necrosis and tumor regrowth have been seen to cause progressive decline in KPS due to neurological impairment. This decline often results in cessation of systemic cancer therapy and transition of the patient to hospice care regardless of lesional pathology. Currently, limited data are available to compare the functional outcomes of LITT to other treatment modalities. However, early results suggest that a successful LITT procedure may preserve the KPS score, improve quality of life, and preserve cognition in many cases. In several series, preservation or improvement of the KPS score was reported in 43.3–75% of the patients, with the median follow-up time ranging from 3 to 6.5 months (Table 5.3). Similar to the other treatment modalities, these numbers may be affected by the patients' baseline KPS scores. For example, in the series by Chaunzwa et al., KPS score preservation was much more likely for those with a preoperative KPS score of 70 or higher (59%), compared to 100% of those with a preoperative KPS score of 60 who all deteriorated and died after LITT [11]. Similarly, the LAASR study had a median baseline KPS score of 85 and reported a stable to improved KPS score in 60% of their patients at 6 months post-LITT [5].

Early results have also reported no significant impact of LITT on cognition, as measured by the pre- and postoperative Hopkins Verbal Learning Test-Revised (HVLT-R) scores and Mini-Mental State Examination (MMSE) scores [5]. Furthermore, although a decline in Social Well-Being scores and Emotional Well-Being scores overall has been reported [5], Smith et al. found that LITT results in statistically significant improvement of overall mental health and vitality at 12 months, as measured by the Short-Form Health Survey (SF-36) [12].

In practice, functional outcomes and mental health effects in patients with metastatic in-field recurrence may be influenced by multiple factors other than LITT treatment alone. These factors can include baseline functional status and mental health, duration, type and success of systemic

Table 5.3 Published neurological outcomes in LITT patients with metastatic in-field recurrence

Series	Number of patients	Median follow-up (months)	Percent with neurological improvement	Percent with stable or improved KPS
Carpentier, 2008 [7]	4	3	N/A	75%
Torres-Reveron, 2013 [8]	6	3	67%	N/A
Rao, 2014 [9]	15	6	71.4%	N/A
Chaunzwa, 2018 [11]	30	6	48%	43.3%
Ahluwalia, 2018 [5]	42	6.5	27.3%	60%

KPS Karnofsky Performance Score, *N/A* not available

cancer therapy, and the presence of disease progression elsewhere. Larger series with a longer follow-up time are needed to fully understand the long-term effects of LITT on patient's mental health, functional status, and quality of life.

Steroid Dependence

Steroids are an effective tool to treat symptomatic perilesional edema but are often associated with significant adverse effects when used chronically. These adverse effects include weight gain, hypertension, difficult-to-control diabetes, impaired wound healing, GI ulceration, osteoporosis, and infection. In addition, it is thought that immunosuppression facilitates the progression of cancer [20]. Therefore, the inability to wean steroids is one of the most robust indications today for the use of LITT [11]. Most studies reported that following LITT, the majority of patients are able to wean off steroids within one to two months [8–11, 21], with the percentages ranging from 66.7% of patients within one month [21] to 100% within two months [8]. Chaunzwa et al. cited detailed information on preoperative and postoperative steroid usage and reported that 73.3% of their patients were able to stop steroids, with the median time to cessation of 4.5 weeks [11]. Both lesional volume and the corresponding FLAIR volume were recorded in this study post-LITT. Their results suggested that although the lesional volume as measured by contrast-enhanced images may initially increase at 6 weeks, a FLAIR reduction of as much as 36% was seen at that time, with the trend in FLAIR reduction continuing at 6 months follow-up. A larger reduction in FLAIR volume was found to be associated with an increased ability to stop steroids. In a study by Hernandez et al., 25% of patients with preoperative steroid use were continued on steroids indefinitely, whereas only approximately 13.5% with no preoperative steroid use had to be continued on steroids post-LITT [4]. The authors concluded that LITT should be offered prior to metastatic in-field recurrence becoming symptomatic, as patients with preoperative steroids use tended to remain dependent on steroids postoperatively and were more likely to experience post-LITT complications.

Interestingly, only 31% of patients in the LAASR study were able to stop or reduce steroids by their 3-month follow-up [5]. Although the authors did not offer an explanation to this finding, it is worth mentioning that 42.9% of the patients in this series were dependent on steroids use at baseline, compared to 26.7% as reported by Rao et al. [9], or 33% as reported by Chaunzwa et al. [11]. Moreover, the average pre-LITT volume in the LAASR study was larger at 6.4 cm^3 compared to 3.7 cm^3 reported by Rao et al., which may explain the smaller percentage of patients being able to stop steroids. The ability to wean steroids was not statistically significantly different between the radiation necrosis group and the tumor regrowth group [5]. Patel et al. proposed that patients who required high-dose steroids preoperatively may not benefit as much from LITT [13]. The effect of preoperative steroid dosages on neurological outcomes was not investigated.

Our institutional experiences are in line with those published by Hernandez et al. In our experience, offering LITT early before patients become dependent on steroid and while the targets and the surrounding FLAIR are small best facilitates the ability to wean off steroids post-LITT. In addition, obtaining an early post-LITT MRI within 2 weeks has also facilitated decision-making regarding the length of steroid taper. In some patients, a significant visible decrease in the amount of perilesional edema was seen by 2 weeks post-LITT and anecdotally in these patients, even if immunotherapy is re-initiated, these patients seemed to be able to remain off steroids without recurrence of their symptoms and eventual resolution of the LITT lesion on imaging.

LITT as an Alternative to Craniotomy

In the early years, LITT was initially proposed for deep targets where a craniotomy may incur excess morbidity. However, LITT is now increasingly performed for easy-to-access targets due to it being perceived as minimally invasive. In our experience, patients are much more likely to agree to LITT than a craniotomy when offered the option of both choices, even with the knowledge that a craniotomy may be needed as a sal-

vage therapy should LITT fail. Only one single-institution retrospective study has been published comparing LITT to craniotomy for the management of metastatic in-field recurrence. This series included a total of 75 patients: 41 (55%) treated with craniotomy and 34 (45%) treated with LITT. No significant difference was found between the two surgical options in the ability to wean off steroids, the ability to initiate or resume postoperative immunotherapy, progression-free survival (PFS), or overall survival (OS) [22]. Given the retrospective nature of this study, the overall mean volume treated by craniotomy was larger than that treated by LITT (8.1 cm^3 vs 4.1 cm^3). Craniotomy was therefore found to result in a higher rate of relief of preoperative symptoms. To control for the volume difference between the two groups, 14 patients with lesions >3 cm diameter were excluded in the subanalysis. Overall survival and local control were even more significantly associated with the pathology of the lesion rather than the type of procedure, with greater PFS and OS reported in the radiation necrosis group compared to the recurrent tumor group. A larger randomized prospective study of more directly comparable targets is needed in order to validate these results.

Disruption of Blood-Brain Barrier after LITT

Other than the direct effect of laser heat on the lesion itself, early results by Leuthardt et al. have demonstrated a potentially useful unintended effect of LITT in disrupting blood-brain barrier (BBB) in glioma patients [23]. In this study, pharmacokinetic parameters and brain-specific enolase (BSE) were measured following a LITT procedure. The authors found that a forward volume transfer constant reflecting capillary permeability and peritumoral BBB disruption peaked immediately after LITT and was persistently elevated for another 4 weeks. Serum BSE, on the other hand, demonstrated a steady rise after LITT, peaked by 2–3 weeks, and remained elevated for up to 6 weeks. The authors concluded that there is a prolonged window after LITT during which BBB is reversibly disrupted. Reversible BBB disruption may conceivably play a role in enhancing the effectiveness of a therapeutic agent after LITT for many patients with metastatic in-field recurrence. A study is now ongoing looking to see if a similar effect might be found after LITT for metastatic in-field recurrence.

Conclusion and Future Development

In summary, multiple retrospective and prospective series have demonstrated that LITT offers a safe and efficacious treatment modality for patients with metastatic in-field recurrence. The indications for LITT continue to expand and highlight some of the strengths of LITT, including accessibility to deep-seated targets, minimally invasive access, stabilization of good KPS scores, ability to wean off steroids, and favorable cognitive, functional, and survival outcomes. Better outcomes are obtained after LITT if lesions are treated when they are smaller in size thus allowing for more complete ablation of the lesion. Larger prospective series with longer follow-up periods comparing LITT to other treatment modalities are needed to clarify the role of LITT in an armamentarium of options available for treating patients with metastatic in-field recurrence. Futures studies might investigate steroid use and its correlation to imaging changes, local changes in tumor and brain microenvironment after LITT, and the relationship of these changes to post-LITT therapies. In addition, techniques by which to ensure total ablation of larger lesions also need to be developed.

References

1. Sneed PK, Mendez J, Vemer-van den Hoek JG, Seymour ZA, Ma L, Molinaro AM, et al. Adverse radiation effect after stereotactic radiosurgery for brain metastases: incidence, time course, and risk factors. J Neurosurg. 2015;123(2):373–86. https://doi.org/10.3171/2014.10.JNS141610.
2. Miyatake S, Nonoguchi N, Furuse M, Yoritsune E, Miyata T, Kawabata S, et al. Pathophysiology, diagnosis, and treatment of radiation necrosis in the brain. Neurol Med Chir (Tokyo). 2015;55(Suppl 1):50–9.
3. Furuse M, Nonoguchi N, Kawabata S, Miyatake S, Kuroiwa T. Delayed brain radiation necrosis: patho-

logical review and new molecular targets for treatment. Med Mol Morphol. 2015;48(4):183–90.
4. Hernandez RN, Carminucci A, Patel P, Hargreaves EL, Danish SF. Magnetic resonance-guided laser-induced thermal therapy for the treatment of progressive enhancing inflammatory reactions following Stereotactic radiosurgery, or PEIRs, for metastatic brain disease. Neurosurgery. 2019;85(1):84–90. https://doi.org/10.1093/neuros/nyy220.
5. Ahluwalia M, Barnett GH, Deng D, Tatter SB, Laxton AW, Mohammadi AM, et al. Laser ablation after stereotactic radiosurgery: a multicenter prospective study in patients with metastatic brain tumors and radiation necrosis. J Neurosurg. 2018;130(3):804–11. https://doi.org/10.3171/2017.11.JNS171273.
6. Rosomoff HL, Carroll F. Reaction of neoplasm and brain to laser. Arch Neurol. 1966;14(2):143–8.
7. Carpentier A, McNichols RJ, Stafford RJ, Itzcovitz J, Guichard JP, Reizine D, et al. Real-time magnetic resonance-guided laser thermal therapy for focal metastatic brain tumors. Neurosurgery. 2008;63(1 Suppl 1):ONS21–9. https://doi.org/10.1227/01.neu.0000335007.07381.df.
8. Torres-Reveron J, Tomasiewicz HC, Shetty A, Amankulor NM, Chiang VL. Stereotactic laser induced thermotherapy (LITT): a novel treatment for brain lesions regrowing after radiosurgery. J Neuro-Oncol. 2013;113(3):495–503. https://doi.org/10.1007/s11060-013-1142-2.
9. Rao MS, Hargreaves EL, Khan AJ, Haffty BG, Danish SF. Magnetic resonance-guided laser ablation improves local control for postradiosurgery recurrence and/or radiation necrosis. Neurosurgery. 2014;74(6):658–67. https://doi.org/10.1227/NEU.0000000000000332.
10. Ali MA, Carroll KT, Rennert RC, Hamelin T, Chang L, Lemkuil BP, et al. Stereotactic laser ablation as treatment for brain metastases that recur after stereotactic radiosurgery: a multiinstitutional experience. Neurosurg Focus. 2016;41(4):E11.
11. Chaunzwa TL, Deng D, Leuthardt EC, Tatter SB, Mohammadi AM, Barnett GH, et al. Laser thermal ablation for metastases failing radiosurgery: a multicentered retrospective study. Neurosurgery. 2018;82(1):56–63. https://doi.org/10.1093/neuros/nyx142.
12. Smith CJ, Myers CS, Chapple KM, Smith KA. Long-term follow-up of 25 cases of biopsy-proven radiation necrosis or post-radiation treatment effect treated with magnetic resonance-guided laser interstitial thermal therapy. Neurosurgery. 2016;79(Suppl 1):S59–72.
13. Patel PD, Patel NV, Davidson C, Danish SF. The role of MRgLITT in overcoming the challenges in managing infield recurrence after radiation for brain metastasis. Neurosurgery. 2016;79(Suppl 1):S40–58.
14. Patel NV, Jethwa PR, Barrese JC, Hargreaves EL, Danish SF. Volumetric trends associated with MRI-guided laser-induced thermal therapy (LITT) for intracranial tumors. Lasers Surg Med. 2013;45(6):362–9. https://doi.org/10.1002/lsm.22151.
15. Patel PD, Hargreaves EL, Danish AF, Weiner J, Danish SF. Volumetric trends of progressive infield recurrences after stereotactic radiosurgery of metastatic intracranial tumors. J Radiosurg SBRT. 2018;5(4):293–304.
16. Nath SK, Sheridan AD, Rauch PJ, Yu JB, Minja FJ, Vortmeyer AO, et al. Significance of histology in determining management of lesions regrowing after radiosurgery. J Neuro-Oncol. 2014;117(2):303–10. https://doi.org/10.1007/s11060-014-1389-2.
17. Patel P, Patel NV, Danish SF. Intracranial MR-guided laser-induced thermal therapy: single-center experience with the Visualase thermal therapy system. J Neurosurg. 2016;125(4):853–60.
18. Beechar VB, Prabhu SS, Bastos D, Weinberg JS, Stafford RJ, Fuentes D, et al. Volumetric response of progressing post-SRS lesions treated with laser interstitial thermal therapy. J Neuro-Oncol. 2018;137(1):57–65. https://doi.org/10.1007/s11060-017-2694-3.
19. Carpentier A, McNichols RJ, Stafford RJ, Guichard JP, Reizine D, Delaloge S, et al. Laser thermal therapy: real-time MRI-guided and computer-controlled procedures for metastatic brain tumors. Lasers Surg Med. 2011;43(10):943–50. https://doi.org/10.1002/lsm.21138.
20. Stewart T, Tsai SC, Grayson H, Henderson R, Opelz G. Incidence of de-novo breast cancer in women chronically immunosuppressed after organ transplantation. Lancet. 1995;346(8978):796–8.
21. Rammo R, Asmaro K, Schultz L, Scarpace L, Siddiqui S, Walbert T. The safety of magnetic resonance imaging-guided laser interstitial thermal therapy for cerebral radiation necrosis. J Neuro-Oncol. 2018;138(3):609–17. https://doi.org/10.1007/s11060-018-2828-2.
22. Hong CS, Deng D, Vera A, Chiang VL. Laser-interstitial thermal therapy compared to craniotomy for treatment of radiation necrosis or recurrent tumor in brain metastases failing radiosurgery. J Neuro-Oncol. 2019;142(2):309–17. https://doi.org/10.1007/s11060-019-03097-z.
23. Leuthardt EC, Duan C, Kim MJ, Campian JL, Kim AH, Miller-Thomas MM, et al. Hyperthermic laser ablation of recurrent glioblastoma leads to temporary disruption of the peritumoral blood brain barrier. PLoS One. 2016;11(2):e0148613. https://doi.org/10.1371/journal.pone.0148613.

LITT Treatment of High-Grade Gliomas

6

Daria Krivosheya, Gene H. Barnett, and Alireza M. Mohammadi

Introduction

Glioblastoma (GBM) is the most common malignant primary brain tumor, accounting for 14% of all newly diagnosed primary brain tumors, and with all malignant gliomas, accounting for about 25% [1]. Despite much effort extended to treat GBM, the median survival of patients with newly diagnosed tumors remains poor, in the range of 16 months, with standard treatment using radiation and temozolomide [2, 3]. Although newer interventions such as tumor-treating fields [4] or vaccines [5] are available and being actively studied, their impact on survival is measured in months rather than years.

The challenge of treating GBM results from the inherent nature of the tumor. Having originated from glial origins, tumor cells migrate down white matter pathways spreading significant distances at times and resulting in satellite tumor formation [6]. Related to this are the limitations of surgical resection of GBM. Regardless of resection of all visible tumors, the remaining infiltrating cells will result in recurrence. Despite this limitation, a number of studies have demonstrated a survival advantage for patients undergoing aggressive surgical resection over biopsy only for diagnosis when both options were followed by radiation and chemotherapy [2, 7, 8]. Furthermore, two large retrospective series correlated the residual volume of tumor with patient survival and showed incremental improvement in survival, which became significant at 78% and 89% of tumor resection with maximal benefit at greater than 98% and 95% of tumor resection [9, 10]. Prospective randomized controlled studies looking at the use of intraoperative adjuncts such as 5-aminolevulinic acid (5-ALA) and intraoperative MRI (iMRI) also showed that maximizing resection of GBM results in improved survival [11, 12]. The infiltrative nature of the tumor was further highlighted in a recent study showing that when, in addition to resection of the contrast-enhancing portion of the tumor, resection of greater than 50% of the surrounding high T2 signal on MRI was achieved, patient survival was further prolonged [13]. Therefore, much emphasis is presently made to maximize the extent of tumor resection in patients with GBM.

D. Krivosheya · A. M. Mohammadi (✉)
Department of Neurosurgery, Cleveland Clinic, Cleveland, OH, USA
e-mail: mohamma3@ccf.org

G. H. Barnett
Rose Ella Burkhardt Brain Tumor and Neuro-Oncology Center, Department of Neurosurgery, Cleveland Clinic, Cleveland, OH, USA

V. L. Chiang et al. (eds.), *Laser Interstitial Thermal Therapy in Neurosurgery*,
https://doi.org/10.1007/978-3-030-48047-9_6

There are a number of challenges, however, related to GBM resection, one of which is related to tumor location. Many gliomas are adjacent to or involve eloquent cortical or subcortical areas, making gross total resection of the tumor impossible without producing a new neurological deficit. This limits the degree of resection that can be achieved in these patients because a new postoperative neurological deficit can significantly shorten patient survival and, thus, should be avoided [14]. Other tumors involve deep subcortical structures that are difficult to access surgically and are traditionally offered only a biopsy, as effective cytoreduction cannot be achieved without neurological morbidity. Other challenges relating to this patient population are that many glioma patients are elderly and frail and may not be able to medically tolerate a craniotomy for tumor debulking, or they may have difficulty with wound healing resulting in wound infection and breakdown complications especially given the need for subsequent chemotherapy and radiation treatments.

The search for new ways of achieving maximal cytoreduction in these difficult patients has led to the exploration of other treatment modalities. Among these, laser interstitial thermal therapy (LITT) is of great interest as a minimally invasive technique. It has the advantage of being able to reach deep and difficult-to-access targets with minimal cortical injury, and through a small scalp stab incision, thus, minimizing the surgical footprint and avoiding wound healing complications. Moreover, unlike ionizing radiation, laser ablation therapy so far has no known cumulative toxicity and can be repeated in patients with recurrent tumors. These advantages of the LITT technique have sparked great enthusiasm in exploring its use to treat high-grade gliomas in an effort to maximize survival. This chapter examines the literature to date on the use of LITT in the treatment of high-grade gliomas.

Clinical Vignette (Fig. 6.1).

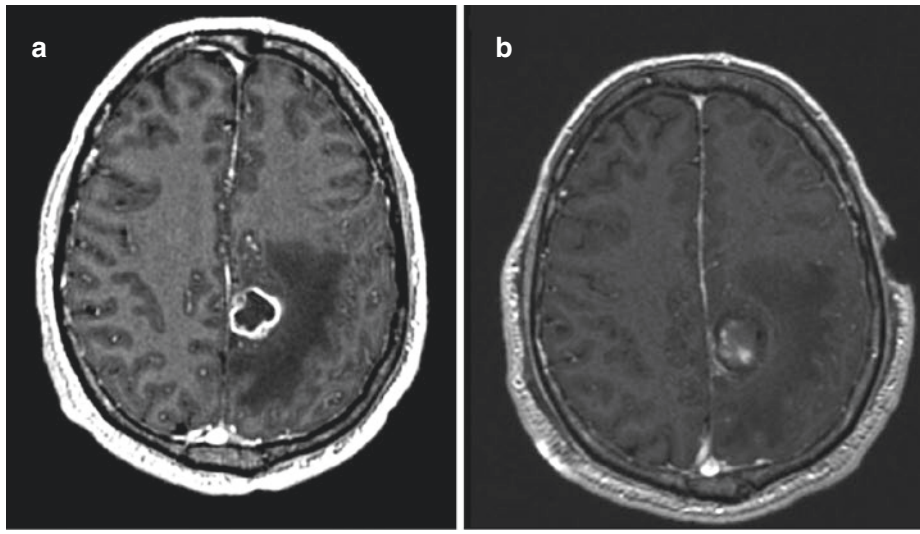

Fig. 6.1 Clinical vignette: A 41-year-old gentleman diagnosed with a left frontal glioblastoma (**a**) underwent biopsy and laser ablation with complete ablation of the lesion (**b**) followed by radiation/temozolomide. He had resolution of the lesion at 1-year (**c**) and 2-year (**d**) follow-up. He was stable after 7 years at the primary site (**e**), however, he developed a new focus of GBM (biopsy-proven) remote from the initial tumor in the lateral left frontal lobe (**f**)

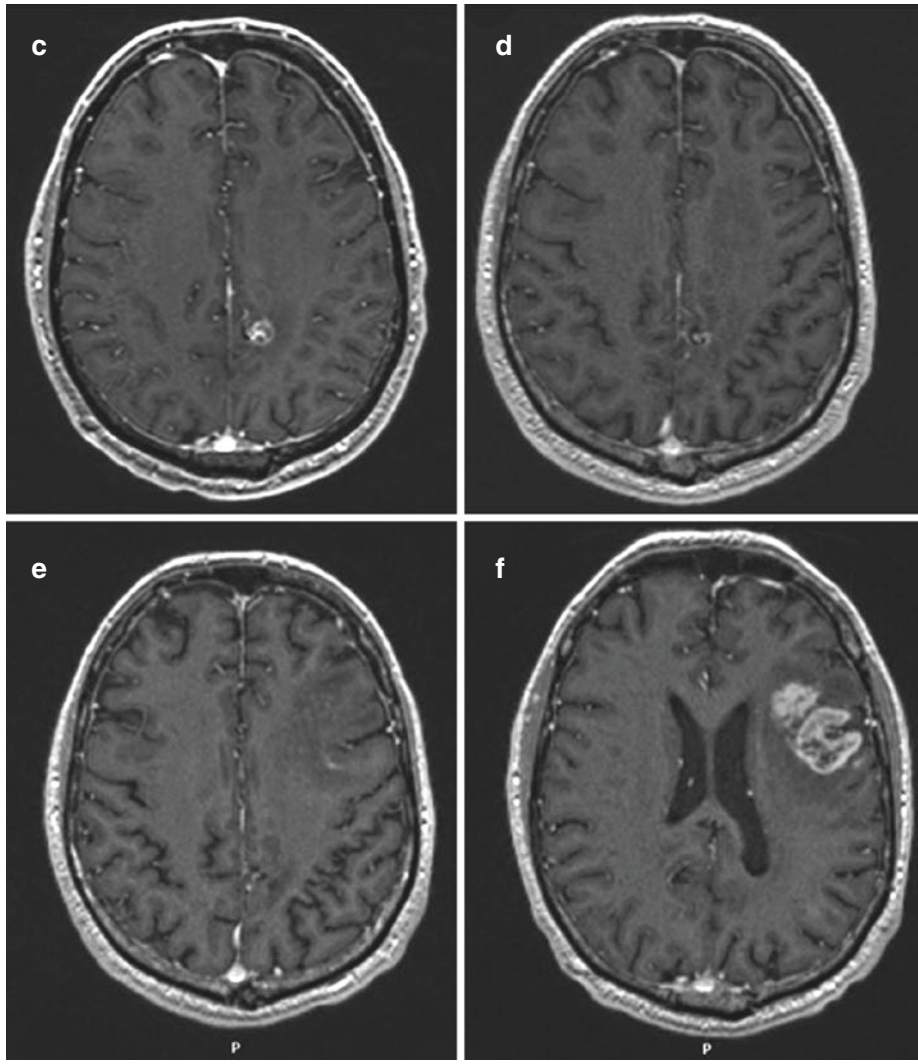

Fig. 6.1 (continued)

LITT as a Treatment Modality for Cytoreduction

Early experience with using laser thermal therapy was reported by Jethwa et al. in 2012 where 20 tumors (six glioblastomas and one anaplastic astrocytoma) were treated with the Visualase System (Medtronic) [15]. They reported good ablation of the tumors with only one complication among the glioma cohort where the patient developed intractable postoperative edema necessitating decompressive craniectomy. Indications for the LITT procedure included tumor recurrence post-surgery and adjuvant treatment, poor craniotomy candidates, or deep location of the tumor that was inaccessible to open surgery, and they reported an average hospital stay of one day post-procedure. It was concluded that LITT is a feasible salvage technique in patients with malignant glial neoplasms by destroying tumor tissue in a minimally invasive manner with a low complication rate.

To better define the highest effective treatment dose, Sloan et al. conducted a prospective multicenter phase I study in ten patients with recurrent high-grade gliomas [16]. Using the NeuroBlate System (Monteris Medical), which allows monitoring of the extent of thermal damage using thermal damage threshold (TDT) lines, three heat thresholds were studied: tissue treated to the equivalent of 43 °C for 2, 10, and 60 minutes defined as the yellow, blue, and white TDT lines, respectively. This was a dose-escalation study where the first three patients had their tumors treated to the yellow TDT line and were observed for signs of toxicity. Given that no toxicity was observed in the following 14 days, the next patient cohorts were then treated with the higher doses. Patients were followed for 6 months or until death. In this study, the average size of the treated tumors was 6.8 cm^3, and an average of 78% of tumor volume was encompassed by the treatment TDT lines. Two patients developed transient postoperative neurological deficits, and two patients suffered neurological deterioration after the procedure, both in the highest dose treatment group (43 °C for 60 minutes). The median overall survival (OS) in the study was substantially greater (at 316 days) when compared to historical studies typically reporting 90–150 days [17]. Furthermore, progression-free survival (PFS) at 6 months was double the historical average (15%) at greater than 30%. In summary, this study identified the blue TDT line as the optimal treatment level to achieve tumor ablation while avoiding complications. Furthermore, they showed that LITT is well tolerated and can be an effective treatment modality that may result in prolonged patient PFS and OS.

The impact of LITT on tumor control was next examined in a retrospective multicenter study conducted by Mohammadi et al. [18]. Thirty-four patients with high-grade gliomas treated at four institutions were identified. Of these, 19 patients were treated with laser thermal therapy as first-line surgical treatment, and 16 patients had recurrent tumors. All patients had tumors in difficult locations that could not be effectively treated with open surgical resection. The average follow-up in the study was 7.2 months, with 71% of tumors progressing at the latest follow-up and 35% of patients dying. Median PFS in the study was 5.1 months, and while the median OS was not reached in the study, the projected OS at 1 year was 68%. To examine the role of cytoreduction, patient outcomes were correlated with the extent of TDT line coverage of the tumor. Favorable PFS of 9.7 months (compared to 4.6 months in remaining cases) was seen in patients where less than 0.05 cm^3 of the tumor volume was not covered by the yellow line and where the volume between the yellow and blue lines was less than 1.5 cm^3. Smaller tumor size is also positively correlated with good outcome, as it is easier to ensure complete coverage of smaller targets. Furthermore, this study looked at the pattern of tumor recurrence after treatment and showed that in the majority of cases (12 patients) the tumor recurred at the edge of the treated volume, with five cases recurring within the treated volume, five patients recurring within 2 cm of the treated area, and only one patient having a remote focus of recurrence. Thus, this study showed the importance of maximizing the extent of tumor coverage to prolong patient survival—analogous to maximizing the extent of tumor resection during craniotomy.

Thomas et al. retrospectively looked at their single-institution outcomes of patients with GBM treated with LITT therapy [19]. They identified eight newly diagnosed patients and 13 patients with recurrent tumors that underwent laser ablation using the Visualase System. Among the newly diagnosed patients, none of the patients responded to treatment and displayed radiographic or clinical progression after treatment with median PFS of 1.5 months and median OS of 8 months. These results are similar to those seen in patients who undergo biopsy only for diagnosis followed by standard radiation and chemotherapy. In the recurrent GBM group, the average time to treatment after diagnosis was 16 months. There were no new postoperative neurological deficits, but one patient developed postoperative status epilepticus. The median time to clinical or radiographic progression was 5 months, and median OS was greater than 7 months. Five patients in this group had radio-

graphic response post-treatment with decrease in tumor size. They had smaller tumor sizes (8.5 vs 17.4 cc) and 60% had IDH1 mutation. The median time to radiographic tumor progression was 9 months. Overall, with the two patient populations being quite different, they concluded that LITT is a good modality for the treatment of recurrent GBM and the use of laser thermal therapy in newly diagnosed tumors needed further investigation.

A recent meta-analysis of the use of LITT in newly diagnosed high-grade gliomas was performed by Ivan et al. [20]. They identified 25 patients across four publications that reported clinical outcomes of newly identified WHO grade 3 and grade 4 gliomas. The mean tumor volume was 16.5 cm^3. The extent of LITT coverage was reported in nine patients with an average of 82.9%. Postoperative outcomes were reported in 13 patients with no new permanent postoperative deficits and with only 2 major complications, including a fulminant CNS infection and postoperative cerebral edema requiring hemicraniectomy in the immediate postoperative period. The mean follow-up in the study was 7.6 months, with 12 patients still followed or lost to follow-up. The mean PFS was found to be 5.1 months and median OS was 14.2 months which is similar to survival reported in other studies for newly identified HGG ranging from 8.5 to 14.5 months. Therefore, upfront treatment of HGG followed by standard of care chemotherapy and radiation may result in outcomes comparable to those of open surgical resection.

Lee et al. performed a meta-analysis of the use of laser thermal therapy in recurrent high-grade gliomas [21]. They identified six articles and included 63 patients with 64 lesions treated. Tumor size ranged from 0.37 to 68.9 cm^3. The range of tumor coverage was between 78% and 100%. Seven patients developed a new postoperative neurological deficit (12%). In addition, 3 patients suffered a vascular injury (3%), and wound infection was reported in one patient (2%). Due to highly variable outcomes reported across the included studies, no meaningful outcome measure could be generated in the study and it was concluded that LITT is a relatively safe treatment modality that results in accurate ablation of tumor tissue with complication rates similar to open craniotomy.

Butterfly gliomas involving the corpus callosum are particularly challenging to treat and are generally considered non-operative tumors. Therefore, a minimally invasive biopsy/LITT therapy approach that would not just provide a tissue specimen but also deliver thermal energy providing cytoreduction is an appealing strategy. Recently, a multicenter retrospective review of patients harboring glioblastomas in the corpus callosum was carried out [22]. Fifteen patients with newly identified or recurrent glioblastomas were identified. Of these, nine were diagnosed de novo. IDH1 mutation was positive in 42% of these patients. The mean tumor volume was 18.7 cm^3 ranging from 0.3 to 62.8 cm^3, and greater than 90% tumor coverage with the blue TDT lines was achieved. Median PFS was 3.4 months, but the median OS was 18.2 months with two patients surviving longer than 40 months after the procedure. Adjusted OS that excluded patients with recurrent glioblastomas was 8.5 months. Median survival was significantly longer for recurrent tumors compared to newly diagnosed (20.0 vs 7.0 months). Complications occurred in six patients: two developed permanent postoperative hemiparesis, one patient had intracerebral hemorrhage, one patient developed hydrocephalus, one patient was re-admitted with ventriculitis, and one patient had significant cerebral edema requiring hemicraniectomy. Larger tumor volume size (>15 cm^3) positively correlated with the increased rate of postoperative complication. The authors concluded that LITT is an effective and safe procedure for patients with GBM involving the corpus callosum providing a similar survival advantage as open surgical resection compared to biopsy alone (7.0 vs 3.5 months) [23].

Finally, the most recent analysis of patients with newly identified GBM diagnosed by biopsy and treated with laser ablation was undertaken retrospectively across multiple centers including Cleveland Clinic, Washington University of St Louis, and Yale University [24]. The outcomes of 24 patients included in the study were compared

to a propensity-matched cohort of biopsy-only patients from Yale and Duke University—institutions that were not routinely performing LITT for newly diagnosed high-grade gliomas at that time. The two groups were matched based upon patient factors such as age (<70 vs ≥70) as well as tumor characteristics such as location (deep vs lobar) and volume (<11 cm^3 vs ≥11 cm^3). Multifocal lesions, as well as brainstem and infratentorial lesions, were excluded from the study. All patients were treated with the NeuroBlate System. Both groups received postoperative standard of care chemotherapy and radiation treatment. Primary end points were OS and PFS. Other primary end points were disease-specific (DS) OS and PFS, where patients with death because of medical causes are censored at the time of death as a competitor for tumor progression. Across the study, neither median PFS nor OS showed any significant difference between the laser ablation group and the biopsy cohort (PSF 4.3 vs 5.9 months, OS 14.4 vs 15.8 months, respectively). When the laser ablation group was subdivided into three treatment groups based on the extent of coverage of the tumor into favorable, intermediate, and unfavorable, the favorable coverage group was associated with significantly better PFS, DS-PFS, DS-OS, compared to other groups but no difference in OS. Increased age and tumor volume were risk factors for decreased OS. Overall, the multivariable analysis demonstrates that the extent of coverage in laser ablation treatment of newly identified GBM correlates with PFS, DS-OS, and DS-PFS, thus supporting the effectiveness of this modality in the treatment of appropriately selected newly identified glioblastomas.

Combining LITT with Surgical Approaches

LITT can be used as a stand-alone therapy. When treating larger lesions, however, there is a higher incidence of postoperative tumor swelling and herniation requiring decompressive craniotomy. One way to minimize the risk of herniation and postoperative emergency is to perform minimally invasive partial tumor debulking purely to relieve mass effect immediately after laser ablation. Wright et al. retrospectively looked at their outcomes in 9 patients with large (>10 cm^3) high-grade gliomas and one patient with malignant melanoma metastasis where laser ablation was followed by trans-sulcal partial resection of the treated lesion [25]. The median tumor volume enclosed by the yellow line was 83% and 73% for the blue line. They had one postoperative infection, two patients with worsening of neurological function, one of which was transient, and one patient with postoperative hydrocephalus. They found that the median progression-free survival in these patients was 9.3 months, which favorably compared to the 4.6 months in a similar cohort of patients treated with LITT alone [18]. Furthermore, the median OS was 16.1 months, which was longer than 10.6 months (316 days) reported in a recent study, despite smaller tumor size in the latter (6.8 cm^3) [16]. Overall, they concluded that in patients with high-grade glioma with tumors greater than 10 cm^3 that are difficult to access with conventional surgical techniques, laser ablation followed by partial resection may provide a survival advantage in this patient population. Further studies with higher numbers of patients would be needed to test this treatment algorithm.

Disruption of Blood-Brain Barrier

Effective delivery of a chemotherapeutic agent to high-grade gliomas is difficult due to the presence of the blood-brain barrier (BBB), which limits the size and composition of molecules that can be used to treat brain tumors. By disrupting the BBB, one could improve the delivery of chemotherapeutic agents to the tumor. Different strategies geared to disrupt or bypass BBB have included convection-enhanced drug delivery through catheters implanted into the tumor, intra-arterial mannitol injections, and focused ultrasound. Recent evidence suggests that laser interstitial therapy may also affect tissues sur-

rounding the treatment zone resulting in transient endothelial cell dysfunction.

Laser ablation produces several zones of damage. The core region consists of a coagulum of permanently and irreversibly damaged tissue. The tissues surrounding the coagulum are exposed to lower temperatures that reach 40 °C. These lower temperatures are insufficient to result in cell death but instead temporarily disrupt cellular physiological functions, and as a consequence may result in transient BBB disruption. This suggestion was formulated following the observation of the presence of a peripheral ring of contrast enhancement on postoperative MRI imaging of lesions treated with laser ablation. This finding was speculated to represent a region of BBB disruption and was further supported in a rodent model. Evans blue dye, a compound that under normal physiological conditions does not cross the BBB, when injected intravenously, was observed to accumulate on the periphery of the lesion treated with laser ablation [26].

Recently, Leuthardt et al. used an advanced MRI methodology to demonstrate blood-brain barrier disruption [27]. They used serial imaging with dynamic contrast-enhanced MRI in 14 patients that were treated with laser ablation to measure the transfer coefficients (Ktrans) on the periphery of the produced lesion. Using Ktrans values as a measure of permeability, they found that Ktrans coefficients peaked immediately after the treatment and then gradually declined over the following 4 weeks. In addition, they measured serum brain-specific enolase (BSE) as a marker of BBB breakdown. They found that the levels gradually increased postoperatively, peaking at 3 weeks, followed by a gradual decline and normalization at 6 weeks. These findings taken together indicate that there is a zone of BBB breakdown that lasts several weeks following laser ablation procedure. Thus, the administration of chemotherapeutic agents in the immediate postoperative period may have greater penetration into the residual infiltrating tumor and have the potential to exert a greater clinical effect.

Sensitization to Radiation

Radiation therapy is one of the cornerstones of glioma treatments and has been shown to prolong patient survival. There have been several studies that suggested that hyperthermia may sensitize tumor cells to radiation therapy and increase the clinical effect of both treatments [28–30]. The synergistic effects of hyperthermia and radiation were studied in vitro and in a rodent model with mice bearing glioma xenografts [31]. Glioma stem cell cultures that were exposed to 42 °C for 1 hour followed by radiation showed decreased survival, proliferation and DNA repair, and promoted cell death. These effects were greatest in cultures exposed to both radiation and heat. On the molecular level, they observed decreased levels of AKT phosphorylation, a key protein kinase in a major growth and survival pathway, in cells exposed to both therapies, and rescue of phosphorylation levels resulted in improved cell survival in the face of both radiation and hyperthermia. In the in vivo glioma model of mice bearing glioma xenografts, exposing animals to both heat and radiation consistently reduced tumor size and improved animal survival. Further studies are needed to explore the clinical potential of combining hyperthermia with radiation treatment in humans.

Future Direction

Larger multicenter prospective studies are underway or planned to further evaluate the safety and efficacy of laser ablation in different subtypes of newly diagnosed and recurrent gliomas. Aside from the cytoreductive benefit of laser ablation that is comparable to surgery, additional investigations are also needed to confirm any potential clinical benefit of blood-brain barrier disruption or sensitization to radiation in the actual clinical setting to further validate these initial promising reports. Moreover, with recent enthusiasm in immunotherapy of glioma, the effect of releasing a large number of antigens into the bloodstream trig-

gered by laser ablation, in combination with checkpoint inhibitors to enhance immune response or other immunotherapies, is another interesting subject. Several ongoing studies are currently investigating this effect of laser therapy, and initial results will be available in the next few years.

Conclusion

In summary, there is increasing evidence for the use of LITT to treat newly identified and recurrent high-grade gliomas, especially for deep-seated and difficult-to-access tumors. LITT appears to result in prolonged progression-free survival, and in some cases, overall survival. Furthermore, the combination of laser ablation and subsequent trans-sulcal tumor resection may further improve the survival of patients with larger tumors. Additional benefits of laser therapy may include temporary disruption of blood-brain barrier and improved delivery of chemotherapeutics, as well as sensitization to radiation. As our experience with this technology grows, and as it becomes more widely used, future studies involving larger numbers of patients will help further define the impact of this modality of treatment.

References

1. Ostrom QT, Gittleman H, Truitt G, Boscia A, Kruchko C, Barnholtz-Sloan JS. CBTRUS statistical report: primary brain and other central nervous system tumors diagnosed in the United States in 2011–2015. Neuro Oncol. 2018;20(Suppl 4):iv1–iv86. https://doi.org/10.1093/neuonc/noy131.
2. Stupp R, Hegi ME, Mason WP, van den Bent MJ, Taphoorn MJB, Janzer RC, et al. Effects of radiotherapy with concomitant and adjuvant temozolomide versus radiotherapy alone on survival in glioblastoma in a randomised phase III study: 5-year analysis of the EORTC-NCIC trial. Lancet Oncol. 2009;10(5):459–66. https://doi.org/10.1016/S1470-2045(09)70025-7.
3. Stupp R, Mason WP, van den Bent MJ, Weller M, Fisher B, Taphoorn MJB, et al. Radiotherapy plus concomitant and adjuvant temozolomide for glioblastoma. N Engl J Med. 2005;352(10):987–96.
4. Stupp R, Taillibert S, Kanner A, Read W, Steinberg D, Lhermitte B, et al. Effect of tumor-treating fields plus maintenance temozolomide vs maintenance temozolomide alone on survival in patients with glioblastoma: a randomized clinical trial. JAMA. 2017;318(23):2306–16. https://doi.org/10.1001/jama.2017.18718.
5. Sampson JH, Heimberger AB, Archer GE, Aldape KD, Friedman AH, Friedman HS, et al. Immunologic escape after prolonged progression-free survival with epidermal growth factor receptor variant III peptide vaccination in patients with newly diagnosed glioblastoma. J Clin Oncol. 2010;28(31):4722–9. https://doi.org/10.1200/JCO.2010.28.6963.
6. Wilson CB. Glioblastoma: the past, the present, and the future. Clin Neurosurg. 1992;38:32–48.
7. Omuro A, DeAngelis LM. Glioblastoma and other malignant gliomas: a clinical review. JAMA. 2013;310(17):1842–50. https://doi.org/10.1001/jama.2013.280319.
8. Simpson JR, Horton J, Scott C, Curran WJ, Rubin P, Fischbach J, et al. Influence of location and extent of surgical resection on survival of patients with glioblastoma multiforme: results of three consecutive Radiation Therapy Oncology Group (RTOG) clinical trials. Int J Radiat Oncol Biol Phys. 1993;26(2):239–44.
9. Lacroix M, Abi-Said D, Fourney DR, Gokaslan ZL, Shi W, DeMonte F, et al. A multivariate analysis of 416 patients with glioblastoma multiforme: prognosis, extent of resection, and survival. J Neurosurg. 2001;95(2):190–8.
10. Sanai N, Polley M-Y, McDermott MW, Parsa AT, Berger MS. An extent of resection threshold for newly diagnosed glioblastomas. J Neurosurg. 2011;115(1):3–8. https://doi.org/10.3171/2011.2.JNS10998.
11. Senft C, Bink A, Franz K, Vatter H, Gasser T, Seifert V. Intraoperative MRI guidance and extent of resection in glioma surgery: a randomised, controlled trial. Lancet Oncol. 2011;12(11):997–1003. https://doi.org/10.1016/S1470-2045(11)70196-6.
12. Stummer W, Pichlmeier U, Meinel T, Wiestler OD, Zanella F, Reulen HJ, et al. Fluorescence-guided surgery with 5-aminolevulinic acid for resection of malignant glioma: a randomised controlled multicentre phase III trial. Lancet Oncol. 2006;7(5):392–401.
13. Li YM, Suki D, Hess K, Sawaya R. The influence of maximum safe resection of glioblastoma on survival in 1229 patients: can we do better than gross-total resection? J Neurosurg. 2016;124(4):977–88. https://doi.org/10.3171/2015.5.JNS142087.
14. McGirt MJ, Mukherjee D, Chaichana KL, Than KD, Weingart JD, Quinones-Hinojosa A. Association of surgically acquired motor and language deficits on overall survival after resection of glioblastoma multiforme. Neurosurgery. 2009;65(3):463–70. https://doi.org/10.1227/01.NEU.0000349763.42238.E9.
15. Jethwa PR, Barrese JC, Gowda A, Shetty A, Danish SF. Magnetic resonance thermometry-guided laser-induced thermal therapy for intracranial neoplasms: initial experience. Neurosurgery. 2012;71(1

Suppl Operative):133–45. https://doi.org/10.1227/NEU.0b013e31826101d4.
16. Sloan AE, Ahluwalia MS, Valerio-Pascua J, Manjila S, Torchia MG, Jones SE, et al. Results of the NeuroBlate System first-in-humans phase I clinical trial for recurrent glioblastoma: clinical article. J Neurosurg. 2013;118(6):1202–19. https://doi.org/10.3171/2013.1.JNS1291.
17. Barker FG, Chang SM, Gutin PH, Malec MK, McDermott MW, Prados MD, et al. Survival and functional status after resection of recurrent glioblastoma multiforme. Neurosurgery. 1998;42(4):709–23.
18. Mohammadi AM, Hawasli AH, Rodriguez A, Schroeder JL, Laxton AW, Elson P, et al. The role of laser interstitial thermal therapy in enhancing progression-free survival of difficult-to-access high-grade gliomas: a multicenter study. Cancer Med. 2014;3(4):971–9. https://doi.org/10.1002/cam4.266.
19. Thomas JG, Rao G, Kew Y, Prabhu SS. Laser interstitial thermal therapy for newly diagnosed and recurrent glioblastoma. Neurosurg Focus. 2016;41(4):E12.
20. Ivan ME, Mohammadi AM, De Deugd N, Reyes J, Rodriguez G, Shah A, et al. Laser ablation of newly diagnosed malignant gliomas: a meta-analysis. Neurosurgery. 2016;79(Suppl 1):S17–23.
21. Lee I, Kalkanis S, Hadjipanayis CG. Stereotactic laser interstitial thermal therapy for recurrent high-grade gliomas. Neurosurgery. 2016;79(Suppl 1):S24–34.
22. Beaumont TL, Mohammadi AM, Kim AH, Barnett GH, Leuthardt EC. Magnetic resonance imaging-guided laser interstitial thermal therapy for glioblastoma of the corpus callosum. Neurosurgery. 2018;83(3):556–65. https://doi.org/10.1093/neuros/nyx518.
23. Chaichana KL, Jusue-Torres I, Lemos AM, Gokaslan A, Cabrera-Aldana EE, Ashary A, et al. The butterfly effect on glioblastoma: is volumetric extent of resection more effective than biopsy for these tumors? J Neuro-Oncol. 2014;120(3):625–34. https://doi.org/10.1007/s11060-014-1597-9.
24. Mohammadi AM, Sharma M, Beaumont TL, Juarez KO, Kemeny H, Dechant C, et al. Upfront magnetic resonance imaging-guided stereotactic laser-ablation in newly diagnosed glioblastoma: a multicenter review of survival outcomes compared to a matched cohort of biopsy-only patients. Neurosurgery. 2018;85(6):762–72. https://doi.org/10.1093/neuros/nyy449.
25. Wright J, Chugh J, Wright CH, Alonso F, Hdeib A, Gittleman H, et al. Laser interstitial thermal therapy followed by minimal-access transsulcal resection for the treatment of large and difficult to access brain tumors. Neurosurg Focus. 2016;41(4):E14.
26. Sabel M, Rommel F, Kondakci M, Gorol M, Willers R, Bilzer T. Locoregional opening of the rodent blood-brain barrier for paclitaxel using Nd:YAG laser-induced thermo therapy: a new concept of adjuvant glioma therapy? Lasers Surg Med. 2003;33(2):75–80.
27. Leuthardt EC, Duan C, Kim MJ, Campian JL, Kim AH, Miller-Thomas MM, et al. Hyperthermic laser ablation of recurrent glioblastoma leads to temporary disruption of the peritumoral blood brain barrier. PLoS One. 2016;11(2):e0148613. https://doi.org/10.1371/journal.pone.0148613.
28. Jones EL, Oleson JR, Prosnitz LR, Samulski TV, Vujaskovic Z, Yu D, et al. Randomized trial of hyperthermia and radiation for superficial tumors. J Clin Oncol. 2005;23(13):3079–85.
29. Man J, Shoemake J, Zhou W, Fang X, Wu Q, Rizzo A, et al. Sema3C promotes the survival and tumorigenicity of glioma stem cells through Rac1 activation. Cell Rep. 2014;9(5):1812–26. https://doi.org/10.1016/j.celrep.2014.10.055.
30. Overgaard J, Gonzalez Gonzalez D, Hulshof MC, Arcangeli G, Dahl O, Mella O, et al. Randomised trial of hyperthermia as adjuvant to radiotherapy for recurrent or metastatic malignant melanoma. Lancet. 1995;345(8949):540–3.
31. Man J, Shoemake JD, Ma T, Rizzo AE, Godley AR, Wu Q, et al. Hyperthermia sensitizes glioma stem-like cells to radiation by inhibiting AKT signaling. Cancer Res. 2015;75(8):1760–9. https://doi.org/10.1158/0008-5472.CAN-14-3621.

LITT for Pediatric Brain Tumors

7

George W. Koutsouras,
Monserrat Almaguer Ascencio,
and Zulma Tovar-Spinoza

Introduction

Brain tumors represent the leading cause of cancer deaths in the pediatric population. Open surgical resection of brain tumors can potentially result in permanent cognitive deficits and other lasting neurological dysfunction. Chemotherapy has multiple known side effects and radiation therapy carries the risk of life-lasting radiation-induced brain damage or secondary brain tumors [1]. Thus, it is advantageous to be able to offer a therapeutic modality that provides a less invasive surgical option that has no long-term side effects. Laser-induced thermal therapy (LITT) is a novel procedure that expands treatment choice for several intracranial pathologies. Its use in brain tumors dates as early as 1990; however, the first reported case of MRIgLITT for pediatric patients was only as recent as 2011 by Jethwa and colleagues [2]. Subsequently, MRIgLITT has been reported to be useful in cases of difficult to access lesions, patients with high surgical risk, or in cases of tumor recurrence and need for repeated and/or staged resections [3].

Through its application of placing a laser fiber into the tumor, the procedure is effective at destroying tumor cells. Laser light is used to create an accurate lesion in the target tissue by inducing acute coagulative necrosis by thermal ablation [4] causing fragmentation of DNA, therefore, promoting cellular apoptosis, according to published hypotheses [5]. Advances in technology have allowed the integration of magnetic resonance imaging into the LITT procedure (MRIgLITT), enabling monitoring of tissue ablation in real-time. The current LITT systems use color-coded temperature maps overlaid on MR images. From this, an irreversible damage zone is calculated based upon the time and temperature history data from individual voxels in the treatment zone [6].

The Role and Outcome of MRIgLITT-Treated Pediatric Brain Tumors

The reports of using MRIgLITT on pediatric brain tumors are scarce and were initially limited to deep lesions such as thalamic tumors or hypothalamic hamartomas (HHs). As the use of the MRIgLITT technology evolved, the criteria for selection of patients for this treatment expanded. Jethwa et al. reported the first case of MRIgLITT

G. W. Koutsouras
Department of Neurosurgery, Upstate University Hospital, Syracuse, NY, USA

M. A. Ascencio
Department of Neurosurgery, Hospital Civil de Guadalajara "Dr. Juan. I. Menchaca", Guadalajara, Jalisco, Mexico

Z. Tovar-Spinoza (✉)
Department of Neurosurgery, SUNY Upstate Medical University, Syracuse, NY, USA
e-mail: tovarspz@upstate.edu

V. L. Chiang et al. (eds.), *Laser Interstitial Thermal Therapy in Neurosurgery*,
https://doi.org/10.1007/978-3-030-48047-9_7

in a pediatric patient in 2011 on a child with a thalamic primitive neuroectodermal tumor (PNET) with good 6-month outcome [2, 6, 7], promoting the use of MRIgLITT as a desirable alternative surgical option to deeply seated intracranial lesions. Further reports by Tovar-Spinoza et al. [4, 8] included a heterogeneous group of tumors such as recurrent medulloblastomas and other PNETs, ependymomas, HHs, pilocytic astrocytomas (PCAs), choroid plexus xanthogranulomas, gangliogliomas, brain stem/midbrain/thalamic gliomas, and subependymal giant cell astrocytomas (SEGAs) (Table 7.1) that were successfully treated with MRIgLITT and showed volumetric reduction in the size of the treated tumors at follow-up of up to 3 years.

Other authors have described the treatment of recurrence of interventricular ependymomas presenting after recurrence and frontal or temporal gangliogliomas [4, 6].

Low-grade gliomas account for more than 50% of all pediatric brain tumors. In our experience, the use of MRIgLITT for low-grade gliomas has accounted for more than 50% of all the treated pediatric brain tumors, with good resultant tumor reduction reported [6].

Pilocytic astrocytomas are traditionally treated with surgical resection. The first case of PCA reported to be surgically managed using MRIgLITT was described by our center in the case of a 17-year-old patient with a cystic thalamic PCA [6]. This tumor was initially managed by endoscopic cyst fenestration and resection at first diagnosis. On tumor recurrence, MRIgLITT was used [6]. After 7 years, there is no evidence of recurrence of the tumor and the patient remains asymptomatic. We further described five other cases of PCA treated with MRIgLITT, in various deeply seated locations including two at the thalamic midbrain junction, one in the hypothalamus, one in the cerebellar peduncle, and one in the cerebellar vermis. One midbrain-thalamic case developed transient perioperative complication with hemiparesis and akinetic mutism due to software limitations on visualizing the ablation, but symptoms improved and along with the other PCAs treated, all were without recurrence at 16–28 months of follow-up [6]. An additional study by Miller and colleagues reported the treatment of a juvenile PCA with MRIgLITT with the novel use of robotic stereotactic guidance. They also reported no recurrence of tumor growth after 196 days of follow-up [7].

Subependymal giant cell astrocytoma treatment usually involves an open surgical or endoscopic resection. These tumors typically arise at the interventricular foramen of Monro with incompletely resected tumors often requiring reoperation to reduce the mass effect and CSF outlet obstruction with a described postoperative complications as high as 49%. In 2016, Buckley et al. reported three cases of successful MRIgLITT-treated SEGA, all with an underlying diagnosis of tuberous sclerosis, all with prior treatment, either with everolimus or craniotomy, and none with peri-operative complications [9]. A median relative reduction in tumor volume of 67% (range 28–70%) on MRI at 3–6-month follow-up was reported. We also have experience with the treatment of two intraventricularly located SEGA, requiring everolimus adjuvant therapy. One showed a volume reduction in the lesion [8], while the other did not [6]. Dadey and colleagues described two cases of SEGA treated with MRIgLITT in two teenagers: one had undergone tumor recurrence from two prior resections; in the other, MRIgLITT was chosen as an option over open surgery. With a short follow-up of fewer than 9 months, both cases reportedly showed overall reduced tumor size and no evidence of recurrence [10].

With regard to complications, Karsy et al. described the development of obstructive hydrocephalus 9 months following a second laser ablation of a SEGA located within the foramen of Monro; it was hypothesized that obstruction was due to the development of intraventricular adhesions following MRIgLITT as tumor size was stable on imaging [11, 12]. Buckley et al. also utilized thermal ablation for a hypothalamic ganglioglioma and a hypothalamic pleomorphic xanthoastrocytoma. Unfortunately, both cases were complicated by acute obstructive hydrocephalus requiring replacement or revision of a ventriculoperitoneal shunt [9]. Tumors in both cases continued to progress despite LITT therapy.

Table 7.1 Case series and case reports of the use of MRIgLITT in brain tumors in the pediatric population. Those series of cases combined with adults or other non-tumor pathologies are not included [6, 8–11, 24]

Author (year)	Tumor type, no. of cases if more than 1	Age, yrs.	Localization, no. of cases if more than 1	Preoperative treatment, no. of cases if more than 1	Median lesion dimensions; median tumor volume	Reduction in tumor volume (%/cm^3)	Laser ablation system	Follow-up, days or months	Complications	Postop treatment	Clinical Outcomes
Buckley (2016)	HH, 6	5.5 (3.3–24.6)	Hypothalamic	NS	0.85 × 0.63 × 0.75 cm; 0.19 cm^3	50%, no residual hamartoma	Visualase	292 d (55–566 d)	Intralesional hemorrhage (16.7%), suboptimal placement of the laser catheter (16.7%), transient ipsilateral weakness (33%), dysphasia (16.7%)		67% complete seizure freedom
	SEGA, 3	13 (7.5–19)	Foramen of Monro	67% neoadjuvant everolimus and craniotomy for resection	1.6 × 1.6 × 1.9 cm; 4.1 cm^3 (1.4–4.1 cm^3)	67% (28–70%)	Visualase	852 d (370–885 d)	None	Everolimus	
	Ganglioglioma	13.9	Hypothalamic	Craniotomy for subtotal resection	3.1 × 3.7 × 3.0 cm; 18 cm^3	Tumor progression 113%	Visualase	683 d	Acute post ablation obstructive hydrocephalus	Craniotomy of cyst resection, drafenib	
	Xanthoas-trocytoma	8.8	Hypothalamic, suprasellar, third ventricle	Stereotactic biopsy and VP shunt, chemotherapy	6.1 × 6.0 × 4.9 cm; 94 cm^3	Tumor progression 113%	Visualase	272 d		Lenalidomide	
	Optic glioma	18.4	Hypothalamic, third ventricular	VP shunt, chemotherapy; subtotal craniotomies, 2	1.8 × 2.6 × 2.7 cm; 6.6 cm^3	NS		179 d	Post-ablation hemorrhage in the ablation zone and transient worsening of a baseline visual field cut	None	80% without the need for adjuvant therapy
Dadey (2016)	SEGA	13	Left lateral ventricle	Craniotomies for resection of bilateral SEGAs, 2; fenestration of the septum pellucidum	1.7 × 1.4 × 2.1 cm	1.2 × 0.9 × 1.2 cm	IMRIS Inc.; Monteris diffusing tip laser probe	9 m	None	NS	
	SEGA	14	Foramen of Monro	AED	1.6 × 1.7 × 1.9 cm	NS	ROSA robotic device–assisted LITT (Medtech)	4 m	Worsened hydrocephalus	NS	Improvements in behavior and personality

(continued)

Table 7.1 (continued)

Author (year)	Tumor type, no. of cases if more than 1	Age, yrs.	Localization, no. of cases if more than 1	Preoperative treatment, no. of cases if more than 1	Median lesion dimensions; median tumor volume	Reduction in tumor volume (%/cm^3)	Laser ablation system	Follow-up, days or months	Complications	Postop treatment	Clinical Outcomes
Karsy (2018)	SEGA	5	Foramen of Monro	Immunotherapy	NS	NS	Visualase	18 m	Gadolinium extravasation into the ventricle	NS	NS
Tovar-Spinoza (2016) [6]	Gliomas, 9	9.72 (1.5–17)	Thalamus; intraventricular; frontal; midbrain-thalamus; hypothalamus; mesial temporal; posterior fossa, 3	ETV; craniotomy + radiation + chemotherapy, 2; craniotomy, 2	8.4 cm^3 (0.87–11.73 cm^3)	Median reduction 61.6%	Visualase/ NeuroBlate	48 m (13–46 m)	Transient leg weakness ($n = 1$), hemiparesia, akinetic mutism, eye movement disorder ($n = 1$)	Everolimus ($n = 1$)	88.8% no recurrence progression
Tovar-Spinoza (2016) [8]	PCA, 6; ependymoma; recurrent medulloblastoma; choroid plexus xanthogranuloma, 2 lesions in 1 patient; SEGA; ganglioglioma	10.3 (4–17)	Frontal lobe; hypothalamus; thalamus, 2; thalamus-midbrain; ventricles, 3; pons; posterior fossa (vermian, peduncle, and tentorial), 3	Open surgery, 5; Oncological treatment, 3	6.79 cm^3	Mean reduction 2.61 cm^3	Visualase	24.5 m (12–35 m)	Transient right leg weakness ($n = 1$) and transient hemiparesis, akinetic mutism, and eye movement disorder ($n = 1$)	Everolimus ($n = 1$)	
Wright (2018)	HH	1.8	Hypothalamus and tuber cinereum		10 × 11 × 15 mm	Disconnection and ablation of the HH	NeuroBlate SideFire laser probe	24 m	None		Seizure free

AED antiepileptic drug, *ETV* endoscopic third ventriculostomy, *HH* hypothalamic hamartoma, *NS* not specified, *PCA* pilocytic astrocytoma, *SEGA* subependymal giant cell astrocytoma, *VP* ventriculoperitoneal

Hypothalamic hamartomas are rare benign lesions that most typically present in children as epileptogenic foci, yielding gelastic seizures, but can also yield to precocious puberty and significant behavioral issues. Open surgical management has been fraught with significant life-threatening complications related to the approach to this region making stereotactic radiosurgery and MRIgLITT viable options. The goal of MRIgLITT in hamartoma epilepsy treatment is to disconnect the hamartoma from the brain tissue, relieving the brain from abnormally firing cells [9, 13, 14]. However, we have also treated giant HH in a staged fashion and in one symptomatic patient with precocious puberty with post-ablation normalization of the endocrine profile. Buckley et al. reported the results of six patients treated with MRIgLITT. Half of the patients developed complications including intralesional hemorrhage in one patient, transient ipsilateral motor weakness in two patients, and stuttering speech with expressive dysphasia in one patient. All symptoms subsequently improved. Complete seizure control (Engel Class I) was seen in four patients (67%) and in the three patients with long-term radiographic follow-up, no residual hamartoma was noted with changes in the ablation zone consistent with gliosis and encephalomalacia. Du and colleagues reported the treatment of eight patients with HH [15, 16]. All patients but one were seizure-free at 6 months follow-up with only one case complicated by epidural hematoma at the laser introduction site [16].

The largest series of HHs treated using LITT however is reported by Curry et al. [17] who report the outcome of 71 pediatric patients treated with LITT. In this series, 93% of patients were seizure-free at 1 year despite 25% of patients having failed prior surgical or radiosurgical interventions. Fourteen patients (20%) required one additional ablation and two patients required two additional ablations to achieve seizure freedom. Seizure rate improvement was noted to be instantaneous for the majority of patients. Complications included one case of worsened diabetes insipidus, one case of severe short-term memory loss related to mamillary body injury, four patients with wound healing issues, and three patients with transient hyponatremia. These results are compared today with those for stereotactic radiosurgery such as reported by Kameyama et al. who described 100 patients with HHs, including adults and children. Using radiosurgery 71% seizure control can be obtained after a single treatment with only two patients developing complication, and greater seizure control can be obtained with subsequent treatments without any additional complications [18]. The relative roles of radiosurgery versus MRIgLITT remain unknown at this time.

Advantages of Using MRIgLITT in Children

Most of the reported literature for choosing MRIgLITT over craniotomy is present within the adult population [19–21]. In pediatrics, MRIgLITT was initially advocated in treating lesions located deep within cortical tissue, beside eloquent brain areas, resistant to other treatment modalities with patients' preference for minimally invasive therapy, and as a salvage/palliative therapy in patients who could no longer tolerate the side effects of chemotherapy or who were not candidates for palliative radiation therapy—similar indications to adult patients. Specific to pediatrics, however, treating deep small intracranial tumors, such as brain stem gliomas and HHs, with MRIgLITT has also become attractive.

Independent of the pathology [6], MRIgLITT has significant advantages in the pediatric population; MRIgLITT can be performed under conscious moderate sedation, local anesthesia, or general anesthesia; it also can be completed in one or multiple sessions, or at one session MRIgLITT can be used to treat more than one target. As LITT technology is compatible with MRI (MRIgLITT), it also allows real-time precision of the ablated area at the moment of treatment—especially significant for lesions that are not easily demarcated during open surgery with post-ablation control images obtained in the same surgical session. The minimal invasiveness of the MRIgLITT procedure offers less overall blood loss, less postoperative pain, shorter hospital

stay, and reduced perioperative morbidity. There are additional cosmetic benefits including the use of a stab incision (no need for hair shaving) and the use of absorbable sutures for skin closure, which reduce the anxiety of postoperative suture removal [8].

Decreasing length of hospital stay allows less disruption of family life, optimizing time away, so children can return to regular activity and school. However, the most important consideration for using MRIgLITT remains to be the possible avoidance of chemotherapy and radiation therapy, both of them offering deleterious side effects, especially in the forming brain. This will require possibly changing or innovating the current treatment protocols. Although surgical resection currently remains the gold standard of treatment for children or adults, many MRIgLITT studies are describing equivalent outcomes of cytoreduction with less periprocedural complications with considerations made that in choosing cases for treatment, lesions no greater than 3 cm in greatest diameter are ideal [19]. Larger lesions are amenable for treatment but either need to be staged or planned for multiple ablations, since the procedure can be staged and repeated as many times as needed, which is important for recurrences.

Technical Considerations when Using MRIgLITT in the Pediatric Population

There are two currently used systems available to administer MRIgLITT therapy: The NeuroBlate System (Monteris Medical) and the Visualase System (Medtronic). The NeuroBlate system utilizes neodymium-doped yttrium aluminum garnet (Nd:YAG) laser, while the Visualase system uses a 980 nm diode laser. Both systems have been described in the adult and pediatric literature, without clear evidence comparing the differences between technology and application in adult or pediatric patients. However, both systems have been designed for patients older than 2 years old when the skull can hold the bolts without risk of moving. For patients younger than 2 years, using pinned head fixation frames for navigation and stereotaxis is challenging. Currently, the gel DORO multi-purpose skull clamp for pediatrics (Pro-med Instruments) is the most available for these instances. Hooten et al. recently reported the use of a frameless navigation technique with a mini-frame tripod system and intraoperative reference points as an alternative to treat a 6-month-old child [22].

Each laser system has shown to be compatible with several types of patient-probe interfaces. Traditional Leksell Stereotactic frames (Elekta), the ClearPoint SmartFrame (MRI Interventions), and the robotic ROSA device (Medtech) have all been used for stereotaxy in treating pediatric lesions [7]. Customized 3D frames, such as the STarFix devices (FHC), may come in handy when performing ablation in posterior fossa lesions, as well as in mesiotemporal lobe lesions requiring precise targeting to spare the nearby structure [10]. Miller et al. were the first to demonstrate the use of STarFix for MRIgLITT. Of the five patient series, two patients were children with seizure foci. More recently, some studies express the use of the ROSA in the context of MRIgLITT in pediatric neurosurgery in five pediatric patients, with biopsy and/or MRIgLITT therapy for a variety of pediatric neuro-oncological tumors [7]. The patients did not experience a recurrence in their follow-up, and one required a subsequent lesional resection. No complications were reported.

For both LITT systems, the size of the bolt is still ominous for small heads with thin bone, with the subsequent risk for bolt instability, fractures, and bolt-generated-artifacts in the MRI images. The bolt materials can be plastic for the Visualase but are titanium only for the NeuroBlate system. For some cases like HHs, the pediatric neurosurgeon might prefer the 1.65 mm diameter Visualase laser rather than the 2.2 or 3.3 mm diameter NeuroBlate system laser [23], although that will depend on the size of the HH planned disconnection to the brain and size of the lesion, keeping in mind that both systems will generate an approximated 1.5 cm lesion in the long-term follow-up. This lesion can be expanded with the use of the 3.3 mm NeuroBlate SideFire laser. To date, there

is no 2.2 mm NeuroBlate SideFire laser available. In the treatment of a HH, Wright described the utilization of a side-firing NeuroBlate probe (versus a standard diffusion probe) that allowed for differentiating the direction of ablation, which ultimately resulted in a seizure-free outcome after ablation [24]. Additional components of the NeuroBlate system allow for multiple trajectories to treat larger lesions or the use of multiple laser fibers during an ablation procedure [6].

The real-time visualization of the ablation is to be considered. Each laser system can be observed with real-time temperature monitoring, using MR thermography (MRT). MRT uses the temperature dependency of the proton resonance frequency. The available software allows the operating neurosurgeon to set the temperature limits to inside the borders of a lesion [8]. In the Visualase system the crossed automatic turn-off points are established manually by the surgeon so that structures can be safeguarded during the ablation, especially in cases such as HH where multiple structures at risk surround the ablation target. However, the software is restricted to using single or 2D T1-weighted spin-echo sequences and may not allow full peri-lesional at-risk structure visualization. NeuroBlate offers the same advantage but the turnoff is manually controlled by the surgeon who, in this case, has 2D or 3D views of the ablated area. The volumetric view constitutes a critical factor when precise ablation limits are crucial in eloquent areas like brainstem lesions as inadvertent heating could potentially leak on the blinded MRI view during the ablation [8].

Within the case series and case reports reviewed [2, 6, 8–11, 24], in the pediatric population, post-ablation results show a considerable decrease in the volume of lesions using both systems, except Buckley et al., where they used the Visualase system, which reported two cases (ganglioglioma and xanthoastrocytoma) with the progression of the lesion in 113% [9]. A multicenter, prospective cohort study (LAANTERN), including pediatric and adult patients, is currently ongoing with the goal of recruiting up to 1000 patients using the NeuroBlate system under MRIgLITT. Primary outcome measures include local control failure rates and overall quality of life.

Regarding the choice of one system over another, in the pediatric population, we must consider the maturity and closure of the skull sutures; the location, characteristics, and size of the lesion; and eloquent and adjacent vascular target structures. Knowing the technical specifications of each system the pediatric neurosurgeon can determine which option is most appropriate for each patient.

Complications

The MRIgLITT-associated risks can be due to two categories related to the insertion of the laser and application of the thermal energy. In a series of 102 patients (both children and adults) treated using frameless stereotaxy, several complications were described: the most frequent complication observed was the onset of new neurological deficits, followed by perilesional edema or hemorrhage, infection, inaccurate laser placement, thermal injury, and rarely death. In another recent review, neurological deficits [12, 19, 25] may occur in up to 11% of cases, catheter malposition in 1–2% of cases, and vascular injuries, such as intraventricular hemorrhage, detailing the need for management by intervention in up to 3% of patients.

Blood-brain barrier disruption is implicated in the incidence of periprocedural edema. In our center's experience, post-ablation edema peaks at 3–4 days [4]. To reduce this complication, we recommend utilizing lower thermal energies with longer ablations. However, the literature is not clear on this issue. Edema is also treated with a dose of dexamethasone during the ablation, with possibly a longer course of steroids [8]. We use 0.5–1 mg/kg/day of dexamethasone from the day of ablation with a 2-week weaning off plan with the additional gastric protection.

In the treatment of HHs, near-precise dosimetry calculations are crucial for sparing adjacent cortical tissues from incidental thermal damage. Karsy et al. described a review of complications like intraventricular extravasation of gadolinium

causing ventricular adhesion and obstruction [11]. In a case series including 49 MRIgLITT procedures, Buckley described differences in complication occurrence depending on the location of a lesion. In three pediatric tumors ablated within the hypothalamus, intralesional hemorrhage or hydrocephalus occurred [9].

Conclusion

MRIgLITT continues to be a promising option for the treatment of pediatric brain tumors. The technique is still developing and remains a salvage tool for most conditions. Future reports, however, will likely show that MRIgLITT will become the primary option in treating certain brain tumors, especially those located in deep, eloquent areas, thus reducing perioperative complications, increasing patient willingness to consider surgical management, and possibly improving long-term outcomes.

References

1. Dang M, Phillips PC. Pediatric brain tumors. Continuum (Minneap Minn). 2017;23(6):1727–57. https://doi.org/10.1212/CON.0000000000000545.
2. Jethwa PR, Lee JH, Assina R, Keller IA, Danish SF. Treatment of a supratentorial primitive neuroectodermal tumor using magnetic resonance-guided laser-induced thermal therapy. J Neurosurg Pediatr. 2011;8(5):468–75. https://doi.org/10.3171/2011.8.PEDS11148.
3. Ashraf O, Patel NV, Hanft S, Danish SF. Laser-induced thermal therapy in neuro-oncology: a review. World Neurosurg. 2018;112:166–77. https://doi.org/10.1016/j.wneu.2018.01.123.
4. Riordan M, Tovar-Spinoza Z. Laser induced thermal therapy (LITT) for pediatric brain tumors: case-based review. Transl Pediatr. 2014;3(3):229–35. https://doi.org/10.3978/j.issn.2224-4336.2014.07.07.
5. Heisterkamp J, van Hillegersberg R, Zondervan PE, Ijzermans JNM. Metabolic activity and DNA integrity in human hepatic metastases after interstitial laser coagulation (ILC). Lasers Surg Med. 2001;28(1):80–6. https://doi.org/10.1002/1096-9101(2001)28:1<80::Aid-lsm1020>3.0.Co;2-1.
6. Tovar-Spinoza Z, Choi H. MRI-guided laser interstitial thermal therapy for the treatment of low-grade gliomas in children: a case-series review, description of the current technologies and perspectives. Childs Nerv Syst. 2016;32(10):1947–56. https://doi.org/10.1007/s00381-016-3193-0.
7. Miller BA, Salehi A, Limbrick DD Jr, Smyth MD. Applications of a robotic stereotactic arm for pediatric epilepsy and neurooncology surgery. J Neurosurg Pediatr. 2017;20(4):364–70. https://doi.org/10.3171/2017.5.PEDS1782.
8. Tovar-Spinoza Z, Choi H. Magnetic resonance-guided laser interstitial thermal therapy: report of a series of pediatric brain tumors. J Neurosurg Pediatr. 2016;17(6):723–33. https://doi.org/10.3171/2015.11.PEDS15242.
9. Buckley RT, Wang AC, Miller JW, Novotny EJ, Ojemann JG. Stereotactic laser ablation for hypothalamic and deep intraventricular lesions. Neurosurg Focus. 2016;41(4):E10. https://doi.org/10.3171/2016.7.FOCUS16236.
10. Dadey DY, Kamath AA, Leuthardt EC, Smyth MD. Laser interstitial thermal therapy for subependymal giant cell astrocytoma: technical case report. Neurosurg Focus. 2016;41(4):E9. https://doi.org/10.3171/2016.7.FOCUS16231.
11. Karsy M, Patel DM, Bollo RJ. Trapped ventricle after laser ablation of a subependymal giant cell astrocytoma complicated by intraventricular gadolinium extravasation: case report. J Neurosurg Pediatr. 2018;21(5):523–7. https://doi.org/10.3171/2017.11.PEDS17518.
12. Pruitt R, Gamble A, Black K, Schulder M, Mehta AD. Complication avoidance in laser interstitial thermal therapy: lessons learned. J Neurosurg. 2017;126(4):1238–45. https://doi.org/10.3171/2016.3.JNS152147.
13. Belykh E, Yagmurlu K, Martirosyan NL, Lei T, Izadyyazdanabadi M, Malik KM, et al. Laser application in neurosurgery. Surg Neurol Int. 2017;8:274. https://doi.org/10.4103/sni.sni_489_16.
14. Burrows AM, Marsh WR, Worrell G, Woodrum DA, Pollock BE, Gorny KR, et al. Magnetic resonance imaging-guided laser interstitial thermal therapy for previously treated hypothalamic hamartomas. Neurosurg Focus. 2016;41(4):E8. https://doi.org/10.3171/2016.7.FOCUS16218.
15. Du VX, Gandhi SV, Rekate HL, Mehta AD. Laser interstitial thermal therapy: a first line treatment for seizures due to hypothalamic hamartoma? Epilepsia. 2017;58(Suppl 2):77–84. https://doi.org/10.1111/epi.13751.
16. Shirozu H, Masuda H, Ito Y, Sonoda M, Kameyama S. Stereotactic radiofrequency thermocoagulation for giant hypothalamic hamartoma. J Neurosurg. 2016;125(4):812–21. https://doi.org/10.3171/2015.6.JNS15200.
17. Curry DJ, Raskin J, Ali I, Wilfong AA. MR-guided laser ablation for the treatment of hypothalamic hamaratomas. Epilepsy Res. 2018;142:131–4.
18. Kameyama S, Shirozu H, Masuda H, Ito Y, Sonoda M, Akazawa K. MRI-guided stereotactic radiofrequency thermocoagulation for 100 hypothalamic hamarto-

mas. J Neurosurg. 2016;124(5):1503–12. https://doi.org/10.3171/2015.4.JNS1582.
19. Missios S, Bekelis K, Barnett GH. Renaissance of laser interstitial thermal ablation. Neurosurg Focus. 2015;38(3):E13. https://doi.org/10.3171/2014.12.FOCUS14762.
20. Diaz R, Ivan ME, Hanft S, Vanni S, Manzano G, Jagid J, et al. Laser interstitial thermal therapy: lighting the way to a new treatment option in neurosurgery. Neurosurgery. 2016;79(Suppl 1):S3–7. https://doi.org/10.1227/NEU.0000000000001435.
21. Sharma M, Krivosheya D, Borghei-Razavi H, Barnett GH, Mohammadi AM. Laser interstitial thermal therapy for an eloquent region supratentorial brain lesion. Neurosurg Focus. 2018;44(VideoSuppl2):V4. https://doi.org/10.3171/2018.4.FocusVid.17737.
22. Hooten KG, Werner K, Mikati MA, Muh CR. MRI-guided laser interstitial thermal therapy in an infant with tuberous sclerosis: technical case report. J Neurosurg Pediatr. 2018;23(1):92–7. https://doi.org/10.3171/2018.6.PEDS1828.
23. Rahmathulla G, Recinos PF, Kamian K, Mohammadi AM, Ahluwalia MS, Barnett GH. MRI-guided laser interstitial thermal therapy in neuro-oncology: a review of its current clinical applications. Oncology. 2014;87(2):67–82. https://doi.org/10.1159/000362817.
24. Wright J, Chugh J, Wright CH, Alonso F, Hdeib A, Gittleman H, et al. Laser interstitial thermal therapy followed by minimal-access transsulcal resection for the treatment of large and difficult to access brain tumors. Neurosurg Focus. 2016;41(4):E14. https://doi.org/10.3171/2016.8.FOCUS16233.
25. Patel P, Patel NV, Danish SF. Intracranial MR-guided laser-induced thermal therapy: single-center experience with the Visualase thermal therapy system. J Neurosurg. 2016;125(4):853–60. https://doi.org/10.3171/2015.7.JNS15244.

LITT in the Treatment of Adult Epilepsy

8

Bartosz T. Grobelny, Jon T. Willie, and Robert E. Gross

Introduction

Laser interstitial thermal therapy (LITT) was first introduced into use in oncological neurosurgery in 1991 [1]. It was not until 2008 that the technique was reported with the current system of real-time MRI thermography [2] and until 2012 that the first series of patients treated for medically intractable epilepsy was published [3].

The current FDA-cleared (510k) uses for LITT are to "necrotize or coagulate soft tissue through thermal therapy" under MRI guidance [4, 5]. Although both current commercially available systems – Medtronic's Visualase® (Louisville, CO) and Monteris Medical's NeuroBlate® (Plymouth, MN) – are similarly cleared for use in neurosurgery, neither are FDA-approved for any specific indication such as epilepsy or tumor. At the time of writing of this chapter, the SLATE (Stereotactic Laser Ablation for Temporal Lobe Epilepsy) Trial investigating mesial temporal lobe laser ablation for mesial temporal sclerosis (MTS) is ongoing [6, 7].

Despite only a specific subset being studied in a prospective clinical trial, a multitude of epilepsy patients have been treated with MRg-LITT across a wide range of etiologies ranging from lesional (e.g., MTS, malignant neoplasms, cavernous malformations, cortical malformations, hypothalamic hamartomas) to non-lesional (neocortical non-lesional and generalized epilepsy requiring disconnection surgery).

Indications

Broadly, the indications for LITT ablation in epilepsy patients are similar to the indications for open surgical resections. As in the latter, it is limited (albeit not without exception) to patients with drug-resistant epilepsy, namely failure to achieve freedom from disabling seizures after trials of at least two antiepileptic drugs. For focal ablations, a patient needs to undergo a comprehensive evaluation for localization of the seizure onset zone (SOZ) with a thorough history and analysis of seizure semiology, and non-invasive long-term video-EEG monitoring with electroclinical correlation. Neuroimaging includes 3-Tesla MRI imaging of the brain to look for structural abnormality, at a minimum, but many centers also routinely perform interictal fluorodeoxyglucose-positron emission tomography (FDG-PET) to look for region(s) of hypometabolism and/or magnetic source imaging (MSI) with magneto-encephalography (MEG) to localize irritative zones characterized by the dipoles

B. T. Grobelny
Neurological and Spine Surgery, Saint Luke's Hospital of Kansas City, Kansas City, MO, USA

J. T. Willie · R. E. Gross (✉)
Department of Neurosurgery, Emory University School of Medicine, Atlanta, GA, USA
e-mail: rgross@emory.edu

V. L. Chiang et al. (eds.), *Laser Interstitial Thermal Therapy in Neurosurgery*,
https://doi.org/10.1007/978-3-030-48047-9_8

associated with interictal epileptiform discharges. Additionally, subtractive ictal/interictal single photon emission computed tomography (SPECT) is frequently useful for localization of the seizure onset zone. Neurocognitive assessment, functional MRI, and intracarotid amobarbital (Wada) test can also help in localization of seizure pathology as well as to help predict risks of ablation.

In patients in whom the non-invasive workup results in uncertain localization of the SOZ, additional investigation using intracranial EEG is used to best localize the onset of the seizures and spread pattern. In addition to its other advantages [8] we find that the use of stereo-EEG (SEEG) uniquely works together with LITT, offering a completely minimally invasive workup and treatment plan, and often avenues of therapy in the same trajectories as the diagnostic electrodes were placed.

Techniques

Successful laser ablation using MRg-LITT depends upon a composite of accurate stereotactic delivery of the laser catheter and careful and skillful execution of the thermal ablation. Stereotactic delivery of the device can be performed in a variety of ways, but it must be sufficiently accurate and precise for the procedure to be effective and safe. Since we have only used the Visualase system, we will describe the different methods that we currently employ (or have employed in the past) with this particular system that has allowed us to best treat epileptic lesions.

Choice of Trajectory

The success of any LITT procedure begins with the choice of trajectory, the goal of which is to maximally ablate the targeted structure(s) while minimizing the risk of ablation of non-involved areas or of damage to uninvolved traversed brain ("collateral damage"). The choice of trajectory naturally depends on the anatomy of the anticipated lesion volume. A planned spherical lesion gives the most flexibility in terms of approach while an elliptical or cylindrical lesion ideally is approached so that the trajectory is in line with the long axis of the planned lesion as much as possible. In order to minimize the chance of hemorrhagic complications, fine adjustments of the trajectory need to be made to avoid vasculature both at the surface and the depths of the brain along the path of the laser catheter. Another consideration is the avoidance of the ventricles to lessen the chance of path deflections and heat sinks. Lastly, the angle of incidence to the skull is an important consideration in trajectory planning and accuracy: those that deviate greatly from orthogonality to the skull surface stand the risk of skiving when drilling the skull surface and inserting the catheter, with resultant targeting inaccuracy.

Due to its inherent complexity and multiple anatomical considerations, the trajectory planning for stereotactic laser amygdalohippocampotomy (SLAH) will be discussed in detail in the part of this chapter pertaining to mesial temporal lobe epilepsy.

Anesthesia and Positioning

In nearly all cases, laser ablations for adult epilepsy are performed with the patients under general endotracheal anesthesia, for several reasons: (1) having a seizure in the MRI scanner would be hazardous to the patient; (2) the LITT technique requires co-registration of the GRE images with the high-resolution anatomical image in MRI space, which is compromised by any patient movement; (3) ablation sessions can be lengthy and many patients would not tolerate MR imaging for that length of time, or at least it would add unnecessary challenge to the procedure; and (4) the majority of cases do not require awake functional testing; in the cases that do, we will often perform radiofrequency ablation with awake monitoring first. However, on very rare occasion we have performed MRg-LITT with an awake epilepsy patient with focal motor seizures without impaired awareness and a high degree of

cooperativity. In all cases careful padding is necessary, and we routinely use sequential compression devices to prophylax against deep vein thrombosis.

Patients are positioned in the MRI scanner in such a way as to facilitate access to all planned trajectories. For many targets this can be with the patient supine with the head turned to a certain degree. However, certain trajectories like that for our SLAH approach requires that the patient be prone. Lateral positioning in the MRI scanner is difficult. We pin the head when using the ClearPoint® (Clearpoint Neuro; Irvine CA) system (an entirely interventional MRI-based navigation system and skull mounted frame that allows for insertion and manipulation of the laser catheter) which we use for the majority of our de novo insertions, including supine and prone cases. In the cases where a patient has an insertion bolt and/or laser catheter placed with a system that uses a stereotactic headframe, we typically leave the headframe base ring on during the procedure within the MRI coils as it helps maintain head position. Otherwise, the patient is positioned in such a way as to avoid pressure on the laser catheter (if previously inserted) or to maintain access to the bolt(s) when inserting them in the MR scanner.

Choice of MRI Coils

Whenever the patient does not have a neurostimulator device in place (e.g., vagal nerve or deep brain stimulator) we employ flexible receive-only coils. For patients with laser insertion or SEEG bolts already present we typically use the transmit-receive birdcage coil. This makes draping of a sterile field somewhat cumbersome, though the bars of the coil do not usually sterically hinder the access to the bolts when the head is appropriately positioned. For cases in which we use the ClearPoint system to directly target within the MRI scanner, we use a single 6-channel body coil curled in a U-shape underneath the head. Some centers use two parallel 6-channel body coils flanking either side of the head instead. Either allows for enough room to attach and manipulate the ClearPoint frame as well as to insert the laser fiber through it. The quality of the imaging can be affected by the choice of head coil, but is usually sufficient. In the event that signal-to-noise ratio is suboptimal, repositioning or choosing a different coil can be beneficial.

Single Lesions or Ablation Tracts

For treatments that require the ablation of only a single lesion or lesioning only within a single tract, there is a considerable amount of flexibility in terms of the stereotactic technique used to place the laser fiber catheter depending on surgeon preference as well as the availability of stereotactic equipment. Broadly speaking, one can either perform the stereotactic placement of the laser and/or its bolt inside the operating room or in the interventional/intraoperative MRI.

In the operating room the laser fiber catheter can be inserted using virtually any stereotactic method that is sufficiently accurate and precise, including but not limited to conventional frames, custom-printed frames, or frameless stereotactic approaches (including robotic assistants). Typically a skull bolt is inserted over a stereotactically guided insertion rod, and then the laser catheter is inserted through the bolt since it is not feasible to hold the catheter using the frame while the patient is transported. Ideally, insertion accuracy is verified by a thin-cut intraoperative CT of the head merged to preoperative planning MRI with either the laser fiber catheter or the metallic insertion rod (if the ultimate placement of the laser will be in the MRI suite) in place, because this is the step where it is most easy to revise the placement to achieve optimal location. With a stereotactic frame, intraoperative C-arm fluoroscopy can be used but it only provides a sagittal view, and therefore is unable to detect medial/lateral displacements which are equally as important. In lieu of intraoperative imaging (see below for MRI), extraoperative CT or MR (which of course is necessary anyway) can be used, but few surgeons will elect to return to the OR for replace-

ment if a minimal amount of suboptimal catheter accuracy is detected at this stage (and what would be done differently, anyhow?)

When there is a single fiber to be used, it is inserted in the OR, and then the patient is transported to the MRI-suite for the MR-guided ablation. Great care needs to be taken to keep the laser in place and intact in the process. Multiple fibers can also be placed in this manner. Alternatively, if the MRI suite is qualified to serve as a sterile field, the bolts can be placed in the OR and the sterile field sealed at the entry site with a sterile adhesive drape such as Ioban™ (3M; St. Paul, MN) with the plan to re-prep before reopening and inserting the fiber(s) in the MR. Although not in the "indications for use" of the Visualase laser fiber assembly, one fiber can be moved from bolt to bolt in this way (checking for integrity after each ablation track). In either case, if a stereotactic headframe is used (either in isolation or in combination with a robotic assistant) the base ring is kept on for transport as it can aid with head positioning in the MRI. With the laser in place in the MRI suite a volumetric MRI scan is performed to verify the placement of the laser fiber(s) and the MRI-thermometry and ablation may begin.

Multiple Ablation Tracts

In many cases multiple tracts need to be used to achieve the ablation goal in epilepsy patients. Often the ablation targets are of anatomic areas instead of single lesions that cannot be adequately covered with a single ovoid cylindrical lesion. Examples of this are temporopolar ablations, insular ablations, and corpus callosum ablations.

We described above the technique of inserting multiple catheters with a stereotactic frame or robot. Alternatively, multiple trajectories can be planned and executed using the ClearPoint system in the MRI suite, or in the OR using intraoperative MRI [9]. This provides a high degree of accuracy for single catheters, particularly for long trajectories such as temporal ablations from a posterior approach but is also very well suited for multiple trajectories, especially if subsequent passes are influenced by the previous ablation volume [10]. Anatomy allowing, one can attempt multiple ablation trajectories from a single craniostomy (Fig. 8.1a) or one may need to move and remount the frame (or mount multiple frames) in order to achieve the desired goals (Fig. 8.1b). Use of ClearPoint offers greater adaptability of the plan should an initial planned trajectory not result in the desired ablation volume. On the other hand, the ClearPoint system can be time-intensive with multiple trajectories. When performing laser callosotomies (see below) with more than two trajectories (Fig. 8.2), we now favor inserting the bolts in the OR using the robot rather than ClearPoint, which we used initially.

Coupling MRg-LITT to SEEG

Utilizing the SEEG method of diagnostic intracranial EEG also allows for the natural transition to the use of laser ablation, coupling together two minimally invasive techniques. Provided the hypothesis of seizure onset zone is narrow enough, the SEEG electrode trajectories may be planned in such a way that to allow division of the studied brain into adjacent cylindrical volumes that can correspond to potential ablation volumes. If a certain area provides a strong enough hypothesis for seizure onset, special hybrid stereotactic bolts can be inserted at the time of SEEG electrode implantation that can accommodate first a depth electrode (albeit, in some embodiments, not a reduced diameter one) and eventually a laser cannula (Fig. 8.3). However, it is not absolutely necessary to use the hybrid bolts in order to laser ablate seizure foci through SEEG trajectories on the same admission as the intracranial monitoring. We have developed a method in which we remove the SEEG electrodes and bolts in the interventional MRI suite leaving only the bolts whose trajectories we plan to use for ablation. With those bolts remaining implanted, the patient is carefully positioned in the MRI with the head in the birdcage coil. The bars of the coil are carefully draped out

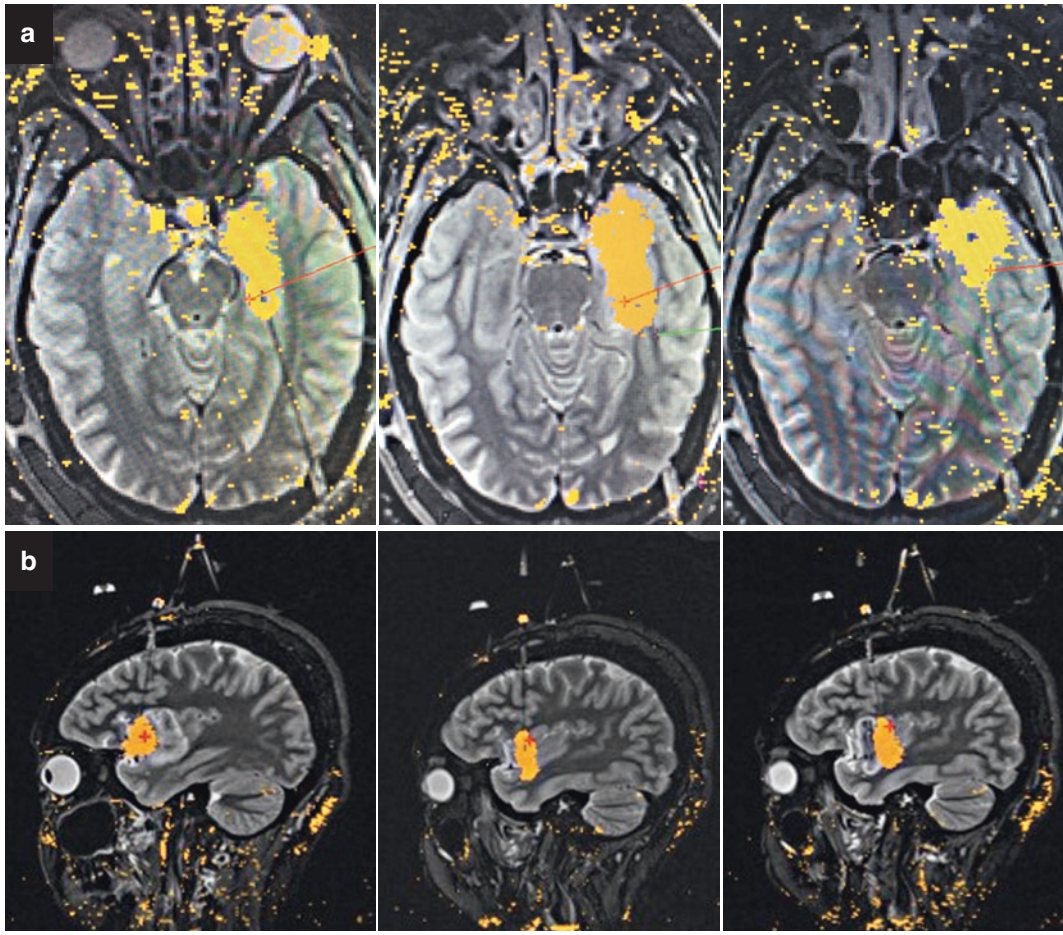

Fig. 8.1 Multiple LITT Technique with ClearPoint. (**a**) Temporal pole, amygdala, and hippocampus ablation through single bur hole and mounting of the SmartFrame. (**b**) Insula ablation through two bur holes and remounting of the SmartFrame

in a sterile fashion when positioned over the head. When the sterile draping is complete, the screwdriver for the bolts is placed through the spaces between the bars onto the bolts and used as a guide to define the trajectory needed to be taken by the laser catheter. The bolts are removed in this fashion and the laser fiber is inserted along the same trajectory as shown by the long screwdriver, with a post-electrode-implantation CT of the head as a guide for what depth from the skin to insert the laser catheter. While recreating complex 3D trajectories may seem difficult in this scenario, we have actually found that the birdcage coil imposes constraints on the trajectories and provides ready spatial references that allow for the accurate replacement of the catheter in line with the prior electrode trajectories (Fig. 8.4). We only do this for relatively short and safe trajectories, such as within the parietal lobe. Moreover, sometimes the SEEG trajectories are not the ideal ones for an ablation, such as medial temporal lobe and insula; for these targets we bring the patient back at a later time for ablation using one of the other techniques described above.

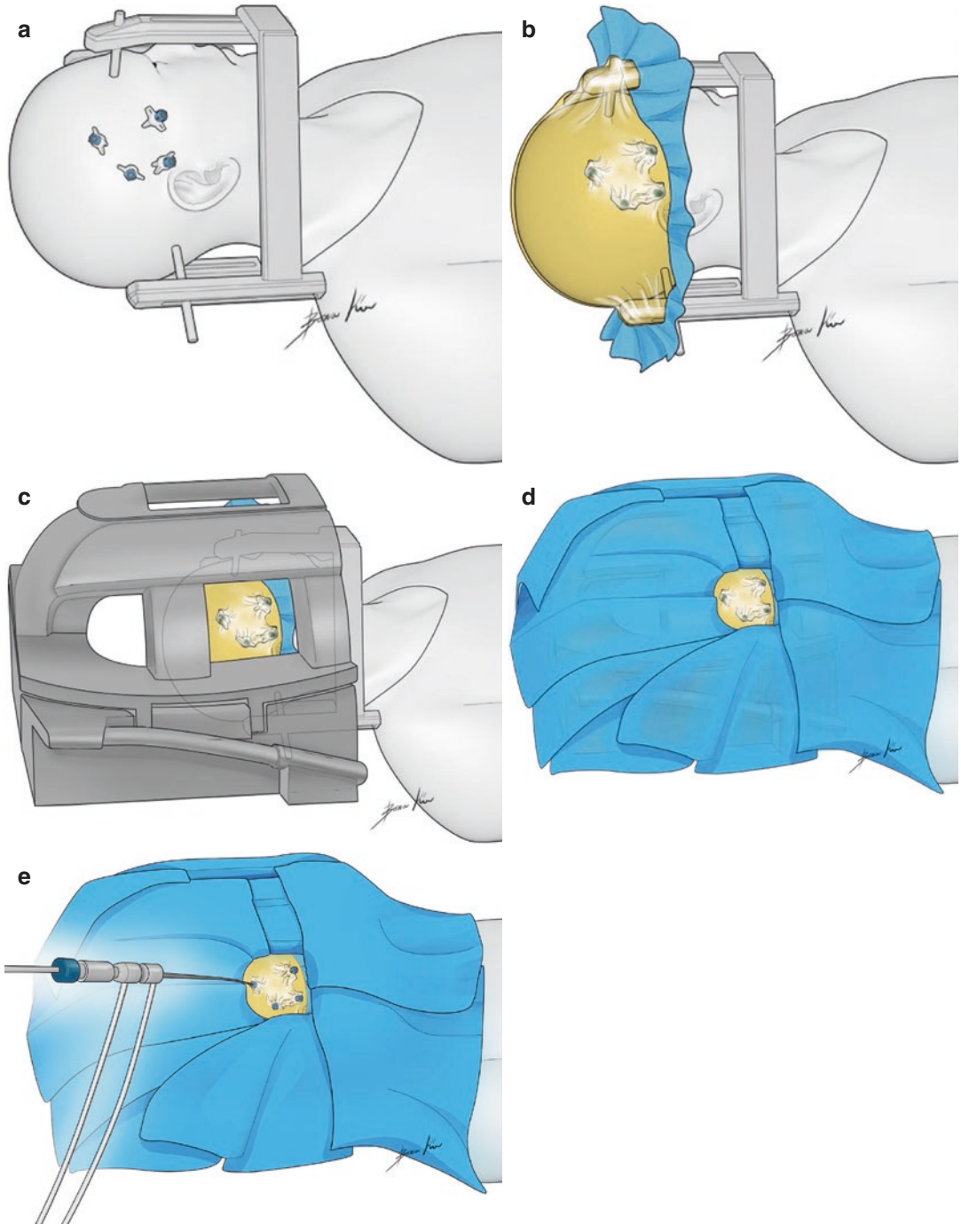

Fig. 8.2 LITT Technique with Bolt. (**a**) Multiple bolts placed. (**b**) Bolts in head covered in Ioban. (**c**) Bolts with bird-cage coil. (**d**) Patient head and coil after sterile draping. (**e**) Visualase fiber placed through a bolt

Fig. 8.3 Standard and Dual-Purpose SEEG Bolts. SEEG heads (above) and corresponding bolts (below) from AdTech Medical that accommodate only an SEEG electrode (left) or has sufficient internal diameter to pass either an electrode or the Visualase laser fiber

Specific Use Cases

Medial Temporal Lobe Epilepsy

Medial temporal lobe epilepsy remains the most common etiology in surgical epilepsy [11]. The only randomized controlled evidence in resective epilepsy is for anterior temporal lobectomy (ATL; as compared to medical therapy) [12, 13]. In a similar vein, SLAH is the most common laser ablation procedure being performed for the treatment of epilepsy and subsequently has been the best-studied laser ablation procedure. Of all laser ablations for epilepsy at our institution at the time of writing this chapter, 56% (101/182) have been SLAHs. Of those, 67% (68/101) have been for MTS.

In patients with unilateral MTS, ipsilateral concordant ictal onsets from the anterior temporal lobe on video EEG, and ipsilateral concordant hypometabolism on PET scan, we offer SLAH as a first-line treatment at our institution. Contraindications are similar to those for open resection, such as bilateral seizure onsets, and risk for global amnesia in patients with widespread (i.e., both verbal and visuospatial) memory decline; responsive neurostimulation or deep brain stimulation is offered to these patients. We do offer selective amygdalohippocampectomy to patients with non-dominant MTS, but not dominant side patients due to the risk of naming decline. In patients with non-lesional MRI we have a low threshold to pursue intracranial monitoring to confirm the seizure onset zone prior to ablation. In cases of confirmed non-dominant medial temporal lobe onsets in MRI-normal patients we offer medial temporal lobe ablation or anterior temporal lobectomy as the first line, whereas responsive neurostimulation is first line for patients with dominant medial temporal lobe onset, due to risk of verbal memory decline.

Ablations that fail to achieve seizure freedom in these patients are re-evaluated with non-invasive studies. Particular attention is paid to whether the procedure achieved the anatomical ablation goals, as these patients may be candidates for re-ablation or craniotomy for anterior temporal lobectomy. Patients in whom the ablation was anatomically complete (with respect to the hippocampus and uncus) may progress to ATL or undergo invasive monitoring. In patients in whom we have failed to achieve seizure freedom and that were subsequently studied with SEEG, we have found onsets in the anterior temporal lobe, parahippocampal gyrus, entorhinal cortex, residual amygdala, posterior cingulate cortex, and even contralateral medial temporal lobe [14]. Many of these patients received repeat laser ablations or temporal lobectomies with resultant seizure freedom or at least seizure improvement [15].

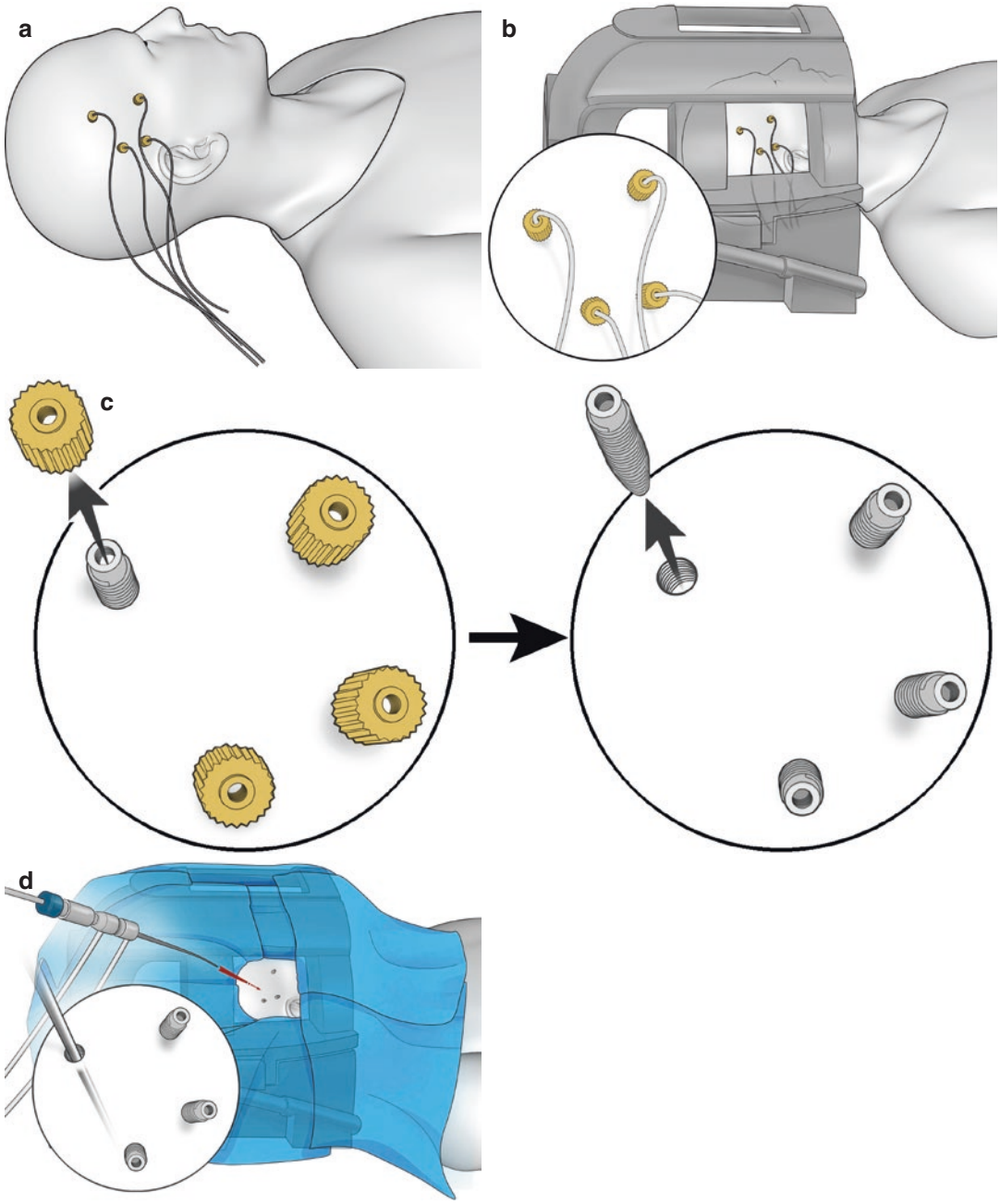

Fig. 8.4 Combined SEEG/LITT Approach. (**a**) SEEG electrodes in place. (**b**) Patient with SEEG electrodes positioned inside the MRI coil with inset showing detail of electrodes and bolts. (**c**) Detail of removing a particular SEEG cap/electrode (left) and bolt (right). (**d**) Patient positioned inside sterilely draped MRI coil with Visualase fiber entering craniostomy left by the removed SEEG bolt. Inset shows this in greater detail, recreating the prior SEEG electrode trajectory

Medial Temporal Lobe Epilepsy Ablation Technique: Stereotactic Amygdalohippocampotomy

Stereotactic methods in order to place the stereotactic bolt and/or laser cannula are chosen based on availability and preference of the surgeon. We prefer to use the ClearPoint system for intraoperative trajectory planning and alignment as it gives us the most confidence in terms of accuracy in a long trajectory, as well as giving us the option of planning a second trajectory "on the fly" should the first ablation not achieve desired anatomical goals. However, patients' girth may be too great to fit in the MR tube in the prone position, especially in 60 cm bore magnets; these patients need to undergo bolt followed by catheter placement in the OR with a different stereotactic technique than ClearPoint.

General endotracheal anesthesia is induced in the interventional MRI suite (diagnostic MR outfitted and certified as an operating room). Hair is usually clipped in a 5 cm × 5 cm square patch that is centered 5 cm lateral and 5 cm superior to the external occipital protuberance on the side of planned ablation. In the case of stereotactic workflows that include the use of a headframe, this area needs to be kept clear of steric hindrance from any fixation posts. The patient is positioned prone on gel rolls and head pinned after being turned slightly to the ipsilateral side. Great care is taken to pad all pressure points as the patient's arms are strapped down to their side. Particular care needs to be taken with obese patients that there is no pressure on the arms in the tube. In the case that stereotactic bolts have already been placed prior to transport to MRI, the patient can be positioned supine with sufficient head turn to access the posterolaterally placed device. Skin preparation and sterile draping is performed as per the usual protocol. Most patients receive 10 mg intravenous dexamethasone and 1000 mg levetiracetam, and weight-appropriate broad-spectrum antibiotic prior to incision. We affix the ClearPoint SmartGrid in the shaved area of the scalp and begin our intraoperative planning scans.

Planning of the trajectory begins with the selection of the initial target point in the center of the head of the hippocampus in the coronal plane, at the level of the midpoint of the cerebral peduncle in the axial plane. An initial entry point is chosen in the center or slightly inferior part of the posterior part of the hippocampal body, in a coronal plane somewhere between the lateral mesencephalic sulcus and the tectal plate. Coronal T1 and T2 Inversion Recovery sequences are both useful in this step. The entry point is extended posteriorly to the cortical surface and adjusted for vasculature along the path (see below). The target point is then extended anteriorly to pass through the amygdala and anteromedial uncus to the medial temporal pole.

The trajectory is then inspected throughout its length to avoid vasculature such as occipital cortical vessels and basal temporal posterior cerebral branches whose trajectories can often come superiorly and close to the planned trajectory. Care is taken to remain inferior to the lateral ventricle if possible, because this may be a clue that the trajectory deviated too superiorly, subjecting the thalamus to risk, or too laterally, subjecting the optic radiation to risk; in addition the ventricle can cause trajectory deflection. Choroid plexus is avoided if possible to minimize intraventricular hemorrhage. After adjustment, the track needs to be inspected to insure that any changes made to avoid complications maintain the previously mentioned anatomical goals of the trajectory. Often both scalp entry point and target point need to be modified in tandem to achieve the optimal trajectory (Fig. 8.5).

The structures that we aim to ablate are the head and body of the hippocampus (as far posteriorly as the tectal plate), the subiculum, inferomedial amygdala, and the uncinate gyrus. We also aim to include the hippocampus within the posterior uncal apex, although this is challenging given its medial and superior location. Unless intracranial EEG suggests onsets in entorhinal, perirhinal, or fusiform cortices, we typically avoid these structures in the ablation plan, although the white matter (containing the perforant pathway) is often encompassed. Individual

anatomy, such as a larger or more curved hippocampus may require the use of a second trajectory to cover all desired structures.

A misplaced trajectory can have consequences specific to the subsequent location of the ablation. A trajectory that is too medial risks injury of the third or fourth cranial nerves in the cavernous sinus dura resulting in an extraocular movement palsy and diplopia. These are usually temporary and likely occur from thermal spread to the nerves. The cerebral peduncles are also medial but separated by the ambient cistern and we have

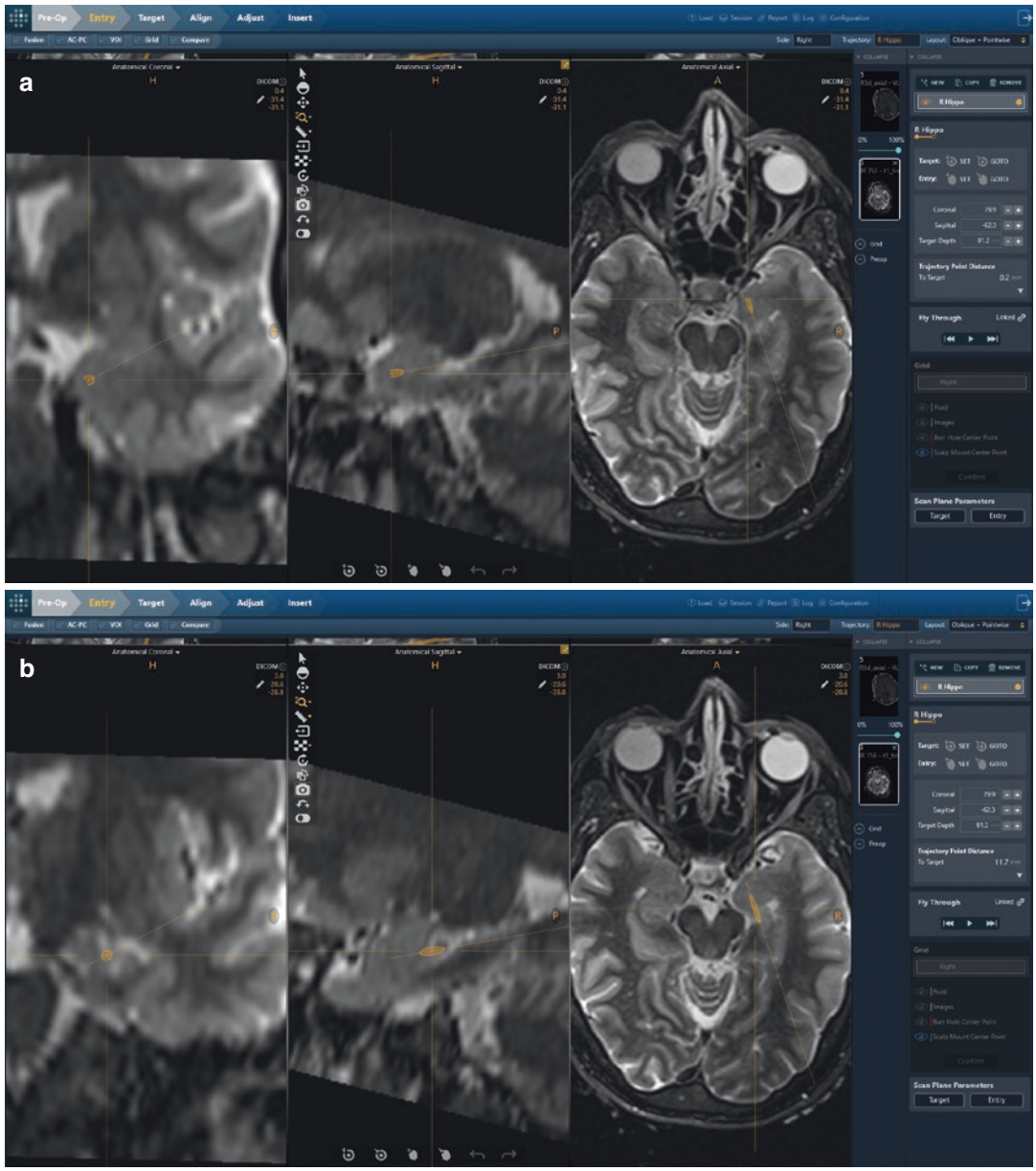

Fig. 8.5 SLAH Trajectory as Viewed in the Three Cardinal Planes in the IR Sequence in the Clearpoint Planning Station. (**a**) Trajectory in the amygdala. (**b**) Pes hippocampus. (**c**) Body of the hippocampus. (**d**) Exiting the hippocampus posterior to the mesencephalic sulcus

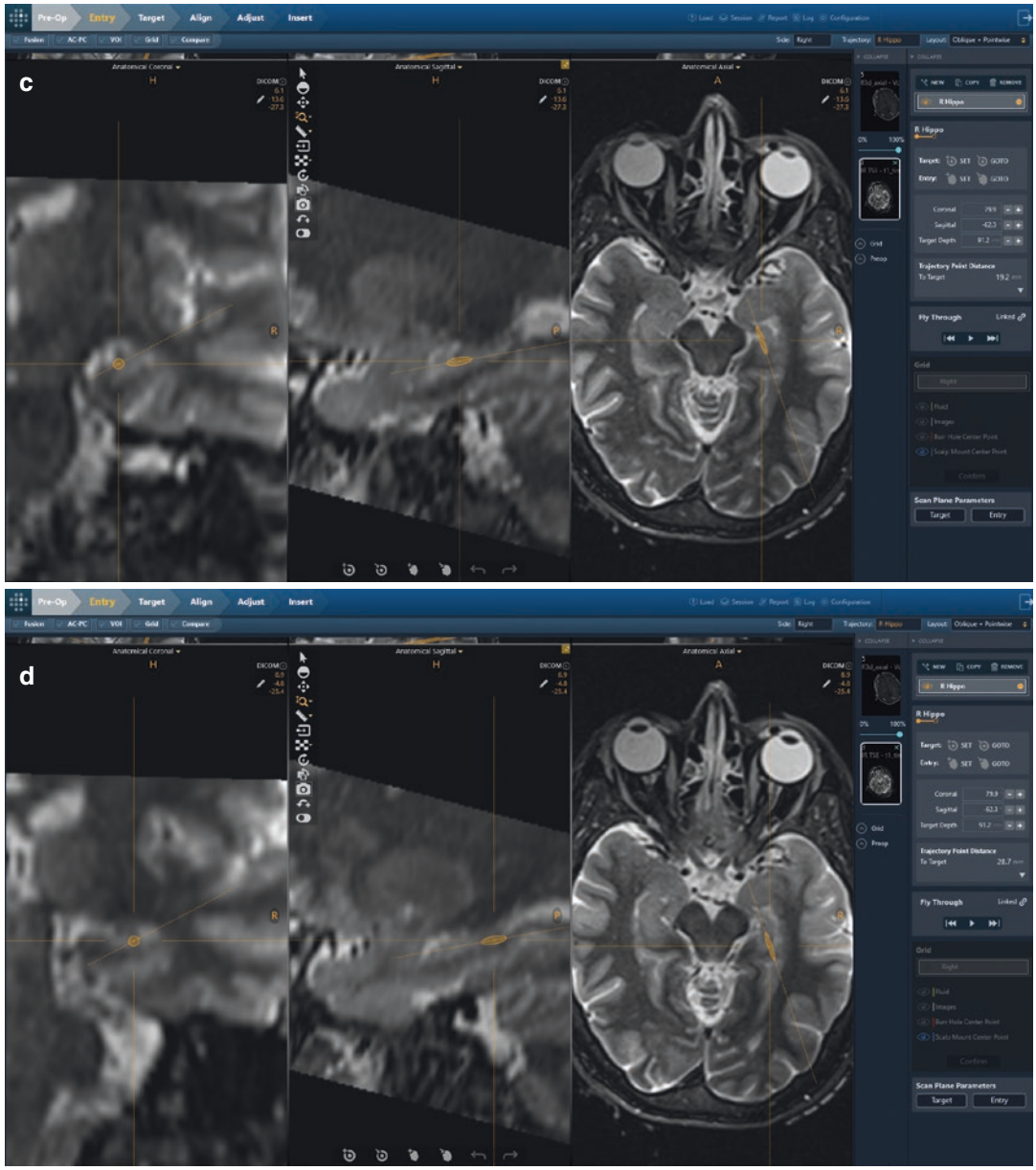

Fig. 8.5 (continued)

never seen injury to these long tracts. This kind of trajectory can also result in insufficient lateral hippocampal ablation.

A trajectory that is too lateral risks injury to the optic radiations within the external sagittal stratum at the posterior end of the ablation and resultant partial visual field deficit (homonymous superior quadrantanopia). Conversely, the medial pes hippocampus and uncinate gyrus may be insufficiently ablated.

Trajectories that are too inferior typically are not associated with unintended neurological deficits, but will very likely result in insufficient ablation of the hippocampal pes and/or body, especially if the trajectory is on the inferior side of the pial boundary of the hippocampal sulcus.

Finally, a trajectory that is too superior can result in injury to the optic tract as it runs above the amygdala (very unusual). Additionally, the lateral geniculate nucleus of the thalamus may be damaged above the hippocampal body posterior to the inferior choroid point with a resultant homonymous hemianopsia [9, 15, 16]. This kind of trajectory also puts the patient at risk for having an insufficient ablation of the subiculum.

Due to the intricacies of finding the appropriate trajectory some have investigated whether there is a reasonable computer-assisted way to better plan these trajectories. Vakahria et al. retrospectively compared historical medial temporal ablations with theoretical ablations extrapolated from computer-modeled trajectories and found that the computer-modeled trajectories had shorter length, better ablation coverage of the amygdala and hippocampus, and overall larger safety margins from critical structures [17].

Medial Temporal Lobe Epilepsy Outcomes

At the time of writing of this chapter ten publications had reported experience of 20 or more patients treated for mesial temporal lobe epilepsy with SLAH [15, 16, 18–25] (Table 8.1). The number of patients treated ranged from 20 [19] to 231 [25], with the largest series being a multicenter cohort that encompassed many of the patients reported in the single-center reports. The largest single-center (58 patients) cohort published is from our own group's experience [15]. Most patients treated had MTS present – ranging from 52.3% [24] to 85% [19]. These studies varied in their technique for placement of the laser fiber, both between as well as within studies. They also varied in their use of intracranial monitoring to confirm medial temporal lobe epilepsy onsets ranging from none of the patients [18] to non-lesional patients [21, 22], or even most patients irrespective of pathology [24].

These studies also varied in methods of reporting their seizure outcomes. Six studies report group outcomes at one year or more [15, 16, 18, 19, 22, 25] whereas others reported using 6 months as their minimum follow-up [20, 21, 23, 24], though they reported mean follow-up greater than one year for their cohorts. At the 6-month time point reported seizure freedom ranged between 53% [19] and 79.5% [21]. For the groups reporting all overall outcomes after 6 months seizure freedom ranged between 47.5% [20] and 67.4% [21]. Seizure freedom at one year or longer ranged between 36% [19] and 65% [16]. Patients with MTS had better outcomes than those that did not – seizure freedom in MTS patients was reported at 67.6% [21] to 73% [24] after at least 6 months and 56% [22] to 73% [16] after at least one year. Patients without MTS showed seizure freedom between 16% [23] and 66% [21] after 6 months and between 33% [15] and 62% [16] after at least one year.

We previously calculated that, of 168 currently (at the time) reported SLAHs with one-year postoperative outcomes, overall 96 (57.1%) were seizure-free, and 63.7% (58 of 91) of MTS patients [26]. Wu et al. reported the retrospective outcomes of 231 patients after SLAH at last follow-up at/beyond 12 months [25]. Based on the centers involved there were at most 50 patients overlapping the previously reported series so this series is ~80% unique patients, and it did not include the two largest previously reported series [15, 21] so it is not biased by those centers (including our own). Engel class I outcomes were achieved in 134 of 231 patients (58.0%) at one year and 96 of 167 patients (57.5%) at 2 years. This seizure-free outcome rate in the entire cohort is strikingly similar to the previously and mostly (~80%) distinct cohort. In the Wu et al. cohort, there was no statistically significant difference in outcome in patients with or without MTS; as to whether this is a power issue is not easy to discern as the number of seizure-free patients in these two subgroups is not provided. However, it appears that ~60% of MTS patients and ~52% of non-MTS patients were Engel 1, with a large confidence interval around the latter.

Where reported, repeat laser ablations were performed in 3.3% [22] to 15.5% [15] of patients and anterior temporal lobectomies in 3.3% [22] to 20% [19]. Combining the experience of multiple

Table 8.1 Published Series of Laser Amygdalohippocampotomy

Study	*N*	%MTS	Visual Field Complication	Cranial Nerve Complication	Follow-Up	Engel I Seizure Outcomes
Kang et al. (2016) [19]	20	85%	5%	5% (transient)	6 months, 1 year	53% (6 months), 36% (1 year)
Jermakowicz et al. (2017) [16]	23	65%	4.3%	0%	1 year	65% (all), 73% (MTS), 62% (non-MTS)
Tao et al. (2018) [24]	21	52%	4.8%	0%	>6 months last f/u	73% (MTS), 30% (non-MTS)
Grewal et al. (2018) [30]	23	78%	34.8%	0%	>1 year last f/u	72% (MTS), 40% (non-MTS)
Donos et al. (2018) [21]	43	79%	0%	0%	6 months, last f/u	79.5% and 67.4% (overall: 6 months and last f/u), 67.6% and 66.6% (last f/u: MTS and non-MTS)
Youngerman et al. (2018) [22]	30	60%	3.3%	0%	>1 year last f/u	55.6% (MTS), 58.3% (non-MTS)
Le et al. (2018) [23]	29	79%	3.4%	10.3% (3.4% permanent)	>6 mo last f/u	73% (MTS), 17% (non-MTS)
Gross et al. (2018) [26]	58	74%	8.6%	6.9% (transient)	>1 year last f/u	60.5% (MTS), 33.3% (non-MTS)
Tatum et al. (2019) [20]	29	79%	5%	0%	>6months last f/u	47.5%
Wu et al. (2019) [25]	231	74%	5.1%	–	1 year, 2 years, last f/u	58.0% (1 year), 57.5% (2 years), 58.0% (last)

centers, 5 of 13 repeat SLAH procedures (38.5%) yielded seizure freedom, although in our own hands it was 4 of 9 [15, 22, 24]. From the same studies additional anterior temporal lobectomies in patients who failed repeat SLAH yielded 1 seizure-free patient out of 6 operations. Although Kang et al. report 3 out of 4 patients becoming seizure-free after an anterior temporal lobectomy after a failed single SLAH, they did not attempt repeating a laser ablation first in any [19].

Aside from the presence of MTS, several other factors have been examined for their relationship to seizure freedom. Differences in ablation volumes examined within case series were not found to be associated with different rates of seizure freedom [18, 19, 21, 24] though, where reported, there are noticeable differences between series in ablation volumes – Grewal et al. [18] report 63% ablation of hippocampus and 43% ablation of amygdala whereas Donos et al. [21] report ablation proportions of 70.9% and 73.7%, respectively. Jermakowicz et al. found in their series that sparing of the medial hippocampal head and lateral trajectories were associated with lack of seizure freedom [16] while Wu et al. found that prioritizing the ablation of the amygdala, hippocampal head, rhinal cortices, and parahippocampal gyrus were associated with a greater chance of seizure freedom [25]. The use of invasive monitoring did not appear to have a clear effect on seizure freedom in these patients [21, 22, 25]. Though intracranial EEG affords better seizure focus localization in patients whose non-invasive studies are not all concordant, this patient population compared to that with a lesional well-localized epilepsy in which invasive monitoring is not necessary are expected to have poorer postsurgical seizure outcomes. One study found that de novo postoperative temporal intermittent rhythmic delta activity (TIRDA) on scalp EEG was a marker of increased risk of failure to become seizure-free [20].

Complications varied considerably across studies with visual field cuts reported between 0% [21] and 35% [18] though most reporting rates below 10% (Table 8.1). Transient cranial nerve III or IV palsies were reported in 0% [21] to 6.9% while permanent ones were reported

between 0% [21] and 3.4% [23]. Intracerebral hemorrhage rates were reported between 0% [21] and 5% [19]. There were no infections reported.

Neuropsychological outcomes are favorable following SLAH. Confrontational naming largely remains stable with the few patients who change significantly being more likely to have an improvement than a decline [16, 18, 21, 24, 27, 28]. Changes in visual memory varied – some studies reported no change while one report noted significant decline in as many as 47% of the patients, with patients showing deficits after either dominant or non-dominant medial temporal lobe ablations [15, 16, 27]. Verbal memory declines, too, were inconsistently observed after SLAH – some series noting no significant group-wise significant changes [15, 18, 24] while others finding significant declines on certain tests [16, 19, 21, 27]. There were differences in dominant versus non-dominant temporal lobe ablations in this measure – the statistically significant group-wise declines were more frequent in dominant-sided ablations [21] while there were increased chances of improvement in non-dominant-sided ablations [15, 16]. Increased size of ablation correlated with neurocognitive decline only in dominant-sided ablations [21]. Seizure outcomes did not correlate with neuropsychiatric outcomes [28].

Comparisons with Other Procedures

While there are no randomized trials that compare SLAH with ATL or selective amygdalohippocampectomy(SAH), there are several studies that one can use to compare the outcomes after open resection vs. SLAH. The Engel 1 outcomes noted above (~57% in patients ± MTS) are lower when one compares against seizure freedom in either of the two randomized controlled trials of ATL against medical treatment – 64% [12] and 73% [13] – or against a meta-analysis of SAH vs ATL, which has one-year post-op seizure-free rates of 67% and 75% for the two procedures, respectively [29]. However, the comparison is not ideal since the selection for the randomized controlled trials likely would have excluded some of the patient population retrospectively reported in the open-label "real world" studies, (e.g., some patients with dual pathology). Conversely, retrospective studies generally perform better than prospective trials due to various biases not controlled for. The meta-analysis, too, is not a perfect comparison as its population was 91% MTS patients. However, comparing the seizure freedom rates of MTS-positive patients extrapolated from the meta-analysis supports a larger effect on seizure freedom by larger lesions – 73% seizure freedom after ATL, 66% after SAH, and 64% after SLAH. Meta-analysis of stereotactic radiosurgery (SRS) in temporal lobe epilepsy, too, shows lower rates of seizure freedom compared to open surgery: 42% for all comers, and 50% in lesional (all MTS except for one patient) cases [30].

Operative risk from papers included in the surgical meta-analysis shows rates of death or permanent neurological deficit ranging from 0% to 3.1% for SAH and 0% to 2.4% for ATL [29] as compared to 3.3% of permanent symptomatic neurological deficit (permanent cranial nerve palsies and hemianopsias) from our combined analyzed patient series. There have been no deaths reported from the SLAH procedure. The overall rate of visual field deficits from the reports of SLAH analyzed is 7.8%. Reported visual field deficits from temporal lobectomy range from 28% to 55% [12, 31, 32] while the SRS meta-analysis yielded visual field deficits reported in 12.7% [30].

Neuropsychological outcomes from the two procedures were examined head-to-head in one study. Our group found that there was no decline in naming or object recognition in our SLAH patients whereas 88% of patients after open resections (SAH or TLE) showed worsening (95% of dominant resections declined in at least one measure of naming, whereas 85% of non-dominant-sided resections declined in object recognition or familiarity) [28]. A meta-analysis of neuropsychological outcomes after temporal lobe resections found that 23% of right and 21% of left-sided patients showed a decline in visual memory [33] whereas all but one studies of SLAH [27] showed no significant changes postoperatively. Verbal memory declines are seen in both open surgery

and SLAH patients with a predilection toward more frequent memory decline if the dominant temporal lobe is operated on – decline in an average of 44% of dominant and 20% of non-dominant open surgeries [33] compared to 30.4% of dominant and 12.5% of non-dominant SLAHs in the series reviewed [15, 16, 24, 27].

Lesional and Non-Lesional Focal Neocortical Epilepsies

General Approach

Of course pathologies other than MTS and onset zones other than the medial temporal lobe can be treated with MRg-LITT as well, including both non-lesional and lesional focal neocortical etiologies such as cavernous malformations, focal cortical dysplasias, periventricular nodular heterotopias, epileptogenic tumors, hypothalamic hamartomas, cortical tubers, malignant gliomas, and metastatic tumors (the last four of these pathologies will be discussed in other chapters of this book).

Many lesional focal epilepsies can be treated de novo with laser ablation, that is, do not need invasive monitoring. In these cases, MRg-LITT is performed much as described above for the medial temporal lobe, with either frame- or frameless-based implantation of skull anchors for the guidance of the laser catheter, or with MRI-platforms such as ClearPoint. We and others have treated each of the above etiologies with both skull anchors and ClearPoint (Figs. 8.2 and 8.6).

Of course, many instances warrant further study with invasive monitoring, including some lesional epilepsies with alternative hypotheses and non-lesional epilepsies. With a long delay, over the last decade SEEG has become the dominant invasive monitoring technique beyond Europe where it was started in the 1960s. While historically, and in regions where laser ablation is not yet available, the only subsequent treatment option following SEEG was open resection (or the rarely effective multiple subpial transection), or radiofrequency ablation we now can marry SEEG very effectively with MRg-LITT. In some instances, following seizure and functional mapping with SEEG, the most logistical approach is to remove the electrodes and then on the same or subsequent admission perform MRg-LITT in just the same way as a de novo case, as described above. Instances such as this include onsets that are identified in the medial temporal lobe (treated as above) and the insula (Fig. 8.1b), because the trajectories used for SEEG are dissimilar to the most effective and safe approach needed for the laser ablation.

In other instances, however, the SEEG trajectories are ones that can be easily co-opted for insertion of the laser catheter and subsequent ablation, allowing ablation of the seizure onset zone during the electrode removal procedure through the existing SEEG electrode anchor bolts or even without, through the twist drill craniostomies (see above). When a sufficiently strong hypothesis exists a priori, as when there is a visible lesion, or perhaps even a region of dipoles identified with MEG, the depth electrodes can be inserted through the hybrid "laser bolts" that can subsequently accommodate replacement of the electrode with the laser catheter. In fact we may insert more than one to tar-

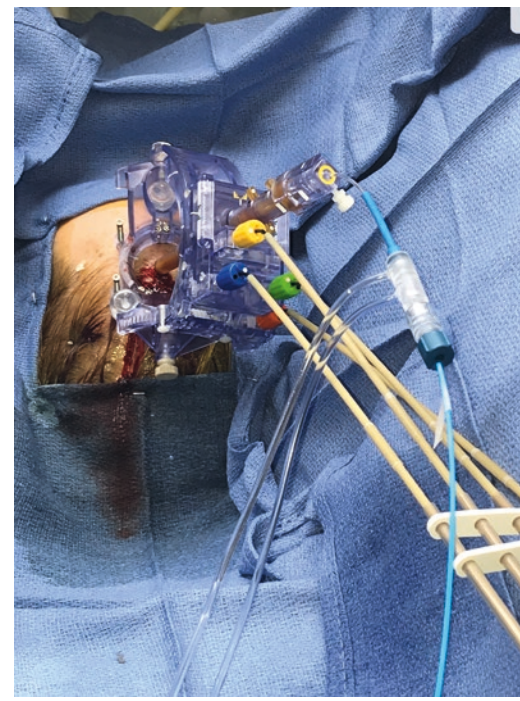

Fig. 8.6 Laser Ablation Through ClearPoint

get the same region as needed, in a distinctly non-classical SEEG approach. It should be noted that we do not use more than a few hybrid bolts, because the depth electrodes that go through them are not reduced diameter ones (Ad-Tech, although reduced diameter electrodes that go through the laser bolt are available from PMT), and the skin defect left by these larger bolts may not be trivial and more prone to poor healing. As noted above, an alternative approach when the hypothesis is not strong enough to use the laser bolts, but when ultimately SEEG identifies a region that can be ablated, is to simply remove the usual smaller anchor bolt and electrode and slide the laser catheter through this craniostomy under careful intraoperative MRI visualization to make sure there is no deviation from the intended trajectory (Fig. 8.4). Again, this is not done if there is any vasculature at risk nearby, as for example in the insular region.

Outcomes from Laser Ablation of Neocortical Epilepsies

Malformations of Cortical Development

Several small reports show seizure freedom in 64% of patients with focal cortical dysplasias solely treated through laser ablation [3, 34–38]. This compares favorably with seizure freedom rates in the 51–53% range from published open surgical series [39, 40]. There is also a report showing the effective use of LITT in combination with open resection to treat a focal cortical dysplasia [41]. Periventricular nodular heterotopia (PVNH) is particularly well-suited to treatment with stereotactic laser ablation; in fact there is much precedent for treating these typically small- to moderate-sized lesions by ablation with radiofrequency thermocoagulation [42]. The appeal of stereotactically treating these lesions with LITT is obvious given their deep location making the surgical approach treacherous, and their size. Patients with this pathology often exhibit other lesional pathology and their seizure onset zones may localize to more than just a particular heterotopia (such as the overlying neocortex), thus intracranial SEEG investigation is highly recommended [43]. Though ablating a single heterotopia may suffice to achieve seizure freedom, one may need to pursue further surgical treatment as well [44].

Cavernous Malformations

Although not necessarily intuitive, stereotactic laser ablation of epileptic cortical cavernous malformations is a safe alternative to open resection, particularly since some of these lesions may not be easily surgically accessible [45] (Fig. 8.7). Usually, invasive monitoring is not required in these lesional cases. We reported Engel I outcome in 82% of patients 1 year after treatment with laser ablation [46], which is on par with a reported Engel I outcome of 83% from a meta-analysis of surgical resections [47]. There were no hemorrhagic complications in our series of 19 patients.

Non-Lesional Epilepsies

Thus far, there are only a handful of reports of outcomes from MRg-LITT of non-lesional epilepsies. The insula, in which there is a considerable risk of surgical morbidity from resecting between the branches of the middle cerebral artery, is particularly well suited to this stereotactic technique [48]. In this example, the anatomy lends itself to parasagittal approaches down the long axes of the gyri of the insula with lower rates of neurological deficit than open surgery [49, 50] (Fig. 8.1b). Two published series of 20 and 14 (with likely overlap of patients) cite 50% [35] and 43% [51] seizure freedom, respectively, after laser ablation of non-lesional insular seizure foci. Cingulate epilepsy also lends itself to this kind of minimally invasive approach [52] (Fig. 8.8).

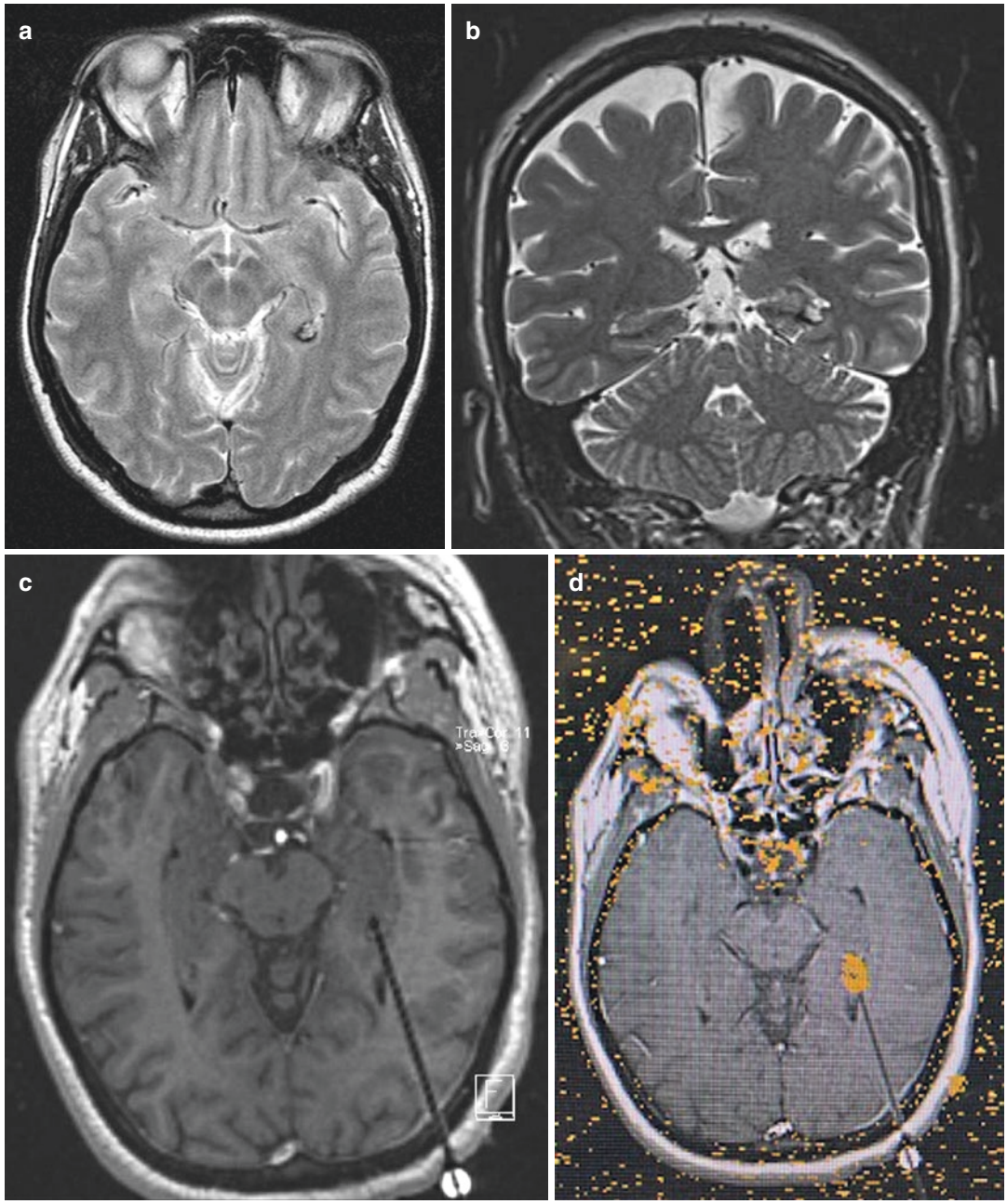

Fig. 8.7 Laser Ablation of Cavernous Malformation. (**a**) Axial FLAIR MRI and (**b**) coronal T2 of cavernous malformation deep in the left temporal lobe adjacent to the tail of the hippocampus in a right-handed dominant young woman. Surgical approach for resection cannot be done without either significant incursion on the white matter tracts and/or resection on the brain. (**c**) Axial MRI thermography image with laser cannula in the lesion shows a posterior approach to the lesion. (**d**) Axial MRI thermography of the lesion shows the maximal cross section volume. This patient is free of seizures and auras at 6 months with no memory or language complaints

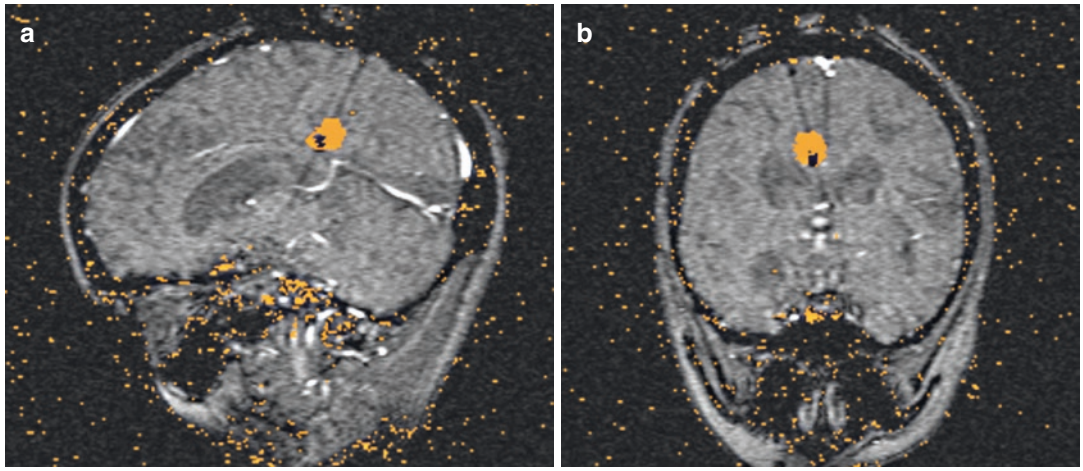

Fig. 8.8 Sagittal (**a**) and coronal (**b**) ablation map from MRI thermography demonstrating LITT of a posterior cingulate seizure focus

A review of our center's LITT ablations of neocortical non-lesional epilepsy patients shows a 1-year seizure-free rate of 43% in the 7 patients who have reached that time point for us [38]. As a comparison, a meta-analysis of surgical series of this class of patients reveals a 50% seizure-free rate in these patients [53].

Corpus Callosotomy

Corpus callosotomy for the treatment of drop attacks and/or secondarily generalization lends itself to MRgLITT as well. In this case, from 3 to 5 stereotactic bolts are inserted, depending on whether an anterior two-thirds vs. a complete callosotomy is being performed. We have also done laser callosotomy using the ClearPoint system, but this can be quite time-consuming since the tower needs to be relocated several times. In our series of 16 patients we have been able to reduce atonic seizures by 50% or more in 75% (9/12) patients and generalized tonic-clonic seizures in 62% (8/13; manuscript under review) [54]. Two patients had hemorrhagic or ischemic complications. The topic of corpus callosotomy using laser ablation is covered more extensively in the chapter on pediatric epilepsy surgery.

Conclusion

Since its introduction in 2010, stereotactic laser ablation is proving to be a safe and effective method for the treatment of focal epilepsy. While the most evidence thus far is for medial temporal lobe epilepsy, there is increasing evidence of effectiveness in treating other etiologies of focal epilepsy such as cavernous malformations, focal cortical dysplasias, periventricular nodular heterotopias, and non-lesional neocortical epilepsy. Though the rates of seizure-freedom appear slightly lower for MRgLITT compared to standard open resection for medial temporal lobe epilepsy there is growing evidence that stereotactic laser amygdalohippocampotomy can yield improved neuropsychological outcome and lower surgical morbidity compared to open surgeries. Whether the therapeutic window can also be increased for neocortical epilepsies will require much more evidence (manuscript under review). At this early stage, laser ablation seems to be on par with open resection in terms of seizure outcomes.

References

1. Bettag M, Ulrich F, Schober R, Furst G, Langen KJ, Sabel M, et al. Stereotactic laser therapy in cerebral gliomas. Acta Neurochir Suppl (Wien). 1991;52:81–3.
2. Carpentier A, McNichols RJ, Stafford RJ, Itzcovitz J, Guichard J-P, Reizine D, et al. Real-time magnetic resonance-guided laser thermal therapy for focal metastatic brain tumors. Neurosurgery. 2008;63(1 Suppl 1):ONS21–8; discussion ONS28–9.
3. Curry DJ, Gowda A, McNichols RJ, Wilfong AA. MR-guided stereotactic laser ablation of epileptogenic foci in children. Epilepsy Behav. 2012;24(4):408–14.
4. Administration FD. Visualase thermal therapy system 510(k). Food and Drug Administration: Rockville; 2007.
5. Administration FD. Monteris medical NeuroBlate system 510(k). Silver Spring: Food and Drug Administration; 2013.
6. Stereotactic Laser Ablation for Temporal Lobe Epilepsy (SLATE) ClinicalTrials.gov: U.S. National Library of Medicine; 2019 [updated 1/9/19]. Available from: https://clinicaltrials.gov/ct2/show/NCT02844465.
7. Sperling MR, Gross RE, Alvarez GE, McKhann GM, Salanova V, Gilmore J. Stereotactic Laser Ablation for Mesial Temporal Lobe Epilepsy: A prospective, multicenter, single-arm study. Epilepsia, 2020; epi.16529. https://doi.org/10.1111/epi.16529.
8. Gonzalez-Martinez J, Mullin J, Vadera S, Bulacio J, Hughes G, Jones S, et al. Stereotactic placement of depth electrodes in medically intractable epilepsy. J Neurosurg. 2014;120(3):639–44.
9. Willie JT, Laxpati NG, Drane DL, Gowda A, Appin C, Hao C, et al. Real-time magnetic resonance-guided stereotactic laser amygdalohippocampotomy for mesial temporal lobe epilepsy. Neurosurgery. 2014;74(6):569–85.
10. Bentley JN, Isbaine F, Gross RE, Willie JT. Accuracy of stereotactic laser amygdalohippocampotomy ablations using an MRI-targeting platform. Manuscript in preparation.
11. Sadler RM. The syndrome of mesial temporal lobe epilepsy with hippocampal sclerosis: clinical features and differential diagnosis. Adv Neurol. 2006;97:27–37.
12. Wiebe S, Blume W, Girvin J, Eliasziw M. Group EaEoSfTLES. A randomized, controlled trial of surgery for temporal lobe epilepsy. N Engl J Med. 2001;345(5):311–8.
13. Engel J Jr, McDermott MP, Wiebe S, Langfitt JT, Stern JM, Dewar S, et al. Early surgical therapy for drug-resistant temporal lobe epilepsy: a randomized trial. JAMA. 2012;307(9):922–30.
14. Bullinger K, Alwaki A, Gross R, Willie J. When laser fails: the role for intracranial monitoring following seizure recurrence after stereotactic laser amygdalohippocampectomy (SLAH). New Orleans: American Epilepsy Society; 2018.
15. Gross RE, Stern MA, Willie JT, Fasano RE, Saindane AM, Soares BP, et al. Stereotactic laser amygdalohippocampotomy for mesial temporal lobe epilepsy. Ann Neurol. 2018;83(3):575–87.
16. Jermakowicz WJ, Kanner AM, Sur S, Bermudez C, D'Haese P-F, Kolcun JPG, et al. Laser thermal ablation for mesiotemporal epilepsy: analysis of ablation volumes and trajectories. Epilepsia. 2017;58(5):801–10.
17. Vakharia VN, Sparks R, Li K, O'Keeffe AG, Miserocchi A, McEvoy AW, et al. Automated trajectory planning for laser interstitial thermal therapy in mesial temporal lobe epilepsy. Epilepsia. 2018;59(4):814–24.
18. Grewal SS, Zimmerman RS, Worrell G, Brinkmann BH, Tatum WO, Crepeau AZ, et al. Laser ablation for mesial temporal epilepsy: a multi-site, single institutional series. J Neurosurg. 2018;1:1–8.
19. Kang JY, Wu C, Tracy J, Lorenzo M, Evans J, Nei M, et al. Laser interstitial thermal therapy for medically intractable mesial temporal lobe epilepsy. Epilepsia. 2016;57(2):325–34.
20. Tatum WO, Thottempudi N, Gupta V, Feyissa AM, Grewal SS, Wharen RE, et al. De novo temporal intermittent rhythmic delta activity after laser interstitial thermal therapy for mesial temporal lobe epilepsy predicts poor seizure outcome. Clin Neurophysiol. 2019;130(1):122–7.
21. Donos C, Breier J, Friedman E, Rollo P, Johnson J, Moss L, et al. Laser ablation for mesial temporal lobe epilepsy: surgical and cognitive outcomes with and without mesial temporal sclerosis. Epilepsia. 2018;59(7):1421–32.
22. Youngerman BE, Oh JY, Anbarasan D, Billakota S, Casadei CH, Corrigan EK, et al. Laser ablation is effective for temporal lobe epilepsy with and without mesial temporal sclerosis if hippocampal seizure onsets are localized by stereoelectroencephalography. Epilepsia. 2018;59(3):595–606.
23. Le S, Ho AL, Fisher RS, Miller KJ, Henderson JM, Grant GA, et al. Laser interstitial thermal therapy (LITT): seizure outcomes for refractory mesial temporal lobe epilepsy. Epilepsy Behav. 2018;89:37–41.
24. Tao JX, Wu S, Lacy M, Rose S, Issa NP, Yang CW, et al. Stereotactic EEG-guided laser interstitial thermal therapy for mesial temporal lobe epilepsy. J Neurol Neurosurg Psychiatry. 2018;89(5):542–8.
25. Wu C, Jermakowicz WJ, Chakravorti S, Cajigas I, Sharan AD, Jagid JR, et al. Effects of surgical targeting in laser interstitial thermal therapy for mesial temporal lobe epilepsy: a multicenter study of 234 patients. Epilepsia. 2019;60(6):1171–83.
26. Gross R. The latest on lasers: improving the outcome of MRg-LITT Amygdalohippocampotomy. Epilepsy Curr. 2018;18(6):382–6.
27. Greenway MRF, Lucas JA, Feyissa AM, Grewal S, Wharen RE, Tatum WO. Neuropsychological outcomes following stereotactic laser amygdalohippocampectomy. Epilepsy Behav. 2017;75:50–5.
28. Drane DL, Loring DW, Voets NL, Price M, Ojemann JG, Willie JT, et al. Better object recognition and naming outcome with MRI-guided stereotactic laser

amygdalohippocampotomy for temporal lobe epilepsy. Epilepsia. 2015;56(1):101–13.
29. Josephson CB, Dykeman J, Fiest KM, Liu X, Sadler RM, Jette N, et al. Systematic review and meta-analysis of standard vs selective temporal lobe epilepsy surgery. Neurology. 2013;80(18):1669–76.
30. Grewal SS, Alvi MA, Lu VM, Wahood W, Worrell GA, Tatum W, et al. Magnetic resonance–guided laser interstitial thermal therapy versus stereotactic radiosurgery for medically intractable temporal lobe epilepsy: a systematic review and meta-analysis of seizure outcomes and complications. World Neurosurg. 2019;122:e32–47.
31. Tecoma ES, Laxer KD, Barbaro NM, Plant GT. Frequency and characteristics of visual field deficits after surgery for mesial temporal sclerosis. Neurology. 1993;43(6):1235–8.
32. Egan R, Shults W, So N, Burchiel K, Kellogg J, Salinsky M. Visual field deficits in conventional anterior temporal lobectomy versus amygdalohippocampectomy. Neurology. 2000;55(12):1818–22.
33. Sherman EMS, Wiebe S, Fay-McClymont TB, Tellez-Zenteno J, Metcalfe A, Hernandez-Ronquillo L, et al. Neuropsychological outcomes after epilepsy surgery: systematic review and pooled estimates. Epilepsia. 2011;52(5):857–69.
34. Kamath AA, Friedman DD, Hacker CD, Smyth MD, Limbrick DD Jr, Kim AH, et al. MRI-guided interstitial laser ablation for intracranial lesions: a large single-institution experience of 133 cases. Stereotact Funct Neurosurg. 2017;95(6):417–28.
35. Perry MS, Donahue DJ, Malik SI, Keator CG, Hernandez A, Reddy RK, et al. Magnetic resonance imaging-guided laser interstitial thermal therapy as treatment for intractable insular epilepsy in children. J Neurosurg Pediatr. 2017;20(6):575–82.
36. Devine IM, Burrell CJ, Shih JJ. Curative laser thermoablation of epilepsy secondary to bottom-of-sulcus dysplasia near eloquent cortex. Seizure. 2016;34:35–7.
37. Cobourn K, Fayed I, Keating RF, Oluigbo CO. Early outcomes of stereoelectroencephalography followed by MR-guided laser interstitial thermal therapy: a paradigm for minimally invasive epilepsy surgery. Neurosurg Focus. 2018;45(3):E8.
38. Koch P, Ramesha S, Graf D, Cabaniss B, Gross R, Willie J, editors. Stereotactic laser ablation for neocortical epilepsy. New Orleans: American Epilepsy Society; 2018.
39. Choi SA, Kim SY, Kim H, Kim WJ, Kim H, Hwang H, et al. Surgical outcome and predictive factors of epilepsy surgery in pediatric isolated focal cortical dysplasia. Epilepsy Res. 2018;139:54–9.
40. Fauser S, Essang C, Altenmüller D-M, Staack AM, Steinhoff BJ, Strobl K, et al. Long-term seizure outcome in 211 patients with focal cortical dysplasia. Epilepsia. 2015;56(1):66–76.
41. Ellis JA, Mejia Munne JC, Wang S-H, McBrian DK, Akman CI, Feldstein NA, et al. Staged laser interstitial thermal therapy and topectomy for complete obliteration of complex focal cortical dysplasias. J Clin Neurosci. 2016;31:224–8.
42. Cossu M, Mirandola L, Tassi L. RF-ablation in periventricular heterotopia-related epilepsy. Epilepsy Res. 2018;142:121–5.
43. Thompson SA, Kalamangalam GP, Tandon N. Intracranial evaluation and laser ablation for epilepsy with periventricular nodular heterotopia. Seizure. 2016;41:211–6.
44. Esquenazi Y, Kalamangalam GP, Slater JD, Knowlton RC, Friedman E, Morris SA, et al. Stereotactic laser ablation of epileptogenic periventricular nodular heterotopia. Epilepsy Res. 2014;108(3):547–54.
45. McCracken DJ, Willie JT, Fernald BA, Saindane AM, Drane DL, Barrow DL, et al. Magnetic resonance thermometry-guided stereotactic laser ablation of cavernous malformations in drug-resistant epilepsy: imaging and clinical results. Operative Neurosurg. 2016;12(1):39–48.
46. Willie JT, Malcolm JG, Stern MA, Lowder LO, Neill SG, Cabaniss BT, et al. Safety and effectiveness of stereotactic laser ablation for epileptogenic cerebral cavernous malformations. Epilepsia. 2019;60(2):220–32.
47. Shang-Guan H-C, Wu Z-Y, Yao P-S, Chen G-R, Zheng S-F, Kang D-Z. Is extended lesionectomy needed for patients with cerebral cavernous malformations presenting with epilepsy? A meta-analysis. World Neurosurg. 2018;120:e984–e90.
48. Bouthillier A, Nguyen DK. Epilepsy surgeries requiring an operculoinsular cortectomy: operative technique and results. Neurosurgery. 2017;81(4):602–12.
49. Perry MS, Donahue DJ, Malik SI, Keator CG, Hernandez A, Reddy RK, et al. Magnetic resonance imaging–guided laser interstitial thermal therapy as treatment for intractable insular epilepsy in children. J Neurosurg. 2017;20(6):575.
50. Hawasli AH, Bandt SK, Hogan RE, Werner N, Leuthardt EC. Laser ablation as treatment strategy for medically refractory dominant insular epilepsy: therapeutic and functional considerations. Stereotact Funct Neurosurg. 2014;92(6):397–404.
51. Hale AT, Sen S, Haider AS, Perkins FF Jr, Clarke DF, Lee MR, et al. Open resection vs laser interstitial thermal therapy for the treatment of pediatric insular epilepsy. Neurosurgery. 2019 Oct 1;85(4):E730–6.
52. Marashly A, Loman MM, Lew SM. Stereotactic laser ablation for nonlesional cingulate epilepsy: case report. J Neurosurg. 2018;22(5):481.
53. Engel J Jr, Wiebe S, French J, Sperling M, Williamson P, Spencer D, et al. Practice parameter: temporal lobe and localized neocortical resections for epilepsy. Epilepsia. 2003;44(6):741–51.
54. Willie JT, Gross RE, Qiu D, Winkel D, Fasano RE. Minimally invasive stereotactic laser ablation of the corpus callosum in adults with intractable epilepsy. Houston: American Epilepsy Society; 2016.

9 LITT in Adult Functional Neurosurgery: Movement Disorders

Meghan Harris and Jessica Anne Wilden

Rationale for LITT in Movement Disorders

Lesions of the motor cortex, brainstem, and spinal cord were among the first procedures performed for movement disorders. By mid-century, pallidotomy, thalamotomy, and sub-thalamotomy were routine procedures performed for Parkinson's disease (PD), essential tremor (ET), and dystonia. Surgery declined for PD in particular after the introduction of levodopa in the 1960s. With the recognition of levodopa complications, however, there was revived interest in movement disorder surgery in the late 1980s, and this combined with further surgical refinements led to the resurgence of posteroventral pallidotomy for PD [1]. The resurgence was short-lived: with the seminal work of Benabid and colleagues and others, the safety and effectiveness of deep brain stimulation (DBS) was demonstrated and then commercially developed. Like pallidotomy and thalamotomy, it results in sustained improvements in core motor symptoms, including action or resting tremor, rigidity, and bradykinesia while minimizing medication side effects like dyskinesia and wearing OFF phenomenon [2–5]. DBS is currently FDA approved for Parkinson's disease (PD) and essential tremor (ET) as well as for primary generalized dystonia under a humanitarian device exemption. Nevertheless, while remarkably effective – and non-destructive – DBS is a high maintenance therapy that is typically offered to patients with good health, robust cognition, younger age, and a strong support system that can bear the burden of repeated travel to a multidisciplinary clinic for long-term management.

As the population ages and the prevalence of Parkinson's disease and tremor disorders increases, the need for diversified surgical therapies is apparent. In our clinic, elderly patients, particularly in the late eighth decade and up, are presenting for definitive treatment of medically intractable action or resting tremors. These tremors are severe and threaten the patient's independence. Patients who are in relatively good health want to be given surgical options that are effective and tolerable even at an advanced age, which is a reasonable expectation of our society. Other issues to consider are the inconvenience and cost of repeated travel for DBS titration, particularly on a fixed income like Social Security Insurance. Large swaths of the US house rural retirees who cannot access a large academic medical center.

Ablative procedures have made a comeback for these reasons among others. Traditionally a radiofrequency (RF) probe was used to make a lesion in the thalamus or the globus pallidus

M. Harris
Department of Neurology, Highland Clinic, Shreveport, LA, USA

J. A. Wilden (✉)
Surgical Movement Disorder Clinic, Tristate Neurosurgery, Willis-Knighton Hospital System, Shreveport, LA, USA

V. L. Chiang et al. (eds.), *Laser Interstitial Thermal Therapy in Neurosurgery*,
https://doi.org/10.1007/978-3-030-48047-9_9

internus in the operating room using conventional frame-based methodology with or without microelectrode recording [6, 7]. Effectiveness of this technique was a ~ 30–70% reduction in symptoms including tremors, bradykinesia, rigidity, and drug-induced dyskinesias, sustained long term, with rare but potentially serious side effects [8–14]. Stereotactic radiosurgery (SRS) has also been used to create 4 mm thalamotomy lesions in the Gamma Knife suite. In several series essential or Parkinsonian tremor improved ~60% on average, sustained for 6 years and beyond [15], though not all patients were "responders" with up to 20% of Parkinsonian tremors not having significant clinical improvement [16]. Side effects were relatively common, occurring in 6–8% of patients [15], and included unpredictable and disabling radiation necrosis affecting the internal capsule as seen in one of our own patients despite using a low-dose (120 Gy) and a well-described target [17]. Clinical effect on tremor can also be delayed several weeks to months after SRS, which is a disadvantage, particularly to very elderly patients. MRI-guided high-intensity focused ultrasound (HIFU) is a widely recognized and recently FDA-approved method for unilateral thalamotomy in essential tremor and tremor-predominant Parkinson's disease [18]. The novelty of HIFU is the ability to create a destructive lesion using focused ultrasonic waves without an incision. Although incisionless, HIFU nonetheless destroys thalamic tissue and, like other procedures, has the potential for side effects and adverse events, which are relatively uncommon [19]. The effectiveness of HIFU has been demonstrated in the short and the long term [20–22], though chronic data over ~4 to 10 years has yet to be published. The major limitations of HIFU for both community and academic institutions remain the cost and the MRI logistics as well as barriers to reimbursement, particularly among private insurance carriers. Ultrasound, by its nature, also has treatment limitations based on patient's scalp and skull thickness as well as hair concerns [23]: shaving the entire head for HIFU is a distinct downside given the elective nature of the procedure. Intraprocedural testing of the tremor effect, performed in ultrasound and RF ablations, is usually seen as a positive, even necessary, aspect by physicians. However, it is critical to recognize that this may be a negative for the patient with claustrophobia in a head frame, generalized anxiety, low education, difficulty cooperating with tasks, poor concentration, and/or medical conditions that impede breathing in the supine position.

In order to adapt to our patients' needs, our clinic desired an alternative tremor procedure that met the following criteria: (1) no hardware, (2) no titration, (3) fast results, (4) no intraprocedural patient participation, (5) minimal incision, and (6) minimal recovery time. MRI-guided laser interstitial thermal therapy (MRg-LITT) for thalamotomy or pallidotomy, previously reported in a single case [24], was our answer and is described in detail below. This procedure is performed in an MRI suite using live imaging guidance and the ClearPoint stereotactic system, which may provide superior accuracy to more traditional frame-based techniques [25]. Laser ablation systems are capable of creating a small focal lesion without injury to surrounding critical structures. The surgeon can see the temperature change as well as the cumulative estimated tissue damage on the laser work station in real time [26], offering an alternative means of control of the ablation zone as compared to RF lesioning in the awake patient and potentially allowing the procedure to be completed under general anesthesia. Incision and hair shave required are minimal, and there is no head frame placement while awake, all of which may greatly improve the patient experience.

Patient Selection

As we alluded to above, this procedure is best applied to a relatively narrow category of patients. If a patient meets standard, accepted criteria for deep brain stimulation for ET or PD, then we recommend DBS over any type of lesioning, including LITT, which is reflected in the fact that laser thalamotomy/pallidotomy only comprises ~10–15% of our movement disorder cases.

Common factors that favor laser surgery over DBS include:

- Advanced age (usually 75 years or older)
- Medically fragile (e.g., history of stable but significant cardiac disease)
- Inability to follow up for DBS management
- Inability of patient or family member to adjust DBS system at home
- Patient preference (e.g., refusal to accept implanted hardware)

We prefer to perform this procedure under general anesthesia due to our intra-MRI technique and to maximize patient comfort. The incision, blood loss, and operative time are typically much less than for DBS, which is helpful in patients with a history of cardiopulmonary disease. In our experience, insurance does not affect patient eligibility because both Medicare and private insurers have recognized and reimbursed this procedure under the same code for RF lesioning (i.e., creation of a stereotactic lesion in thalamus or pallidum).

Interventional MRI

The accuracy required and the general debility of this patient population is best served in our hands by performing the entire procedure in the MRI scanner. The entire process at our center, including anesthesia induction, target planning, frame placement, laser application, and postoperative imaging, is performed in a diagnostic MRI suite (Philips 1.5 T) adapted for surgical procedures as previously described for DBS lead placement. The ClearPoint disposable SmartFrame and its partner software (MRI Interventions, Irvine, CA) are used in conjunction with the Visualase laser platform (Medtronic, Louisville, CO) to make focused lesions in the ventral intermediate thalamus for essential tremor or the globus pallidus internus for Parkinson's disease.

Section I: Induction, Head Frame, and Sterile Field

The anesthesiologist does a full assessment of the patient in the preoperative holding area and transfers the patient to an anteroom directly outside of the main MRI chamber. The patient is intubated on a surgical stretcher using standard techniques; we often use a GlideScope in our elderly patients to prevent significant neck extension given the high likelihood of cervical spondylosis. No special anesthetic agents are necessary since there is no intraoperative monitoring. Two large-bore IVs are placed as well as a Foley catheter in patients who report pre-existing urinary incontinence. Antibiotics are administered, sequential compression devices are used for deep vein thrombosis prophylaxis, and surgical time-out is performed. The patient is then moved onto the MRI-compatible table, which is wholly covered by a gel mat and a sheet. The patient is then fitted with additional padding, including an Aquagel sacral protector pad and foam underneath the elbows and heels. The patient's arms are tucked by both sides of the body with the sheet, ensuring that all IVs and oxygen/BP monitoring are still functioning properly in the final position. *Note: Anesthesia has extremely limited access to the patient during the case as the bulk of the patient's body is within the bore of the MRI. It is thus critically important that all lines and monitors are satisfactory prior to entry to MRI.*

The patient's head is secured in a four-point MRI-compatible head holder (MRI Interventions, Irvine, CA), with flexible MRI receiving coils on each side of the head. Head position for laser surgery, like DBS, is neutral without excess extension or flexion and should be midline with the nose in a sagittal plane that is perpendicular to the floor. *Note: There is no pressure measurement on the MRI-compatible head frame, unlike the Mayfield. Pins are tightened to a finger-tight level, and the head is checked for movement in the A-P and lateral directions*. If any movement occurs, pins are tightened a few turns further, and the process is repeated until the head is secure. Two important points are as follows: (1) MRI receiving coils must be placed on either side of the patient's head before tightening the pins, and (2) care must be taken to not accidentally puncture an MRI receiving coil while tightening the pins because this will affect imaging quality later in the case. We place an absorbent padding

between the head and the coil to protect the coils from fluid and the patient's skin from heating. Once the head is secured, an additional safety time-out is performed during which all staff make sure no MRI-unsafe items are being taken into the main MRI chamber, including cell phones, pens, jewelry, medication patches, needles, and the like. Anesthetic goals are also reviewed at this time, including a SBP goal of less than 120 and an end-title CO2 level of 35–40 as well as ample hydration to prevent venous collapse with subsequent tearing or infarction. We do not administer mannitol or steroids.

The patient on the MRI table is moved into the main scanning chamber and secured onto the gantry, taking care not to disrupt any of anesthesia's lines/equipment. Isocenter is marked at the level of the coronal suture. The patient's head is then moved to the back of the MR bore, where the sterile field is established (Fig. 9.1). One can use four blue towels to define the sterile field versus a full ClearPoint drape (MRI Interventions, Irvine, CA). We have done both but prefer a full drape for these cases so the surgeon can access the mechanical drill and bipolar cautery easily without contamination. Draping the field in the MRI suite involves attaching elastic tabs, which are color-coded and numbered for simplicity, to the near and far end of the bore to keep the field sterility intact between scanning at the center of the bore and operating at the back of the MRI.

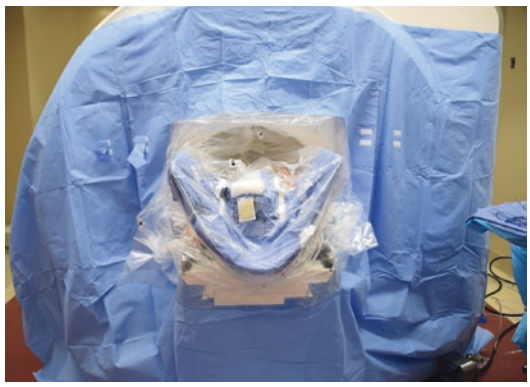

Fig. 9.1 The sterile field is prepared in a converted diagnostic MRI

Section II: General Targeting and SmartFrame Placement

Patients undergo a preoperative screening MRI on a 3T non-operative scanner the day prior to surgery. These high-quality scans are imported into the ClearPoint software the evening prior to surgery. The surgeon plans a tentative target and trajectory to ensure the procedure is feasible prior to subjecting the patient to general anesthesia.

Intraoperatively, after the sterile field has been established, a ClearPoint marking grid is placed on the scalp in the region of the coronal suture. The patient is moved back to the center of the bore for a contrast-enhanced image. For laser cases, we give a half dose (10–20 mL) of gadolinium at the beginning of the case to assess the vasculature near our planned trajectory and save the other half dose to be given at the end of the case to check the lesion. The acquired T1W images are imported into ClearPoint software. The preoperative coordinates that were planned the day prior are imported into the ClearPoint software session that is active during surgery. The anatomic target is inspected for accuracy and adjusted as needed; the trajectory is reviewed to make sure it does not violate the lateral ventricle or cross major vascular structures. *Note: Unlike a DBS lead, the tip of the Visualase catheter is somewhat sharp and may be more prone to vascular disruption. Avoid crossing vascular structures and sulci whenever possible. We drive SBP down to around 100 during insertion.*

The ClearPoint software proposes an entry point on the marking grid based on the desired target and trajectory. *Note: The marking grid has a fluid-filled top cover that must be peeled off the plastic grid base prior to marking the scalp.* A "screwdriver-like" punch tool is used to mark the entry point on the scalp through the plastic marking grid base (Fig. 9.2). The grid base itself is then peeled off. A disposable two-piece surgical apparatus called the SmartFrame is centered over the marked entry point and secured to the skull with six small screws that go through the scalp and seat into the bone (Fig. 9.3). *Note: We recommend using all six screw sites on the frame to secure the device to ensure stability.* The

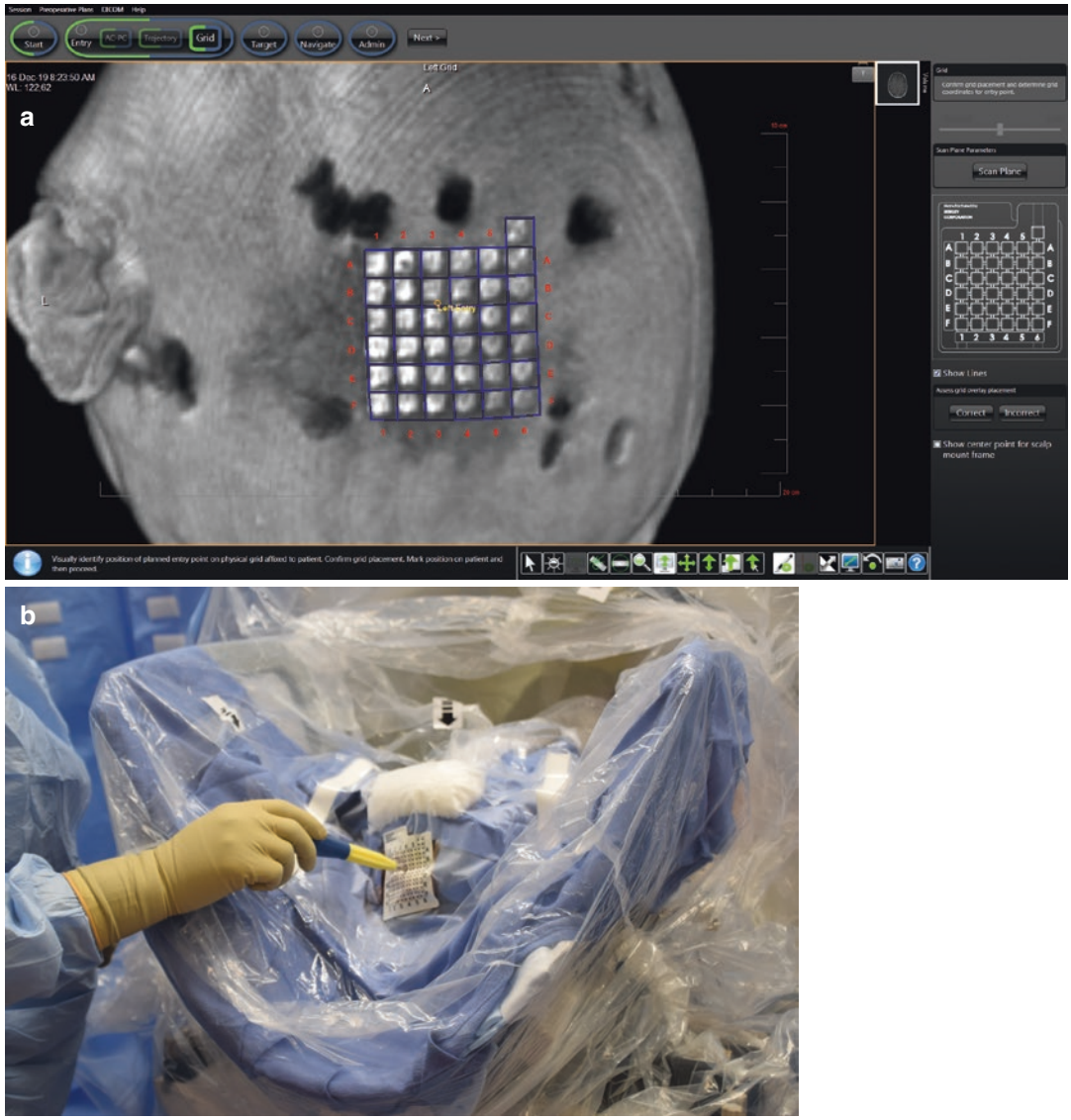

Fig. 9.2 (**a**) The ClearPoint software projects the scalp entry point on the surface marking grid. (**b**) A punch tool is used to pierce the marking grid base through the scalp and superficial skull to define the projected entry

SmartFrame consists of a base and a top piece that has colored hand knobs and a center cannula that will guide the laser into place, obviating the need for a laser-specific bone anchor. A remote-control system can be attached to the colored knobs on the SmartFrame to allow ease of adjustment without leaning into the center of the bore. Once firmly secured, the SmartFrame should exhibit no significant movement, or accuracy will be adversely affected.

Section III: SmartFrame Adjustment and Burrhole Creation

High-resolution imaging is obtained through the target region, and the surgeon confirms the target and trajectory. The best sequence for target confirmation may vary, but in general a T1W sequence is used for the thalamus, and an inversion recovery (IR) sequence is used for the pallidum. High-resolution imaging is then obtained

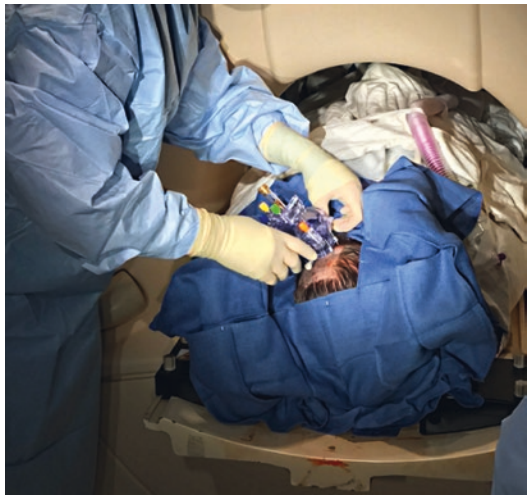

Fig. 9.3 The ClearPoint stereotactic SmartFrame is mounted to the patient's head

through the plane of the SmartFrame and identifies three built-in frame fiducials. ClearPoint software then calculates the adjustments to the SmartFrame knobs to point the center cannula at the target. Initial large adjustments of the SmartFrame controls are performed based on axial imaging using the pitch (orange) and roll (blue) knobs. Fine adjustments are then made based on oblique sagittal and coronal imaging using the X (green) and Y (yellow) knobs until the predicted error is less than 1 mm from target.

There are distinct modifications to the laser protocol that are needed to successfully create a small lesion in a critically eloquent area like the thalamus or pallidum. Submillimetric accuracy during these procedures is paramount, so we change our drilling and ablation protocols to accommodate. For larger targets like tumors or the temporal lobe for epilepsy, we use a standard method: A 3–4 mm stab incision is made followed by a 3 mm burrhole with the manual ClearPoint drill. There is no direct vision when drilling, and the drill tip is passed through the outer and inner tables of the skull by feel. A sharp metal stylette in the ClearPoint drill kit is used to puncture the dura prior to laser insertion. Unfortunately, this method can be fraught with minor inaccuracies if the laser is slightly deflected by the bony or dural edge. While a 1–2 mm error may not significantly affect a tumor ablation, this could have a major impact on a movement disorder case in which the entire lesion size is 4 to 8 mm.

Our modified protocol is as follows: A 1.5 cm linear incision is made over the entry site. The ClearPoint hand drill is used to mark the outer table of the skull at the entry point. The top of the SmartFrame is removed for better access to the incision. Meticulous hemostasis is achieved using bipolar cautery, and the skin edges are retracted with sutures secured to the drape. An MR-compatible high-speed mechanical drill (Stryker) is used to make a 6–8 mm burrhole centered at the marked location. The dura is coagulated and opened completely under direct vision so as to not obstruct any potential entry point. One may use loupes and a headlight to facilitate this process given the small field of view. *Note: A surgical headlight can typically be worn at the back of the MRI bore without interaction with the magnetic field, though the surgeon should not lean into the bore when wearing this equipment.*

Once the exposure is complete, the top of the SmartFrame is re-applied, and the patient is moved to isocenter for repeat scans to confirm that the center cannula is pointing at the target. Typically, only small adjustments are needed to re-establish an accuracy of ~1 mm if the frame is well-secured to the skull. The software calculates the depth needed to reach the target, and a ceramic, MRI-compatible ClearPoint stylette is measured appropriately. *Note: The ceramic stylette is extremely fragile, so handle the stylette and tighten the depth stop with care.* The ceramic stylette is inserted into a peel-away sheath that is inserted through the center cannula down to the target. When the stylette is at target, a high-resolution axial T1W image is obtained and provides a radial error. We generally accept an error of less than 0.6 mm for either DBS or laser ablation. *Note: When operating at the back of the bore, anesthesia is not readily visible to the surgeon. Verbally confirm that blood pressure is at the desired level prior to insertion of any device into the brain. High blood pressure during insertion increases risk of stroke/bleed.*

Section IV: Laser Preparation, Ablation, and Assessment

A radial error of greater than 0.6 mm is not acceptable for thalamotomy and pallidotomy. In that case, the patient is returned to the back of the bore, the stylette is removed, the center cannula is readjusted per software recommendations, and the stylette is reinserted and reassessed. If the radial error is acceptable, then the ceramic stylette is removed, and the Visualase laser apparatus, consisting of a catheter, saline lines, and the laser itself, is opened onto the sterile field.

The Visualase catheter is measured using a depth stop similar to the ceramic stylette. However, an adjustment needs to be made to the calculated depth. To understand this adjustment, it is necessary to review the types and heating properties of the laser. The Visualase laser diffusing tip comes in two lengths, 10 mm and 3 mm. *Note: Both lasers heat symmetrically around the light source but differ as to where the heating starts. The 10 mm laser starts heating at its center, or ~ 5 mm from the tip. The 3 mm laser starts heating at its posterior edge, or ~ 3 mm from the tip* (personal communication, Medtronic Inc., Louisville, CO). This is critically important in terms of depth calculation. For creation of small lesions, we use the 3 mm laser and low power percentages (25% or less); as a result, the laser will primarily damage tissue only around its starting point and not around its entire length. In contrast, at higher power percentages (50% or greater), the laser heats around its entire length creating an oblong or spherical lesion for 10 and 3 mm, respectively. This means that final depth calculation for the catheter is equal to ClearPoint calculated depth for the ceramic stylette +3 mm adjusting for the catheter's plastic tip beyond the laser fiber +3 mm adjusting for the length of the laser beyond where it will start to heat. *Note: Practically speaking this means that the surgeon adds 6 mm to the recommended ClearPoint depth when placing the depth stop on the Visualase catheter.* It is thus important to review the imaging at least 6 mm beyond the target for any vascular structures or areas of potential injury.

The catheter comes with a stiff stylette that is left in place during laser insertion to ensure it does not deviate from the intended trajectory. Once the catheter is inserted down the cannula and is secured to the SmartFrame, the stiff stylette is removed, and the laser fiber is inserted into the catheter. Once the laser fiber reaches the bottom of the catheter, a catheter locking knob is tightened around the laser so it does not accidently retract during the case (Fig. 9.4). We place a Steri-Strip at the junction of the laser fiber and locking knob to mark the laser depth as well. The patient is then moved back to the center of the bore, and an opening is cut in our sterile drape lateral to the main surgical field. The saline cooling lines are connected to the laser apparatus and then passed distally through the drape along with the distal end of the laser fiber, both of which are connected to the Visualase work station (Medtronic, Louisville, CO). The final position of the laser apparatus is observed, and, if accept-

Fig. 9.4 The Visualase laser catheter is attached to the SmartFrame, and the laser fiber is then inserted and secured prior to the patient moving back to the center of MRI for treatment

able, all laser and saline lines are attached to the surgical drape using Steri-Strips or hemostats to prevent undue movement when the non-sterile lines are manipulated. *Note: There is some flexibility to the laser apparatus so it can bend slightly to accommodate a smaller bore MRI. However, the laser catheter should not go beyond a gentle angular curve because the saline will not flow correctly through the catheter at a sharp 90-degree angle, which will break the catheter. If saline fails to flow around the tip of the catheter, the surrounding brain is more susceptible to unintended heat damage.*

Background imaging is obtained continuously and superimposed on a high-resolution T1 or IR historical image as the Visualase laser is used to achieve controlled ablation of the target area. Direct visual feedback of lesion formation is provided in real time on the Visualase work station in the form of a heat map and a damage estimate. In general, the heat map seems to be more reliable for this indication than the damage estimate; if incongruent, we adjust our approach based on the lesion size and shape on the heat map. The target area is usually covered completely with 3–5 ablations at the same or serial site(s) depending on thalamotomy vs pallidotomy (see below). We use consecutive low power percentages of 10% (1.0 W), 15% (1.5 W), 20% (2.0 W), and +/− 25% (2.5 W) for about 2 minutes each to achieve a small lesion without collateral damage. The ablation site(s) are allowed to cool completely between each run. We alter each patient's particular protocol based on visual feedback. For example, we may stop lesion formation at 20% total power after just 1 minute if heating is significant and fully covering the intended target. Alternatively, we may use up to 25% total power for up to 4 minutes if heating appears to be slow or inadequate. *Note: There is no magic "standard" protocol. Successful treatment is dependent on surgeon engagement and adaptive decision-making.*

After ablation of the target is complete, a T2 and gadolinium-enhanced volumetric T1 MRI are performed to evaluate the area of ablation. *Note: To get a clear picture of the "true ablation," ensure that hypotension is not present, thereby interfering with the flow of contrast into the tissue, and that contrast is injected a full 10 minutes prior to scanning.* We usually ask anesthesia to aim for a SBP around 120 for these final scans. If the lesion is acceptable (see below for details), then the patient is returned to the back of the magnet bore where the Visualase laser is disassembled and the Visualase catheter removed from the brain. The SmartFrame top and base mount are removed. The incision and screw sites are irrigated and cleaned with a sponge. A titanium cover is placed over the burrhole to prevent a long-term cosmetic divot in the frontal region. The wound is closed with a single 2-0 Vicryl in the galea and a single figure-of-eight 2-0 Prolene suture for the skin. The drape is taken down, the patient is moved back into the anteroom of the MRI suite, the patient's head is released from the head frame, and the patient is moved back onto the stretcher for extubation.

Thalamotomy

Targeting and Laser Ablation

Our thalamus target is based on cumulative experience with thalamic DBS and GKS thalamotomy. We start with the following coordinates: X = 10 mm lateral to the wall of the third ventricle for hand tremor, Y = 25% of the AC-PC distance, and Z = 2.5 mm above the AC-PC plane. Based on the HIFU experience of sensory disturbances using the aforementioned Y coordinate [27], we add 1 millimeter to the Y coordinate to place the lesion slightly more anterior than a typical DBS lead. Each thalamotomy target is additionally altered as needed based on direct imaging of the VIM nucleus using a previously described scan protocol adapted to our Philips 3T MRI (Fig. 9.5) [28].

The depth of the lesion has varied slightly case to case. We started by using the depth recommended for GKS targeting with a 4 mm sphere [17], which was 2.5 mm above the AC-PC plane. As we gained experience, it became clear that a laser ablation of ~6 mm in diameter seemed to perform best with no more than 1 to 2 mm of

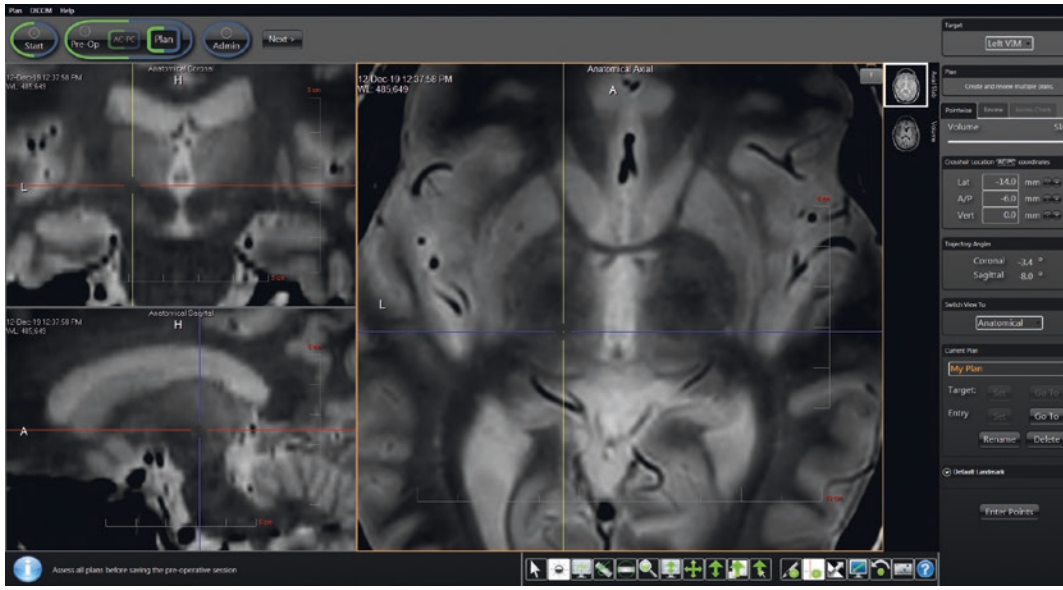

Fig. 9.5 Direct targeting of the VIM nucleus of the thalamus, which appears as the third hypodensity from posterior to anterior on a fast spin echo (FSE) sequence (e.g., hypodensities are as follows: posterior edge of thalamus, ventralis caudalis nucleus, ventralis intermedius nucleus)

lesion extending *below* the AC-PC plane. Our first patient's lesion was conservative and ended 2 mm *above* the AC-PC plane. This placement was deemed too superior when the patient had mild recurrence of hand tremor at 1 year, although he was still markedly better than preoperatively and not clinically affected. This observation is in line with literature suggesting that ablative or DBS therapy must interact with the dentatorubrothalamic tract for good long-term tremor control [29]. Another patient had a lesion that extended 3–4 mm below the AC-PC plane, and, while tremor was abolished, she experienced mild dysmetria and incoordination on exam that were moderately bothersome clinically at 1 year. This is reminiscent of what occurs when using the lowest contact on a DBS lead in a monopolar configuration, which is rarely used in our clinic (best electrode locations are typically contact 1 at AC-PC plane, or contact 2 slightly above AC-PC). Depth is traditionally the most variable parameter in stereotactic space [30], and the margin for error for thalamotomy is narrow. We now typically plan 2 mm above the AC-PC plan, which allows a 6 mm sphere to end 1 mm below the base of the thalamus. This paradigm has resulted in mild or no short-term side effects, no long-term side effects, and excellent sustained tremor suppression as detailed below.

For a thalamic ablation, we set six critical safety points to help define the planned spherical lesion: four points are arranged circumferentially around the target on an axial image, and two points are chosen along the medial capsular border on a coronal image (Fig. 9.6). If heating over 50 degrees occurred at any safety point, the laser automatically shut off. Heating is applied "low and slow," using 10% power, 15% power, 20% power, and 25% power as needed, each for 1–3 minutes, allowing the heat map to normalize between each session. As mentioned above, the exact procedure varies slightly depending on visual feedback, but we do not recommend using more than 25% of total power in this area regardless. The ablation is performed at the same site and depth without any pull-backs on the laser fiber for each run. A ~ 5–6 mm enhancing spherical ablation is subsequently created in the VIM thalamic region on post-procedural MRI (Fig. 9.7).

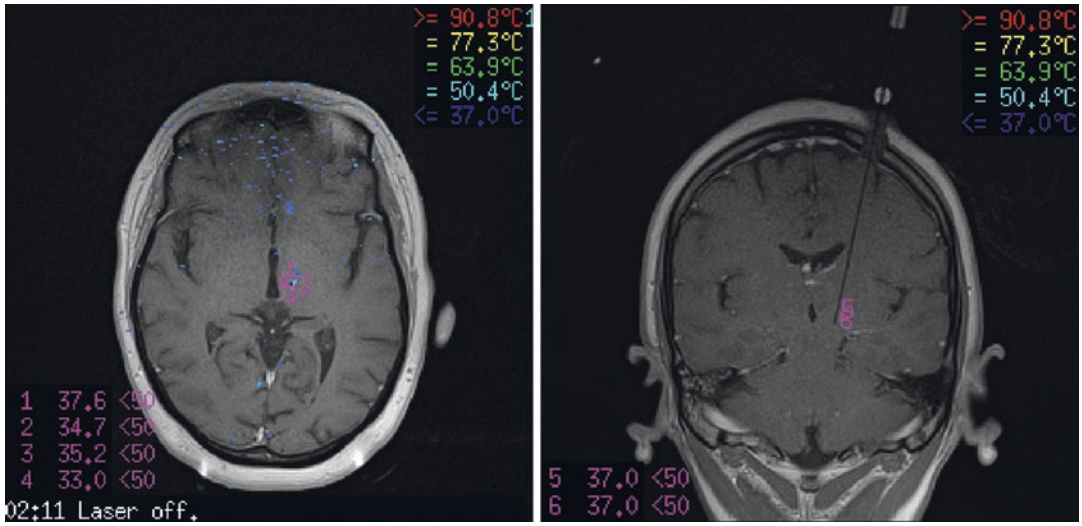

Fig. 9.6 Six critical safety points are chosen for thalamotomy planning on axial and coronal MRI scan

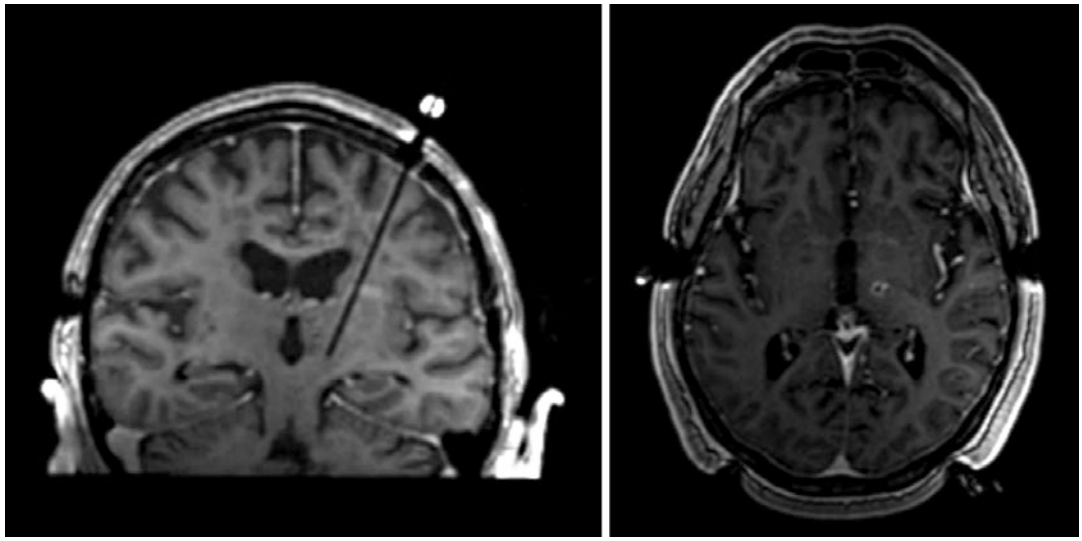

Fig. 9.7 Thalamotomy: axial and coronal T1W image demonstrating laser placement and a 6 mm spherical ablation in the thalamus

Results and Discussion

We recommend the reader review our initial outcomes publication for a detailed description of the first 13 patients [31]. Up to and beyond that cohort, we have continued to offer this procedure to patients who meet appropriate selection criteria. Tremor suppression and functional improvement improved by 83% and 72%, respectively, and have been sustained in all essential tremor patients except our very first patient who was treated minimally and had a slight, non-disabling recurrence after 1 year. Short-term side effects occur frequently, which is not unexpected due to swelling associated with thermal injuries [32] and the incredibly tight anatomy of the thalamus. In fact, we now expect and counsel patients on the likelihood of experiencing a mild, short-term side effect while acutely recovering, which resolves by 4–6 weeks with a long-term suppres-

sion of tremor. Specifically, we counsel patients to expect one or more of the following *short-term issues* after effective thalamic ablation surgery: (1) mild imbalance, (2) mild incoordination of treated hand, and (3) mild sensory disturbances in the thumb/index finger and/or corner of the mouth/tongue. Interestingly these side effects often occur together as a triad immediately after surgery in patients who then fare the best in terms of function and tremor outcome with all side effects resolving after ~ 1 month. *Note: We emphasize that successful surgery is often associated with "mild" temporary side effects that are not functionally disabling. If any of these side effects are severe or persistent for months, then over-treatment and/or suboptimal lesion location must be considered, and patients may have a prolonged or difficult recovery.*

We have successfully abolished a midline head tremor associated with significant blepharospasm in a patient who had a contralateral DBS in place to control dominant right-hand tremor; there were no procedural issues completing the laser ablation in the presence of DBS hardware. Finally, it is notable that three of our patients underwent staged bilateral lesioning procedures spaced 3–12 months apart and did not suffer obvious neurocognitive or functional decline, suggesting that bilateral treatment is feasible in carefully selected patients.

Pallidotomy

Targeting and Laser Ablation

Early on, we treated a tremor-predominant Parkinson's patient with unilateral laser thalamotomy. The tremor was dramatically and immediately diminished but recurred significantly by 6 months. We postulated that Parkinson's patients may be better served by pallidotomy, which we first performed in the fall of 2017. Our pallidotomy target is the same as that used in standard DBS or RF ablation [5, 6]. We start with the following coordinates: X = 18–22 mm lateral to midline, Y = 2 to 3 mm anterior to the mid-commissural point, and Z = 4 mm below the level of the AC-PC plane. Each target is additionally altered as needed based on direct imaging of the posterolateral GPi nucleus using an inversion recovery sequence. An effective pallidotomy lesion needs to extend at least 4–5 mm below the level of the AC-PC plan to be effective [6]. This ablation thus involves a series of laser pull-backs to accomplish an oblong shape, twice as long as it is wide, extending from just above the dorsolateral optic tract to 3–4 mm above the AC-PC plane (Fig. 9.8).

For a pallidal ablation, we again start by setting six critical safety points: four points are arranged circumferentially around the target on an axial image at the level of the AC-PC plane and two points are chosen along the lateral capsular border on a coronal image. Heating is applied as described above. However, a "low and slow" series of incremental ablations is performed at four different sites at the following depths to create the pallidotomy: 4 mm, 2 mm, at the AC-PC plane, and 1–2 mm above the AC-PC plane. The Visualase catheter is inserted about 10 mm beyond the target depth calculated by ClearPoint to compensate for the 6 mm described above + an additional 4 mm to position the start of the lesion just above dorsolateral OT. Direct visualization of the tip of the catheter 10 mm below the GPi localizes it lateral to the OT and medial to the temporal horn. The laser fiber is inserted fully into the catheter for the first series of ablations and is pulled back by 2 mm for each subsequent run. *Note: It is useful to mark the laser fiber with a dark marker in 2 mm increments prior to insertion because it is difficult to measure accurately while retracting the laser in the center of the bore.* Interestingly we have seen heating in this manner with respect to the pallido-capsular border along the length of the pallidum likely due to the low powers employed. We have not seen significant T2 changes in the internal capsule indicating damage (Fig. 9.8).

Results and Discussion

At the writing of this chapter, we have performed 17 pallidotomies, so a comprehensive analysis of

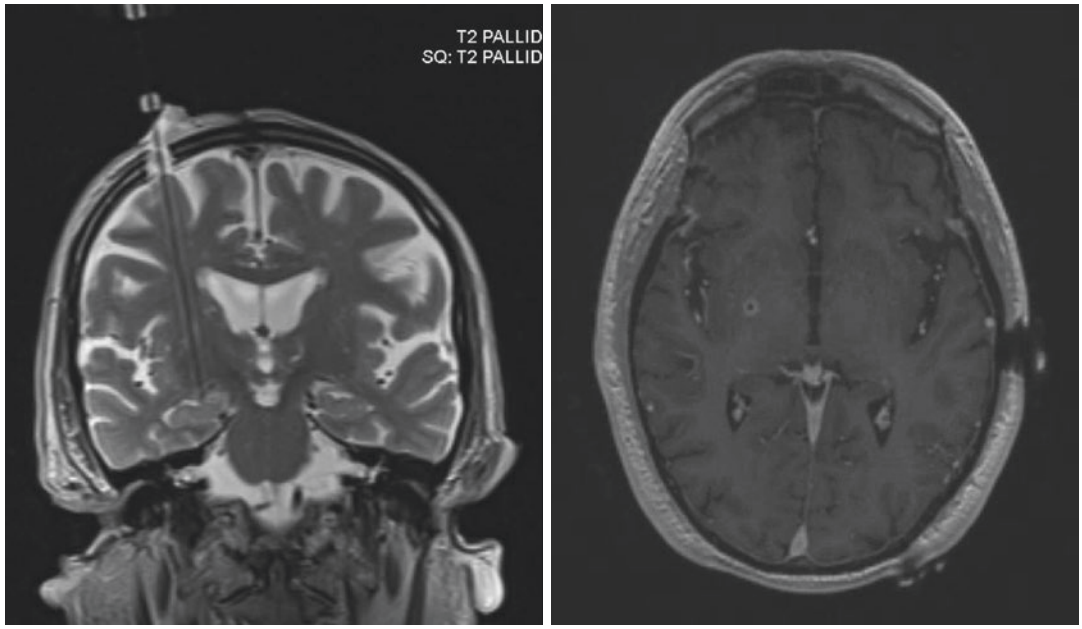

Fig. 9.8 Pallidotomy: coronal T2W and axial T1W image demonstrating laser placement and a 6 mm spherical ablation in the posterolateral globus pallidus internus

long-term results is not feasible. However, all patients have experienced a significant reduction in resting tremor, bradykinesia, and rigidity on the treated side as well as improved arm swing and general mobility on both physical exam and self-report. These results have been sustained through 6- to 12-month follow-up with no clear decrements. Unlike thalamotomy, side effects of pallidotomy, even in the short-term, have been sparse, likely due to anatomic differences between the structures. Only one patient reported mild facial weakness immediately postoperatively, which resolved after 4 weeks. Though we are early in our experience, laser pallidotomy may be a powerful tool in the armamentarium of treatment options for a subset of Parkinson's disease patients.

Conclusions

MRg-LITT for movement disorders, specifically laser thalamotomy and pallidotomy, has demonstrated promising early results for essential tremor and Parkinson's disease in patients who are not candidates for further medical or DBS therapy. We have performed this procedure using a commercial laser ablation work station in conjunction with the ClearPoint System in a converted diagnostic MRI suite and have achieved safe, reliable outcomes. However, these outcomes would be best supplemented by a multi-institution clinical trial in the future to further define the indications and expectations of LITT for movement disorders.

References

1. Benabid AL, Chabardes S, Torres N, Piallat B, Krack P, Fraix V, et al. Functional neurosurgery for movement disorders: a historical perspective. Prog Brain Res. 2009;175:379–91.
2. Limousin P, Pollak P, Benazzouz A, Hoffmann D, Le Bas JF, Broussolle E, et al. Effect of parkinsonian signs and symptoms of bilateral subthalamic nucleus stimulation. Lancet. 1995;345(8942):91–5.
3. Benabid AL, Pollak P, Gervason C, Hoffmann D, Gao DM, Hommel M, et al. Long-term suppression of tremor by chronic stimulation of the ventral intermediate thalamic nucleus. Lancet. 1991;337(8738):403–6.

4. Follett KA, Weaver FM, Stern M, Hur K, Harris CL, Luo P, et al. Pallidal versus subthalamic deep-brain stimulation for Parkinson's disease. N Engl J Med. 2010;362(22):2077–91.
5. Weaver FM, Follett KA, Stern M, Luo P, Harris CL, Hur K, et al. Randomized trial of deep brain stimulation for Parkinson disease thirty-six-month outcomes. Neurology. 2012;79(1):55–65.
6. Vitek JL, Bakay RAE, Hashimoto T, Kaneoke Y, Mewes K, Zhang JY, et al. Microelectrode-guided pallidotomy: technical approach and its application in medically intractable Parkinson's disease. 1998; https://doi.org/10.3171/jns.1998.88.6.1027.
7. Garonzik IM, Hua SE, Ohara S, Lenz FA. Intraoperative microelectrode and semimicroelectrode recording during the physiological localization of the thalamic nucleus ventral intermediate. Mov Disord. 2002;17(Suppl 3):S135–44.
8. Laitinen LV, Bergenheim AT, Hariz MI. Leksell's posteroventral pallidotomy in the treatment of Parkinson's disease. J Neurosurg. 1992;76(1):53–61.
9. Schuurman PR, Bosch DA, Merkus MP, Speelman JD. Long-term follow-up of thalamic stimulation versus thalamotomy for tremor suppression. Mov Disord. 2008;23(8):1146–53.
10. Lozano AM, Lang AE, Galvez-Jimenez N, Miyasaki J, Duff J, Hutchinson WD, et al. Effect of GPi pallidotomy on motor function in Parkinson's disease. Lancet. 1995;346(8987):1383–7.
11. Baron MS, Vitek JL, Bakay RA, Green J, Kaneoke Y, Hashimoto T, et al. Treatment of advanced Parkinson's disease by posterior GPi pallidotomy: 1-year results of a pilot study. Ann Neurol. 1996;40(3):355–66.
12. de Bie RM, de Haan RJ, Nijssen PC, Rutgers AW, Beute GN, Bosch DA, et al. Unilateral pallidotomy in Parkinson's disease: a randomised, single-blind, multicentre trial. Lancet. 1999;354(9191):1665–9.
13. Vitek JL, Bakay RAE, Freeman A, Evatt M, Green J, McDonald W, et al. Randomized trial of pallidotomy versus medical therapy for Parkinson's disease. Ann Neurol. 2003;53(5):558–69.
14. Akbostanci MC, Slavin KV, Burchiel KJ. Stereotactic ventral intermedial thalamotomy for the treatment of essential tremor: results of a series of 37 patients. Stereotact Funct Neurosurg. 1999;72(2–4):174–7.
15. Young RF, Li F, Vermeulen S, Meier R. Gamma knife thalamotomy for treatment of essential tremor: long-term results. J Neurosurg. 2010;112(6):1311–7.
16. Duma CM, Jacques DB, Kopyov OV, Mark RJ, Copcutt B, Farokhi HK. Gamma knife radiosurgery for thalamotomy in parkinsonian tremor: a five-year experience. J Neurosurg. 1998;88(6):1044–9.
17. Niranjan A, Raju SS, Kooshkabadi A, Monaco E 3rd, Flickinger JC, Lunsford LD. Stereotactic radiosurgery for essential tremor: retrospective analysis of a 19-year experience. Mov Disord. 2017
18. Elias WJ, Huss D, Voss T, Loomba J, Khaled M, Zadicario E, et al. A pilot study of focused ultrasound thalamotomy for essential tremor. N Engl J Med. 2013;369(7):640–8.
19. Elias WJ, Lipsman N, Ondo WG, Ghanouni P, Kim YG, Lee W, et al. A randomized trial of focused ultrasound Thalamotomy for essential tremor. N Engl J Med. 2016;375(8):730–9.
20. Zaaroor M, Sinai A, Goldsher D, Eran A, Nassar M, Schlesinger I. Magnetic resonance-guided focused ultrasound thalamotomy for tremor: a report of 30 Parkinson's disease and essential tremor cases. J Neurosurg. 2017:1–9.
21. Zrinzo L. Thalamotomy using MRI-guided focused ultrasound significantly improves contralateral symptoms and quality of life in essential tremor. Evid Based Med. 2017;22(2):64.
22. Gallay MN, Moser D, Rossi F, Pourtehrani P, Magara AE, Kowalski M, et al. Incisionless transcranial MR-guided focused ultrasound in essential tremor: cerebellothalamic tractotomy. Journal of therapeutic ultrasound. 2016;4:5.
23. Ghanouni P, Pauly KB, Elias WJ, Henderson J, Sheehan J, Monteith S, et al. Transcranial MRI-guided focused ultrasound: a review of the technologic and neurologic applications. AJR Am J Roentgenol. 2015;205(1):150–9.
24. San Luciano M, Katz M, Ostrem J, Martin A, Starr P, Ziman N, et al. Effective interventional magnetic resonance image-guided laser ablations in a Parkinson's disease patient with refractory tremor. Movement Disorders Clinical Practice. 2016;3(3):312–4.
25. Ostrem JL, Ziman N, Galifianakis NB, Starr PA, Luciano MS, Katz M, et al. Clinical outcomes using ClearPoint interventional MRI for deep brain stimulation lead placement in Parkinson's disease. J Neurosurg. 2016;124(4):908–16.
26. Buttrick S, Komotar RJ. Introduction for laser interstitial thermal therapy (LITT) in neurosurgery supplement. Neurosurgery. 2016;79(Suppl 1):S1–2.
27. Elias WJ. A trial of focused ultrasound Thalamotomy for essential tremor. N Engl J Med. 2016;375(22):2202–3.
28. Spiegelmann R, Nissim O, Daniels D, Ocherashvilli A, Mardor Y. Stereotactic targeting of the ventrointermediate nucleus of the thalamus by direct visualization with high-field MRI. Stereotact Funct Neurosurg. 2006;84(1):19–23.
29. Chazen JL, Sarva H, Stieg PE, Min RJ, Ballon DJ, Pryor KO, et al. Clinical improvement associated with targeted interruption of the cerebellothalamic tract following MR-guided focused ultrasound for essential tremor. J Neurosurg. 2018;129(2):315–23.
30. Starr PA, Martin AJ, Ostrem JL, Talke P, Levesque N, Larson PS. Subthalamic nucleus deep brain stimulator placement using high-field interventional magnetic resonance imaging and a skull-mounted aiming device: technique and application accuracy. J Neurosurg. 2010;112(3):479.
31. Harris M, Steele J, Williams R, Pinkston J, Zweig R, Wilden JA. MRI-guided laser interstitial thermal thalamotomy for medically intractable tremor disorders. Mov Disord. 2019;34(1):124–9.
32. Pisipati S, Smith KA, Shah K, Ebersole K, Chamoun RB, Camarata PJ. Intracerebral laser interstitial thermal therapy followed by tumor resection to minimize cerebral edema. Neurosurg Focus. 2016;41(4):E13.

LITT for Intractable Psychiatric Disease

10

Wael F. Asaad and Nicole C. R. McLaughlin

Rationale for LITT in Psychiatric Neurosurgery

The surgical treatment of intractable psychiatric disease has a long history of motivating or quickly adopting new operative tools. For example, after Jean Talairach demonstrated in the 1940s that selective lesions of the anterior internal capsule might capture many of the benefits of the more radical frontal lobotomies [1], Lars Leksell was quick to follow in the 1950s by applying the new technique of radiosurgery toward the same end [2]. In fact, "functional" neurosurgery through the lesioning of white matter tracts was a primary motivation for the development of the Gamma Knife for radiosurgery in subsequent decades. A strong parallel is now seen in the early application of high-intensity focused ultrasound to obsessive-compulsive disorder (OCD) [3]. Laser thermal ablation (aka MR-guided laser interstitial thermal therapy, MRg-LITT), likewise, has been undertaken quickly as a tool for the treatment of intractable, debilitating psychiatric disease.

The persistence of lesion procedures for intractable mental illness is occasionally regarded with suspicion given the questionable history of such procedures in the early to mid-twentieth century [4] and the more recent availability of less destructive options such as deep brain stimulation (DBS). Indeed, DBS is approved for intractable obsessive-compulsive disorder (OCD) in the United States under a Food and Drug Administration (FDA) Humanitarian Device Exception (HDE) [5]. The potential adjustability of DBS (different stimulation contact locations, amplitudes, frequencies, pulse widths, patterns, etc.) compared to the static and permanent nature of lesions also may bias some to believe that DBS or stimulation more generally should be the preferred approach to these cases [6].

However, lesions do continue to have an important role in psychiatric neurosurgery. Foremost, lesions have good efficacy, generally on par with stimulation [7–12]. Meanwhile, the side-effect profile of lesions is generally more favorable than DBS. Specifically, if one extrapolates from DBS applications in movement disorders (where the experience is much greater than in psychiatric procedures), it appears highly likely that thermal lesion procedures are associated with fewer infections and certainly do not run the risks of adverse events associated with implanted hardware [10, 13–17]. Furthermore,

W. F. Asaad (✉)
Departments of Neurosurgery and Neuroscience, Brown University and Rhode Island Hospital; The Carney Institute for Brain Science, Brown University, Providence, RI, USA
e-mail: wael_asaad@brown.edu

N. C. R. McLaughlin
Department of Psychiatry and Human Behavior, Butler Hospital/Alpert Medical School of Brown University, Providence, RI, USA

V. L. Chiang et al. (eds.), *Laser Interstitial Thermal Therapy in Neurosurgery*,
https://doi.org/10.1007/978-3-030-48047-9_10

for patients who often travel large distances to experienced centers for these procedures, returning home with an atypical DBS system (one that is implanted at an unusual target for a rare indication) that requires closer follow-up and intermittent adjustments may present difficulties due to a lack of local, specialized care. This is especially important in severe OCD and depression. In addition, the tolerability of implanted hardware in patients with severe psychiatric disease may be low in some cases due to compulsive behaviors (e.g., "picking") or troublesome thoughts (e.g., concerns over "mind control" or "loss of self" more generally), as well as concerns for potential non-compliance (e.g., not charging batteries leading to exacerbation of symptom severity). Finally, the naive notion that lesions are purely destructive and cause only loss of function is misguided: lesions in appropriately selected cases can in fact improve performance on some cognitive tests [18].

Lesions for psychiatric neurosurgery can be created using any one of several techniques, such as radio-frequency (RF) ablation, LITT, focused ultrasound (FUS), or radiosurgery (RS). In general, thermal lesions (RF or LITT) are likely to produce more consistent lesion volumes than those resulting from the delayed tissue response to radiation in RS [19, 20]. In the latter, adverse events, such as delayed cyst formation, potentially with serious neurological sequelae, have occasionally been observed [9], whereas to our knowledge this type of complication has not been reported for thermal lesions. Furthermore, in the generally younger psychiatric surgical population, avoidance of ionizing radiation is a potentially important factor because there may be many decades remaining during which secondary tumor formation can occur, especially given the high doses of radiation needed to create functional lesions in grossly normal brain tissue (120 to 180 Gy). Thermal lesions also have the advantage that they are immediate rather than delayed by several months, potentially providing earlier symptom relief.

Compared to RF and LITT, RS and FUS have the advantage of being able to create lesions of various geometries not confined to a linear trajectory (FUS, however, is currently most capable when targeted at deeper structures toward the center of the head, whereas targets for psychiatric indications, such as the anterior internal capsule or especially anterior cingulate, may push or exceed its present boundaries). Nonetheless, in most cases, the targeted anatomy may be well-suited to a linear trajectory (such as the anterior ventral internal capsule) or can be approached in a more tailored manner (e.g., the "six-pack" RF cingulotomy consisting of three separate lesions in each hemisphere oriented along the anterior to posterior direction, or the potential posterior parietal longitudinal approach which would be suitable for LITT with several "pull-back" steps). At this time, there are no confirmed advantages for curved or non-cylindrical lesions, so linearly constrained trajectories have been considered adequate thus far.

An advantage for LITT over RF ablation is the ability to create a lesion under direct, near-real-time visualization. While there is a fairly good relationship between RF lesion procedure parameters (i.e., probe size, temperature, and time) and lesion size [21–23], there are nevertheless some variability and the potential for non-uniform heat spread if the probe is near a heat sink such as a CSF space or blood vessel. Magnetic resonance thermometry during the LITT procedure makes relative temperature readings that are used to model the lesion using the Arrhenius equation [24]. However, one must keep in mind that the visualized lesion model is an estimate, albeit one created with more direct data than the textbook estimates used to guide RF procedures; while there is typically good correspondence between the damage estimate and the actual resulting lesion [25], blood perfusion along with dynamic changes in the optical and thermal properties of the tissue can affect the damage estimate and thereby leave some uncertainty about precise lesion size [26, 27]. Of course, because the LITT procedure is performed within the MRI scanner, post-ablation images to confirm initial lesion size are easily obtained.

There are important fundamental differences between the thermal mechanisms of the LITT and RF lesioning techniques. LITT is dependent

upon the conversion of photons to heat in the target tissue (and the heat transfer properties of the tissue). This, in turn, is dependent upon the optical properties of the tissue [28]. RF ablation, on the other hand, creates heat by exposing molecules to an alternating electromagnetic field (established between the probe tip and distant grounding pads), similar in principle to a microwave oven; the density of this field is highest near the tip and drops off exponentially with distance [29]. In both cases, the final lesion is a function of the spatiotemporal heat distribution. These different methods of heat generation result in distinct lesion characteristics, such that RF lesions appear to transition more gradually to normal tissue while LITT lesions tend to have more distinct boundaries [30]. Therefore, particularly in psychiatric neurosurgery where the optimal targets and lesion configurations are still hotly debated, such differences must be kept in mind. Ultimately, a simple mapping of RF surgical experience to LITT experience in this domain may or may not be realized.

Especially in psychiatric neurosurgery, where there is a relative sparsity of evidence to guide optimal therapeutic intervention, rigorous data collection and trial design are needed. In this vein, RS and FUS have the advantage that clinical trials can include untreated control groups without the need for an invasive sham procedure. Therefore, in the ideal case, the lesion method chosen should optimize patient benefit and hopefully also to allow rigorous scientific determination of the procedure's efficacy.

Lastly, because instruments for laser ablation are cleared by the US FDA as "tools" for the general creation of lesions within the brain rather than as specific therapies for particular diseases, undertaking LITT for psychiatric disease can avoid the "investigational" label that would be applied to DBS procedures other than for the five approved indications (Parkinson's disease, essential tremor, epilepsy, dystonia, and OCD, with the latter two under an HDE) and their specific, corresponding targets. Nevertheless, guidelines put forth by the American Society for Stereotactic and Functional Neurosurgery (ASSFN) emphasize that psychiatric neurosurgical procedures should be considered investigational, and so rigorous data collection and thoughtful trial design are strongly encouraged [31]. In addition, local approval by the institutional review board (IRB) may be sought as appropriate.

Patient Selection

Psychiatric neurosurgery for intractable, debilitating psychiatric disease is best undertaken after a multi-disciplinary review by clinicians experienced in managing these rare cases. Experienced centers typically employ a psychiatric neurosurgery committee consisting of psychiatrists, neurologists, neurosurgeons, neuropsychologists, and often a community representative. Patients are typically referred by local treating psychiatrists or occasionally primary care physicians. Some patients self-refer upon reading relevant literature online, but comprehensive documentation of medical and psychiatric history and prior outpatient and inpatient treatments are required from the local primary care physician, psychiatrist, and therapist prior to approval for surgery. It is essential that patient expectations are assessed prior to surgery. Psychiatric neurosurgeries are often construed by patients and families as the "last hope" for patients. Thus, consequences may be disastrous (e.g., suicide) if there is lack of post-surgical improvement.

The type of procedure offered, if any, varies with the particular indication and target, the patient's preferences and circumstances, and the experience of the treating clinicians. Patients are informed that the surgical approach to psychiatric disease consists of either neuro-stimulation (typically deep brain stimulation, DBS) or ablation (creation of a lesion). If a patient prefers ablation and this is agreed to be a reasonable modality, the options available at the performing institution are presented (at our institution, these would include RS, RF, and LITT), along with options that may be available elsewhere (e.g., FUS). Patients who cannot undergo MRI and who desire a lesion could be considered for RF or RS approaches depending on the protocol at the performing institution. In our case, we generally

refrain from ablative procedures for psychiatric indications if the patient cannot have an MRI because there is significant cross-patient variability of the relevant target locations and geometries that would not be appreciated on computed tomography (CT) alone.

Though guidelines may differ slightly across centers and will vary according to the particular psychiatric disorder, at our institution, approval for OCD surgery is generally reserved for:

1. Patients with severe, treatment-resistant OCD, typically of at least 5 years in duration, which has caused functional interference and poor quality of life. Severity is typically based on the YBOCS, with a score over 26 to 30.
2. Patients who have failed all conventional treatments. Prior treatment trials must be clearly documented and judged as adequate. Medication trials typically include trials of a serotonin re-uptake inhibitor (often high-dose trials are needed in OCD), as well as a neuroleptic trial and trials of clonazepam and clomipramine. Behavioral therapy should include at least 20 sessions of exposure and response/ritual prevention, the gold standard treatment for OCD.
3. Patients without severe personality disorders or current comorbid substance abuse.
4. Patients who are 18 years of age or older and can provide appropriate informed consent; though not mandatory, family support is recommended and likely contributes to improved outcomes after surgery.

In addition, the ability to comply with follow-up treatments should also be taken into consideration, particularly with regard to DBS, where batteries require frequent charging and patients need to return for frequent post-surgical visits. Significant neurological conditions (e.g., extensive white matter disease, stroke) may be relative contraindications, as can be medical conditions that may increase surgical risk.

With both ablative and stimulation procedures, patients should continue to receive treatment with a psychiatrist and a therapist skilled in ERP. The majority of patients remain on psychiatric medications post-surgery, though there may be a decrease in the number of prescribed medications. In the case of DBS, access to specialized psychiatric neurosurgery teams is recommended for clinical monitoring and device adjustment. Patients will need continued battery replacements, and future costs, particularly of DBS, should be considered. Long-term follow-up is essential to track clinical change and adverse effects.

Technical Considerations

The geometry of the target in ventral capsulotomy for OCD is favorable for LITT. Based upon our experience with RS capsulotomy, the target is defined as the bottom third of the anterior internal capsules, bilaterally, about 8–10 mm anterior to the posterior border of the anterior commissure (Fig. 10.1). The trajectory is typically through the superior or middle frontal gyrus about 3–5 cm anterior to the coronal suture. The laterality of the entry sites is selected to avoid vessels and to match the coronal angle of the ventral internal capsules as best as possible.

These procedures are typically performed under general anesthesia in order to minimize patient movement during laser ablation within the MRI. Even small movements can translate the targeted region out of the scanning plane during ongoing imaging, and this could result in incorrect estimates of lesion volume and place non-targeted tissues at risk. While there may be strategies and devices to mitigate this concern, because there is as yet no validated immediate behavioral marker of long-term procedural success — and there is likewise no known utility of side-effect testing for this target — there is not currently a benefit to having an awake patient, although studies in this domain are ongoing.

Using standard stereotactic methods, the laser fiber is inserted to the bottom of the internal capsule, and intra-operative CT images are obtained. These CT images are co-registered to pre-op MRI and the trajectory of the laser fiber is confirmed. At our institution, the patient is then transported under anesthesia to a separate MRI

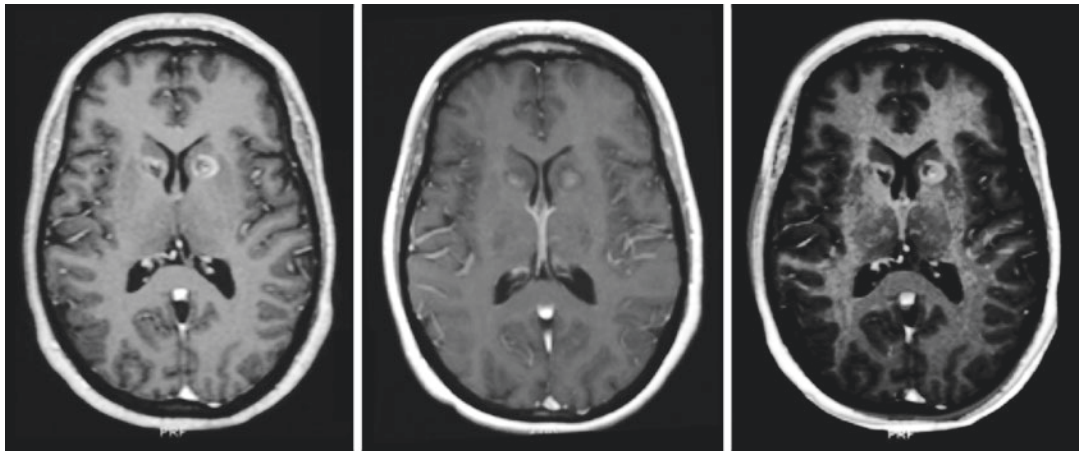

Fig. 10.1 Evolution of LITT capsulotomy lesion over the first 24 hours. T1 post-contrast images are shown. The right overlay image shows the relative differences between the two individual scans to the left. Note the contrast-enhancing core on post-op day 1 resides within the ring-enhancing portion evident immediately after the procedure on day 0

suite where the laser ablation is performed. Because we use two laser fibers (one in each hemisphere), we connect the cooling circuit to both of these in series. The distance (and CSF space) between the fibers in bilateral capsulotomy is sufficient that this is not strictly necessary to prevent heat from one fiber damaging the contralateral fiber; however, cooling both catheters at all times eliminates the potential error of delivering heat through an uncooled catheter.

"Background" images (T1- or T2-based) are acquired to serve as a reference for the thermography maps ("T-maps") that will be obtained at short intervals (every 6 to 8 seconds) during the ablation. The choice of background image sequence is left to the surgeon and perhaps the psychiatric team, if present, to highlight the relevant anatomy. In general, maximizing contrast between gray and white matter would be desirable for capsulotomy or cingulotomy.

For anterior capsulotomy, we use Visualase laser fibers (Medtronic, Inc., Louisville, CO) with 3 mm diffusing tips. Full laser power is set to 10 watts, and a test dose of thermal energy is given with the laser at 15–25% power. Once the desired heat distribution is confirmed on the T-map, laser power is increased to about 35–55% of maximum until the damage estimate is considered appropriate. At this point, the laser fiber is withdrawn about 2 mm and the lesion is extended dorsally. Usually, 2–3 "pull-backs" are performed in this fashion. Heat spread into the caudate medially or globus pallidus laterally should be minimized; "low" temperature markers placed in these structures can help limit collateral damage. Occasionally, modulating the balance between temperature and time can influence the extent of the lesion, depending on unobserved factors such as blood perfusion in different tissue compartments (e.g., gray vs. white matter); empiric testing of these parameters in individual cases may yield a more desirable lesion configuration.

Expected Outcomes

Most of the outcome data for capsulotomy in OCD arises from experience with RS or RF lesions. Because the characteristics of laser thermal lesions differ from those created by other techniques, and because the precise lesion configuration yielding maximal patient benefit is still unclear, extrapolating from earlier experience with other surgical approaches may have relevant limitations.

Nonetheless, to the best of our knowledge, targeting the ventral third of the anterior internal capsule should yield benefit in approximately 40–60% of appropriately selected patients with intractable OCD who have failed other available treatments [9, 11, 32]. In a large RS capsulotomy series [9], female gender, positive employment status, and later age of onset were predictive of a good response to treatment. The symptomatic OCD subtype may also be relevant for the outcome following capsulotomy; those with contamination fears and taboo thoughts may be more likely to improve than those with hoarding or the need for symmetry and order [33, 34]. Lastly, because we have observed cases of RS capsulotomy in which treatment response was absent and visible lesions were not created despite high doses (150 Gy) of radiation, we anticipate that these sorts of therapeutic failures – which appear to be due to lack of adequate lesion formation – will be infrequent or absent in LITT capsulotomy.

There are as yet no reports of LITT cingulotomy for either OCD or depression. Broadly, dorsal cingulotomy may be less efficacious than capsulotomy for intractable OCD [12]; in depression, dorsal cingulotomy may provide some benefit in a third of patients with about another third gaining benefit from a second, subcortical lesion (subcaudate tractotomy, together known as "limbic leukotomy") [10]. The precise cingulate location conferring efficacy and the optimal lesion size have yet to be fully understood; RF cingulotomy for OCD and depression at experienced centers evolved to a "six-pack" approach consisting of three anterior-to-posterior lesions in each hemisphere along the cingulum bundle placed a few centimeters anterior to the coronal suture [35]. Replicating this with LITT would require multiple re-insertions of the laser probe, simultaneous insertion of multiple (expensive, single-use) probes, or the use of a more efficient trajectory (e.g., parietal longitudinal approach along the axis of the cingulum bundle).

Even though thermal lesions (RS, LITT, and FUS) are created much more rapidly than radiation-induced lesions (RS), there is nevertheless an evolution of lesion architecture over time in the setting of time-dependent changes in symptoms. Thermal lesions have been associated with gradual improvement in OCD over many weeks or months, and this may or may not be sustained over years [36]. To what extent these therapeutic results parallel changes in brain structure vs. plasticity-driven alterations in brain function is unknown.

Conclusions

LITT for psychiatric neurosurgery is expected to provide a relatively safe and effective means of treating intractable, debilitating psychiatric disease. Experienced centers performing these procedures should apply a thoughtful, multi-disciplinary approach to patient selection and should strive to elucidate the unique characteristics of LITT psychosurgery while contextualizing it within the broad, cross-institutional experience with ablative and stimulation-based psychiatric interventions.

Ablation and stimulation both continue to have important roles in psychiatric neurosurgery. The different targets and mechanisms of lesions vs. DBS (e.g., in OCD, a capsulotomy lesion is typically anterior to the ventral capsule/ventral striatum target used for DBS) generally render comparisons of efficacy between these techniques inexact. Furthermore, because there is a wide range of efficacy reported across studies even within a treatment modality, there is no obvious "winner" in terms of the optimal approach. Therefore, the chosen treatment should be tailored to the needs and circumstances of the patient, and for the overall benefit of this patient population through rigorous trial design and data collection.

References

1. Talairach J, Hecaen H, David M. Lobotomies prefrontal limitee par electrocoagulation des fibres thalamo-frontales a leur emergence dubras anterieur de la capsule interne. Revue Neurologique, IV Congres Neurologique International. 1949;83.
2. Leksell L. Stereotactic radiosurgery. J Neurol Neurosurg Psychiatry. 1983;46(9):797–803.
3. Jung HH, Kim SJ, Roh D, Chang JG, Chang WS, Kweon EJ, et al. Bilateral thermal capsulotomy with MR-guided focused ultrasound for patients with

treatment-refractory obsessive-compulsive disorder: a proof-of-concept study. Mol Psychiatry. 2015 Oct;20(10):1205–11.
4. Caruso JP, Sheehan JP. Psychosurgery, ethics, and media: a history of Walter freeman and the lobotomy. Neurosurg Focus. 2017;43:1.
5. Youngerman BE, Chan AK, Mikell CB, McKhann GM, Sheth SA. A decade of emerging indications: deep brain stimulation in the United States. J Neurosurg. 2016;125(2):461–71.
6. Lapidus KAB, Kopell BH, Ben-Haim S, Rezai AR, Goodman WK. History of psychosurgery: a psychiatrist's perspective. World Neurosurg. 2013;80(3–4):S27.e1–16.
7. Pepper J, Hariz M, Zrinzo L. Deep brain stimulation versus anterior capsulotomy for obsessive-compulsive disorder: a review of the literature. J Neurosurg. 2015;122(5):1028–37.
8. Greenberg BD, Malone DA, Friehs GM, Rezai AR, Kubu CS, Malloy PF, et al. Three-year outcomes in deep brain stimulation for highly resistant obsessive-compulsive disorder. Neuropsychopharmacology. 2006;31(11):2384–93.
9. Rasmussen SA, Norén G, Greenberg BD, Marsland R, McLaughlin NC, Malloy PJ, et al. Gamma ventral Capsulotomy in intractable obsessive-compulsive disorder. Biol Psychiatry. 2017.
10. Sheth SA, Neal J, Tangherlini F, Mian MK, Gentil A, Cosgrove GR, et al. Limbic system surgery for treatment-refractory obsessive-compulsive disorder: a prospective long-term follow-up of 64 patients. J Neurosurg. 2013;118(3):491–7.
11. Gupta A, Shepard MJ, Xu Z, Maiti T, Martinez-Moreno N, Silverman J, et al. An international radiosurgery research foundation multicenter retrospective study of gamma ventral Capsulotomy for obsessive compulsive disorder. Neurosurgery IV ed. 2018;30(3):400.
12. Brown LT, Mikell CB, Youngerman BE, Zhang Y, McKhann GM, Sheth SA. Dorsal anterior cingulotomy and anterior capsulotomy for severe, refractory obsessive-compulsive disorder: a systematic review of observational studies. J Neurosurg. 2016;124(1):77–89.
13. Zhan S, Liu W, Li D, Pan S, Pan Y, Li Y, et al. Long-term follow-up of bilateral anterior capsulotomy in patients with refractory obsessive-compulsive disorder. Clin Neurol Neurosurg. 2014;119:91–5.
14. Christmas D, Eljamel MS, Butler S, Hazari H, MacVicar R, Steele JD, et al. Long term outcome of thermal anterior capsulotomy for chronic, treatment refractory depression. J Neurol Neurosurg Psychiatry. 2011;82(6):594–600.
15. Hardaway FA, Raslan AM, Burchiel KJ. Deep brain stimulation-related infections: analysis of rates, timing, and seasonality. Neurosurgery. 2018;83(3):540–7.
16. Rumalla K, Smith KA, Follett KA, Nazzaro JM, Arnold PM. Rates, causes, risk factors, and outcomes of readmission following deep brain stimulation for movement disorders: analysis of the U.S. Nationwide readmissions database. Clin Neurol Neurosurg. 2018;171:129–34.
17. Abode-Iyamah KO, Chiang H-Y, Woodroffe RW, Park B, Jareczek FJ, Nagahama Y, et al. Deep brain stimulation hardware-related infections: 10-year experience at a single institution. J Neurosurg. 2018:1–10.
18. Csigó K, Harsányi A, Demeter G, Rajkai C, Németh A, Racsmány M. Long-term follow-up of patients with obsessive-compulsive disorder treated by anterior capsulotomy: a neuropsychological study. J Affect Disord. 2010;126(1–2):198–205.
19. Okun MS, Stover NP, Subramanian T, Gearing M, Wainer BH, Holder CA, et al. Complications of gamma knife surgery for Parkinson disease. Arch Neurol. 2001;58(12):1995–2002.
20. Ohye C, Higuchi Y, Shibazaki T, Hashimoto T, Koyama T, Hirai T, et al. Gamma knife thalamotomy for Parkinson disease and essential tremor: a prospective multicenter study. Neurosurgery. 2012;70(3):526–35; discussion535–6.
21. Alberts WW, Wright EW, Feinstein B, Bonin Von G. Experimental radiofrequency brain lesion size as a function of physical parameters. J Neurosurg. 1966;25(4):421–3.
22. Pecson RD, Roth DA, Mark VH. Experimental temperature control of radiofrequency brain lesion size. J Neurosurg. 1969;30(6):703–7.
23. Cosman ER, Nashold BS, Bedenbaugh P. Stereotactic radiofrequency lesion making. Appl Neurophysiol. 1983;46(1–4):160–6.
24. McNichols RJ, Gowda A, Kangasniemi M, Bankson JA, Price RE, Hazle JD. MR thermometry-based feedback control of laser interstitial thermal therapy at 980 nm. Lasers Surg Med. 2004;34(1):48–55.
25. Patel NV, Frenchu K, Danish SF. Does the thermal damage estimate correlate with the magnetic resonance imaging predicted ablation size after laser interstitial thermal therapy? Oper Neurosurg (Hagerstown). 2018;15(2):179–83.
26. Jiang SC, Zhang XX. Effects of dynamic changes of tissue properties during laser-induced interstitial thermotherapy (LITT). Lasers Med Sci. 2005;19(4):197–202.
27. Schwarzmaier HJ, Yaroslavsky IV, Yaroslavsky AN, Fiedler V, Ulrich F, Kahn T. Treatment planning for MRI-guided laser-induced interstitial thermotherapy of brain tumors--the role of blood perfusion. J Magn Reson Imaging. 1998;8(1):121–7.
28. Menovsky T, Beek JF, van Gemert MJ, Roux FX, Bown SG. Interstitial laser thermotherapy in neurosurgery: a review. Acta Neurochir. 1996;138(9):1019–26.
29. Hong K, Georgiades C. Radiofrequency ablation: mechanism of action and devices. J Vasc Interv Radiol. 2010;21(8 Suppl):S179–86.
30. LaRiviere MJ, Gross RE. Stereotactic laser ablation for medically intractable epilepsy: the next generation of minimally invasive epilepsy surgery. Front Surg. 2016;3:64.
31. Bari AA, Mikell CB, Abosch A, Ben-Haim S, Buchanan RJ, Burton AW, et al. Charting the road

forward in psychiatric neurosurgery: proceedings of the 2016 American Society for Stereotactic and Functional Neurosurgery workshop on neuromodulation for psychiatric disorders. J Neurol Neurosurg Psychiatry. 2018.
32. Rück C, Karlsson A, Steele JD, Edman G, Meyerson BA, Ericson K, et al. Capsulotomy for obsessive-compulsive disorder: long-term follow-up of 25 patients. Arch Gen Psychiatry. 2008;65(8):914–21.
33. Gentil AF, Lopes AC, Dougherty DD, Rück C, Mataix-Cols D, Lukacs TL, et al. Hoarding symptoms and prediction of poor response to limbic system surgery for treatment-refractory obsessive-compulsive disorder. J Neurosurg. 2014;121(1):123–30.
34. Rück C, Larsson KJ, Mataix-Cols D. Predictors of medium and long-term outcome following capsulotomy for obsessive-compulsive disorder: one site may not fit all. Eur Neuropsychopharmacol. 2012;22(6):406–14.
35. Shields DC, Asaad W, Eskandar EN, Jain FA, et al. Prospective assessment of stereotactic ablative surgery for intractable major depression. Biol Psychiatry. 2008;64(6):449–54.
36. Lopes AC, Greenberg BD, Canteras MM, Batistuzzo MC, Hoexter MQ, Gentil AF, et al. Gamma ventral capsulotomy for obsessive-compulsive disorder: a randomized clinical trial. JAMA Psychiat. 2014;71(9):1066–76.

LITT in Pediatric Epilepsy

11

Sara Hartnett and Daniel J. Curry

Introduction

Epilepsy affects 1 in 100 children. Drug-resistant epilepsy, defined as inadequate seizure control despite adequate trials of two anti-seizure medications, occurs in approximately 40% of pediatric patients [1, 2]. Delayed seizure control is associated with developmental delay, depression, anxiety, behavioral problems, and autism and has a negative effect on brain development and quality and quantity of life [3]. Epilepsy surgery is a treatment option for these children to remove or destroy the primary epileptogenic focus and improve seizure control. Open resection of well-defined epileptic foci has been shown to achieve a control rate of up to 75–80% [4]. Cerebral plasticity during infancy and childhood also offers potential benefits of enhanced functional recovery following surgery [5]. However, surgery is not without risk. Major complication rates for open epilepsy surgery range from 1.6 to 6.6% and minor complications from 12.5 to 17.5% as reported in the literature [6, 7]. These estimated risks do not account for surgeries in eloquent areas, deep-seated lesions, or patients who require reoperation [8]. Reoperation for refractory epilepsy can achieve seizure-free outcome in 60–70% of cases but with a complication rate of 50%, with 35% of patients developing new-onset neurologic deficits [2].

Minimally invasive surgical techniques hold potential for achieving similar seizure control outcomes with reduced complications compared to open resective surgery. Laser interstitial thermal therapy (LITT) is a stereotactically guided percutaneous minimally invasive procedure which delivers light energy to target tissue via a fiber-optic catheter resulting in thermal ablation of tissue [9]. LITT was first described in 1983 by Bown [10] and first applied in the treatment of brain lesions by Sugiyama et al. in 1990 [11]. Improvements in technology over the past decades have improved its efficacy and reduced the risks of thermal damage to surrounding normal brain tissue. In 2007, the US Food and Drug Administration approved the first magnetic resonance (MR)-guided laser interstitial thermal therapy (MRgLITT) system for use in brain soft tissue. MRgLITT enables monitoring of tissue ablation in real time, therefore reducing the risk of thermal damage to the surrounding normal brain parenchyma. In 2010, the first child was treated for epilepsy with MRgLITT [12]. Since that index case, 179 cases of pediatric epilepsy treated with MRgLITT have been reported [13].

S. Hartnett
Neurosurgery and Brain Repair, University of South Florida, Tampa, FL, USA

D. J. Curry (✉)
Department of Neurosurgery, Section of Pediatric Neurosurgery, Texas Children's Hospital/Baylor College of Medicine, Houston, TX, USA
e-mail: djcurry@bcm.edu

V. L. Chiang et al. (eds.), *Laser Interstitial Thermal Therapy in Neurosurgery*,
https://doi.org/10.1007/978-3-030-48047-9_11

Patient Selection/Diagnostic Tools/ Work-Up

Requirements for candidates for epilepsy surgery – after demonstration of medical intractability – include demonstration of semiology consistent with the proposed hypothetical focus as correlated by video EEG, high-resolution MR imaging (possibly functional and connectivity studies), and neuropsychological evaluation. Most patients also undergo metabolic studies (PET and SPECT) and magnetoencephalographic (MEG) studies. Surgical treatment of epilepsy requires that the surgeon is able to identify the epileptogenic focus, determine its relationship to eloquent structures, and access the tissue for resection, ablation, disconnection, or stimulation. Any of those modalities can be used alone or in combination. Precise localization of the epileptogenic focus is a prerequisite for seizure-free outcome but can be challenging in non-lesional or multi-lesional epilepsy. Most epilepsy surgery centers utilize a recurring multi-disciplinary conference including epileptologists, neurosurgeons, neuropsychologists, and neuroradiologists to review the extensive pre-operative evaluation and discuss each case to determine if a patient is a candidate for ablative surgery. The diagnostic tools in combination create a hypothesis of a seizure onset zone and a three-dimensional seizure propagation network to determine the extent of epileptic activity before surgery. The 3D network can then be confirmed, as needed, with invasive stereo-electroencephalography (sEEG).

Technique

Pre-incision and Anesthesia

All anesthesia lines and monitors must be MRI safe, and a standard patient MRI safety screening form should be completed. In cases where ablation is the surgical goal without the need for intraoperative or postoperative electrophysiology, the patient may undergo general inhalational anesthesia; total intravenous anesthesia (TIVA) is not necessary in these cases. Chemical paralysis is utilized to prevent unwanted movement that can result in errant ablation. If the ablation is near vital structures, the patient is given high-dose steroids to minimize the effects of edema. In some ablation targets, such as hypothalamic hamartoma, a week of pre-operative steroids has been found to reduce the effects of the immediate edema. An arterial line is not necessary. Bladder decompression is achieved using an indwelling catheter. A surgical team pause is performed, and antibiotics are administered.

Delivering the Laser

MRgLITT is dependent on accurate stereotactic targeting aided by identification and minimization of possible sources of error during all stages of the procedure. MRgLITT procedural workflows are dependent on institutional resources and practice patterns and utilize frame-based, mini-frame-based, frameless, and robotic systems to transfer stereotaxic location from the planning system to a bone-anchored bolt which holds the laser in the desired trajectory (although a bone anchor is not necessary with certain stereotactic systems). Ablations may be carried out in an intraoperative MRI after placement of the fiber conventionally outside the magnetic field, in a separate diagnostic MRI suite after stereotactic placement of laser probe in a traditional operating room, or entirely in an intraoperative MRI suite using MR-compatible delivery systems.

Frame-Based Stereotaxy

In general, arc-centered stereotactic frames including Leksell and Cosman-Roberts-Wells (CRW) are commonly used and are the gold standard for performing stereotactic/functional neurosurgery. Frame-based stereotaxy requires a working frame and computer software package which allows planning. The frame can be placed in the pre-operative area or following induction with general anesthesia. Stereotactic imaging with frame in place can be either MRI or CT with co-registration to pre-operative

imaging used for surgical planning. In pediatrics, frame-based stereotaxy has two significant concerns: skull thickness and head circumference. Any rigid fixation of the pediatric skull requires special attention to pin forces. If the forces of fixation can be distributed among additional pins, this should be utilized. Only enough force to achieve fixation need be used, and no additional tightening must be done after registration since this will move the target with respect to the center of the frame. Additionally, care must be taken during positioning to avoid tangential forces on the pins from the body, which over time can loosen the fixation. Lastly, the time between target registration and surgery on the trajectory should be minimized to disallow accumulating slippage error.

Frameless Stereotaxy

A plethora of frameless stereotactic systems maintain useable accuracy while avoiding the need to frame the cranium; examples include the use of AxiEm™ (Medtronic, Inc.) and multiaxial arm stereotaxy (Medtronic Vertek Arm, BrainLab Varioguide). Accuracy of these systems can be augmented with the use of bone fiducials or trusted points for registration of the patient space with the MRI space by recapitulating a series of fiducials, or trusted points. There are a number of mini-frame systems using bone-fixed targeting, such as STarFix microTargeting system (Fred Hare Co.), Clearpoint System (MRI Interventions), or Nexframe (Medtronic, Inc.), which first register or fuse the patient space with the imaging space by fiducials and then register the fiducial space with the mini-frame fixed to the surgical section of the skull.

Robotized stereotactic assistant (ROSA™, Zimmer Biomet) and Neuromate (Renishaw) are other frameless stereotactic systems applicable to LITT (Fig. 11.1). Robotized assistants are published with submillimetric accuracy [14]. ROSA™ and Neuromate can be more efficient than frame-based targeting when multiple trajectories are needed. In particular, laser ablations for multifocal epilepsy based on sEEG that require transition between electrode and laser placement are facilitated by the robotic systems.

Overall, there appears to be equipoise in accuracy and risk profiles among frameless systems making the local resources the most important factor determining system selection. Although prospective randomized study between frame-based and frameless (BrainLab Varioguide) stereotaxy reports similar diagnostic specimen rates, trajectory accuracy, and complication rate in stereotactic biopsies, frameless stereotaxy for laser ablation specifically is reported to be associated

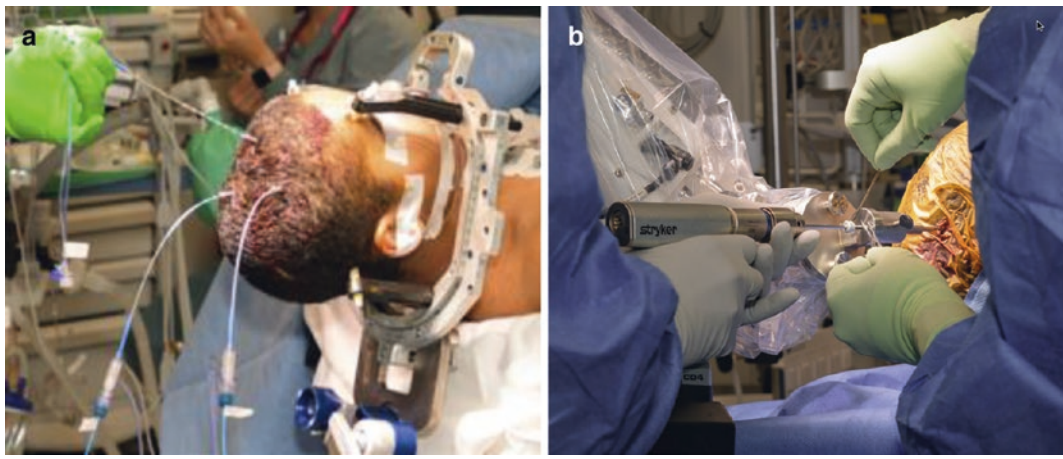

Fig. 11.1 Stereotactic MRgLITT of pediatric multifocal epilepsy. (**a**) Multiple catheters are held to the treatment trajectories by titanium anchor bolts in a child with multifocal epilepsy. (**b**) Stereotactic robot-assisted establishment of trajectories into a seizure onset zone via a 3.4 mm burr hole

with higher adverse events including hemorrhage and neurological deficits [15, 16].

Trajectory Planning

Stereotactic trajectories have inherent risks independent of what is passed through the brain. Imaging considerations when planning a trajectory should take into account the anatomical variance in skull thickness, subarachnoid spaces, blood vessels, ventricular volumes, and lesion target volumes. Ependymal surfaces should be avoided when possible in addition to minimizing the number of pial surfaces to be transgressed. Neck flexion or any other position which restricts venous outflow should be avoided since it may cause intracranial veins to become more conspicuous and increase the risk of rupture during stereotaxy. Avascular trajectories are planned with a diameter at least twice that of the estimated error of the system so that error in any direction will have less opportunity for vascular injury.

Planning for Heat Sinks

Although there is no quantification technique that exists for the identification of heat sinks a priori near the target, experience has led to strategies to mitigate the effect of heat sink on lesion reduction. Common heat sinks are cisterns, such as the ambient and quadrigeminal cistern in MTLE or the suprasellar cistern in HH, where the combination of CSF and arterial pulsations greatly dissipates applied thermal energy. Ventricles are also heat sinks, especially those with high flow rates by scarring and narrowing from previous surgery, such as the foramen of Monro. Sulci can also house heat sinks, especially those that possess a moderately large artery which increases pulsations. Lastly, there are considerable iatrogenic heat sinks from previous surgery and partial resections which can limit ablation volume, although the thermodynamics of these resection cavities are slower, and less pulsatile, and can be overcome with longer duration ablations. Occasionally indirect evidence of heat sinks can be encountered on planning imaging as noticeable flow voids on T2 imaging or as increased signal on the raw thermal image. Generally, we adopt our targeting to compensate for a heat sink by placing the laser as close to the heat sink as possible for the high-magnitude heat sinks (cisterns) and place the laser one third of the proposed ablation diameter closer to the moderate heat sinks on the oblique planar view. These adjustments should allow the heat to spread in the opposite direction of the heat sink as the power of the laser is increased.

Implanting the Laser

An orthogonal trajectory when drilling should be used as much as possible to minimize the risk of deflection of the drill by the bone/dura and thus loss of stereotactic accuracy. If an oblique trajectory is necessary, serial drilling using a smaller drill bit to create a pilot hole will help with unintentional movement at the bony surface. Rigid guidance of the anchor bolt into the bone is optimal, or if this is not possible, screwing of the plastic anchor bolt into the bone can be done by hand over the stylet guided to target by rigid stereotaxy. Dural penetration is also simplified by orthogonal puncture, with obliquity complicating the haptic feedback and maximizing the length of the dural opening. Monopolar cautery is applied to an obturator during durotomy to reduce the possibility of hemorrhage with dural penetration.

Each stereotactic pass involves creating a corridor first with a straight metal obturator to target depth (although this is not in the “indications for use” of the laser catheter). The obturator is placed to target depth slowly and steadily through the axial plane, focusing on the haptic feedback as the tip passes through structures of variable densities. In MR-compatible systems, sharp- or blunt-tipped ceramic stylets are used to establish the trajectory. Once the skull bolt is secured and the corridor of the trajectory established with a probe, the catheter, followed by the laser fiber (Visualase) or the laser probe (NeuroBlate), is placed down to target and secured.

Since 2012, we have utilized a combined technique with SEEG and laser ablation. Use of the wider inner diameter anchor bolt (Depthalon, PMT Corporation) allows the electrode of the ictally confirmed seizure onset zone to be replaced sterilely with a Visualase cannula, obviating the need for further surgery provided the trajectory was planned for optimal ablation in addition to SOZ localization. This allows the use of SEEG localizing data to plan the laser ablation on the same admission. Alternatively, Cobourn et al. demonstrated that staged sEEG and MRgLITT, separated by 2–4 months, can be used safely and effectively to localize and ablate epileptogenic foci in a minimally invasive paradigm for treatment of medically refractory lesional epilepsy in pediatric populations [17]. Both approaches integrate invasive EEG data in the surgical plan while maintaining a minimally invasive paradigm.

Intraoperative Imaging and Thermometry

Once the laser is delivered to the target, an MRI is obtained to confirm targeting. The imaging protocol begins with the acquisition of 3D T1 MRI from which the treatment planes can be selected. Proton resonance frequency is the most widely used temperature-sensitive MRI imaging parameter for real-time MRTI [18]. MR guidance allows precise monitoring of the thermal ablation zone, protecting critical and eloquent structures [19]. Photons emitted from the fiber-optic laser are absorbed by the tissue leading to molecular excitation and subsequent release of thermal energy within the target tissue. MRTI does not measure the absolute temperature of a sample but measures the temperature difference between the sample and a designated reference temperature image [18]. Temperature information and time of ablation are incorporated into a mathematical model of thermal tissue destruction to provide a quantitative estimate of tissue necrosis displayed in real time as an orange "Thermal Damage Estimate" [18]. Thermally induced time-dependent irreversible cell damage occurs between 43°C and 60°C, whereas temperatures above 60°C result in instantaneous coagulative necrosis. There is a sharp temperature drop-off at the border of the ablation zone creating a sharp margin between viable and nonviable tissue which can be monitored with real-time MRI thermal imaging.

The shape of the ablation zone frequently conforms to the target lesion, despite limitations in the directional probe. This phenomenon is attributed to microthermodynamic properties of target tissue, which tend to encase rather than disperse thermal energy [12].

MR Thermogram Limitations

The MR thermogram can be prone to artifact and signal drift. Artifacts that are frequently encountered are pulsation artifact and artifact from fixation devices. Pulsation artifact is mostly unavoidable but can occasionally be minimized by scanning in a plane that does not include a pulsatile large artery. Occasionally the direction of scanning can also be adjusted to move the pulsation artifact away from the area of interest. Fixation devices can also obscure the thermogram, the most impactful of which is the signal void created by titanium anchor bolts near the surface of the brain. Potential solutions to this problem include the use of a less rigidly fixated plastic anchor bolt to visualize surface ablations, use of derrick-style frame (Clearpoint, Nexframe, STarFix) that keeps the top of the trajectory free of metal artifact, or an ablation performed without thermography – dosed by the laser parameters at the deeper, thermally visualized portion of the trajectory. To address thermography signal drift, the NeuroBlate (Monteris) system has stabilization points within a limited field to minimize the effect of drift. In the Visualase system, using a high limit point far from the ablation zone to monitor the phenomenon can detect it, and resetting the phase once drift is detected mitigates this inaccuracy.

Confirmational Imaging

Confirmational imaging is obtained using diffusion-weighted imaging (DWI), or higher-resolution diffusion tensor imaging (DTI), FLAIR imaging, and enhanced T1 sequences. The laser fiber and catheter are removed, the stab wound is closed, and an additional sequence of fast field echo (FFE) or gradient recalled echo (GRE) or susceptibility-weighted imaging (SWI) is obtained to evaluate for hemorrhage.

Postoperative Care

Postop care in stereotactic laser ablation is typically quite minimal due to the small size of the incision typically needed to place the laser catheter. Due to this lack of access-related morbidity, many patients can leave the hospital the next day. The majority of the postoperative care concerns are related to the edema created by the thermal ablation. If the thermal ablation is performed adjacent to vital structures, such as in the ablation of a hypothalamic hamartoma or in targets abutting the motor strip, high-dose steroids typically minimize the symptoms related to the severe and rapid onset edema commonly encountered following thermal ablation. Activity restrictions typical of post-craniotomy care are not required.

Imaging and Radiologic-Pathologic Correlation of Lesions Treated with LITT

Ablated lesions radiologically demonstrate a thin peripheral rim of enhancement, variable T1 and T2 central signal due to blood and protein products, and surrounding edema on T1-contrasted images [20] (Fig. 11.2). Serial follow-up performed more than a month after the procedure should demonstrate a continuous decrease in the size of the ablated lesion and stable or decreased enhancement [21].

There are five histologically separate concentric zones (Fig. 11.3) [22]. The histologic view of the lesion has a central zone, which includes the probe track, filled with CSF, blood, and coagulation necrosis. Outside that is a peripheral zone, which includes thrombosed vessels and distended cell bodies [22]. Beyond the peripheral zone is the marginal zone, which includes an area of reversible post-surgical perifocal edema, edematous tissue, and axonal swelling without thrombosis.

Commercially Available Laser Ablation Systems

Two major LITT platforms are in use today. Subtle differences in workflow exist related to the laser ablation system and software that is chosen. Both systems are MR/head compatible and utilize probe tip cooling to maximize target zone heating penetration by controlling temperatures at probe-tissue interface.

Medtronic Visualase

In cases where the target is in non-eloquent cortex, in which completeness of the lesion ablation is the primary objective, a single oblique treatment plane is selected that encompasses the entire trajectory. In lesions abutting eloquent tissue, two treatment planes are selected, one obliquely inclusive of the trajectory and one selected to optimally visualize adjacent structures that are to be preserved, typically in an orthogonal plane. Adding treatment planes has practical consequences on the refresh time of the near real-time MR thermography (Fig. 11.4), with the refresh time of a single plane being 3.5 seconds and 7 seconds for two planes. When choosing the fiber diffuser length (3 mm or 10 mm), the proximity of eloquent tissue along the longitudinal axis of the trajectory should be considered. If the eloquent tissue is within 3 mm proximal or distal to the heat source, then a the

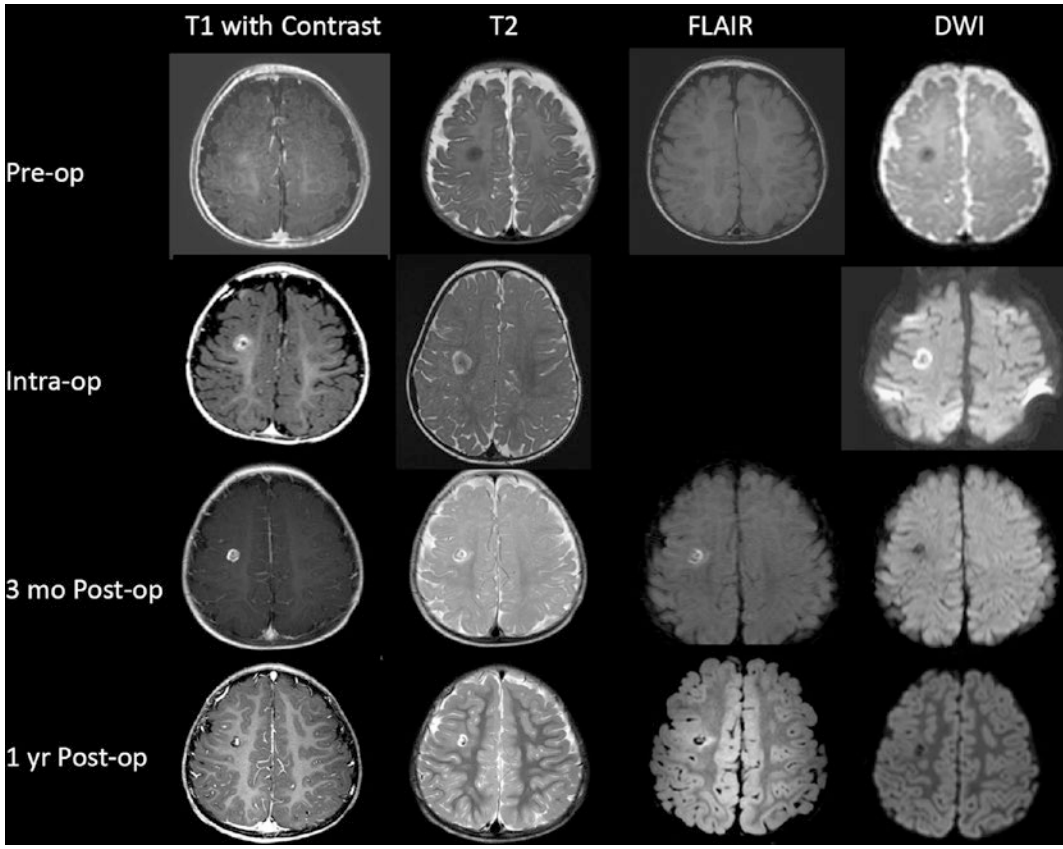

Fig. 11.2 The radiologic evolution of MRgLITT-treated focal cortical dysplasia in a 12-month-old child. MRI sequences of T1 with gadolinium, T2, FLAIR, and DWI are shown at separate times during the treatment process. Images are taken pre-operatively, intraoperatively (we do not routinely obtain FLAIR sequences during the ablation), 3 months after the operation, and 1 year after the operation. Note the steady contracture of the T1 gadolinium infused ablation area, the resolution of the increase of the DWI signal, and the persistence of the FLAIR signal in the lesion

3 mm fiber should be chosen as it can create a wide (axial) but short (longitudinal) heat field that can be monitored with two or less planes (Fig. 11.5). If such eloquent tissue is not nearby, then the 10 mm diffuser tip fiber can be chosen to maximize the ablation volume. Once the planes are established, background images are obtained, the sequence of which is chosen to optimize contrast between the lesion and the surrounding brain, and they are then fused to a continuous MR thermogram. A test dose of heat, typically 15% of a 15 W laser setting on a 10 mm diffuser, or 8% of a 10 W laser setting on a 3 mm diffuser, is applied, and the depth of the laser fiber within the cannula is adjusted to optimize the application of heat to the center of the lesion.

Use of Low-Limit Markers

When ablating a target abutting vital structures, low-limit markers, designed to automatically turn the laser off when the pixel under that marker reaches 50°C, are placed approximately 1–2 mm from the structure to be preserved, in the direction of the heat source. The current software offers three of these markers to distribute along the structures to be preserved, but in complex

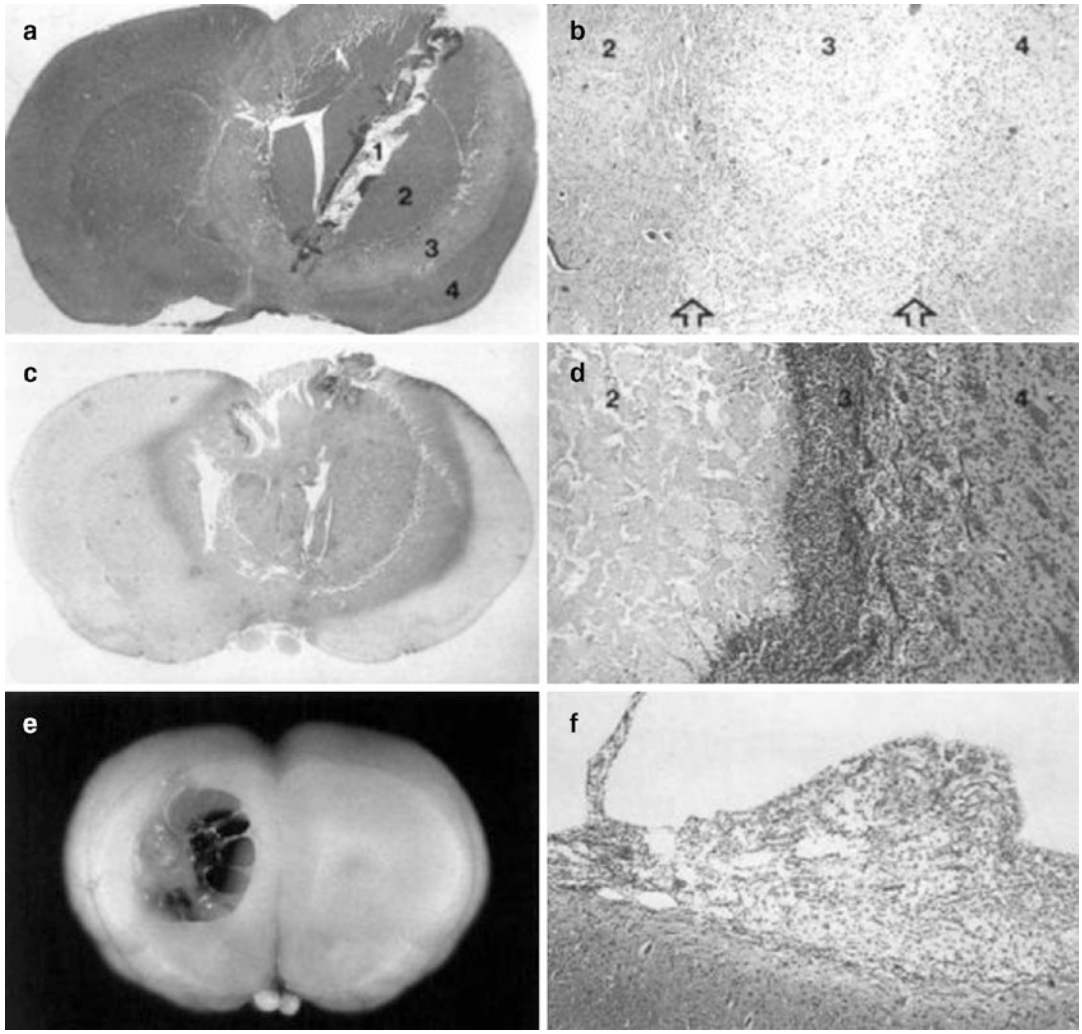

Fig. 11.3 Neuropathological changes in interstitial laser hyperthermia. (**a**) Frontal section of rat brain with a very large acute lesion to illustrate the zonal architecture. 1, track of the laser probe; 2, coagulation; 3, edema; 4, adjacent normal brain tissue. Masson X5. (**b**) Higher magnification of the zones 2, 3, and 4 with arrows marking their borders. The coagulation zone shows minor histological changes, whereas the zone of edema is pale due to vacuolization and contains darkly staining neurons. H&E, X30. (**c**) Immunohistochemical decoration by albumin of the serial section, showing a breakdown of the blood-brain barrier in the entire lesion but not in the peripheral brain tissue. PAP method X5. (**d**) Early reactive changes in the tissue zones corresponding to (b). One week postoperatively, the necrosis is obvious by loss of nuclear staining and is demarcated by granulation tissue originating from the viable periphery. H&E X50. (**e**) Histology of the cyst wall, showing strands of fibrous tissue with interspersed siderophages but very little changes in the underlying brain tissue. Masson x50. (**f**) Histology of cyst wall, showing strands of fibrous tissue with interspersed siderophages but very little changes in the underlying brain tissue. From Masson, Schober et al. *Lasers Surg Med* 1993 13:234–41 [22]. Reprinted with permission from John Wiley and Sons

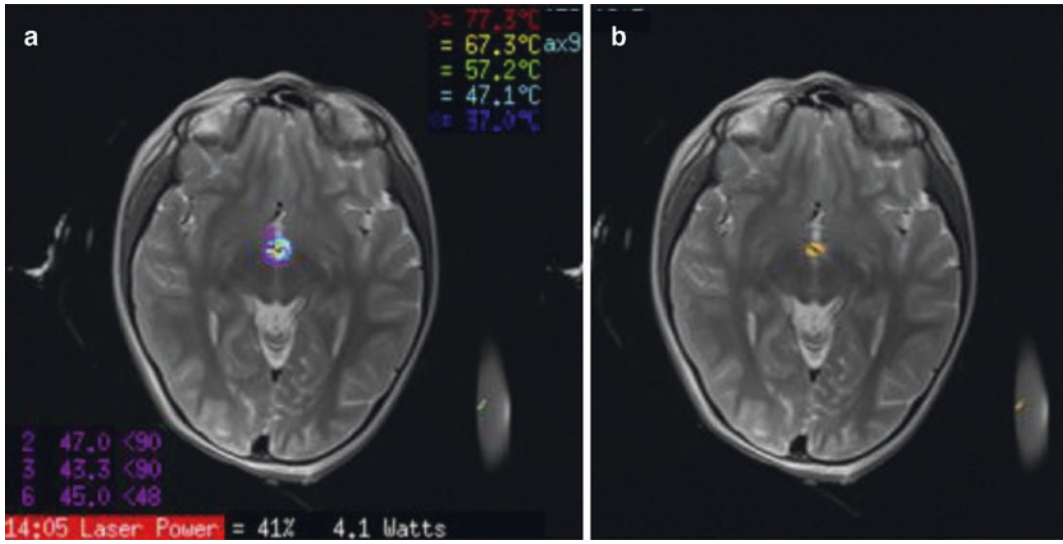

Fig. 11.4 MRgLITT of a hypothalamic hamartoma with Visualase Laser Ablation System. (**a**) MR thermography superimposed onto an anatomic background image showing the temperature changes occurring at the region of interest as the laser is turned on. Note the low-limit marker #6 monitoring the right mammillothalamic tract and repurposed high-limit markers #2 and #3 monitoring the left mammillothalamic tract and the right fornix, respectively. (**b**) A treatment damage estimate (TDE), in orange pixels, accumulates over the target lesion, in this case a hypothalamic hamartoma, as the temperature steadily escalates to tissue coagulation

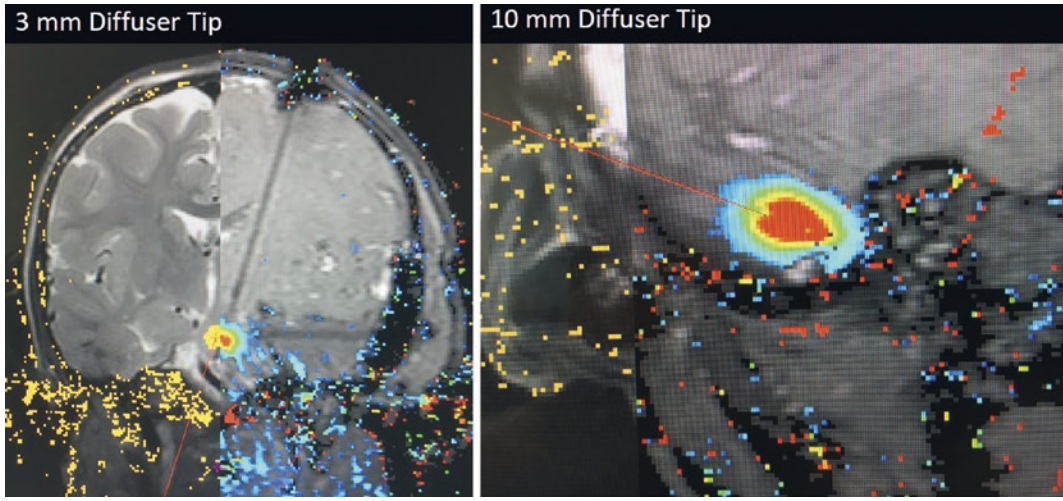

Fig. 11.5 Diffuser tips of the fiber-optic laser fibers available in the Visualase Laser Ablation System. Split-screen thermograms of stereotactic laser ablations of hypothalamic hamartomas performed in the oblique coronal plane, with the right of the split screen showing a TDE superimposed upon a T2 coronal background image and the left showing the source thermogram. The image on the left has a wide, short, toroid-shaped ablation zone created by a 3 mm diffuser tip. The ablation zone on the right is longer at the comparable width and is the ablation zone created by a 10 mm diffuser-tipped fiber

lesion targeting, such as hypothalamic hamartoma, more low-limit markers are needed. In those scenarios, high-limit markers, used to monitor the temperature near the heat source to avoid catheter damage from overheating, can be borrowed to serve as monitor markers, but they need to be visually monitored for manual laser shutoff. Also, we have lowered the temperature of the low limit from 50°C to 48°C for an additional margin of safety (indications for use of the Visualase laser system actually recommend 43°C). One high-limit is reserved for monitoring the temperature at the heat source.

Once the low-limit markers are in place, the laser is turned on to allow the heat within the lesion to increase until the irreversible damage estimate, as calculated and projected onto the image on the basis of the Arrhenius equation, overlaps the lesion as visualized on the background image. This is optimally performed by adjusting the laser wattage to keep the high-limit marker from 85°C to 89°C to maximize the heat delivery. After the irreversible damage map covers the lesion, the laser is discontinued.

Using the Monteris NeuroBlate

The Monteris NeuroBlate software automatically monitors the imaging in five views: sagittal oblique, coronal oblique, and three oblique axial views along the ablation trajectory (Fig. 11.6). The thermogram is automatically fused to the background imaging, the sequence of which is selected to optimize lesion contrast. Eight temperature reference points are placed within a focused thermal field to minimize the artifactual drift of the MR thermogram data, and after a number of iterations, the thermogram is stabilized, and the background thermogram color turns green. The laser is then engaged, at only one intensity, and two clinically relevant

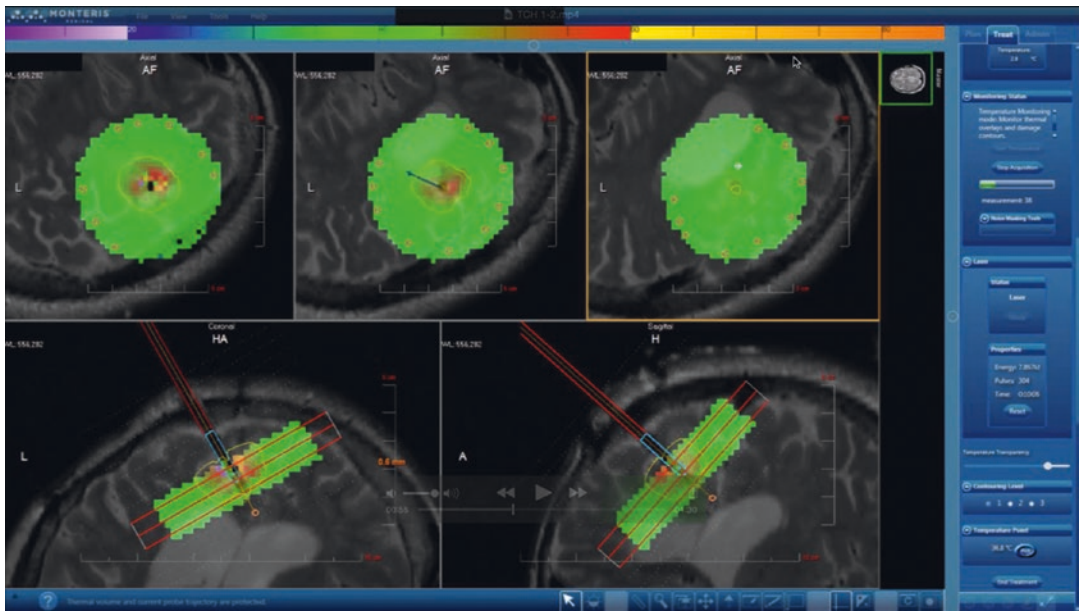

Fig. 11.6 MRgLITT with the NeuroBlate (Monteris, Inc.) System. A screenshot of a laser ablation of an area of encephalomalacia-causing seizures. The treatment is done in five planes at one laser power with a 6 mm diffuser. Note the points placed in around the area of interest to stabilize the thermogram. Note also the directional nature of the laser, perceived by the asymmetric color-coded heat emanating from the probe in the center of the field

thermal dose threshold (TDT) contours of damage, apoptotic TDT contour in yellow and the coagulation TDT contour in blue, expand over time. Once the blue TDT contour contains the target, the laser is turned off. One can choose diffuse or side-fire laser probes, the latter of which provides directional laser energy offering a theoretical advantage of selectivity in brief ablations.

Indications

Hypothalamic Hamartoma

Hypothalamic hamartoma (HH) is the most common indication of MRgLITT in pediatric epilepsy with Curry et al. providing the largest series with 71 pediatric patients [23] (Fig. 11.7). The goal of MRgLITT is not necessarily ablation of the entire hamartoma but rather complete disconnection of the hamartoma from the hypothalamus and mammillary bodies. The most metabolically active portion of the lesion could be targeted by pre-operative PET scanning. Disconnection is usually sufficient to achieve total remission of gelastic seizures [23]. Recent data has shown that 57% of lesion destruction predicts an 83% chance of freedom from gelastic seizures [24].

The trajectory described is in an oblique coronal plane angled anteriorly beginning in the frontal lobe, traversing the anterior limb of the internal capsule and ending in the inferior portion of the hamartoma near its junction with the mammillary bodies. The surgical trajectory results in minimal corridor-related morbidity making it safely repeatable, allowing the technique to be used in an incremental fashion in situations of high risk [23]. In the series published by Curry (2018), there was a 1.5% rate of memory deficit, compared to the 15% permanent memory deficit in open surgery or 7% in endoscopic resection [25, 26]. Four percent of patients had a single episode of hyponatremia as opposed to near universal prolonged serum sodium fluctuation associated with open resection [23].

Mesial Temporal Sclerosis

Temporal lobe epilepsy represents the most common localization-related epilepsy syndrome, and it has been demonstrated that temporal lobectomy is superior to medical management [27]. In pediatric mesial temporal lobe epilepsy (MTLE), however, the surgical outcomes are less robust than in adult series and are particularly vulnerable to failure in volumetrically smaller resections [28]. Although there have been published series on the application of LITT for adult MTLE, there have been no series published in children. Table 11.1 summarizes the published cases to date of pediatric patients undergoing LITT of the mesial temporal lobe.

Gross et al. presented a case series demonstrating seizure-free rates for mesiotemporal epilepsy with MRgLITT closely approximating those for open temporal lobectomies while potentially improving post-procedural neurocognitive outcomes [29, 30]. A linear trajectory from the lateral occipital region through the long axis of the hippocampal body terminating in the amygdala is usually selected while avoiding traversing the ventricle or any vascular structures [31]. Ablation outcome in MTLE is optimized if the ablation volume includes the head of the hippocampus, half of the amygdala, and the tail of the hippocampus posteriorly to the lateral diencephalic notch [32] (Fig. 11.8). Additional efficacy can be obtained by localizing the seizure onset zone (SOZ) with invasive monitoring [33].

Tuberous Sclerosis

Tuberous sclerosis complex (TSC) is a multisystem disorder that involves the brain, skin, kidneys, heart, and lungs. Epilepsy is the most common clinical manifestation of TSC and is found in as many as

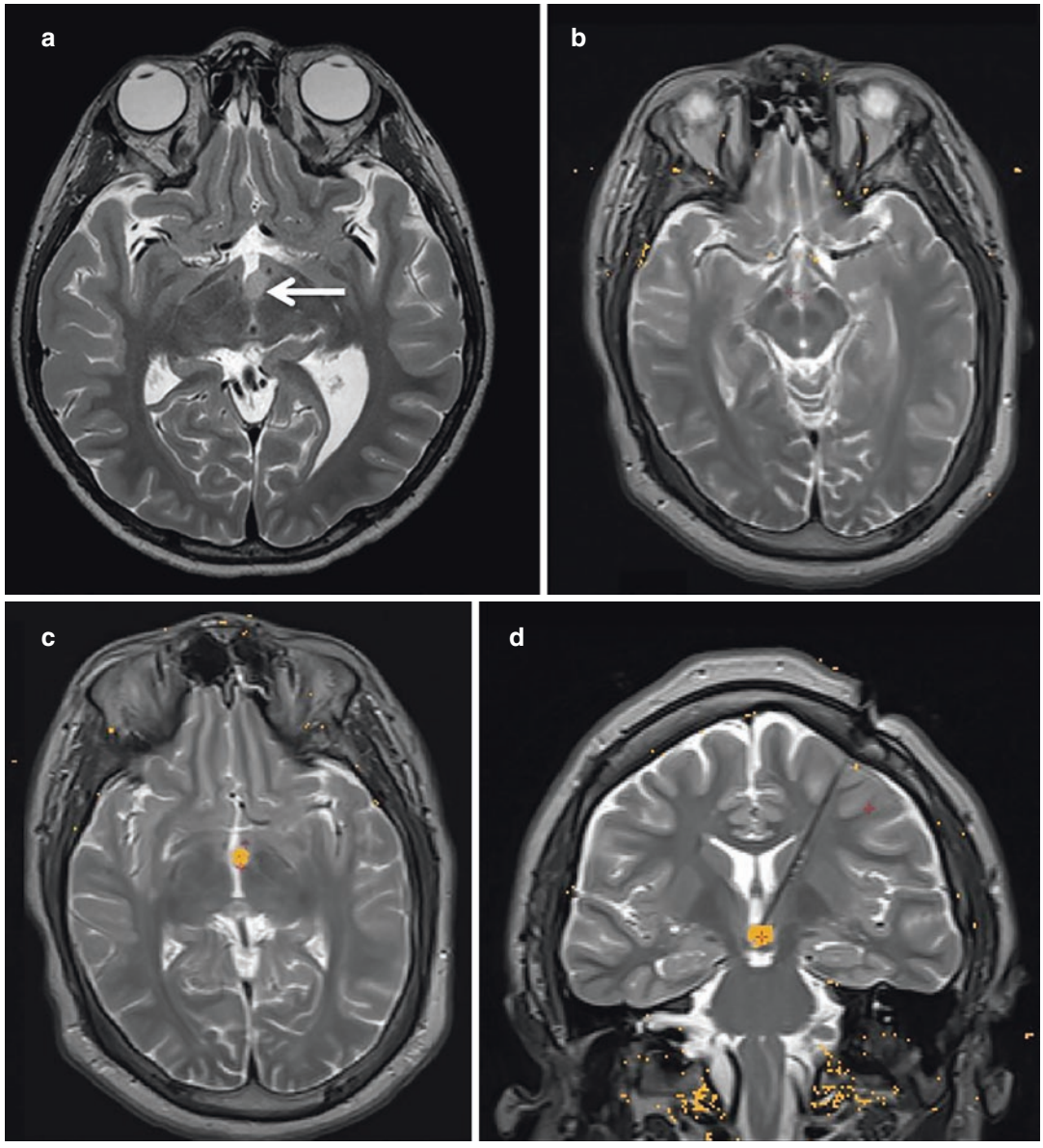

Fig. 11.7 MRgLITT for hypothalamic hamartoma. (**a**) Axial T2 MRI showing a left Delalande Type II hypothalamic hamartoma (*arrow*). (**b**) Axial T2 MRI of the most inferior slice of the lesion showing the catheter in place and low-limit markers on the left and right mammillary bodies. (**c**) Axial T2 MRI of a superior half of the lesion showing a TDE covering the hamartoma and low-limit markers protecting the left fornix and the left mammillothalamic tract. (**d**) Coronal T2 MRI showing the catheter entering the lesion, the TDE covering the lesion, and a high-limit marker near the catheter to prevent overheating. (**e**) Axial T1 MRI with gadolinium enhancement showing the new enhancement of the ablated hamartoma and no ablation outside the lesion. (**f**) Axial DWI imaging confirming thermal injury in the hamartoma. (**g**) Axial and (**h**) coronal T2 MRI showing the lesion site 3 months after ablation with destruction of the lesion with intact left mammillary body, fornix, and mammillothalamic tract

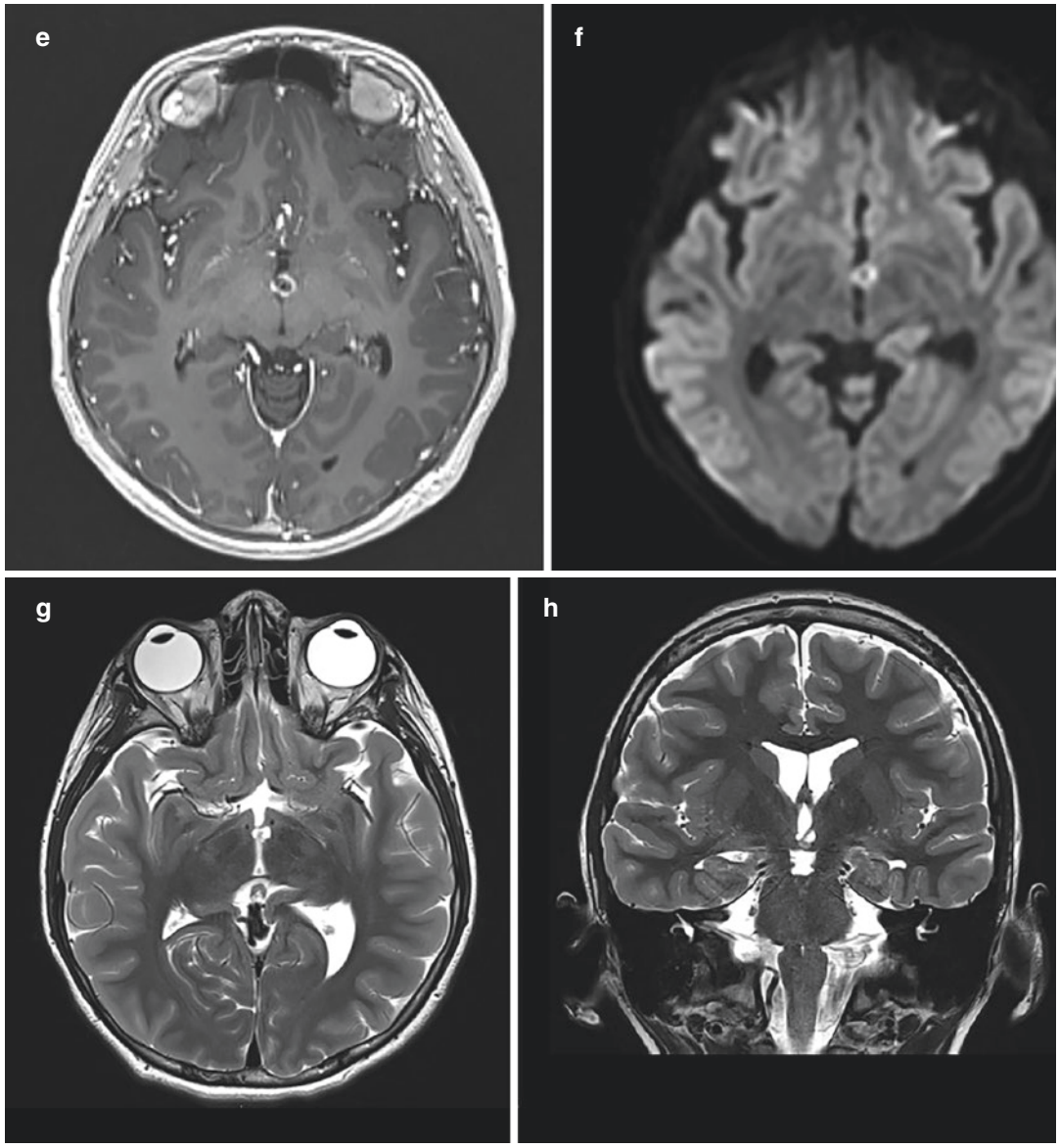

Fig. 11.7 (continued)

Table 11.1 Published experience in MRgLITT in pediatric mesial temporal lobe epilepsy

Center	Age	MTS	Duel	Engel Score
Thomas Jefferson University	11	Y	N	4
	14	Y	N	2
Emory University	18	Y	N	1D
	16	Y	N	1D
	18	Y	Y	2, 1D
Texas Children's Hospital/Baylor College of Medicine	15	Y	Y	1D (late failure)
	17	Y	N	4
	7	Y	Y	1A
	16	Y	Y	2
	16	Y	Y	1D
	11	Y	N	1D
University of Miami	14	N	U	1B
	15	N	U	2
	15	N	U	1B
	11	Y	U	2
	17	Y	U	1A
	15	N	U	4
	5	N	U	3
	2	N	U	2

The table shows the 19 published cases of LITT in pediatric mesial temporal lobe epilepsy. Note the modest Engel 1 outcome (52%) and the relatively increased rate of dual pathology [12, 57–59]

90% of cases. Epileptogenesis has been theorized to result from different morphological and molecular abnormalities observed in the cortical tubers and the perituberal cortex, heterotopic gray matter and associated white matter tract abnormalities. Patients with TSC and epilepsy often present with multiple, bilateral, and disparately located cortical tubers making surgical treatment challenging and increasing the risk of adverse events. Even in patients with multiple tubers, seizures may still rise from a single tuber. Weiner et al. established a three-stage, open craniotomy approach with subdural grids and strips to not only localize the active tuber prior to the initial resection but to repeat the invasive monitoring after resection to extend the resection or resect an emergent focus in the postoperative period [34]. Laser ablation offers a less invasive option to achieve the same goals (Fig. 11.9). After a comprehensive non-invasive seizure localization evaluation, sEEG can replace the need for subdural grid studies via craniotomy to confirm the epileptogenic focus. Stereotactic laser ablation also offers a less invasive option for surgical palliation of the seizure burden in these patients who will likely need repeat surgeries throughout their lives as new seizure foci arise [35]. The first patient with epilepsy to be treated with stereotactic laser ablation was a child with TSC and a large cingulate tuber [12]. Tovar-Spinosa et al. in 2018 presented case series of seven patients, seizure reduction rate comparable to resective surgery and reduction in AED burden [19]. Several other case series have also been reported with successful ablation of tubers in single or staged surgeries.

Cortical Dysplasia

Focal cortical dysplasias (FCD) (Fig. 11.10) are areas of epileptogenic cortical dyslamination without (Type I) or with (Type II) dysmorphic neurons or associated with another lesion like a low-grade tumor (Type III). Focal cortical dysplasia was first targeted with a submental laser ablation by Curry et al., resulting in temporary seizure freedom that was only made permanent with extension of the ablation to the cortical surface [12]. The largest series of laser ablation in cortical dysplasia was reported by Lewis et al. which found a 45% seizure freedom rate in their series [36]. Similar to open surgical resection, success of stereotactic laser ablation in its application to FCD is dependent upon completeness of localization and destruction of the SOZ. Although somewhat less successful than summarized outcomes of open resection, LITT for FCD may offer a low-morbidity initial approach with a reasonable chance of achieving the surgical goals that does not preclude further resection.

Periventricular Nodular Heterotopia

Periventricular nodular heterotopia (PVNH) is a neuronal migration disorder characterized by

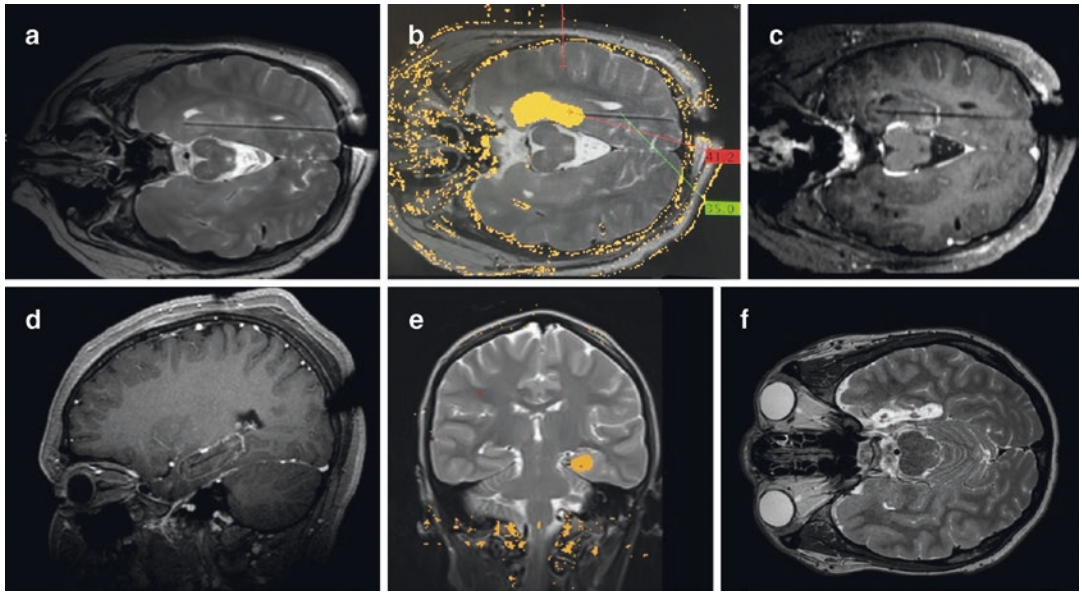

Fig. 11.8 MRgLITT in pediatric mesial temporal lobe epilepsy. (**a**) Axial T2 MRI showing a catheter in the mesial temporal lobe. (**b**) Axial T2 MRI showing the TDE enveloping and taking the shape of the mesial temporal structures, with low-limit markers in the optic radiations and in the Meyer's loop and a high-limit marker near the catheter. (**c**) Axial, and (**d**) sagittal, T1 MRI with gadolinium enhancement showing enhancement in the mesial temporal structures confirming ablation. (**e**) Coronal T2 MRI showing the catheter, the TDE, and low limits placed on the lateral geniculate nucleus to prevent homonymous hemianopsia. (**f**) Axial T2 MRI showing the mesial temporal region 1 year after ablation

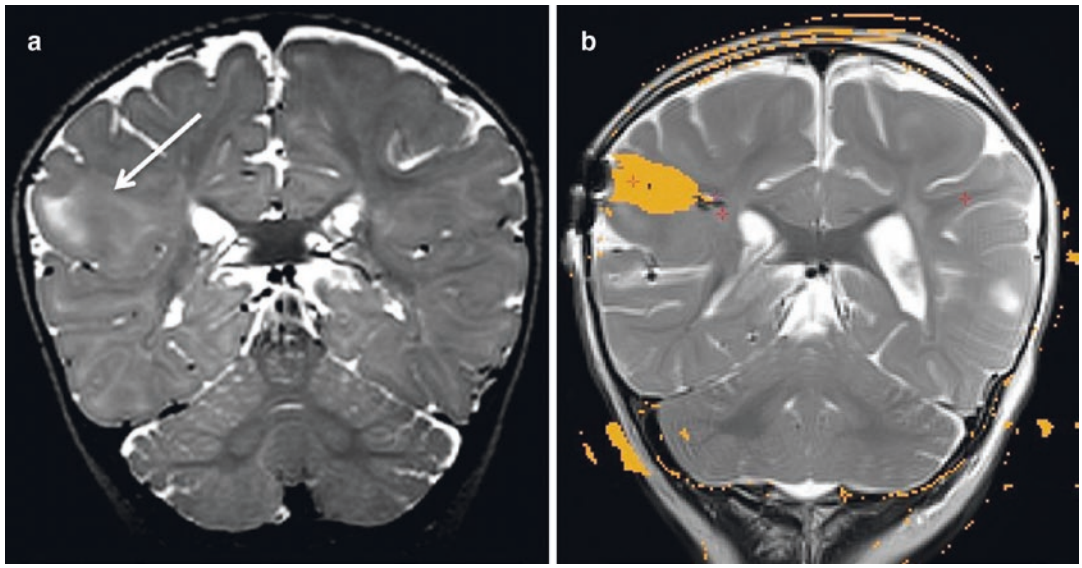

Fig. 11.9 MRgLITT for epilepsy related to tuberous sclerosis complex. (**a**) Coronal T2 MRI of a patient with TSC and a seizure onset zone localized by SEEG to the tuber in the parietal operculum (*arrow*). (**b**) Coronal, and (**c**) axial, T2 MRI with the TDE superimposed upon the target lesion. (**d**) Coronal T1 MRI with gadolinium enhancement showing new enhancement of the target tuber, confirming ablation

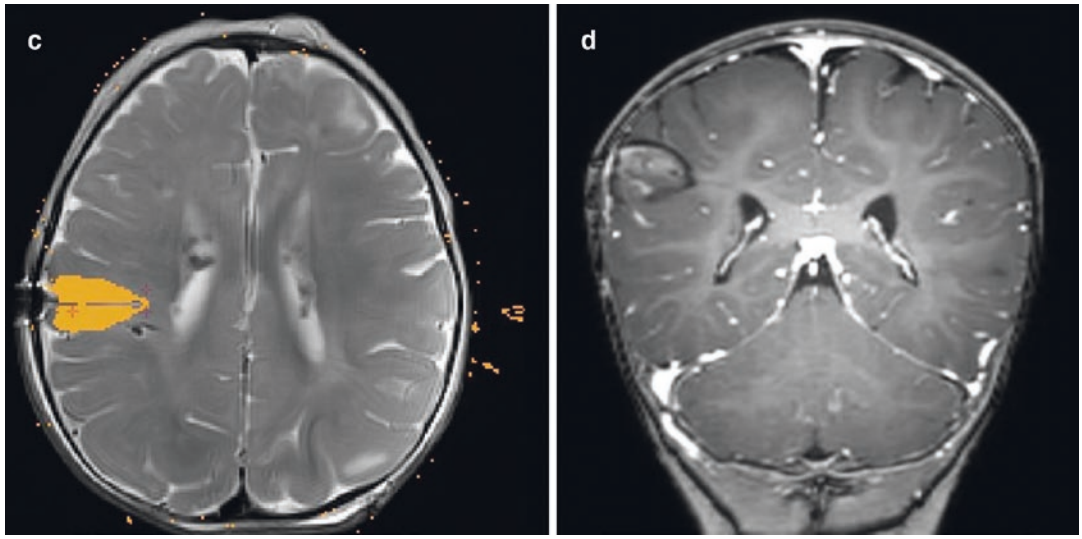

Fig. 11.9 (continued)

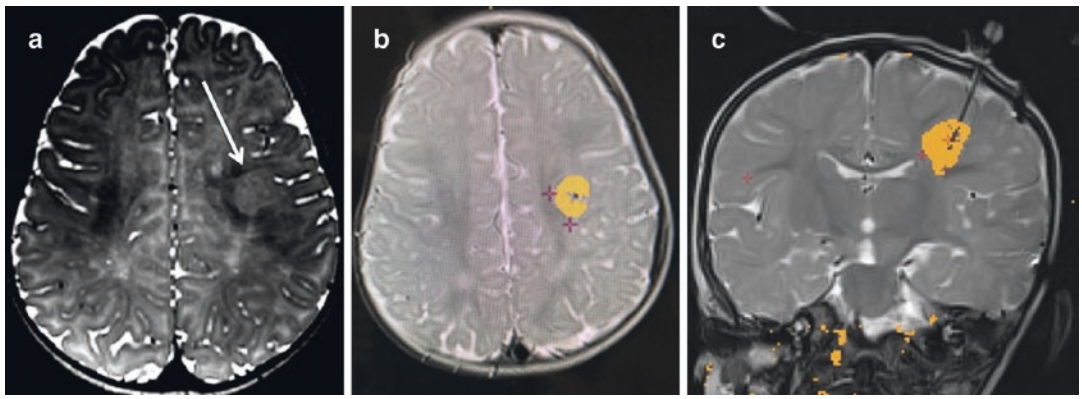

Fig. 11.10 MRgLITT in pediatric cortical dysplasia. (**a**) Axial T2 MRI showing a cortical dysplasia in the left central lobule of a 1-year-old patient (*arrow*). (**b**) Axial and (**c**) coronal T2 MRI showing the laser catheter and the superimposed TDE quantifying the ablation of the target lesion. Low-limit markers are placed on the white matter of the corticospinal tract

subependymal gray matter nodules that fail to migrate from the periventricular germinal matrix. Gray matter heterotopias are visible on MRI along the ventricles and in the white matter, with less distinct and frequently not radiologically visible cortical dysplasia within the projected cortex along the radial glia, making complete radiologic definition of the seizure onset zone challenging. In addition, PVNH frequently presents with dual or multiple radiologic abnormalities that are possibly epileptogenic, such as cortical dysplasia, polymicrogyria, hypothalamic hamartoma, and mesial temporal sclerosis. Resective surgical strategies are difficult due to their deep location, and often are only successful after anatomic lobectomy, typically with a subsequent neurologic deficit. There has been varied success with nodular ablation alone

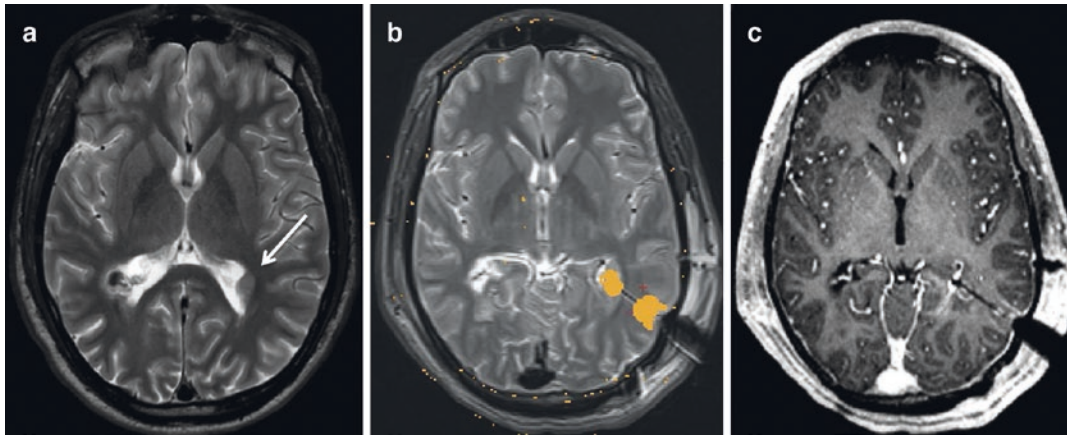

Fig. 11.11 MRgLITT in pediatric periventricular nodule heterotopia. (**a**) Axial T2 MRI showing a patient with bilateral PVNH, the right side of which was ablation at a previous operation. The left PVNH (*arrow*) is targeted on the exhibited operation. (**b**) Axial T2 MRI showing the catheter in a trajectory that was shown to be the seizure onset zone, in the periventricular nodule and in the overlying cortex, by SEEG. The ablation, as estimated by the TDE, therefore covers both the nodule and the overlying cortex with the use of low-limit markers in red protecting the intervening white matter. (**c**) Axial T1 MRI with gadolinium showing new enhancement of the left PVNH and the overlying cortex

[37]. PVNH is thought to act as a pacemaker which seizes independently or with seizures arising from multiple regions within the network simultaneously [38]. Alternatively, PVNH may focus and synchronize epileptogenic activity in overlying cortex requiring resection of both the PVNH and the overlying cortex [39]. There are no dedicated pediatric series of surgically treated patients with PVNH-related epilepsy, but the adult surgical literature is likely reflective of the experience in this congential condition. Esquenazi reported two cases of PVNH patients treated with MRgLITT in adults. One patient remained seizure-free on only one medication. The other required amygdalohippocampectomy after 12 weeks but then remained seizure-free [40]. The same group published a comprehensive review of the 47 patients invasively monitored with PVNH, all adult, and revealed a variety of networks and patient-specific surgical solutions including ablations (both LITT and radiofrequency) and resective [38]. Our own experience with PVNH (Fig. 11.11) supports a necessity of invasive ictal data, ideally with SEEG, and a multi-staged and multi-modal approach to treatment which frequently can include resection, ablation, and responsive stimulation to control the ictal network.

Insular Epilepsy

Insular epilepsy represents a particularly difficult form of surgical epilepsy to diagnose and treat with resection. Diagnostically, insular epilepsy can be difficult – especially in the absence of stereotypical insular semiologies such as hypersalivation, choking, perioral paresthesias, or dysautonomia. Additionally, surface EEG can be unhelpful due to its deep nature, requiring SEEG or depth electrodes to electrophysiologically confirm its presence. Operative treatment of insular epilepsy carries a high risk of vascular injury due to the candelabra-like branches of the middle cerebral artery draped over the geometrically complex structure. LITT has been shown to be a safe and effective approach to insular epilepsy [41] (Fig. 11.12). In a comparison between an open surgical cohort and a LITT cohort of children being treated for insular epilepsy, the two cohorts had comparable outcomes at 2 years postoperatively [42]. Although half of the patients in both cohorts had a transient contralateral hemiparesis, the open cohort also had complications of meningitis and hydrocephalus, leading the authors to conclude that the ablative approach had an advantage in complication avoidance.

Cavernous Malformations

Cavernous malformations are thin-walled clusters of vascular sinusoids lined by endothelial cells intertwined without intervening parenchyma. Supratentorial CCM lead to seizures in up to 70% of patients, and 40% develop medically refractory epilepsy [43]. Patients exhibiting symptoms relatable to intracranial pressure and mass effect benefit from surgical resection. Seizure freedom usually requires additional evaluation to define the seizure onset zone and a more extended lesionectomy to include the hemosiderin ring and gliotic tissue to include the epileptogenic cortex. McCraken et al. (2016) and Willie et al. (2019) published a case series of five patients with epileptogenic cavernomas, most of which were in the temporal lobe, treated with MRgLITT [43, 44]. Four out of five were seizure-free at follow-up. One patient had residual atrophy and blood products at the ablation site and underwent open resection [43].

Corpus Callosotomy

Corpus callosotomy is a commonly performed procedure as a treatment for refractory epilepsy, most commonly for atonic seizures, generalized tonic-clonic seizures, or seizures with multifocal spike-slow wave activity or rapid secondary bisynchronous EEG activity [45, 46]. The first report of using LITT for corpus callosotomy was

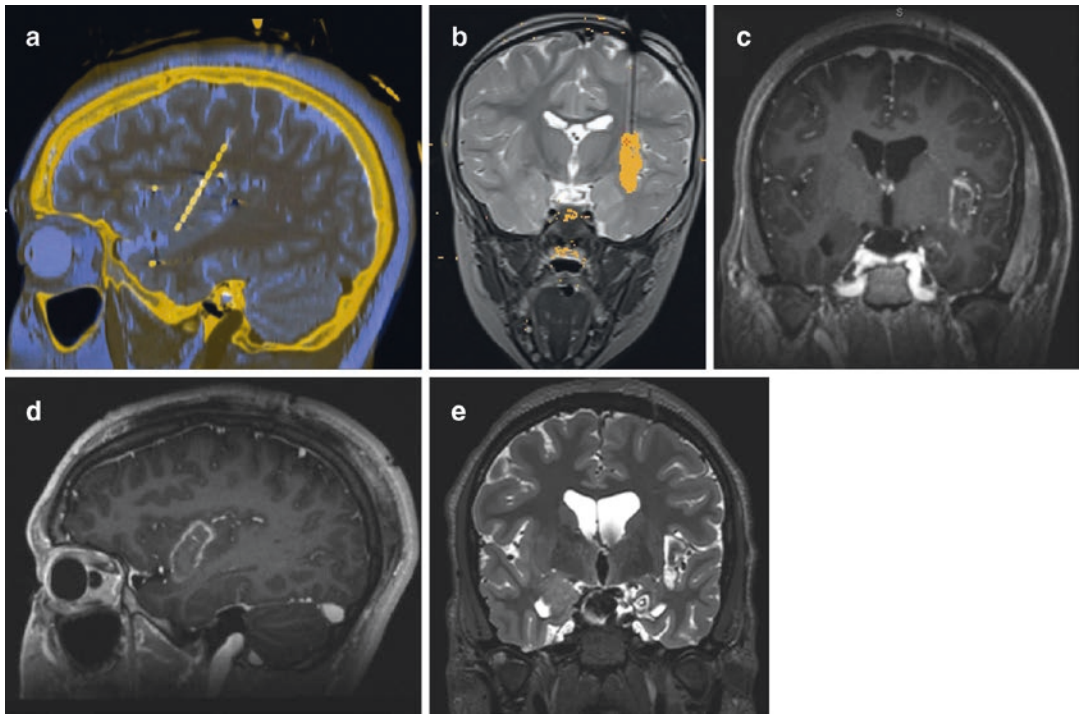

Fig. 11.12 MRgLITT in pediatric insular epilepsy. (**a**) Sagittal view of a T2 MRI fused to a volumetric CT scan showing the placement of the depth electrode found to be the seizure onset zone by SEEG in a patient with insular epilepsy. (**b**) T2 coronal MRI with the superimposed TDE showing the estimated ablation along the middle short gyrus of the left insula, with a low-limit marker protecting the descending white matter tracts. (**c**) Coronal and (**d**) sagittal T1 MRIs with gadolinium enhancement showing new enhancement of the ablated corridor. (**e**) Coronal T2 MRI showing the insular ablation zone 3 months after the operation

in a 10-year-old female by the senior author, with Engel II outcome at 2 years [47]. The technique, designed for this particular patient's malformed rectilinear corpus callosum, utilized one laser in a coronal oblique trajectory to target the genu and rostrum, and a second laser in an oblique axial plane to target the body. Subsequent LITT callosotomies have used three and occasionally four lasers depending upon the curvature of corpus callosum and the extent of the ablation desired. The ablation in the white matter is more rapid than in gray matter and requires precision to avoid the bilateral fornices that hang from the corpus callosum near the junction of the posterior body and the splenium (Fig. 11.13).

A video abstract was published by Karsy et al. utilizing three catheters in a 17-year-old female with expected reduction of her seizures at a brief follow-up period of 9 months [48]. Palma et al. published two pediatric patients undergoing LITT for corpus callosotomy, one primary (with a PVNH ablation) and one residual, showing resolution of their drop seizures lasting up to 3 years [49]. A larger series of ten patients, eight less than 20 years of age, was reported by Roland et al., six of whom were primary and four were residual [50]. Assessment of disconnection was made by resting state functional MRI [50, 51]. The first patient in that series was treated with the Monteris NeuroBlate System, the rest being treated with the Medtronic Visualase System. Five of the eight pediatric patients had an Engel III outcome score or better. Long-term outcomes are unknown.

Another use for LITT in corpus callosotomy is as a salvage procedure, as described in a subset of the patients reported in Palma et al. and Roland et al. An additional three pediatric patients undergoing completion callosotomy were reported by Huang et al. with Engel IV outcomes in two and an Engel II outcome in a third [52]. DTI studies showed residual but attenuated corpus callosal fibers greater than 1-month post-ablation. Average hospital stay was 2 days [52], and there was one report of disconnection syndrome [51] lower than in open series [53].

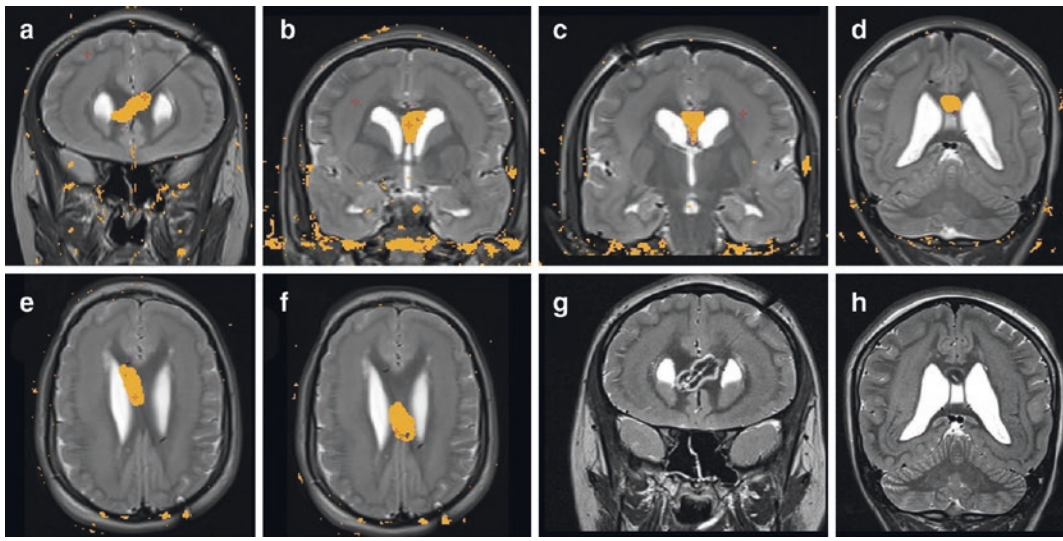

Fig. 11.13 Corpus callosotomy by MRgLITT. Coronal T2 MRIs with the superimposed TDE showing the estimated ablation of the (**a**) rostrum and genu, (**b**) anterior body, (**c**) posterior body, and (**d**) the posterior body/splenium junction. (**e**) Axial T2 MRIs with the superimposed TDE of (**e**) the anterior body and (**f**) the posterior body of the corpus callosum, with low-limit markers placed on the fornices. Coronal T2 MRIs of the (**g**) genu and (**h**) posterior body/splenium junction confirming the ablation with increased T2 signal at the ablation target

Complications

The most common reported complication of LITT is transient neurologic deficit, 19% of all complications [13]. This is dependent upon the target of the ablation and the potential for collateral injury to the target. Examples include dysphagia, weakness, hemianopsia, and minor seizures. The main complication seen in MRgLITT of mesial temporal lobe epilepsy was a visual field cut. Limiting heat exposure along the posterior hippocampus may decrease the frequency of this complication. In addition to limiting the heat exposure, ablation can more safely be performed by using a coronal or sagittal plane to visualize and protect with low-limit markers the lateral geniculate ganglion, the thermal damage of which would result in a homonymous hemianopsia. Cranial nerve neuropathy is also reported, at a higher frequency than with open resection in MTLE [54]. Heat spread along the tentorium or near the cavernous sinus may be the cause of the higher incidence of cranial nerve 3 and 4 palsies. Permanent neurologic symptoms occurred in 3% of patients in current reported case series [13]. Intracranial hemorrhage was reported in 2.5%, infection in 2.5% and deep venous thrombosis (DVT) in 2.5%. Post-ablation edema when seen on imaging is treated with high-dose Decadron tapered over 2 weeks. Other reported complications include intracranial hemorrhage, meningitis, and hydrocephalus due to a trapped ventricle presumably from scar tissue along the ablation tract [13].

In targeting cortical dysplasia, the complication profile is mostly associated with the proximity of eloquent tissues near the target. LITT applied to insular lesions was found to have a minor and transient complication profile, especially as it relates to contralateral weakness, when directly compared to open insular resections for epilepsy [42]. Kuo et al. addressed this complication profile directly in five pediatric patients and found a favorable complication rate near eloquent regions [55]. Barber et al. reported a particularly troubling case of delayed intraventricular and intraparenchymal hemorrhage requiring craniotomy and resulting in hemiparesis [56].

The highest potential for complication in LITT for epilepsy is in the ablation of hypothalamic hamartoma. The target is near the mammillary bodies, fornices, and mammillothalamic tracts, the injury of which could profoundly decrease memory. The HH is also nestled against the medial wall of the hypothalamus, injury of which results in hypothalamic obesity, and is nearby the pituitary stalk, injury of which can result in diabetes insipidus. In the laser ablation of the hypothalamic hamartoma, permanent memory disturbance has been reported in the range of 1.4% [23] to 22% by Du et al. [57]. One particular exemplary complication of memory deficit was published, noting that the contralateral mammillary body was injured despite planning that protected it with a low-limit maker [58]. The report emphasized the additional safety features of lowering the temperature required to trip the laser off to 48 °C from the default of 50 °C and keeping the low-limit marker at least 1.5 mm away from the structure to protect in the direction of the heat source.

Technical failures can also be considered as complications to the procedure although they may not adversely affect the patient or their outcome. Reported failures include inaccurate fiber placement, misregistration error between the frame and navigation, and failure of the cooling mechanism around the catheter [34].

Avoidance of complications can be achieved with the following recommendations: frame-based catheter placement; small, 1.8 mm alignment rod to create a tract; titanium anchor bolts for long trajectories to improve accuracy; narrow gauge instrument for dural puncture via electrocautery; co-registration of MRI and CTA to reduce intracerebral hemorrhage; generalized endotracheal anesthesia with stimulator-proven pharmacologic paralysis to prevent patient movement; the use of as few probes as possible; dose modification of thermal treatment to avoid collateral damage to surrounding tissue; and use of short 3 mm diffusing tip fibers to limit the ablation in planes outside the visualized treatment plane and when structures do not have intervening CSF spaces to act as heat sinks.

Outcomes

There is limited long-term data regarding Engel class outcomes for pediatric patients undergoing MRgLITT. Follow-up intervals vary widely between published case series. In the 127 patients reported, 57.5% of the patients experienced complete remission of their seizures [13]. For HH, 78% of patients reported Engel Class I outcome at 12 months [23]. Only a minority of patients, 6.3%, had no effect on seizures at all. Several authors reported that the therapeutic effect on seizures occurred immediately after the procedure, although "running down" phenomenon of gradual seizure reduction over the first year postoperatively has also been described.

Cognitive outcome studies in pediatrics are rare and difficult to standardize. There are no studies with direct evaluation of cognitive function of children undergoing LITT for epilepsy. Hoppe and Helmstaedtler, in a review of LITT for epilepsy in children, noted that subjectively no cognitive decline and mild improvement occurred in the reports that mentioned cognitive outcome at all [13]. In the adult ablation literature, cognitive studies have mainly focused on temporal lobe epilepsy patients and functions dependent on extra-mesial temporal lobe structures such as naming, verbal fluency, object, and person recognition. Preliminary data suggest MR-guided stereotactic laser ablation may offer a significantly better cognitive outcome than open resection due to the fact there is more focal tissue ablation with less collateral damage to surrounding structures [59, 60]. Stereotactic laser amygdalohippocampotomy appears to have better outcome than open resection for several functions dependent on extra-mesial temporal lobe structures including category-related naming, verbal fluency, and object/familiar person recognition [59]. Episodic, declarative verbal memory can decline following stereotactic laser amygdalohippocampotomy, although early findings suggest comparable or even superior outcomes compared with open resection [61].

Conclusions

MRgLITT has become an established alternative to open surgical resective surgery in the management of pediatric intractable epilepsy. Laser ablation offers comparable outcomes to resective surgery, with a reduction in surgical morbidity, particularly in deep lesions or those in eloquent brain. Adoption of this technical approach into established epilepsy surgery centers is facilitated by the incorporation of workflows from the fields of movement disorder and tumor surgery. This relatively new approach will greatly benefit from future investigation into optimal patient selection, technological improvements in laser power and application, and the understanding of the thermodynamics of the brain. Multicenter prospective trials with standard pre-operative protocols are needed to guide candidate selection so that MRgLITT is performed uniformly, safely, and optimally and so that outcomes and complications can be reported and analyzed accurately.

References

1. Edelvik A, Rydenhag B. Long term outcomes of epilepsy surgery in Sweden. Neurology. 2013.
2. Spencer S, Huh L. Outcomes of epilepsy surgery in adults and children. Lancet Neurol. 2008.
3. Russ SA, Larson K, Halfon N. A national profile of child- hood epilepsy and seizure disorder. Pediatrics. 2012;129:256–64.
4. Ramey WL, Martirosyan NL, Lieu CM, Hasham HA, Lemole GM Jr, Weinand ME. Current management and surgical outcomes of medically intractable epilepsy. Clin Neurol Neurosurg. 2013;115:2411–8.
5. Pindrik J, Hoang N, Smith L, et al. Preoperative evaluation and surgical management of infants and toddlers with drug-resistant epilepsy. Neurosurg Focus. 2018;45:1–9.
6. Guldvog B, Loyning Y, Hauglie-Hanssen E, et al. Surgical treatment for partial epilepsy among Norwegian children and adolescents. Epilepsia. 1994;35:554–65.
7. Rydenhag B, Silander HC. Complications of epilepsy surgery after 654 procedures in Sweden, September 1990-1995: a multicenter study based on the Swedish National Epilepsy Surgery Register. Neurosurgery. 2001;49:51–7.

8. Lewis EC, Weil AG, Duchowny M, et al. MR-guided laser interstitial thermal therapy for pediatric drug-resistant lesional epilepsy. Epilepsia. 2015;56:1590–8.
9. Kahn T, Bettag M, Ulrich F, Schwarzmaier HJ, Schober E, Furst G, Modder U. MRI-guided laser-induced interstitial thermotherapy of cerebral neoplasms. J Comput Assist Tomogr. 1994;18(4):519–32.
10. Bown S. Phototherapy in tumors. World J Surg. 1983;7:700–9.
11. Sugiyama K, Sakai T, Fujishima I, et al. Stereotactic interstitial laser-hyperthermia using Nd-YAG laser. Stereotact Funct Neurosurg. 1990;54:501–5.
12. Curry DJ, Gowda A, McNichols RJ, et al. MR-guided stereotactic laser ablation of epileptogenic foci in children. Epilepsy Behav. 2012;24:408–14.
13. Hoppe C, Helmstaedter C. Laser interstitial thermotherapy (LiTT) in pediatric epilepsy surgery. Seizure: Eur J Epilepsy. 2018; https://doi.org/10.1016/j.seizure.2018.12.010.
14. Sharma JD, Seunarine KK, Tahir MZ, Tisdall MM. Accuracy of robot-assisted versus optical frameless navigated stereoelectroencephalography electrode placement in children. J Neurosurg Pediatr. 2019;23(3):297–302.
15. Dhawan S, He Y, Bartek J Jr, Alattar AA, Chen CC. Comparison of frame-based versus frameless intracranial stereotactic biopsy: systematic review and meta-analysis. World Neurosurg. 2019;127:607–16.
16. Pruitt R, Gamble A, Black K, Schulder M, Mehta AD. Complication avoidance in laser interstitial thermal therapy: lessons learned. J Neurosurg. 2017;126(4):1238–45.
17. Cobourn K, Fayed I, Keating RF, Oluigbo CO. Early outcomes of stereoencephalography followed by MR-guided laser interstitial thermal therapy: a paradigm for minimally invasive epilepsy surgery. Neurosurg Focus. 2018;45:1–9.
18. McNichols RJ, Gowda A, Kangasniemi MK, Bankson JA, Price RE, Hazle JD. MR-thermography based feedback control of laser interstitial thermal therapy at 980nm. Laser Surg Med. 2004;34:48–55.
19. Tovar-Spinoza Z, Carter D, Ferrone D, et al. The use of MRI-guided laser-induced thermal ablation for epilepsy. Childs Nerv Syst. 2013;29:2089–94.
20. Schwabe B, Kahn T, Harth T, et al. Laser-induced thermal lesions in the human brain: short and long-term appearance on MRI. J Comput Assist Tomogr. 1997;21:818–25.
21. Tiwari P, Danish SF, Madabhushi A. Identifying MRI markers to evaluate early treatment related changes post laser ablation for neurologic disorders: preliminary findings. PLoS One. 2014;9(12):e114293.
22. Schober R, Bettag M, Sabel M, et al. Fine structure of zonal changes in experimental Nd:YAG laser induced-interstitial hyperthermia. Lasers Surg Med. 1993;13:234–41; Lagman C, Chung LK, Pelargos PE, et al. Laser neurosurgery: a systematic analysis of magnetic resonance-guided laser interstitial thermal therapies. J Clin Neurosci. 2017;36:20–6.
23. Curry DJ, Raskin J, Ali I, Wilfong AA. MR-guided laser ablation for the treatment of hypothalamic hamartomas. Epilepsy Res. 2018;142:131–4.
24. Gadgil N, Lam SK, Pan IW, LoPresti M, Wagner K, Ali I, Wilfong A, Curry DJ. Staged MR-guided laser interstitial thermal therapy for hypothalamic hamartoma: analysis of ablation volumes and morphological considerations. Neurosurgery. 2019:nzy 378. https://doi.org/10.1093/nrutos/nyz378.
25. Ng Y, Rekate HL, Prenger EC, et al. Transcallosal resection of hypothalamic hamartoma for intractable epilepsy. Epilepsia. 2006;46:1192–2012.
26. Ng YT, Rekate HL, Prenger EC, Wang NC, Chung SS, Feiz-Erfan I, Johnsonbaugh RE, Varland MR, Kerrigan JF. Endoscopic resection of hypothalamic hamartomas for refractory symptomatic epilepsy. Neurology. 2008;70(17):1543–8.
27. Wiebe S, Blume WT, Girvin JP, Eliasziw M. A randomizaed controlled trial for surgery for temporal lobe epilepsy. NEJM. 2001;345(5):311–8.
28. Elliott CA, Broad A, Narvacan K, Steve TA, Snyder T, Urlacher J, et al. Seizure outcome in medically refractory pediatric temporal lobe epilepsy: selective amygdalohippocampectomy versus anterior temporal lobectomy. J Neurosurg Peds. 2018;22(3):276–82.
29. Gross RE, Stern MA, Willie JT, Fasano RE, Saindane AM, Soares BP, Pedersen NP, Drane DL. Stereotactic laser amygdalohippocampectomy for mesial temporal lobe epilepsy. Ann Neurol. 2018;83(3):575–87.
30. Willie JT, Laxpati NG, Drane DL, Gowda A, Appin C, Hao C, Brat DJ, Helmers SL, Saindane A, Nour SG, Gross RE. Real-time magnetic resonance-guided stereotactic laser amygdalohippocampectomy for mesial temporal lobe epilepsy. Neurosurgery. 2014;74(6):569–84.
31. Wu C, Boorman DW, Gorniak RJ, Farrell CJ, Evans JJ, Sharan AD. Effects of anatomic variations on the stereotactic laser amygdalohippocampectomy and proposed protocol for trajectory planning. Neurosurgery. 2015;(Suppl 2):345–56.
32. Jermakowicz WJ, Kanner AM, Sur S, Bermudez C, D'Haese PF, Kolcun JPG, et al. Laser thermal ablation or mesial temporal lobe epilepsy: analysis of ablation volumes and trajectories. Epilepsia. 2017;58(5):801–10.
33. Youngerman BE, Oh JY, Anbarasan D, Billakota S, Casadei CH, Corrigan EK, et al. Laser ablation is effective for temporal lobe epilepsy with and without mesial temporal sclerosis if hippocampal seizure onsets are localized by stereoencephalography. Epilepsia. 2018;59(3):595–606.
34. Weiner HL, Carlson C, Ridgway EB, Zaroff CM, Miles D, LaJoie J, Devinsky O. Epilepsy surgery in young children with tuberous sclerosis: results of a novel approach. Pediatrics. 2006;117(5):1494–502.
35. Connelly MB, Hendson G, Steinbok P. Tuberous sclerosis complex: a review of the management of epilepsy with emphasis on the surgical aspects. Childs Nerv Sys. 2006;22(8):896–908.

36. Lewis EC, Weil AG, Duchowny M, Bhatia S, Rageb J, Miller I. MR-guided laser interstitial thermal therapy for pediatric drug-resistant epilepsy. Epilepsia. 2015;56(10):1590–8.
37. Schmitt FC, Voges J, Buentjen L, Woermann F, Pannek HW, Skalej M, Heinze HJ, Ebner A. Radiofrequency lesioning of epileptogenic perventricular nodular heterotopia: a rational approach. Epilepsia. 2011;52(9):e101–5.
38. Thompson SA, Kalamangalam GP, Tandon N. Intracranial evaluation and laser ablation for epilepsy in periventricular nodular heterotopia. Seizure. 2016;41:211–6.
39. Miandola L, Mia RF, Fancione S, Pellicia V, Gozzo F, Sartoi I, Nobili L, Cardinale F, Cossu M, Meletti S, Tassi L. Stereo-EEG: diagnostic and therapeutic tool for periventricular nodular heterotopia. Epilepsia. 2017;58(11):1962–71.
40. Esquenazi Y, Kalamangalam GP, Slater JD, et al. Stereotactic laser ablation of epileptogenic periventricular nodular heterotopia. Epilepsy Res. 2014;108:547–54.
41. Perry MS, Donahue DJ, Malik SI, Keator CG, Hernandez A, Reddy RK, Perkins FF, Lee MR, Clarke DF. Magnetic resonance imaging-guided laser interstitial thermal therapy as the treatment for intractable insular epilepsy in children. J Neurosurg Pediatr. 2017;20(6):575–82.
42. Hale AT, Sen S, Haider AS, Perkins FF, Clarke DF, Lee MR, Tomycz LD. Open resection versus laser interstitial thermal therapy for the treatment of pediatric insular epilepsy. Neurosurgery. 2019;85:e730–6.
43. McCracken DJ, Willie JT, Fernald B, et al. Magnetic resonance thermometry-guided stereotactic laser ablation of cavernous malformations in drug-resistant epilepsy: imaging and clinical results. Oper Neurosurg. 2016;12:39–48.
44. Willie JT, Malcolm JG, Stern MA, Lowder LO, Neill SG, Cabaniss BT, Drane DL. Safety and effectiveness of stereotactic laser ablation for epileptogenic cerebral cavernous malformations. Epilepsia. 2019;60(2):220–32.
45. Oguni H, Andermann F, Gotman J, Olivier A. Effect of anterior callosotomy on bilateral synchronous spike and wave and other EEG discharges. Epilepsia. 1994;35(3):505–13.
46. Tanriverdi T, Olivier A, Poulin N, Andermann F, Dubeau F. Longer-term seizure outcome after corpus callosotomy: a retrospective analysis of 95 patients. J Neurosurg. 2009;110(2):332–42.
47. Dulce A, Curry DJ, Wilfong AA. Corpus Callosotomy by laser ablation in a pediatric patient. Poster session presented at: American Epilepsy Society Annual Meeting, 2014; Seattle, WA.
48. Karsy M, Patel DM, Halvorson K, Mortimer V, Bollo RJ. Anterior two thirds corpus callosotomy via stereotactic laser ablation. Neurosurg Focus. 2018;44(VideoSuppl2):V2.
49. Palma AE, Wicks RT, Popli G, Couture DE. Corpus callosotomy via laser interstitial thermal therapy: a case series. JNS Pediatrics. 2019;23:303–7.
50. Roland JL, Akbari SHA, Salehi A, Smyth MD. Corpus Callosotomy performed with laser interstitial thermal therapy. J Neurosurg. 2019;13:1–9.
51. Lehner KR, Yeagle EM, Argyelan M, et al. Validation of corpus callosotomy after laser interstitial thermal therapy: a multimodal approach. JNS. 2018;1:1–11.
52. Huang Y, Yecies D, Bruckert L, Parker JJ, Ho AL, Kim LH, et al. Stereotactic laser ablation for completion corpus callosotomy. J Neurosurg Pediatr. 2019;24:433–41.
53. Bower RS, Wirrell E, Nwojo M, Wetjen NM, Marsh WR, Meyer FB. Surgical outcomes after corpus callosotomy for drop attacks. Neurosurgery. 2013;73(6):993–1000.
54. Waseem H, Osborn KE, Schoenberg MR, et al. Laser ablation therapy: an alternative treatment for medically resistant mesial temporal lobe epilepsy after age 50. Epilepsy Behav. 2015;51:152–7.
55. Kuo CH, Feroze AH, Poliachik SL, Hauptman JS, Novonty EJ Jr, Ojemann JG. Laser ablation therapy for pediatric patients with intracranial lesions in eloquent regions. World Neurosurg. 2019;121:e191–9.
56. Barber SM, Tomycz L, George T, Clarke DF, Lee M. Delayed intraparenchymal and intraventricular hemorrhage requiring surgical evacuation after MR-guided laser interstitial thermal therapy for lesional epilepsy. Stereotact Funct Neurosurg. 2017;95(2):73–8.
57. Du XV, Gandhi SV, Rekate HL, Mehta AD. Laser interstitial thermal therapy: a first line treatment for seizures in hypothalamic hamartoma? Epilepsia. 2017;58(Suppl 2):77–84.
58. Zubkov S, Del Bene VA, MacAllister WS, Shepard TM, Devinsky O. Disabling amnestic syndrome following stereotactic laser ablation of hypothalamic hamartoma in a patient with a prior temporal lobectomy. Epilepsy Behav Case Rep. 2015;4:60–2.
59. Drane DL. MRI-guided stereotactic laser ablation for epilepsy surgery: promising preliminary results for cognitive outcome. Epilepsy Res. 2018;142:170–5.
60. Kang JY, Wu C, Tracy J, et al. Laser interstitial thermal therapy for medically intractable mesial temporal lobe epilepsy. Epilepsia. 2016;57:324–34.
61. Cajigas I, Kanner AM, Ribot R, Casabella AM, Mahavadi A, Jermakowicz W, Sur S, Millan C, Saporta A, Lowe M, Velez-Ruiz N, Rey G, Ibrahim GM, Ivan ME, Jagid JR. Magnetic resonance-guided laser interstitial thermal therapy for mesial temporal epilepsy: a case series of outcomes and complications at 2 year follow-up. World Neurosurg. 2019;126:e1121–9.

LITT for Spine Tumors

12

Rafael A. Vega, Dhiego C. A. Bastos, and Claudio E. Tatsui

Introduction

Metastatic epidural spinal cord compression (ESCC) remains a significant source of pain and morbidity impairing the quality of life in individuals with cancer [1]. Approximately 40% of patients with a systemic malignancy will develop spinal metastases, and up to 10% present with symptomatic spinal cord compression [2]. The most common initial symptom is pain, although neurological dysfunctions including weakness, gait instability, loss of sphincter control, or sensory deficits are frequently observed. Not all tumors exhibit the same predilection for bone; the most common metastatic lesions include prostate, lung, and breast carcinoma followed by lymphoma, renal cell carcinoma (RCC), and multiple myeloma. The distribution of metastases along the spinal axis reflects the relative bone mass of each segment and the regional blood flow, with the highest number found within the thoracic spine (60%) followed by the lumbosacral (25%) and cervical spine (15%). Multiple synchronous sites of disease along the spinal column are common and should be considered during the evaluation and treatment of these patients.

As the survival of individuals with metastatic cancer continues to improve from advancements in radiation and systemic therapy, the burden of spinal metastases continues to grow. Treatment of these metastatic lesions is fundamentally palliative, focused on neurologic preservation, restoration of spinal stability, pain relief, and durable local tumor control [3]. Due to the palliative intent of therapy, surgical intervention must have minimal morbidity and low complications. Unfortunately, patients with metastatic disease frequently have multiple medical comorbidities in the face of progressive systemic disease and the impact of surgery on the patient's oncological management and quality of life and must be taken into account. Clinical management of these patients is multidisciplinary at its core, requiring discussions between surgeons, radiologists, medical-oncologists, and radiation-oncologists. The demands on the surgeon are to provide effective surgical intervention associated with minimal disruption to systemic therapy.

The management of spinal metastatic disease associated with ESCC has evolved over the past 40 years. Historically patients were treated with high-dose glucocorticoids and fractionated radiation therapy [4]. In the 1980s, initial efforts at surgical intervention focused on laminectomies for posterior-only decompression of the spinal canal, which were commonly associated with

R. A. Vega (✉)
Division of Neurosurgery, Beth Israel Deaconess Medical Center, Harvard Medical School, Boston, MA, USA
e-mail: rvega@bidmc.harvard.edu

D. C. A. Bastos · C. E. Tatsui
Department of Neurosurgery, The University of Texas MD Anderson Cancer Center, Houston, TX, USA

V. L. Chiang et al. (eds.), *Laser Interstitial Thermal Therapy in Neurosurgery*,
https://doi.org/10.1007/978-3-030-48047-9_12

worsened neurologic and functional outcomes compared with radiation alone. In retrospect, this surgical strategy had several disadvantages including lack of reconstitution of the load bearing capacity of the spine, disruption of the posterior tension band leading to progressive spinal instability, and failure to decompress the spinal cord as the tumor arising from the vertebral body was not removed. In subsequent years, functional outcomes and local control have improved due to further developments in spine instrumentation and popularization of posterolateral, lateral, and anterior approaches allowing circumferential decompression of the spinal canal and revitalization of the role of surgery in the management of spine metastases. In a pivotal study by Patchell et al. [5], individuals with solitary/symptomatic metastatic ESCC were randomized to circumferential decompression/stabilization followed by conventional external beam radiation therapy (cEBRT) or cEBRT alone. Patients in the surgical cohort experienced maintenance and significant improvement in rates of recovery for ambulation, functional performance, pain control, urinary continence, and survival. This study established that appropriately selected surgery offers a meaningful improvement in quality of life with acceptable morbidity when added to radiation therapy.

Tumor histology has an impact on the efficacy of radiation therapy for tumor control. Traditionally, tumors were classified as either radiation-sensitive or radiation-resistant based on their response to conventional fractionated radiation therapy [6]. Radiosensitive histologies include lymphoma, plasmacytoma, multiple myeloma, germ cell tumors, breast cancer, and prostate carcinomas. In response to cEBRT, these tumors have a reported 2-year local control rate of up to 80–90%. In contrast, radioresistant malignancies such as non-small cell lung, thyroid, hepatocellular, colorectal, RCC, melanoma, and sarcomas exhibit much poorer 2-year local control, as low as 30% following radiation therapy.

Advances over the last decade in the development of image-guided stereotaxy and radiation therapy have enabled the delivery of highly conformal and tumoricidal doses of radiation as either a single treatment or hypofractionated (2 to 5) regimen to the spine. Spinal stereotactic radiosurgery (SSRS) delivers radiation to a contoured volume to cover a specific target with a steep dose gradient that spares surrounding tissues such as the spinal cord, nerves, visceral organs, or esophagus. However, despite the highly contoured nature of radiation dose delivery, the predicted falloff of radiation must remain within the constraints of spinal cord and surrounding vital structures tolerance. The biologically effective dose of radiation delivered with SSRS is estimated to be approximately three times greater than with cEBRT, leading to more extensive DNA damage, irrecoverable endothelial damage, and potentially enhanced immune environment with T-cell activation and pro-inflammatory cytokines [7]. Radiosurgery effectively overcomes the previously held histology specific radioresistance, with 12-month local control rates of 85% in even notoriously difficult tumor types such as RCC [8]. Furthermore, due to the conformality of SSRS and relative sparing of surrounding tissues, it is possible to use as a salvage therapy in the setting of prior cEBRT failures for local recurrence [9, 10].

While SSRS is an effective and reliable treatment option for spinal metastases, radiation-induced spinal cord injury remains an important concern [11]. A large multicenter study following over 1000 individuals treated with SSRS found only 6 patients who developed radiation-induced myelopathy, keeping to the widely acceptable dose maximum of 14 Gy to the spinal cord. In the setting of high-grade epidural compression, the toxicity-limiting dose of the spinal cord or cauda equina requires adjustment to the prescribed treatment dose, potentially undertreating the epidural tumor and compromising local control. Lovelock et al. [12] found that local treatment failure was associated with tumors that received less than 15 Gy to any point in the treatment planning volume. A less aggressive surgical strategy proposed by Bilksy et al. designed to stabilize the spine and remove just the epidural tumor, enough to create separation between the residual lesion and the spinal cord to allow a safe margin to deliver a cytotoxic dose of radiation in the setting

of epidural compression, is commonly referred as separation surgery [13, 14]. This approach combined with high-dose single or hypofractionated SSRS is less morbid than attempted gross total resection and is associated with shorter operative times and better tumor control than conventional external beam radiation in cases of ESCC from radioresistant histologies. The aim of surgery in the era of SSRS is (1) neurologic decompression, (2) create separation between tumor and the spinal cord, and (3) provide spinal stabilization as indicated. The extent of tumor resection is not crucial to local control as long as there is an adequate distance between the tumor margin and spinal cord to deliver tumoricidal doses of SSRS, as described above. Separation surgery followed by SSRS represents a paradigm shift in spinal oncology and has dramatically improved treatment of oligometastatic disease.

The ideal surgical intervention for spinal metastases for achieving local tumor control would allow for fast recovery, minimize postoperative pain and morbidity, and limit delays in initiating or interrupting systemic therapies directed at the primary tumor. These notions led to the conception of spinal laser interstitial thermal therapy (sLITT) at the University of Texas MD Anderson Cancer Center in 2013. By its nature, sLITT is a percutaneous minimally invasive procedure that results in immediate ablation of the epidural tumor resulting in a durable decompression of the spinal cord and facilitates an immediate transition to radiotherapy. The indications, patient selection, technical considerations, and nuances of sLITT are discussed below.

Indications for Spinal Laser Interstitial Thermal Therapy

Individuals with metastatic cancer harbor a number of medical comorbidities and are frequently deconditioned. Malnutrition, chronic anemia, chronic steroid use, systemic thromboses (DVT or PE), and prior radiation complicate open surgical intervention. Furthermore, these patients commonly have rapidly progressive disease at other sites in addition to their spine requiring concurrent and systemic therapy with cytotoxic or targeted agents. For these individuals, separation surgery may lead to significant morbidity. Percutaneous techniques have been developed as an alternative to open surgical procedures in certain scenarios to decrease morbidity, limit disruption of systemic therapy or anticoagulation, shorten hospital admissions, decrease pain, and minimize blood loss or transfusions. Currently used methods include CT-guided cryo- or radiofrequency ablation of vertebral tumors [15–17]. Injury to the spinal cord or nerve roots has been documented with radiofrequency ablation, and in animal studies, placement of the electrode immediately adjacent to the posterior cortex of the vertebral body or pedicle led to neural injury [18, 19]. Concern for neurologic injury and the inability to monitor tissue injury in real-time has limited the adoption of these techniques for the ablation of epidural tumors in close proximity to the neural elements. Laser interstitial thermal therapy (LITT) is an alternative method of percutaneous ablation that has seen widespread adoption in the treatment of intracranial tumors and other pathologies [20, 21]. Using this technique, a small laser probe is inserted into the lesion using stereotactic guidance. Energy is transferred from the laser into the surrounding tissue producing a thermal injury sufficient to lead to tumor cell death and coagulative necrosis. The amount of tissue damage is based on a thermal response model in which there is a correlation between temperature, duration of exposure, and the ensuing damage. An advantage of this technology over others is that an intraoperative MRI (iMRI) is used to monitor in real time the heat generation and distribution within a particular region. Using a modified LITT-based approach for the spine, epidural tumors in close proximity to the thecal sac and spinal cord can be ablated while ensuring that there is no thermal injury to the spinal cord (Fig. 12.1) [22–24]. Regions of high-grade epidural compression can safely be ablated using sLITT. This treatment paradigm, similar to separation surgery, requires adjuvant SSRS following laser ablation for effective tumor control. Similar to circumferential decompression, the region of

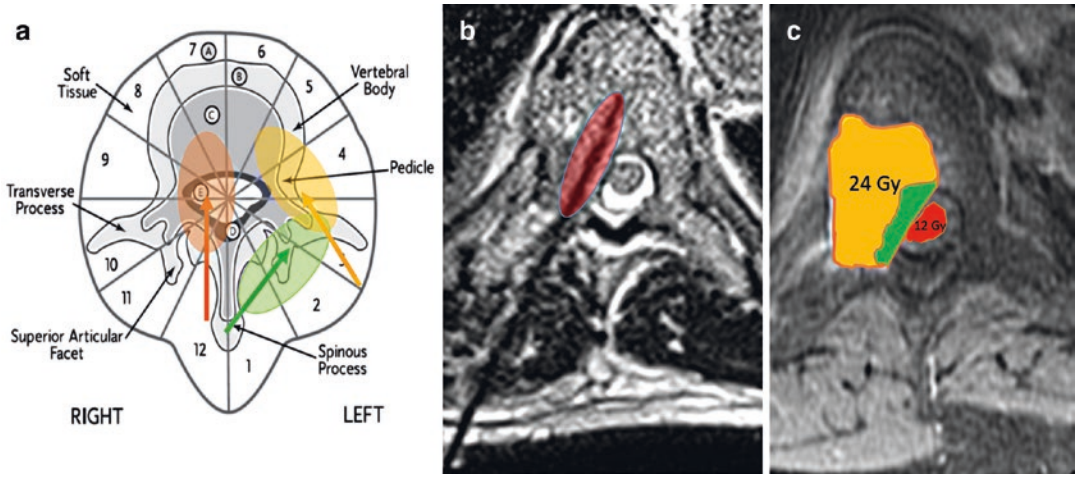

Fig. 12.1 (**a**) Diagram demonstrating the typical approaches (i.e., oblique transpedicular, *yellow arrow*) for spinal laser interstitial thermotherapy (SLITT) based on the location of the metastatic lesion in relation to the spinal cord. (**b**) The ideal distance between the fiber and dura is 5–7 mm, while each fiber covers a 10–12 mm radius. (**c**) Representative illustration of the targeted dose distributions for spine stereotactic radiosurgery after SLITT is preformed: *orange*, at-risk contiguous bone; *green*, area treated by SLITT; *red*, spinal cord

necrotic tissue following thermal ablation creates a separation between viable tumor and the spinal cord facilitating effective doses of SSRS. For individuals that also have spinal instability secondary to pathologic fracture, a percutaneous posterior spinal stabilization procedure can be performed following the LITT treatment in the same setting [25].

Patient Selection

sLITT is a minimally invasive alternative to open circumferential decompression for patients with epidural compression that are candidates for radiosurgery [22, 23]. High-grade epidural compression is typically defined using the Bilsky Scale [13] and classified as grade 1c or higher. In these individuals, the degree of epidural compression would limit treatment with an effective radiosurgery dose. Additional considerations for patient selection include (1) medical comorbidities; (2) need to continue or rapidly resume systemic therapy; (3) normal neurologic exam; (4) ESCC location within the upper cervical, C1–2, or thoracic spine, T2–12; and (5) no contraindications to MRI (e.g., pacemaker or neurostimulator). For patients in which MRI is contraindicated, sLITT cannot be performed without MRI thermography. Similarly, existing instrumentation at the level of ablation typically creates metallic artifact that impairs the accuracy of MRI thermography and precludes its use. We have observed an interval of 3–4 weeks between the sLITT treatment and radiographic decompression of the spinal canal. We recommend that individuals presenting with a neurologic deficit undergo surgical decompression as a faster way to decompress the spinal cord; therefore, we have considered presence of neurological deficits a contraindication for sLITT.

Individuals with debilitating thoracic radiculopathy due to foraminal tumor involvement are ideal candidates for laser ablation [24]. The ablation and destruction of tumor within the foramina and associated sensory nerve typically provides complete resolution of the pain. For the same reason, we restrict the use of sLITT to the upper cervical or thoracic spinal segments to avoid unintentional injury to functional motor nerve roots of the cervical and lumbosacral plexus. For lesions of the mid/lower cervical (C3–T1) and throughout the lumbosacral spine, surgical decompression with visualization and complete

decompression of the functional roots is preferred.

As previously discussed, prior conventional radiation therapy and spinal instability are not contraindications to sLITT. In the case of prior radiation, a percutaneous technique such as sLITT is actually more desirable to avoid wound complications. If there is spinal instability, a percutaneous stabilization with cement augmentation of the pedicle screws is frequently performed following the laser ablation [25]. This can be done during the same case while under general anesthesia or as a staged procedure.

A number of metastatic tumors are notoriously vascular. These include RCC, hepatocellular carcinoma, and thyroid carcinoma. Prior to a circumferential decompression, these tumors typically require embolization preoperative in an effort to decrease the amount of blood loss. It has been our experience that such tumors are safely treated with sLITT without the need of preprocedure embolization with only minimal blood loss.

Technical Considerations

At our institution sLITT is performed within an operating room suite equipped with an iMRI. Following induction of general anesthesia, the patient is placed in the prone position with the upper extremities parallel to the body in a manner that is ergonomic to the surgeon and does not interfere with the use of the C-arm fluoroscope or iMRI [26]. Initially, we have used a CT scan of the spine and C-arm for localization and stereotactic placement of the laser fibers [22, 23]. Currently, we are using the iMRI for coregistration and spinal navigation and have found that this can be accomplished with subcentimeter accuracy [23]. Additionally, the MRI provides better spatial resolution of the tumor and its relation to the neural elements for trajectory planning and insertion of the fibers. After final positioning, but prior to registration MRI, skin fiducials are placed on the region of interest in a unique pattern that distinguishes right-left and rostral-caudal (Fig. 12.2a,b). The surgical site above or below the fiducials is prepped and draped, and a

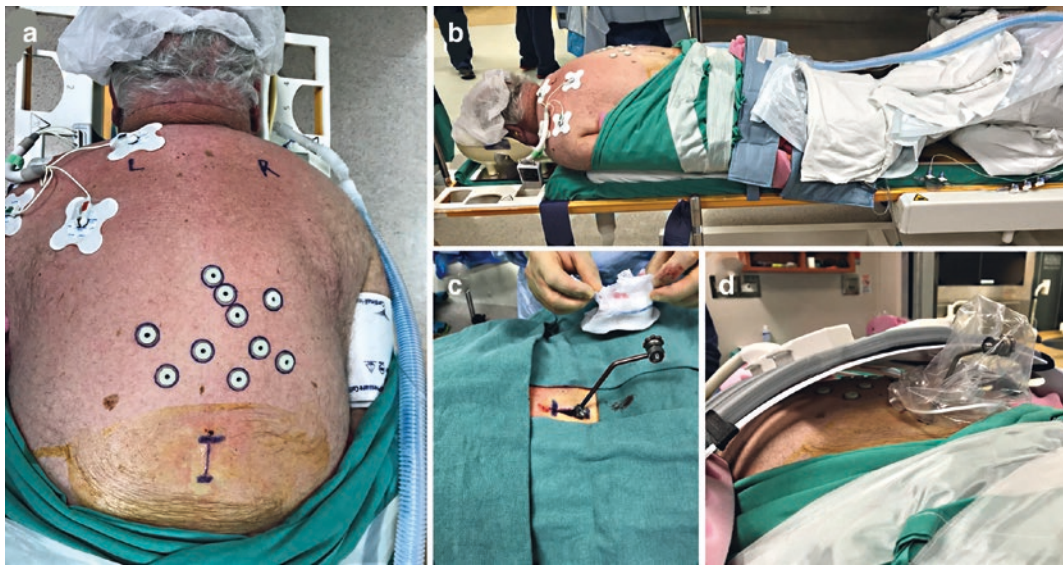

Fig. 12.2 (**a**) Fiducial markers applied in a unique pattern for registration along the dorsal region overlying the tumor. (**b**) Patient in the final prone position on the intraoperative MRI transfer table. (**c**) The skin is prepped and the spinous process clamp is secured. (**d**) Spinal clamp is covered with a sterile plastic bag, and the MRI coil is placed over the plastic fiducial held by a plastic cradle to avoid fiducial displacement

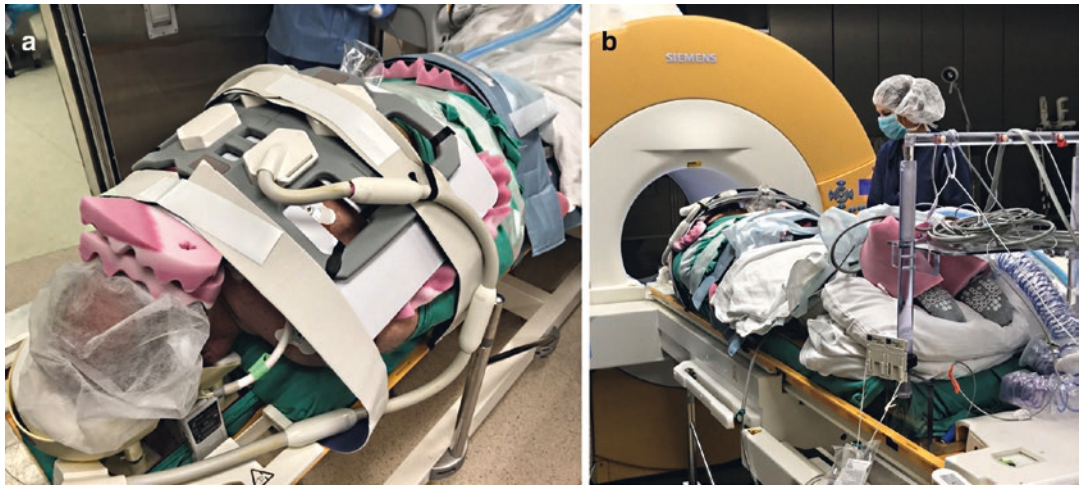

Fig. 12.3 (**a**) The patient is positioned prone with the head placed in a ProneView and arms tucked on each side with foam pads placed throughout. The trunk of the patient is placed over gel rolls to position the spine at a higher level than the arms allowing for clear lateral fluoroscopic images from T3 to the sacrum without interference from the upper extremity skeleton. (**b**) Transferring the patient to the MRI magnet

small incision is made with dissection proceeding to the level of the spinous process. Using subperiosteal dissection, the soft tissues are reflected away from the spinous process, and an MRI-compatible titanium clamp (Medtronic) is secured to a spinous process and covered with a sterile plastic bag (Fig. 12.2c,d). Without displacing the reference array and fiducials, a body matrix coil (Siemens) secured to a plastic cradle is placed over the region of interest, and the patient is positioned within the MRI (Fig. 12.3). A high-resolution T2-weighted image of the segment containing the fiducials (and tumor) is obtained and is used for co-registration and navigation. Following image acquisition, the patient is positioned at a safe distance from the MRI magnet, the sterile plastic bag of the spinous process clamp is removed, and a sterile reference array is attached to the clamp. The registration image series is transferred to a StealthStation S7 system (Medtronic), and co-registration is performed using a point-matching registration with the fiducial markers with a non-sterile navigation probe (Fig. 12.4). The accuracy is confirmed by comparing anatomical landmarks (midline, fiducials, skin surface) to the predicted position of the navigation wand in the inline sagittal and axial reconstructed images in the navigation screen. Significant error will occur if the inline reconstructions are not selected.

Spine navigation using MRI allows for meticulous trajectory and entry point planning with the advantage of easy identification of the spinal cord, tumor, and surrounding cerebrospinal fluid (Fig. 12.4b,c). In our experience we have relied on the Weinstein-Boriani-Biagini tumor classification to select the optimal probe trajectory (Fig. 12.1a) [27]. Typically one of the three trajectories is used based on the location of the epidural disease that is being treated. The most common trajectory is an oblique transpedicular or transforaminal trajectory. This is well-suited to treat disease that is ventral to the spinal cord or canal (zones 4–6 or 7–9). Orthogonal transpedicular or translaminar trajectories can also be used to access different sites of disease intended for treatment. In general the selected trajectory places the laser fiber approximately 6 mm from the dura or thecal sac, and it is assumed that each fiber can achieve a 10 mm diameter of thermal injury. Depending on the extent of disease in the rostral-caudal plane, multiple trajectories may be required to achieve an adequate ablation (Fig. 12.5). We have used up to nine trajectories in a single patient. When planning multiple trajectories, they are placed within 10 mm of one

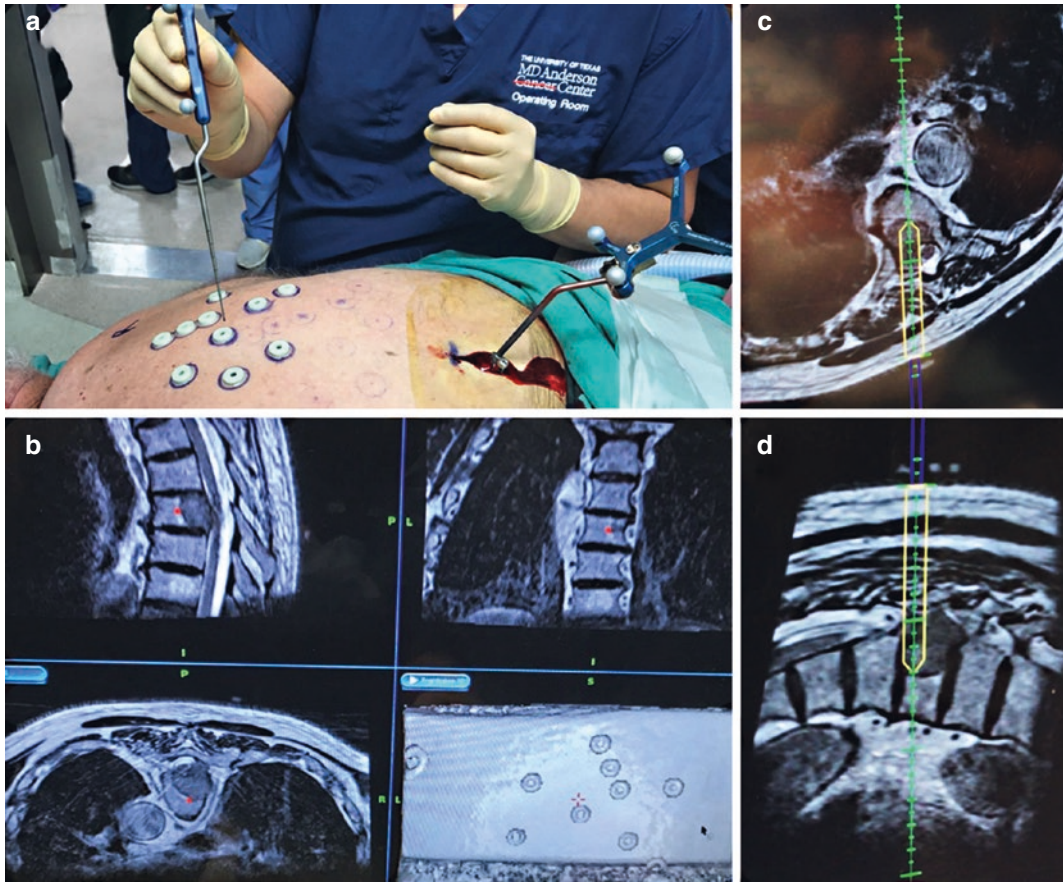

Fig. 12.4 (**a**) Sterile reference array is attached to the clamp, maintain local sterile conditions. Non-sterile probe is used to perform surface matching of fiducials. (**b**) MRI 1 mm axial cuts are obtained and transferred to the standard navigation system for surface registration. (**c**) T2 sequence without contrast imaging is used to verify accuracy inside the fiducials, midline, and the easily palpable spinous processes. Trajectories for placement of the laser catheters and pedicle screws are then marked on the skin in the (**c**) axial and (**d**) sagittal planes

another to ensure that there are no untreated segments between successive ablations. Similarly, bilateral trajectories may be needed to completely treat ventral or lateral epidural disease.

Following selection of the appropriate trajectory(s) and marking of the skin entry point(s), the unsterile fiducials are removed, and the operative field is prepared and draped with standard sterile technique. Special attention is given that draping does not displace the skin and the reference array. A navigated Jamshidi needle (Medtronic) is introduced and the navigation accuracy is again confirmed in easily identifiable landmarks. Small incisions are made at the entry sites and the needle is advanced until it contacts the lamina or other bone surfaces. The C-arm is then used to confirm the location of the Jamshidi needle and verify that the fluoroscopy and spine navigation are commensurate with one another. Next, the Jamshidi is advanced to target depth using navigation. A K-wire is introduced through the Jamshidi needle and exchanged with a 1.65-mm-diameter plastic catheter and stylet (Fig. 12.6). This is repeated in succession for each trajectory. Once all of the cannulas have been inserted (Fig. 12.7), remove the reference array and place sterile towels to cover the skin, allowing exposure of the access cannulas. Each individual access cannula is covered with a sterile plastic bag, and the non-sterile MRI coil is

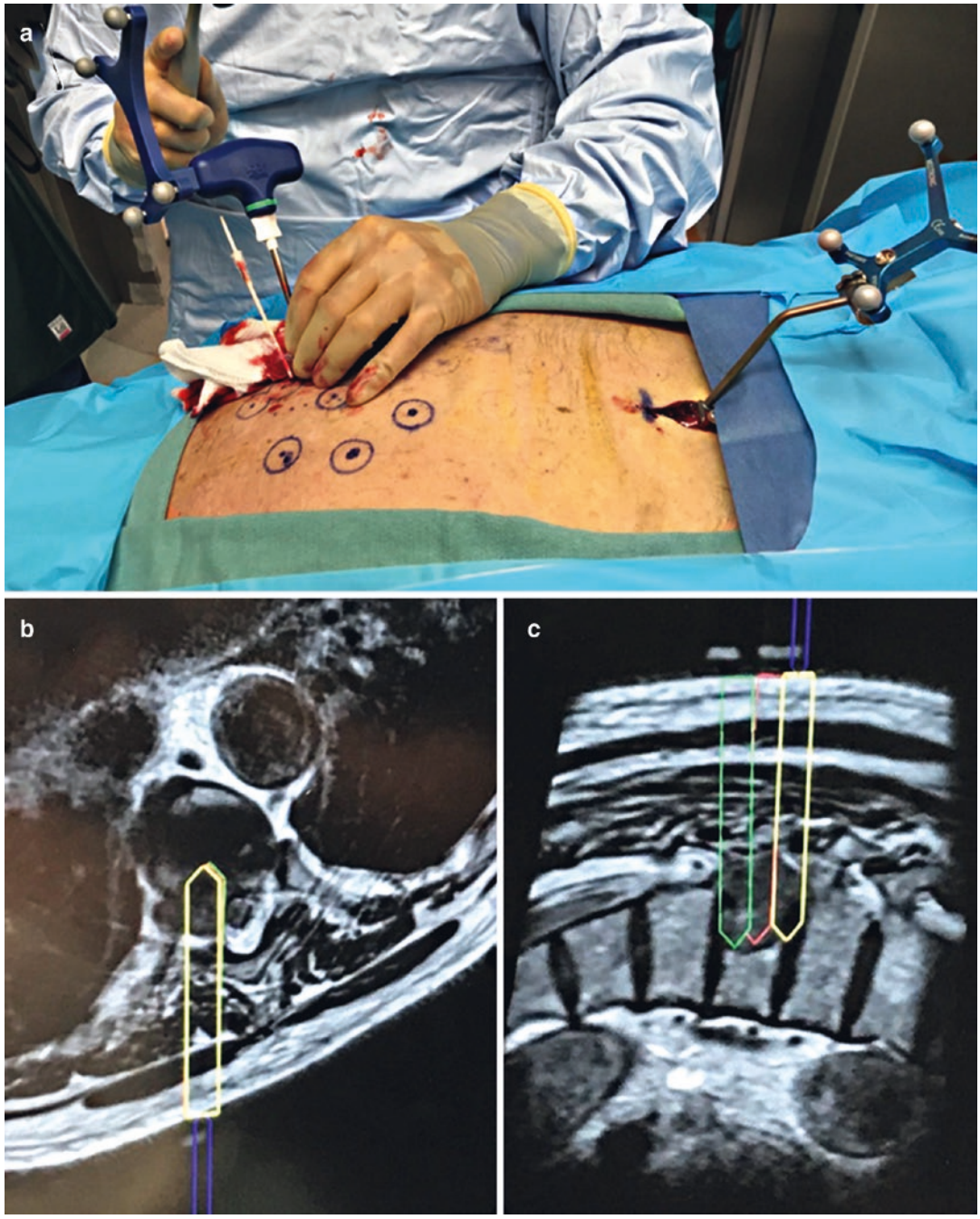

Fig. 12.5 (**a**) Fiducials are removed, the rest of the skin is prepped and draped in the usual sterile fashion. (**b**) Navigated Jamshidi needle is inserted using image guidance, where the diameter of the needle (*yellow*) is increased to position the needle 5–7 mm lateral to the dura. (**c**) This is repeated with multiple trajectories, as needed, to achieve an adequate ablation

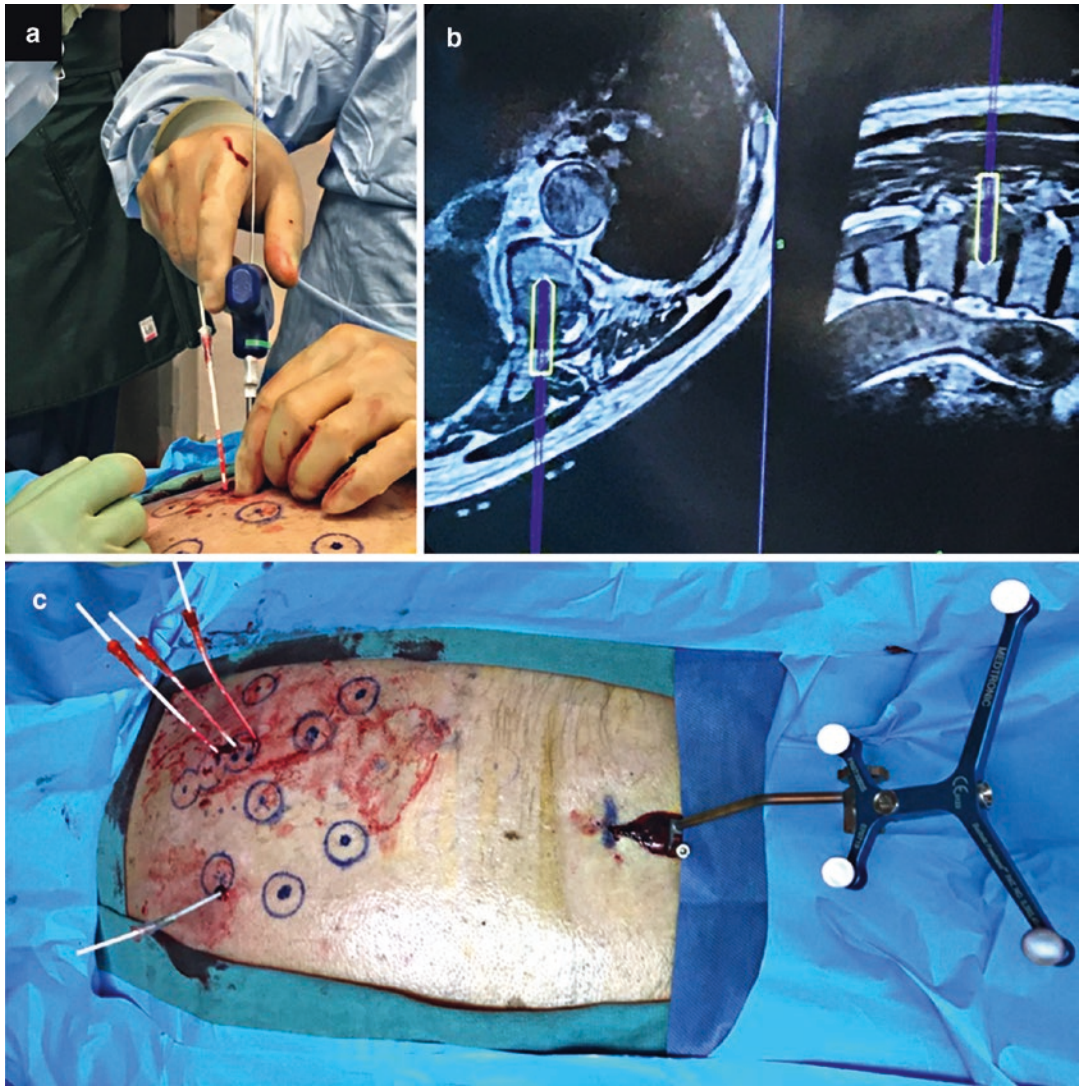

Fig. 12.6 (**a**) K-wires are inserted through the Jamshidi, which is exchanged to a plastic access cannula. A modified plastic introducer is inserted into the plastic cannula to maintain the trajectories (**b**), and additional needles are inserted in tandem to cover the craniocaudal extension of the epidural mass (**c**)

positioned in a way that gives easy access to the plastic bags covering the cannulas. The plastic bags are then removed, without contaminating the access cannulas. Sterile towels are placed over the MRI coil allowing easy access to the cannulas. The patient is transferred to the MRI magnet, and a trajectory localization scan is obtained to confirm the exact axial plane of each access cannula (Fig. 12.8).

The laser fiber consists of a 980-nm diode encased in a catheter that is connected to a 15-W power source (Visualase, Medtronic). A single fiber is introduced into one of the cannulas and advanced to appropriate depth for treatment (Fig. 12.7f). This fiber is subsequently moved to next cannula after each cycle of ablation is completed. MR thermography is based on gradient-echo acquisition and used

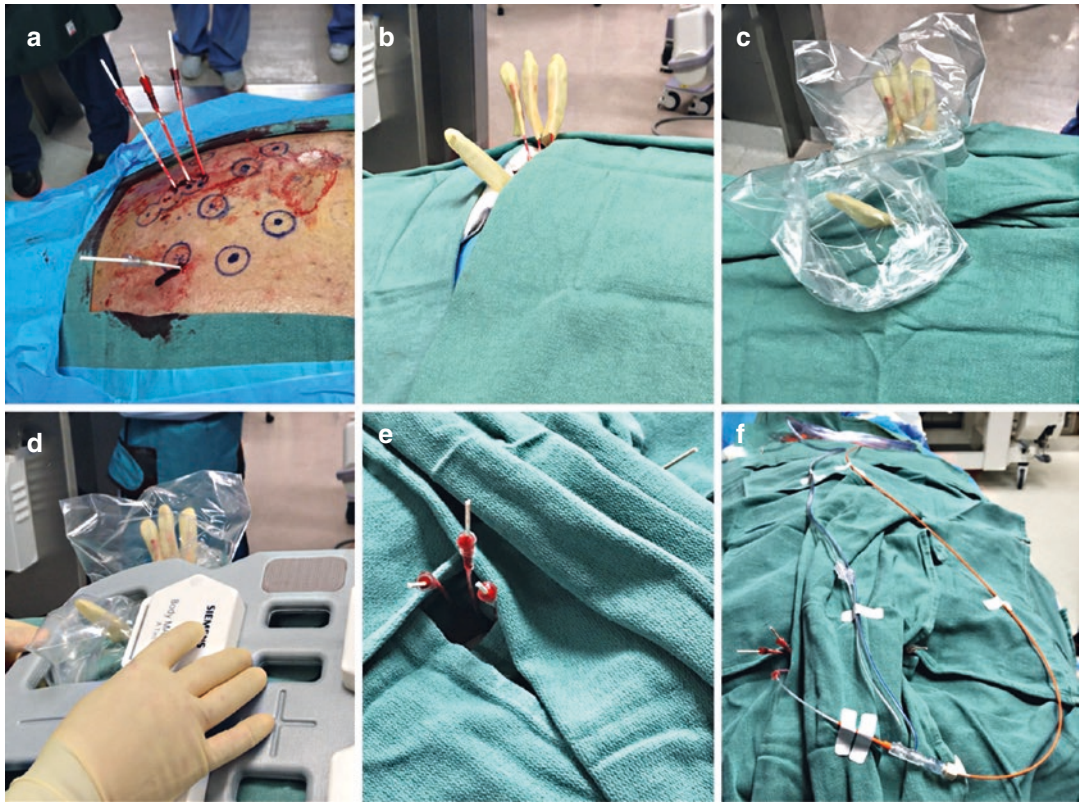

Fig. 12.7 Sequential procedural workflow during the sLITT procedure. (**a**) After the access cannulas are placed, the reference array is removed, and (**b**) sterile towels are placed to cover the exposed areas surround the covered cannulas. (**c**) Sterile plastic bags are placed over the covered access cannulas; (**d**) then the non-sterile MRI coil is positioned over the cannulas in such a way to allow access, for the laser. (**e**) The plastic bags are removed carefully, and sterile towels are again placed over the MRI coil to provide the final level of easy access to the cannulas for the laser ablation. (**f**) The laser probe is then inserted into each cannula, then the patient is transferred back to the MRI magnet, and the trajectory localization scan is obtained to confirm the position of the access cannulas in each plane

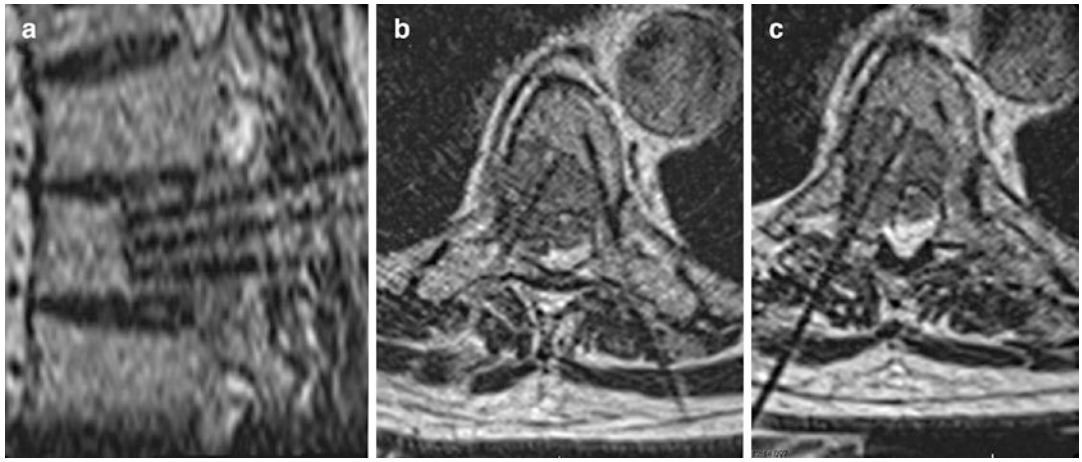

Fig. 12.8 Once the patient is transferred back to the iMRI, a trajectory localization scan is obtained. This MRI T2 sequence is utilized to confirm the exact place for each access cannula in the (**a**) sagittal and (**b,c**) axial planes

throughout the ablation to monitor the heat generated within the tissue. Proton resonance within the tissue is sensitive to temperature, and the difference in phases allows for modeling of the temperature within the exposed tissue. 3-mm slices are acquired every 5 to 6 seconds while the laser is activated. The laser is deactivated when one of the two temperature thresholds are reached. The boundary between dura and tumor is identified and set to an upper temperature limit of 48–50° (Fig. 12.9). A second threshold is set to 90° in the tissue adjacent to the laser fiber to prevent excessive heating of the tumor and tissue carbonization. The thermal maps are sensitive to and degraded by motion. The spine is vulnerable to respirophasic motion and demands that a breath hold be completed during the ablation. Thus, the ablation is performed in cycles in which the laser is active for up to 120 seconds during a breath hold, interrupted by periods of ventilation to allow for adequate oxygenation and recovery from hypercapnia. Typically, the ablation time in total is up to 4 minutes at a single site. The laser fiber is manually advanced or withdrawn as needed to ensure that there is ablation of all of the intended epidural tumor.

After the ablation is complete, the laser fiber and cannulas are removed, and the incisions are closed with an absorbable suture (Fig. 12.10a). To visualize the extent of ablation, a pre- and

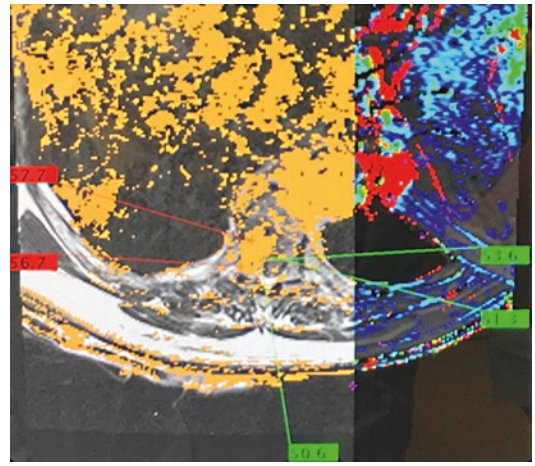

Fig. 12.9 Real-time magnetic resonance thermal imaging for sLITT. A mathematical model of thermal damage is monitored in real time, attained with our imaging software. A carefully monitored ventilator pause is performed by the anesthesiologist during the acquisition of thermal images, where a total of 2 minutes is allowed for each ablation cycle. The T2 image demonstrates real-time heat and temperature monitoring at selected points in the epidural space

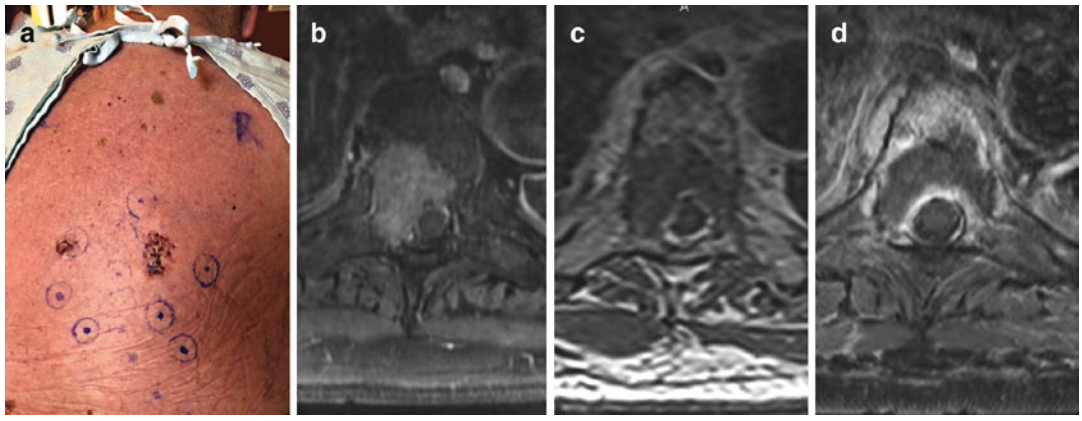

Fig. 12.10 (**a**) After sLITT is performed, closure is performed with absorbable sutures and Dermabond in iMRI suite; then the patient returns to the induction room, repositioned supine, and emerges from anesthesia for extubation. Images obtained from the procedure utilizing iMRI demonstrate the immediate thermal damage from sLITT; (**b**) preoperative T1 with contrast, (**c**) postoperative T1 without contrast revealing a hypointense area corresponding to coagulative necrosis from the ablation. (**d**) After 3 months, postoperative MR imaging reveals the lasting result of our sLITT procedure in conjunction with radiosurgery for achieving durable local control

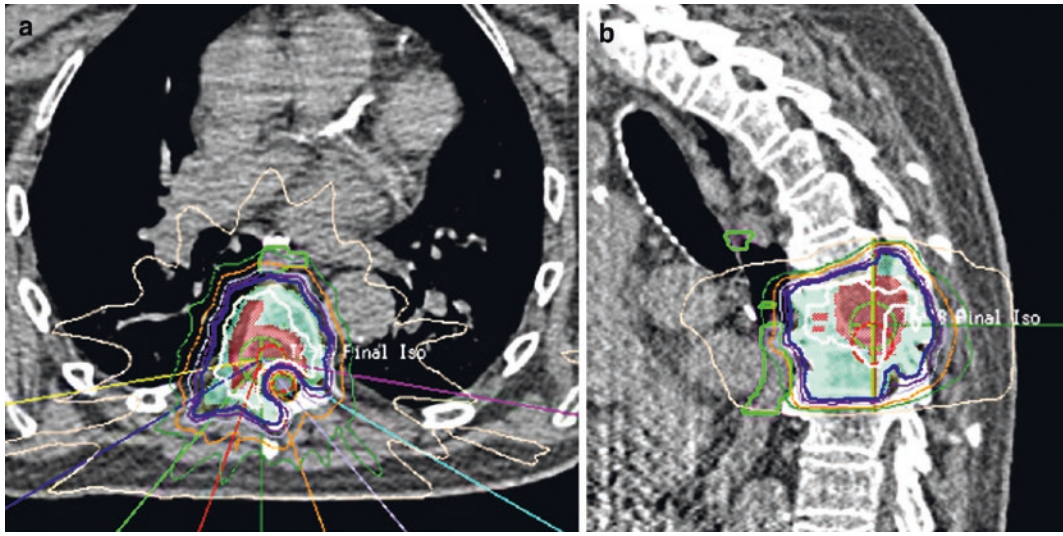

Fig. 12.11 Spine stereotactic radiosurgery (SSRS) is performed following sLITT with the aim of delivering a targeted high dose of radiation to the residual lesion while minimizing the dose to the spinal cord to achieve durable local tumor control. Treatment planning performed using intensity-modulated radiation therapy inverse treatment software. Typical SSRS dosimetry plan in the (**a**) axial and (**b**) sagittal plane

post-contrast T1WI is acquired, again with breath holding. The best way to evaluate the ablated tissue is by performing a subtracted image from the contrast and non-contrast co-planar scans. The region of coagulative necrosis will lack contrast enhancement, which appears as a hypointense or dark area in the subtracted scans (Fig. 12.10c). In our experience this has been an accurate estimation of the ablated volume. For individuals with concomitant spinal instability, a stabilization procedure can be performed under the same anesthetic or as a separate staged surgery. Typically, a percutaneous instrumentation with cement augmentation of the pedicle screws is performed the same day. Once the ablation is completed, the patient is positioned at a safe distance of the MRI magnet, the spinous process clamp is reapplied, and the ink marks of the fiducials are reregistered, allowing image guidance. This is especially helpful in the upper thoracic spine and facilitates the intraoperative workflow. If inaccuracy is verified, we either replace fiducials and repeat the registration scan or use standard fluoroscopic techniques. Rarely we decide to stage the procedure and perform the stabilization part on a separate day using appropriate CT navigation guidance. Generally, our practice is to repeat a MRI of the spine in 6–12 weeks (Fig. 12.10d). If instrumentation is used, a CT myelogram is obtained postoperatively for radiosurgery planning (Fig. 12.11).

Outcomes of sLITT in Facilitating the Treatment of Spine Tumors

In conjunction with radiosurgery, spinal laser interstitial thermal therapy provides effective and durable local tumor control with minimal morbidity. From our initial experience, we reported outcomes of sLITT and SSRS in 19 individuals presenting with radioresistant tumors, the majority of which had progressed despite systemic therapy [22]. Within this cohort seven patients had Bilsky 1c epidural compression, eight had grade 2 compression, and four exhibited grade 3 compression. SSRS was indicated in all subjects for oncologic control but, considering the degree of epidural compression, would have been restricted by toxicity-limiting dose constraints of the spinal cord. sLITT provided a percutaneous alternative to open surgery with the benefit of an abbreviated hospital admission (median of 2 days) and durable tumor control. Progression

was documented in only two patients at 16 and 33 weeks and was ultimately retreated with a subsequent sLITT. Furthermore, there was a statistically significant reduction (22%) in the dimensions of epidural tumor seen at 2 months and improvement in the degree of epidural compression. Pain scores (VAS) were also significantly improved following sLITT. Complications in this series included a transient monoparesis in one patient, wound dehiscence requiring reoperation, and a delayed compression fracture. To date we have performed 110 procedures to treat a variety of tumor histologies. Local tumor progression has been documented at a total of 17 treated sites—15 were in-field recurrences, while 2 were at the treatment margins (unpublished analysis). Median follow-up was 35 weeks for the entire cohort, with time to recurrence measuring a mean of 26 weeks. Approximately one-third of patients also underwent a concomitant stabilization procedure.

From this larger experience, several lessons have emerged. In our current practice, we limit treatment to lesions within the thoracic spine located between T2 and T12 to avoid injury to the cervical or lumbosacral motor nerve roots. Based on the percutaneous nature of the procedure, traversing nerve roots compressed by the epidural tumor cannot be identified and protected. Initial efforts to treat lesions in the upper lumbar spine were complicated by injury to roots at the corresponding level. In addition to level, the presence of a neurologic deficit prior to surgery, however subtle, is an absolute contraindication. Individuals with preexisting deficits have increased potential for neurologic worsening post-ablation. Our series includes a patient treated with mild motor weakness preoperatively and RCC. The procedure itself was uncomplicated and initially well tolerated, but unfortunately the patient had a delayed neurologic decline requiring surgical decompression. Interestingly, review of the pathology obtained from the ablated level at the time of re-operation consisted of necrotic tissue with no viable tumor. A second subject included in this series required an urgent decompression in the setting of a delayed neurologic deficit. In this case the patient was neurologically intact prior to laser ablation but subsequently declined. The patient had received concurrent immunotherapy for RCC, and it was hypothesized that the combination of sLITT and immunotherapy led to a significant immune reaction and edema as these individuals have contraindication to steroids. We do not recommend that individuals treated with immunomodulatory agents presenting with Bilsky 3 degree of spinal cord compression be treated with sLITT. Cases of Bilsky 1c and grade 2 may require special consideration. Similar observations have been made in patients on immunotherapy underlying LITT for cranial tumors that develop severe edema and inflammation.

Although the zone of thermal injury typically measures up to 10 mm in diameter, the ablation is not universally homogenous or predictable. Regions of tumor that are adjacent to spinal fluid, large vessels, or cystic areas are more difficult to treat due to the ability for these structures to dissipate heat and function as a heat sink. Similarly, vascular tumors such as RCC may require longer treatment times and multiple trajectories to properly treat the intended tumor volumes. It has been our experience that a higher volume of tumor ablation per fiber is observed in less vascular tumors like adenocarcinomas (prostate, lung, breast) than highly vascular tumors (thyroid, kidney, liver). Osteoblastic tumors present additional challenges when using sLITT, as highly calcified tissue presents a low MRI signal interfering or decreasing the quality of temperature monitoring by MRI thermography.

Conclusion

Spine laser interstitial therapy is an emerging and minimally invasive method to treat spine metastases. It provides effective and durable local control with minimal morbidity. Compared to other percutaneous techniques, sLITT is unique in offering real-time monitoring of thermal injury. Additional benefits over conventional separation surgery include limited hospital admissions, improved pain control, and minimal blood loss. Furthermore, vascular tumors do not require pre-

operative embolization, and patients with significant medical comorbidities or need for continued systemic therapy can safely be treated. The technology is still early in its development. We expect that future hardware and software improvements facilitate the operative workflow and expand adoption of this technique to other centers. Our experience has been very positive, and we believe that minimal disruption in oncological management, faster recovery, and lower morbidity are current advantages of sLITT over open surgery. A prospective randomized study will be needed to confirm these features and to compare the rates of local control between sLITT and open surgery. In summary, we believe that in selected appropriate cases, sLITT has the potential to replace open surgery allowing a "percutaneous separation surgery" optimizing SSRS and improving outcomes in patients harboring metastatic ESCC.

References

1. Cole JS, Patchell RA. Metastatic epidural spinal cord compression. Lancet Neurol. 2008;7(5):459–66. https://doi.org/10.1016/S1474-4422(08)70089-9.
2. Bach F, Larsen BH, Rohde K, Børgesen SE, Gjerris F, Bøge-Rasmussen T. et al. Metastatic spinal cord compression. Occurrence, symptoms, clinical presentations and prognosis in 398 patients with spinal cord compression. Acta Neurochir. 1990;107(1–2):37–43.
3. Laufer I, Rubin DG, Lis E, Cox BW, Stubblefield MD, Yamada Y, et al. The NOMS framework: approach to the treatment of spinal metastatic tumors. Oncologist. 2013;18(6):744–51. https://doi.org/10.1634/theoncologist.2012-0293.
4. Gilbert RW, Kim JH, Posner JB. Epidural spinal cord compression from metastatic tumor: diagnosis and treatment. Ann Neurol. 1978;3(1):40–51.
5. Patchell RA, Tibbs PA, Regine WF, Payne R, Saris S, Kryscio RJ, et al. Direct decompressive surgical resection in the treatment of spinal cord compression caused by metastatic cancer: a randomised trial. Lancet. 2005;366(9486):643–8.
6. Maranzano E, Latini P. Effectiveness of radiation therapy without surgery in metastatic spinal cord compression: final results from a prospective trial. Int J Radiat Oncol Biol Phys. 1995;32(4):959–67.
7. Greco C, Pares O, Pimentel N, Moser E, Louro V, Morales X, et al. Spinal metastases: from conventional fractionated radiotherapy to single-dose SBRT. Rep Pract Oncol Radiother. 2015;20(6):454–63. https://doi.org/10.1016/j.rpor.2015.03.004.
8. Gerszten PC, Burton SA, Ozhasoglu C, Vogel WJ, Welch WC, Baar J, et al. Stereotactic radiosurgery for spinal metastases from renal cell carcinoma. J Neurosurg Spine. 2005;3(4):288–95.
9. Gerszten PC, Burton SA, Ozhasoglu C, Welch WC. Radiosurgery for spinal metastases: clinical experience in 500 cases from a single institution. Spine. 2007;32(2):193–9.
10. Sahgal A, Larson DA, Chang EL. Stereotactic body radiosurgery for spinal metastases: a critical review. Int J Radiat Oncol Biol Phys. 2008;71(3):652–65.
11. Chang EL, Shiu AS, Mendel E, Mathews LA, Mahajan A, Allen PK, et al. Phase I/II study of stereotactic body radiotherapy for spinal metastasis and its pattern of failure. J Neurosurg Spine. 2007;7(2):151–60.
12. Lovelock DM, Zhang Z, Jackson A, Keam J, Bekelman J, Bilsky M, et al. Correlation of local failure with measures of dose insufficiency in the high-dose single-fraction treatment of bony metastases. Int J Radiat Oncol Biol Phys. 2010;77(4):1282–7.
13. Bilsky M, Smith M. Surgical approach to epidural spinal cord compression. Hematol Oncol Clin North Am. 2006;20(6):1307–17.
14. Laufer I, Iorgulescu JB, Chapman T, Lis E, Shi W, Zhang Z, et al. Local disease control for spinal metastases following "separation surgery" and adjuvant hypofractionated or high-dose single-fraction stereotactic radiosurgery: outcome analysis in 186 patients. J Neurosurg Spine. 2013;18(3):207–14.
15. Nakatsuka A, Yamakado K, Takaki H, Uraki J, Makita M, Oshima F, et al. Percutaneous radiofrequency ablation of painful spinal tumors adjacent to the spinal cord with real-time monitoring of spinal canal temperature: a prospective study. Cardiovasc Intervent Radiol. 2009;32(1):70–5.
16. Masala S, Chiocchi M, Taglieri A, Bindi A, Nezzo M, De Vivo D, et al. Combined use of percutaneous cryoablation and vertebroplasty with 3D rotational angiograph in treatment of single vertebral metastasis: comparison with vertebroplasty. Neuroradiology. 2013;55(2):193–200.
17. Masala S, Roselli M, Manenti G, Mammucari M, Bartolucci DA, Simonetti G. Percutaneous cryoablation and vertebroplasty: a case report. Cardiovasc Intervent Radiol. 2008;31(3):669–72. https://doi.org/10.1007/s00270-007-9223-2.
18. Goetz MP, Callstrom MR, Charboneau JW, Farrell MA, Maus TP, Welch TJ, et al. Percutaneous image-guided radiofrequency ablation of painful metastases involving bone: a multicenter study. J Clin Oncol. 2004;22(2):300–6.
19. Nakatsuka A, Yamakado K, Maeda M, Yasuda M, Akeboshi M, Takaki H, et al. Radiofrequency ablation combined with bone cement injection for the treatment of bone malignancies. J Vasc Interv Radiol. 2004;15(7):707–12.
20. Sharma M, Balasubramanian S, Silva D, Barnett GH, Mohammadi AM. Laser interstitial thermal therapy in the management of brain metastasis and radiation necrosis after radiosurgery: an overview. Expert Rev

Neurother. 2016;16(2):223–32. https://doi.org/10.1586/14737175.2016.1135736.
21. Thomas JG, Rao G, Kew Y, Prabhu SS. Laser interstitial thermal therapy for newly diagnosed and recurrent glioblastoma. Neurosurg Focus. 2016;41(4):E12.
22. Tatsui CE, Stafford RJ, Li J, Sellin JN, Amini B, Rao G, et al. Utilization of laser interstitial thermotherapy guided by real-time thermal MRI as an alternative to separation surgery in the management of spinal metastasis. J Neurosurg Spine. 2015;23(4):400–11. https://doi.org/10.3171/2015.2.SPINE141185.
23. Tatsui CE, Lee SH, Amini B, Rao G, Suki D, Oro M, et al. Spinal laser interstitial thermal therapy: a novel alternative to surgery for metastatic epidural spinal cord compression. Neurosurgery. 2016;79(Suppl 1):S73–82.
24. Thomas JG, Al-Holou WN, de Almeida Bastos DC, Ghia AJ, Li J, Bishop AJ, et al. A novel use of the intraoperative MRI for metastatic spine tumors: laser interstitial thermal therapy for percutaneous treatment of epidural metastatic spine disease. Neurosurg Clin N Am. 2017;28(4):513–24. https://doi.org/10.1016/j.nec.2017.05.006.
25. Tatsui CE, Belsuzarri TA, Oro M, Rhines LD, Li J, Ghia AJ, et al. Percutaneous surgery for treatment of epidural spinal cord compression and spinal instability: technical note. Neurosurg Focus. 2016;41(4):E2.
26. Jimenez-Ruiz F, Arnold B, Tatsui CE, Cata JP. Perioperative and anesthetic considerations for neurosurgical laser interstitial thermal therapy ablations. J Neurosurg Anesthesiol. 2018;30(1):10–7. https://doi.org/10.1097/ANA.0000000000000376.
27. Boriani S, Weinstein JN, Biagini R. Primary bone tumors of the spine. Terminology and surgical staging. Spine. 1997;22(9):1036–44.

Building a LITT Practice

13

Stephen B. Tatter, Adrian W. Laxton, and Daniel E. Couture

Introduction

Laser thermocoagulation of soft tissue in the brain (LITT) was originally introduced in the early 1980s as a tool for treating neoplasms [1]. Use has broadened to include the treatment of epilepsy, movement disorders, cavernous malformations, radiation necrosis/vasculopathy, as well as an expanding variety of types of brain and pituitary neoplasms [2–6]. Advances in magnetic resonance thermography, real-time thermal imaging and feedback control, are rapidly making it a practical solution to previously intractable problems. LITT reduces the "approach risk" of accessing a surgical target and thereby improves the treatment of any disease requiring ablation of intracranial tissue because of its minimally invasive nature. LITT offers shorter lengths of hospital stay, increased patient comfort and satisfaction, the prospect of fewer neuropsychological and focal neurologic sequelae, and decreased patient and caregiver stress [7]. Intensive care unit hospitalization is not routinely necessary after LITT in our experience.

We focus on the technical decisions that the LITT team must make to accomplish this with respect to the choice of laser thermocoagulation platform; intraoperative versus diagnostic MRI scanner for real-time thermometry; anesthesia; head fixation; MRI-intensifying technology; stereotactic trajectory determination, implementation, and confirmation; laser fixation to the skull; and obtaining tissue specimen.

Barriers to overcome in the adoption of LITT include the expense and availability of MRI time, limits to insurance coverage, and the current absence of a Current Procedural Terminology (CPT) code specifically describing the professional services performed by the neurosurgeon. It is also important to remain cognizant of LITT's current regulatory status in the United States as a surgical tool for soft tissue ablation rather than as a treatment indicated for specific diseases. In this sense, it is like a technologically advanced scalpel. We highlight solutions to these potential obstacles in the United States.

LITT Platforms

The first decision required to start a LITT practice is which of the two commercially available systems to deploy: Visualase (Medtronic), NeuroBlate (Monteris Medical), or both. We use both systems and are enthusiastic about the rapid evolution of each that having two choices promotes. In our practice the decision arose in part because of the historical features available as each system evolved. We encourage a team

S. B. Tatter (✉) · A. W. Laxton · D. E. Couture
Department of Neurosurgery, Wake Forest School of Medicine, Winston-Salem, NC, USA
e-mail: statter@wakehealth.edu

V. L. Chiang et al. (eds.), *Laser Interstitial Thermal Therapy in Neurosurgery*,
https://doi.org/10.1007/978-3-030-48047-9_13

starting a new program to fully evaluate both systems for all intended uses.

The two commercially available systems differ in the laser cooling systems used and in their compatibility with different MRI models and installations. NeuroBlate uses carbon dioxide cooling necessitating a tank outside the MRI room with a connection through a magnetically shielded conduit, whereas Visualase uses circulating room temperature saline as the coolant; so the entire system can reside in the room with the scanner when MRI thermometry is underway and can be removed or moved to another scanner readily. MRI thermometry requires high-level knowledge of and real-time access to data from the MRI scanner. In addition to requiring compatibility with the MRI scanner manufacturer, compatibility of the chosen system with the current software version is necessary. Finally, the internal bore diameter of the scanner is a consideration with a larger bore allowing more flexibility with respect to trajectories without the laser hardware colliding with the inner portion of the scanner.

Also important are the software platforms inherent in the choice of LITT platform. Hands-on experience with each software platform via vendor demonstrations or a multi-vendor practical clinic allows the best choice to be made. In Monteris Medical's case, NeuroBlate Fusion Software is used and can incorporate information from other software including Brainlab Elements (Brainlab), while Medtronic's Visualase platform is increasingly optimized with its StealthStation image-guidance technology. It is important to note that software evolves rapidly and that the interoperability between different vendors is not currently seamless. There is also potential interoperability across image-guidance systems from different vendors, so the pairings described are not mutually exclusive. Future improvements in software to watch for include ease of integration of a variety of imaging modalities such as DTI-tractography and, perhaps most importantly, the real-time calculation of dose-volume histograms during treatment to allow quantitative assessment of the extent of target (and non-target) ablation.

Once the choice of system(s) is made, both vendors provide technical expertise to ensure compatibility with the remaining decisions the stereotactic neurosurgeon faces. Many of the decisions with regard to head fixation, tissue acquisition, and stereotaxy are best made based on one's current practices. A "dry run" of the entire procedure with operating suite, imaging suite, and vendor staff is necessary to ensure successful interfaces at each step without encountering procedural incompatibilities or compromises.

In our practice, Medtronic's Visualase system is the primary ablative surgical platform we use for treating epilepsy. Its shorter working distance allows optimization of long trajectories while avoiding collisions with the inner bore of the MRI scanner. It offers the smallest diameter laser fiber currently on the market with a 1.65 mm diameter and requires a 3.2 mm burr hole. Monteris Medical now also has diffusion tip laser technology dubbed FullFire that addresses working distance limitations.

Again, in our practice, most tumors are ablated with Monteris Medical's NeuroBlate using the SideFire laser that offers an element of directionality not inherent in a diffusing tip laser probe. This directionality allows for the volume of ablation to potentially conform more precisely to the target volume in some cases but not all. The extent of directionality of a side fire laser is determined by local factors such as the nature of the tissue, the presence and type of vasculature, and reduced by the length of time for which the laser must be fired to ablate the most distant edge of the target. Similar or better conformality can also be achieved by using multiple laser trajectories at the cost of associated additional time and risk. The direction of the laser can be rotated while the laser is firing using the MRI-compatible NeuroBlate Robotic Probe Driver (Monteris Medical). The depth of the laser can also be changed robotically but not while the laser is firing.

Intraoperative Versus Diagnostic MRI Scanner

LITT is the "killer application" for intraoperative MRI in the same way that spreadsheets were for the dawn of personal computers. Access to an intraoperative MRI therefore serves as the ideal starting point for a LITT practice. It allows more rapid scheduling of patients, greater throughput, and more control over the entire process for the treating neurosurgeon. It has the potential to offer better outcomes by allowing multiple trajectories to be accomplished to optimally increase the extent of target tissue ablation and decrease the volume of non-target tissue ablated. However, if an intraoperative MRI is not in place, securing one is usually a formidable undertaking. Finding suitable space for an intraoperative MRI suite and justifying its cost versus return on investment are the first two hurdles to overcome. In the absence of enthusiastic and wealthy charitable givers, doing so usually requires engineering and pro forma financial plans specific to one's institution. Vendors of intraoperative MRI systems have resources to support this. Specifying compatibility with LITT systems early in the process is, of course, mandatory. In some states approval by a certificate of need (CON) process is necessary; a research exemption may be used to facilitate this, if applicable.

If an intraoperative MRI scanner capable of MRI thermometry is not available, use of a diagnostic scanner is the default. A diagnostic scanner near the operating suites may be ideal if available. This allows for induction of anesthesia, biopsy when indicated, and fixation of the laser holding apparatus to the skull in the most controlled environment. If intraoperative CT is available, the trajectory can be confirmed and access for additional trajectories created if it appears necessary. While LITT under local anesthesia has been described, use of a nearby diagnostic MRI scanner generally requires the patient to be transported under general anesthesia to the MRI suite for laser thermocoagulation. So transport to the MRI thermometry-compatible diagnostic scanner must be practical with respect to distance and obstacles to be traversed.

Systems are available and can be designed to perform entire neurosurgical procedures in a diagnostic MRI scanner without the requirement for routine, planned transport from the operating room. The most widely deployed are ClearPoint (MRI Interventions) and STarFix (FHC, Inc.) neuro-navigation systems. The former uses an MRI-compatible mechanical positioning system, while the latter uses a custom 3D printed stereotactic frame that can accommodate multiple trajectories. Implementation of these systems can, for example, incorporate MRI-compatible drills; so they can be used to create additional trajectories in the MRI scanner, which can be beneficial in settings in addition to a diagnostic scanner somewhat remote to the operating room to the point that it is even used in some institution's intraoperative MRI suite.

Stereotactic Components for LITT

Successful LITT requires creating an environment for stereotaxy in which every step is compatible with the MRI thermometry LITT platform being used. Many of the decisions with regard to preoperative imaging, anesthesia, head immobilization, co-registration, trajectory planning, stereotactic navigation, intraoperative imaging, tissue acquisition, MRI-intensifying coils or coilless intensification, and sometimes devices to hold the laser in position may be best made based on one's experience with the available solutions, current practices, and the instruments already available in one's home institution. Options listed are illustrative but not likely to be mutually exclusive. Often one vendor's product can be used to supply more than one of the necessary functions. In developing a program, one must have at least one solution available for each of these steps, i.e., pick at least one item from each menu (list) below—substitutions allowed.

Preoperative Imaging

Preoperative anatomic imaging most frequently includes a contrast-enhanced high-resolution MRI to allow vessels to be avoided and to target enhancing lesions. Other imaging modalities can be incorporated into some but not all trajectory-planning software. When choosing a combination of systems for one's LITT program compatibility with imaging modalities, listed here should be considered in light of the planned applications. Importation of co-planar stereotactic arteriography is not yet widely supported. Preoperative imaging modalities:

- MRI with and/or without contrast
- Tractography—diffusion tensor imaging (DTI)
- Functional MRI (fMRI)
- High-resolution CT
- Magnetic resonance angiography/venography (MRA/MRV), computed tomography arteriography/venography (CTA/CTV)
- Positron emission tomography (PET)
- Co-planar arteriography
- Single-photon emission computerized tomography (SPECT)
- Magnetoencephalography (MEG)

Anesthesia

Most LITT procedures are performed under general anesthesia, but anesthesia is not mandatory in a cooperative patient willing and able to hold still during MRI thermometry. The ballet required to move a patient under anesthesia from the operating suite to even a nearby diagnostic MRI scanner for thermometry requires careful choreography by anesthesia, radiology, and neurosurgery working together as a team.

Immobilization

There are two separate intervals of the procedure for which to consider head immobilization: during creation of the laser trajectory and during MRI thermometry as the laser is firing. Head motion during MRI thermometry acquisition cannot be tolerated. Separate solutions for each of these two phases may be optimal. We use the AtamA headrest (Monteris Medical) for both on directional laser cases. It attaches to a transport board that fits in the MRI-docking table, which we use to transport the patient from the OR to the nearby MRI suite. Stereotactic frames, of course, also incorporate co-registration, planning, and stereotactic navigation solutions. Examples of head immobilization solutions:

- Stereotactic frames
  - Leksell Frame (Elekta Instrument AB)
  - CRW Frame (Integra LifeSciences Corporation)
  - RM or ZD Frame (inomed Medizintechnik, GmbH)
  - Stereotactic Frame (Kamcon Bio Technology Systems Private Limited)
  - Aimsystem (Micromar Ind. e Com. LTDA)
  - BMS Frame (Bramsys Ind. e Com LTDA)
- Surgical immobilization systems
  - MAYFIELD with or without MRI compatibility (Integra LifeSciences Corporation)
  - Sugita Stereotactic Frame (Mizuho Medical Co., Ltd.)
- Frameless with padding
  - General anesthesia
  - Local anesthesia in highly selected patients
- AtamA Patient Stabilization System (Monteris Medical)
  - Also provides a platform for patient transport to MRI

Co-registration

Each stereotactic neurosurgeon has preferred methods for accurately co-registering imaging space with intraoperative stereotactic space. One may make use of this preference for LITT or adopt a system specifically acquired for LITT. When considering acquisition of a new system, ease and accuracy of co-registration are important considerations as is the availability of intraoperative imaging such as MRI, CT, and

cone-beam CT. Examples of co-registration solutions:

- Stereotactic frame with attached fiducials
  - With CT or MRI registration in radiology or OR
- Fixed headrest
  - With CT or MRI registration in the OR and a visual or magnetic tracking array
- Implanted fiducials
  - STarFix fiducials (FHC, Inc.)
  - Other implanted fiducials detectable by the image-guidance system used
- Co-registration system specific to surgical robot used
- Frameless
  - Surface matching
  - Fiducials with CT or MRI registration in OR or Radiology

Trajectory Planning and Image Segmentation

The LITT surgeon should be very comfortable with the trajectory planning system to be used to optimize laser trajectories to perform complete or maximum prudent ablation of desired targets while avoiding the need to ablate functioning brain tissue and avoiding vessels. The orthogonal views in the trajectory planning software allow measurement of the edge of the target from the laser, ideally only approximately 1 cm in each direction. Trajectory planning software may also provide tools to segment the target, normal eloquent structures, and white matter tracts. Ideally these can then be exported to the LITT treatment software so that they can be taken into account during real-time ablation. Some of the available treatment planning software packages:

- Conventional stereotactic frames or frameless arms
  - Brainlab Elements (Brainlab)
  - StealthStation (Medtronic)
  - CranialMap (Stryker)
  - Software from specific stereotactic frame manufacturer
- WayPoint Navigator (FHC, Inc.)
  - Custom 3D-printed STarFix frame
  - CRW, Leksell, and other frame based stereotactic systems
- ClearPoint (MRI Interventions)
- Robot-specific planning systems
  - ROSA Brain (Zimmer Biomet Holdings, Inc.)
  - *neuromate* system (Renishaw, plc.)
  - Mazor Robotics Ltd.

Stereotactic Navigation and Drill Guidance

The most frequent approach to LITT uses a stereotactic drill to pierce the calvarium and dura followed by attachment of a skull bolt that holds the laser and or robotic laser guide and through which a biopsy can be performed if desired. This technique makes the accuracy of the trajectory entirely dependent on the accuracy of the drill. Inaccuracy may be introduced by skiving of the drill bit on the calvarial surface before the bit is set into the bone. Non-skiving drill bits and manually setting the bit in the calvarium with a mallet reduce this source of inaccuracy but often do not eliminate it. This highlights the importance of choosing the most reliable stereotactic trajectory and drill guidance system when using a stereotactic drill. A number of systems to be considered for trajectory guidance:

- Conventional stereotactic frames
  - Leksell Frame (Elekta Instrument AB)
  - CRW Frame (Integra LifeSciences Corporation)
  - RM or ZD Frame (inomed Medizintechnik, GmbH)
  - Stereotactic Frame (Kamcon Bio Technology Systems Private Limited)
  - Aimsystem (Micromar Ind. e Com. LTDA)
  - BMS Frame (Bramsys Ind. e Com LTDA)
- Robotic
  - ROSA Brain (Zimmer Biomet Holdings, Inc.)
  - *neuromate* system (Renishaw, plc.)
  - Mazor Robotics Ltd.

- ClearPoint (MRI Interventions)
- Custom made frame
  - STarFix (FHC, Inc.)
- Frameless
  - VarioGuide (Brainlab)
  - Stealth Treon, Vertek (Medtronic)
  - Nexframe (Medtronic)
  - Navigus (Medtronic)

Intraoperative Imaging

Intraoperative imaging confirms the trajectory and ideally is accomplished in a location that allows trajectory modification or the addition of another trajectory if needed. So for diagnostic-MRI LITT, the MRI thermometry scan is not ideal as the first confirmation of trajectory unless an MRI-compatible system to create new trajectories such as those provided by ClearPoint or STarFix is being used. We often use intraoperative CT co-registered back to the planning MRI which had been obtained preoperatively to confirm our trajectory. The scan can be obtained with the biopsy needle at the target or constructed from two points in the electrode-holding bolt. Categorical examples of intraoperative imaging that can be used to confirm the trajectory:

- Operative MRI scanner
- Diagnostic MRI scanner
  - Suggested only if MRI-compatible trajectory creation solution is available
- Intraoperative CT
  - In OR
    Conventional CT
    Cone-beam CT
  - In radiology
    May require return to OR

Laser Holders

Solutions to securing the laser in place fall into two categories with a significant difference. Bolts fixed to the skull offer convenience and minimal invasiveness but make the overall accuracy of the LITT trajectory entirely dependent on the accuracy and stability of the drilling system used to perforate the skull. The other category of laser holders allows a larger calvarial opening to be used so that the accuracy of the trajectory does not depend entirely on the initial drilling. Interestingly, bolt technology is so convenient and minimally invasive that many neurosurgeons incorporate it even when they use a stereotactic system capable of holding the laser without a bolt. Laser holding solutions:

- Visualase Bolt (Medtronic)
- Monteris Medical:
  - Monteris Mini-Bolt
  - Axiiis Stereotactic Miniframe
- ClearPoint (MRI Interventions)
- Custom made frame
  - STarFix (FHC, Inc.)
- Frameless
  - Nexframe (Medtronic)
  - Navigus (Medtronic)

MRI Intensifying Coils

Optimization of MRI signal for thermometry may require intensification solutions that communicate with the scanner using send-receive technology. As for each decision needed to develop a LITT program, verification with the LITT platform manufacturer(s) with whom one works allows verification of state-of-the-art compatibility. MRI signal intensification solutions to consider:

- Rigid Coils
  - Head
  - Body
  - Custom
- Flexible Coils
- Disposable Mats

Prioritizing Patient Access to LITT

Competition for institutional resources to begin any new program is often fierce and requires a strategy to enlist support from the neurosurgery

department, other departments whose patients will benefit, radiology, hospital administration, the capital purchase committee, and under some circumstances, the state CON process, particularly if acquisition of intraoperative MRI is a LITT program development goal. While the capital spending needed to start a LITT program can be modest—similar to that of a modern operating microscope—in most institutions marshaling resources to start a LITT program benefits from a concerted strategic effort by members of the LITT team to enlist the support of all of the stakeholders. Fortunately, the benefits of LITT are large, and the financial incentives should be able to be optimized to be ultimately positive for all institutional stakeholders.

Institutional Support

Achieving departmental support for the acquisition of one or more LITT systems is the first and often the most straightforward step to gaining an institution-wide commitment to LITT, since the benefits of decreased approach risk and of being able to surgically access otherwise inaccessible lesions are obvious to neurosurgeons beginning with tumor and epilepsy surgeons and extending to other areas including functional neurosurgery, vascular neurosurgery, and even spine metastasis neurosurgery. In many institutions enlisting the active support of the Department Chair is crucial. There are many opportunities to lobby for this support—a specific example is listing development of a LITT program as highest priority at one's annual review meeting, i.e., turning a lemon into lemonade.

When a diagnostic MRI scanner or scanners will be the home for MRI thermometry, achieving the support of radiology at both the departmental and hospital levels may be challenging because of limited availability of MRI time. Solutions include performing procedures on weekends or even in the evening when scanner demand often lessens. Once LITT becomes a regularly performed procedure arranging for LITT slots be held until 1 week before, and freeing the time for diagnostic scans at that time if no patient requires LITT then allows the disruption of the diagnostic scanning schedule to be minimized. If necessary, it could be useful to remind recalcitrant decision makers that neurosurgeons are able to free significant amounts of MRI scan time by allowing patients to get diagnostic scans on other scanners even those owned by other institutions if that would be helpful.

Currently there is no CPT code that describes neurosurgeons' LITT work and allows for work-related relative value units (wRVU) to be easily calculated and professional fees or compensation based on wRVUs to be reimbursed resulting in use of the unlisted cranial neurosurgical procedure code, 64999. We arrived at a temporary solution to this deficiency at our institution by deriving an internal tracking value of approximately 42 wRVUs to capture the neurosurgeon's effort in performing a single LITT procedure.

Insurance Coverage

Cranial LITT is not encompassed by a current specific CPT code but is described by two ICD-10CM procedure codes: D0Y0KZZ for laser interstitial thermal therapy of the brain and D0Y1KZZ for laser interstitial thermal therapy of the brain stem. The US Center for Medicare and Medicaid Services (CMS) has assigned inpatient hospitalizations associated with these codes to craniotomy diagnosis-related groups (DRG) for hospital reimbursement DRG 023-027 and 025-027, respectively. The primary difference between the DRGs is the absence (DRG 023 and 027) or presence of major complications and morbidities (DRG 023 and 025) or other complications and morbidities (DRG 026). This establishes the basis for reimbursement for hospitalization and performance of the procedure for patients covered by traditional fee-for-service Medicare.

For other insurers, reimbursement for LITT is generally determined on a case-by-case basis. When seeking prior authorization for payment the use of CPT code 64999, Unlisted Procedure, Nervous System may lead to an initial determination that the proposed procedure is experimental,

despite the fact that the use of these surgical tools is expected to comply with the US FDA labels. This reasoning is of course not strictly applicable as it could be used to categorize the use of any other surgical instrument—such as a scalpel—as experimental. The best solution to this obstacle is often to provide thorough documentation of the likely benefits of LITT in comparison to the alternatives—most often craniotomy or no surgical treatment. Including one or two selected labeled images may sometimes be helpful. Seeking peer review as quickly as possible and if possible with a neurosurgeon has been the most successful approach in our experience. LITT vendors have additional resources that can be made available to help with pre-authorization and with post-procedure appeals for appropriate reimbursement and seeking their support as early in the insurance approval process as possible may be helpful. While it may be tempting to consider an individual patient's interests in taking an adversarial approach with an insurance company—such as by encouraging the patient to seek publicity, encouraging the patient to seek legal representation, or encouraging reporting of physicians at insurance companies to state regulators for practicing medicine outside of licensure or standards of care—we have thus far not needed to resort to such measures.

Working with experts in one's institution on arranging general meetings to discuss the benefits of LITT with insurance company representatives and medical directors is a fruitful long-term strategy. Other avenues to pursue include working together to ensure the inclusion of LITT as an option in specialty organization treatment guidelines for specific indications and working on improving providing even more abundant and compelling outcome, cost, and satisfaction data to support LITT for specific indications.

Building LITT Referrals

Neurologists, radiation oncologists, and medical oncologists often become enthusiastic referral sources after seeing and hearing from their patients who have benefitted from LITT by having better than expected outcomes with less than expected morbidity and stress. Generating their first experience of course often occurs as the result of the care being provided by the LITT team. This is amplified by systematic identification of and communication with the other specialists involved in the care of the problem amenable to LITT treatment. In our practice we endeavor to make this communication in the form of a letter or note at the time of the initial consultation that results in a recommendation for LITT. The communication to the other specialists is often detailed enough to also be used in the insurance pre-authorization process to support the medical necessity of LITT for a given patient. We also work to individually communicate by letter or note with the other specialists and the primary care providers at the time the LITT procedure is performed.

Generating initial referrals from neurologists, radiation oncologists, and medical oncologists when one is not routinely involved in the care of their patients with CNS -disease can benefit from creative approaches. We find that mailings informing specialists of LITT clinical trials including registry trials prove to be a source of numerous referrals. These letters may need to be approved by the governing Institutional Review Board (IRB). Enlisting the resources of the institutional marketing department for advertising to physicians and directly to patients can also generate first referrals. Caveats to consider include relatively low rates of penetration by direct to physician marketing efforts and limitations—rarely but potentially applicable to hospital marketing—related to the FDA labeling of LITT as a surgical tool, like a robot, rather than a treatment approved for a specific condition. Presentations of results at local or regional rounds and specialist society meetings are of course very valuable in generating referrals. Sometimes even presenting to very small groups or individual providers leads to developing relationships with what prove to be the most loyal referrers. Many institutions have outreach coordinators to facilitate this. Some institutions may allow vendor support of these activities, whereas others find this to be a potential conflict of interest and do

not. The value of presenting at internal rounds should also not be missed.

Conclusions

If outcomes are the same or better with minimally invasive approaches than with traditional open surgical approaches, it is inevitable the former will displace the latter because of patient satisfaction. LITT exemplifies this to the extent that one of the authors is fond of saying with tongue in cheek when presenting at neurosurgical meetings that someday the meeting will be entirely about LITT and other minimally invasive approaches and craniotomies will be relegated to the special practical courses on the weekend. For this to come to pass practitioners must make LITT widely available to patients who can benefit from it by building successful integrated practice teams. We hope that this review of the current but rapidly evolving environment for building a LITT practice facilitates this laudable goal.

References

1. Missios S, Bekelis K, Barnett GH. Renaissance of laser interstitial thermal ablation. Neurosurg Focus. 2015;38(3):E13. https://doi.org/10.3171/2014.12.FOCUS14762.
2. Ahluwalia M, Barnett GH, Deng D, Tatter SB, Laxton AW, Mohammadi AM, et al. Laser ablation after stereotactic radiosurgery: a multicenter prospective study in patients with metastatic brain tumors and radiation necrosis. J Neurosurg. 2018;130(3):804–11. https://doi.org/10.3171/2017.11.JNS171273.
3. Mohammadi AM, Hawasli AH, Rodriguez A, Schroeder JL, Laxton AW, Elson P, et al. The role of laser interstitial thermal therapy in enhancing progression-free survival of difficult-to-access high-grade gliomas: a multicenter study. Cancer Med. 2014;3(4):971–9. https://doi.org/10.1002/cam4.266.
4. Rennert RC, Khan U, Tatter SB, Field M, Toyota B, Fecci PE, et al. Patterns of clinical use of stereotactic laser ablation: analysis of a multicenter prospective registry. World Neurosurg. 2018;116:e566–70. https://doi.org/10.1016/j.wneu.2018.05.039.
5. Wicks RT, Jermakowicz WJ, Jagid JR, Couture DE, Willie JT, Laxton AW, et al. Laser interstitial thermal therapy for mesial temporal lobe epilepsy. Neurosurgery. 2016;79(Suppl 1):S83–91.
6. Wu C, Jermakowicz WJ, Chakravorti S, Cajigas I, Sharan AD, Jagid JR, et al. Effects of surgical targeting in laser interstitial thermal therapy for mesial temporal lobe epilepsy: a multicenter study of 234 patients. Epilepsia. 2019;60(6):1171–83. https://doi.org/10.1111/epi.15565.
7. Rennert RC, Khan U, Bartek J Jr, Tatter SB, Field M, Toyota B, et al. Laser ablation of abnormal neurological tissue using robotic NeuroBlate system (LAANTERN): procedural safety and hospitalization. Neurosurgery. 2019 . pii:nyz141; https://doi.org/10.1093/neuros/nyz141.

Index

A
Adult epilepsy treatment, LLIT
  indications, 85, 86
  lesional and non-lesional focal neocortical epilepsies
    cavernous malformations, 100
    general approach, 99, 100
    malformations of cortical development, 100
  medial temporal lobe epilepsy, 91
    contraindications, 91
    outcomes, 96–98
    stereotactic amygdalohippocampotomy, 93–96
  non-lesional epilepsies, 100, 102
  techniques, 86
    anesthesia and positioning, 86, 87
    coupling MRg-LITT to SEEG, 88, 89
    MRI Coils, 87
    multiple ablation tracts, 88
    single lesions/ablation tracts, 87, 88
    trajectory, choice of, 86
5-aminolevulinic acid (5-ALA), 65
Amygdalohippocampectomy, 91
Anterior flex coil, 14
Anterior temporal lobectomy (ATL), 91, 98
AtamA patient stabilization system, 22, 170
AxiEm™, 129

B
Barriers to overcome in LITT, 167
Bilsky Scale, 154
Blood brain barrier (BBB), 52, 81
Bolt, 90
BrainLab and Medtronic techniques, 29
BrainLab and StealthStation systems, 24
Brainlab approach, 25–27
BrainLab's wizard-guided trajectory software, 27
BrainLab™ VarioGuide system, 26
Brain tumors, 75
Butterfly gliomas, 69, 70

C
Capsulotomy, 123
Cardiac implantable electronic device (CIED), 42
Cavernous malformations, 100, 101, 144
Cerebral plasticity, 127
Certificate of need (CON) process, 169
Chemical paralysis, 128
Choroid plexus, 93
Cingulate epilepsy, 100
ClearPoint drape, 108
ClearPoint SmartFrame, 80
ClearPoint software, 24, 108, 109
ClearPoint stereotactic system, 106
ClearPoint system, 7, 24, 87–89, 99, 102, 110, 111, 129, 169, 171, 172
Confirmational imaging, 132
Conventional external beam radiation therapy (cEBRT), 152
Cooled laser fibers/probes, 9
Corpus callosotomy, 102, 144, 145
Cortical dysplasia, 100, 102, 140, 142, 146
Cosman-Roberts-Wells (CRW) frame, 23, 128
Cranial nerve neuropathy, 146
Current Procedural Terminology (CPT) code, 167

D
Deep brain stimulation (DBS), 105–108, 110, 112, 113, 115, 119
Deep venous thrombosis (DVT), 146
Delayed seizure control, 127
Diagnosis related groups (DRG), 173
Dominant *vs*. non-dominant temporal lobe ablations, 98
Drug resistant epilepsy, 127

E
Edema, 81
Electronic subsystems, 11
Emotional Well-Being scores, 61
Endotracheal anesthesia, 93
Epidural hematoma, 46
Epidural spinal cord compression (ESCC), 151–154
Epilepsy surgery, 127, 168
Essential tremor (ET), 105

V. L. Chiang et al. (eds.), *Laser Interstitial Thermal Therapy in Neurosurgery*,
https://doi.org/10.1007/978-3-030-48047-9

F
Fast spin-echo (FSE) sequence, 113
Favorable PFS, 68
Flash-lamped based Nd:YAG lasers, 3
Fluid-attenuated inversion recovery (FLAIR) sequence, 25
Focal cortical dysplasias (FCD), 133, 140
Foley catheter, 107
Fractionated radiation therapy, 151
Frame-based stereotaxy, 128, 129
Frameless stereotaxy, 129, 130

G
Glidescope, 107
Glioblastoma (GBM)
  challenge of treating, 65, 66
  disruption of BBB, 70–71
  immunotherapy of, 71
  malignant melanoma metastasis, 70
  median OS, 70
  minimally invasive technique, 66
  postoperative infection, 70
  radiation therapy, 71
  stand-alone therapy, 70
  surgical resection of, 65
  treatment modality for cytoreduction
    butterfly gliomas, 69, 70
    favorable PFS, 68
    laser thermal therapy, 68
    glioma cohort, 67
    laser thermal therapy, 69
    mean PFS, 69
    median PFS, 68
    NeuroBlate System, 68
    salvage technique, 67
    TDT lines, 68
    Visualase System, 68
    WHO grade 3 and grade 4 gliomas, 69
  tumor-treating fields, 65
Globus pallidus internus, 105–107
Gradient echo scan (GRE), 33

H
High-dose glucocorticoids, 151
High intensity focused ultrasound (HIFU), 106
Hopkins Verbal Learning Test-Revised (HVLT-R) scores, 61
Hypothalamic ganglioglioma, 76
Hypothalamic hamartoma (HH), 75, 79, 81, 135, 137

I
Image-guided stereotaxy, 152
Immobilization, 170
Institutional review board (IRB), 121, 174
Insular epilepsy, 143, 144
Interstitial laser hyperthemia, 134
Interventional MRI, 107
  general targeting and SmartFrame placement, 108–110
  induction, head frame, & sterile field, 107, 108
  laser preparation, ablation and assessment, 111, 112
  Smartframe adjustment and burrhole creation, 109, 110
Intracerebral hemorrhage (ICH), 56
Intracranial hematomas, 46, 47
Intractable psychiatric disease
  outcomes, 123, 124
  patient selection, 121, 122
  rationale for LITT in psychiatric neurosurgery, 119–121
  technical considerations, 122, 123
Intraoperative MRI (iMRI), 65, 153
Inversion Recovery (IR) sequence, 109, 115

K
Ktrans coefficients, 71

L
Laser ablation, 21, 86, 106
  of cavernous malformation, 101
  Clearpoint, 99
Laser ablations, 86, 96
Laser amygdalohippocampotomy, 97
Laser catheter placement, 31–32
Laser catheter types, 20
Laser diffusing fiber (LDF), 21, 31
Laser fiber catheter, 87
Laser insertion techniques, 22
Laser interstitial thermal therapy (LITT), 1, 85
  anesthesia, 170
  awake patient
    choosing appropriate patients, 38–39
    deployment of resources, 38
    eloquent tissue preservation, 37
    patient safety, 37–38
    real-time imaging quantification of tumor eradication, 37
    reduced patient turnaround time, 38
    stacking procedures, 38
  building LITT referrals, 174, 175
  complications of
    fully functional laser system, 48
    hyperthermia-related deficits, 49
    hyperthermic injury, 47–48
    intracranial hematomas, 46, 47
    laser misplacement, 45–46
    LITT-induced deficits, 49
    MR thermometry, 48
    newer navigation systems, 48
    SRS, 49
  co-registration, 170, 171
  fiber tip shape, 19
  frame based LITT
    CRW frame, 23
    Leksell frame, 24

stereotactic frames, 22, 23
trajectory guided mini-frames, 24–25
frameless LITT
Brainlab approach, 26, 27
Medtronic StealthStation system, 25, 27, 29
robotic placement, 29–31
imaging sequence, 43
immobilization, 170
intraoperative imaging, 172
intraoperative versus diagnostic MRI scanner, 169
laser ablation
high-quality images, 33
high temperature, 33
monitoring, 33
MR thermometry images, 34
Neuroblate system, 34
patient positioning, 32
post-ablation, 34
probe and cooling lines, 32
quality of thermometry imaging, 32
real-time thermal and damage imaging, 34
3.3mm fullfire laser, 34
T1 and / or T2 image, 33
laser catheter placement, 31–32
laser holders, 172
lesional metrics and operator experience / preference, 19
long optical fibers, 19
MR-guided laser ablation
epilepsy ablation, 42
falling asleep during ablation, 42
local anesthesia, 39
laser-support device, 39
mild left leg weakness, 42
MR controls, 41
natural interruptions, 41
patient positioning, 40
patient reassurance, 39
pharmacologic preparation, 39, 40
preoperative patient preparation, 39
preparation, 39
psychological comfort, 41
scalp incision and MR ablation, 41
speaker-microphone apparatus, 40
support personnel, 39
technical preparation, 40
thermographic imaging, 41
trajectory planning, 39
MRI intensifying coils, 172
NeuroBlate system, 168
pacemaker patient, 42–43
placement of, 22
planning
deciding on type of laser fiber use, 21–22
determination of trajectory and number of laser fibers, 20, 21
preoperative imaging, 170
prioritizing patient access to, 172, 173
institutional support, 173
insurance coverage, 173, 174
SAR values, 43
stereotactic components, 169
stereotactic navigation and drill guidance, 171, 172
trajectory planning and image segmentation, 171
Visualase system, 168
wavelengths for, 19
Laser light, 75
Laser probe placement and activation, 39
Leksell Arc's scale, 24
Leksell Stereotactic frames, 80
Lesional and non-lesional focal neocortical epilepsies
general approach, 99, 100
outcomes from laser ablation
cavernous malformations, 100
malformations of cortical development, 100
Limbic leukotomy, 124
LITT cingulotomy, 124
Local anesthesia, 38
Low-grade gliomas, 76
Low-limit markers, 133, 136

M

Magnetic resonance-guided laser interstitial thermal therapy (MRg-LITT), 85, 86, 88, 89, 99, 100, 102
cerebral thermal ablations, 6–7
ClearPoint system, 7
control computer, electronics, and user interface, 11–12
fiber probes and cooling, 9
interstitial hyperthermia, 1
lasers
flash-lamped based Nd:YAG lasers, 3
mechanisms of immediate laser interactions, 3
980 nm (Visualase), 3
optical and thermal properties, 3
optical radiation on electromagnetic spectrum, 2–3
secondary mechanisms of laser interactions, 3
1064 nm (NeuroBlate), 3
LITT-induced ablations, 6
MR imaging, 7, 12–15
multi-step LITT process, 7
open surgical procedures, 1
pediatric epilepsy (*see* Pediatric epilepsy, MRgLITT)
position control methods, 9–11
real-time MRI thermometry, 1
skull-mounted trajectory device, 8–9
tissue temperature measurement
MRI thermal imaging sequences, 5–6
PRF shift in human and animal tissues, 5
"stock" MR pulse sequences, 6
thermal dosimetry, 3–5
Magnetic source imaging (MSI), 85
Magnetoencephalographic (MEG) studies, 85, 128
Malformations of cortical development, 100

Mayfield head holder, 26
Medial temporal lobe epilepsy, 91
  contraindications, 91
  outcomes, 96, 97
    neuropsychological, 98
    seizure, 96
  stereotactic amygdalohippocampotomy, 93–96
Median PFS, 68
Medtronic StealthStation system, 25, 27–29
Mesial temporal sclerosis (MTS), 85, 91, 96, 98, 99, 137
Metastatic cancer, 151
Metastatic in-field recurrence
  alternative to craniotomy, 62–63
  basal ganglia lesion, 54
  bilateral occipital regrowing tumors, 55, 56
  complications and postoperative management, 55–57
  contrast-enhanced T1W imaging, 58
  corticosteroids, 52
  craniotomy for resection, 52
  disruption of BBB, 63
  imaging changes, 57–59
  intracranial disease, 54
  local control and survival rates, 60
  NeuroBlate System, 54, 55
  neurological outcomes in, 61
  occipital regrowing tumor, 54
  outcomes of
    local control and overall survival, 59–61
    QOL and neurological outcome, 61, 62
    steroids dependence, 62
  patient selection, 52–53
  pre-operative MRI, 54
  pre-operative planning, 53
  radiation necrosis, 51
  recurrent metastases, 52
  SRS, 51
  steroid taper, 55
  systemic disease, 54
  trajectory planning, 54, 55
  WBRT, 52
Mini-Mental State Examination (MMSE) scores, 61
Minimally invasive surgical techniques, 127, 163
Modern clinical MRI systems, 6
Monopolar cautery, 130
Movement disorders
  interventional MRI, 107
    general targeting and Smartframe placement, 108–110
    induction, head frame, & sterile field, 107, 108
    laser preparation, ablation and assessment, 111, 112
    Smartframe adjustment and burrhole creation, 109, 110
  pallidotomy
    results, 115, 116
    targeting and laser ablation, 115
  patient selection, 106, 107
  rationale for LITT in, 105, 106
  thalamotomy
    results, 114, 115
    short-term issues, 115
    targeting and laser ablation, 112–114
MR thermogram limitations, 131
MR-guided LITT procedures, 7

N
Nd:YAG (1064 nm) lasers, 3
Necrotize or coagulate soft tissue through thermal therapy, 85
NeuroBlate
  Fusion Software, 168
  GUI, 13
  laser insertion, 31
  Mini-Bolt, 8
  Monteris NeuroBlate, 19, 85, 132, 133
  Optic Laser Probe (Monteris Medical), 9
  Robotic Probe Driver, 168
  SideFire laser, 81
  system, 1, 2, 11, 12, 14, 21, 23, 34, 55, 70, 80, 81, 136, 167, 168
Neuromate, 129
NexFrame™, 24, 129
Non-lesional epilepsies, 100, 102

O
Obsessive compulsive disorder (OCD), 119–124
Occipital regrowing tumor, 54
Optic Laser delivery probe, 10

P
Pacemaker patient, 42–43
Pain scores (VAS), 163
Pallidotomy, 116
  results, 115, 116
  targeting and laser ablation, 115
Parkinson's disease (PD), 105, 107
Pediatric brain tumors, MRIgLITT, 77–78
  advantages, 79, 80
  complications, 81, 82
  role and outcomes, 75, 76, 79
    hypothalamic hamartomas, 79
    low-grade gliomas, 76
    pilocytic astrocytomas, 76
    subependymal giant cell astrocytoma, 76
  technical considerations, 80, 81
Pediatric epilepsy, MRgLITT
  commercially available laser ablation systems, 132
  complications, 146
  diagnostic tools, 128
  imaging and radiologic-pathologic correlation, 132
  indications
    cavernous malformations, 144
    corpus callosotomy, 144, 145

cortical dysplasia, 140
hypothalamic hamartoma, 137
insular epilepsy, 143
mesial temporal sclerosis, 137
periventricular nodular heterotopia, 140, 142, 143
tuberous sclerosis complex, 137, 140
low-limit markers, 133, 136
Medtronic Visualase, 132, 133
Monteris NeuroBlate software, 136, 137
outcomes, 147
patient selection, 128
post-operative care, 132
techniques
confirmational imaging, 132
delivering laser, 128
frame-based stereotaxy, 128–130
heat sinks, planning for, 130
intraoperative imaging and thermometry, 131
laser implantation, 130, 131
MR thermogram limitations, 131
pre-incision and anesthesia, 128
trajectory planning, 130
work up, 128
Pediatric mesial temporal lobe epilepsy (MTLE), 137, 141
Pediatric multi-focal epilepsy, 129
Pediatric periventricular nodule heterotopia, 143
Percutaneous separation surgery, 164
Percutaneous stabilization, 155
Percutaneous techniques, 153
Perifocal edema, 6
Periventricular nodular heterotopia (PVNH), 100, 140, 142, 143
Pilocytic astrocytomas, 76
Posterior cingulate seizure, 102
PRF-based MR thermometry, 5, 12
Primitive neuroectodermal tumor (PNET), 76
Progression free survival (PFS), 68
Proton resonant frequency (PRF), 5
Psychosurgery, 124

R
Radiation therapy, 152
Radio-frequency (RF) ablation, 105, 120
Radiosurgery, 152
Refractory epilepsy, 127
RF ablation, 120
RF flex coils, 14
Robotic placement, 29–31
Robotized stereotactic assistant (ROSA™), 30, 80, 129
Robot-specific planning systems, 171

S
ScalpMount, 25
Seizure onset zone (SOZ), 85, 137
Selective amygdalohippocampectomy (SAH), 98
Separation surgery, 153, 163
SideFire laser, 168
Single positron emission computed tomography (SPECT), 86
“Six-pack” approach, 124
Skull-mounted trajectory device, 8–9
SLATE (Stereotactic Laser Ablation for Temporal Lobe Epilepsy) Trial, 85
Social Well-Being scores, 61
Speaker-microphone apparatus, 40
Spinal laser interstitial thermal therapy (sLITT), 153, 154
indications patient selection, 153–155
in spine tumors treatment, 162, 163
technical considerations, 155–157, 159, 161, 162
closure, 161
fiducial markers apply, 155, 158
iMRI, 160
K-wires insertion, 159
patient position, 156
real-time magnetic resonance thermal imaging for, 161
sequential procedural workflow, 160
sterile reference array, 157
Spinal metastatic disease, 151
Spinal stereotactic radiosurgery (SSRS), 152, 153, 162
Spine laser interstitial therapy, 163
Spine stereotactic radiosurgery (SSRS), 162
Standard and Dual-Purpose SEEG Bolts, 91
STarFix devices (FHC), 24, 25, 31, 80, 169, 172
STarFix fiducials, 171
STarFix microTargeting system, 24, 129
StealthStation image-guidance technology, 168
StealthStation Tracer® or O-arm™ imaging system, 27
Stereo-EEG (SEEG), 86, 88, 89, 92, 99
Stereo-electroencephalography (sEEG), 128
Stereotactic amygdalohippocampotomy, 93–96
Stereotactic frames, 22, 23
Stereotactic laser amygdalohippocampotomy (SLAH), 86, 87, 91, 94, 96–99
Stereotactic methods, 122
Stereotactic radiosurgery (SRS), 51, 98, 106
Sterile reference array, 157
“Stock” MR pulse sequences, 6
Subependymal giant cell astrocytomas (SEGAs), 76

T
Thalamotomy
results, 114, 115
short-term issues, 115
targeting and laser ablation, 112–114
Thermal damage estimate (TDE), 33
Thermal dose threshold (TDT), 68, 137
Thermal dosimetry, 3–5
Thermometry, 131
3mm LDF, 21
3-Tesla MRI imaging, 85
Total intravenous anesthesia (TIVA), 128

Trajectory guided mini-frames, 24–25
Trajectory planning, 39
Tuberous sclerosis complex (TSC), 137, 140, 141
TwistPoint XG™ frame, 25
2D gradient recalled echo (GRE), 5–6

V
VarioGuide™ system, 26
Ventral intermediate thalamus, 107
Visualase (Medtronic), 2
Visualase Bolt, 172
Visualase bone anchor, 9
Visualase Cooling Catheter System, 10, 111
Visualase laser system, 9, 11, 12, 59, 68, 80, 81, 86, 107, 135, 136, 167, 168

W
WayPoint Navigator, 171
Whole brain radiation therapy (WBRT), 52
Work-related relative value units (wRVU), 173